THE ROLE OF CHX10 IN THE DEVELOPMENT OF THE VERTEBRATE RETINA

Adam David Rutherford

A thesis submitted for the degree of
Doctor of Philosophy
University College London
University of London, 2001

Developmental Biology Unit
Institute of Child Health
and Department of Biology
University College London
30 Guilford St
London, WC1N 1EH

ABSTRACT

The role of Chx10 in the development of the vertebrate retina

Complex interactions between intrinsic and extrinsic factors regulate the development of the retina from multipotential progenitor cells to the highly organised, mature tissue. Many genes are known to be essential to this process. Chx10 is a homeodomain transcription factor that is essential for the development of the retina and eye in many vertebrate species. Based on previous work embracing *Chx10* gene expression patterns and the analysis of the mutant mouse *Chx10*$^{or\text{-}J/or\text{-}J}$, which has a null mutation in *Chx10*, the established roles of Chx10 in eye development include promotion of cellular proliferation in the neuroblastic retina, specification of bipolar interneurons in the differentiating retina, and maintenance of bipolar cells in the mature retina. In the first section of this thesis, I have explored the role of the human orthologue, CHX10, in the development of the eye, by examining gene expression patterns during embryonic human development.

In a comparative study between the *Chx10*$^{or\text{-}J/or\text{-}J}$ and wild-type mouse, I have investigated the impact that the absence of Chx10 has on the expression of other genes that are required for normal eye development. Notably, the expression of the photoreceptor-specific transcription factor gene *Crx* is significantly delayed, which may lead to the observed photoreceptor phenotype in *Chx10*$^{or\text{-}J/or\text{-}J}$. Chx10 is not expressed in photoreceptors, so, using a primary cell culture of *Chx10*$^{or\text{-}J/or\text{-}J}$ retinal neuroblasts, I investigated possible signalling

mechanisms by which interactions between Chx10 and Crx could be fulfilled, and have demonstrated that retinoic acid may be capable *in vitro* of inducing expression of photoreceptor-specific genes in the absence of Chx10.

In the final part of the thesis, I have identified, cloned and characterised a novel *Chx10*-like human cDNA, found as a fragment of an expressed sequence tag (EST) on Human Genome Project databases. Data presented here demonstrates that this putative novel gene is retinal specific, expressed in the adult retina, and maps to human Chromosome 20.

ACKNOWLEDGEMENTS

The work presented in this thesis was funded by the charity Fight for Sight.

I would like to thank Shomi Bhattacharya (Institute of Ophthalmology, UCL, London), in whose lab I conducted the first year of this research, and Patrizia Feretti and Andy Copp, (Developmental Biology and Neural Development Units, respectively, Institute of Child Health and Great Ormond St. Hospital for Sick Children, UCL, London) for hosting the remaining years. Rod McInnes (Hospital for Sick Children, Toronto, Canada) kindly provided cDNA clones and collaboration. Ray Lund (Institute of Ophthalmology, UCL, London), Cheryl Gregory-Evans (Imperial College, London) and David Latchman (Institute of Child Health) generously provided other essential materials.

I thank all of my family and friends who have unconditionally supported me during this research. In particular, Stephanie Halford, Alison Hardcastle, Iain McKinnell, Sarah Reid, Paul O'Neill, John Chilton and Dianne Vaughan were bastions of sanity in the lab, and in the real world, Trishy, Dad, Nanda, Ben, Jake, Nat, Clemmie, Will and Nicola have always provided support, hilarity and alcohol.

And principally, I would like to thank my supervisors, Jane Sowden (Institute of Child Health) and Hazel Smith (Department of Biology, UCL, London). Without Jane's thoughtful and rigorous input, and splendid friendship, none of what follows would have been even vaguely possible or fun.

DECLARATION

I declare that this thesis is my own composition and that the studies presented here are the results of my own work.

This work has not been, and is not concurrently being, submitted for any other degree or professional qualification.

CONTENTS

CHAPTER 1 – INTRODUCTION

1 Ferda-Percin E., Ploder L.A., Yu J.J., Arici K., Horsford D.J., Rutherford A., Bapat B., Cox D.W., Duncan A.M., Kalnins V.I., Kocak-Altintas A., Sowden J.C., Traboulsi E., Sarfarazi M. and McInnes R.R. **Human microphthalmia associated with mutations in the retinal homeobox gene *CHX10*.** *Nat. Genet.* **25**, 397–401 (2000).

2 Grayson C., Reid S.N., Ellis J.A., Rutherford A., Sowden J.C., Yates J.R., Farber D.B and Trump D. **Retinoschisin, the X-linked retinoschisis protein, is a secreted photoreceptor protein, and is expressed and released by Weri-Rb1 cells.** *Hum.Mol.Genet.* **22**, 1873–1879 (2000).

3 Bibb L.C., Holt J.K.L., Tarttelin E.E., Hodges M.D., Gregory-Evans K., Rutherford A., Lucas R.J., Sowden J.C. and Gregory-Evans C.Y. **Temporal and spatial expression patterns of the *CRX* transcription factor and its downstream targets. Critical differences during human and mouse eye development.** *Hum.Mol.Genet.* **10**, 1571–1579 (2001).

FIGURES CONTENTS

CHAPTER 1 – INTRODUCTION

CHAPTER 3 – ANALYSIS OF THE DEVELOPMENT OF THE HUMAN RETINA

CHAPTER 4 – ANALYSIS OF THE DEVELOPMENT OF THE RETINA OF THE *OCULAR RETARDATION* MOUSE

CHAPTER 5 – INVESTIGATIONS INTO INTERACTIONS BETWEEN CHX10 AND CRX DURING RETINAL DEVELOPMENT

CHAPTER 6 – IDENTIFICATION AND CHARACTERISATION OF A NOVEL *CHX10*-LIKE CDNA

ABBREVIATIONS USED IN THIS THESIS

ABC	avidin–biotin peroxidase complex
AP	alkaline phosphatase
bHLH	basic helix–loop–helix transcription factor
BLAST	basic local alignment search tool
bp	base pair
BSA	bovine serum albumin
CNS	central nervous system
DAB	diaminobenzidine tetrahydrochloride
DMEM	Dulbecco's modified eagle medium
DIG	digoxygenin
DNA	deoxyribonucleic acid
DNase I	deoxyribonuclease I
dNTP	deoxy nucleotide triphosphate
dpc	days post-coitum (mouse)
DPX	dextropropoxyphene
E	embryonic day (mouse)
EDTA	ethylene-diamine tetra-acetic acid
EST	expressed sequence tag
FCS	foetal calf serum
gcl	ganglion cell layer
HCl	hydrochloric acid
HRP	horseradish peroxidase
ilm	inner limiting membrane
inl	inner nuclear layer
ipl	inner plexiform layer
is	inner segment
Kb	kilobase
KCl	potassium chloride
kDa	kilodalton
L Agar	Lennox agar
L Broth	Lennox broth
$MgCl_2$	magnesium chloride

mRNA	messenger RNA
nb	neuroblastic layer
nfl	nerve fibre layer
NaCl	sodium chloride
$NaHCO_3$	sodium hydrogen carbonate
NaOH	sodium hydroxide
OD	optical density
onh	optic nerve head
onl	outer nuclear layer
opl	outer plexiform layer
os	outer segment
PAGE	polyacrylamide gel electrophoresis
PBS	phosphate buffered saline
PCNA	proliferating cell nuclear antigen
PCR	polymerase chain reaction
PFA	paraformaldehyde
Pgm1	phosphogluco-mutase 1
PKC	protein kinase C
RA	retinoic acid
RNA	ribonucleic acid
RNase A	ribonuclease A
RPE	retinal pigmented epithelium
rpm	revolutions per minute
RT-PCR	reverse transcriptase polymerase chain reaction
SDS	sodium dodecyl sulphate
S phase	synthesis phase (of the cell cycle)
SSC	sodium chloride/sodium citrate buffer
TAE	Tris acetate EDTA electrophoresis buffer
TBE	Tris borate EDTA electrophoresis buffer
TBS	Tris-buffered saline
TBST	Tris-buffered saline with Tween-20
TE	Tris-EDTA
wpc	weeks post-conception (human)

CHAPTER 1

INTRODUCTION

CHAPTER 1

INTRODUCTION

1.1 The eye, and its origins

The eye is a highly complex, multi-tissue sensory organ that transmits visual information from the world to the brain for processing.

In this introductory chapter, I aim to describe the structure, function and development of the eye, with specific reference to the genes that influence the development of the retina in the context of the data and discussions presented later in this thesis.

1.1.1 Evolution of the eye

The evolution of the eye has historically been a controversial issue for many evolutionary biologists, and was originally argued by the 19th century theologian William Paley as being such a complex and perfect organ, that it confounded theories of Darwinian evolution (Dawkins 1986, in *The Blind Watchmaker*). But, as described by Dawkins, selection of advantageous characteristics of photoreceptive biology is a stepwise process, and quite adequately explains the complexity of the human eye. Indeed, examination of many living animals reveals that not all photoreceptive organs are as complicated as vertebrate or compound eyes, and these provide answers to the mechanisms of the evolution of a complex organ. For example, the protozoan

Euglena has a patch of cells, called an eyespot, that allows behavioural changes in response to light, and this may be one of the simplest photoreceptive organs in an animal (Gualtieri *et al.* 1992).

Salvini-Plawen and Mayr (1961) suggested that photoreceptive organs have evolved independently at least 40 times, the first being multi-cellular organisms dating to ~530 million years ago. This postulation was based on morphological criteria, for example, the profound and obvious differences between the compound eye of insects, and the lens cells of higher vertebrates. However, molecular similarities between all photoreceptive organs have recently been described, indicating the conservation of genetic pathways that determine the development of visual systems (Gehring 1996). Probably the best example of this involved the identification of *Pax6* (discussed in more detail 1.6.8), a gene with orthologous versions in species as diverse as vertebrates, *Drosophila* and jellyfish (Sun *et al.* 1997). In the naturally occurring mouse mutant with a null mutation in *Pax6*, called *Small eye*, heterozygotes have severe microphthalmia (small eyes), and homozygotes fail to develop large areas of the front of the head (discussed below), including the eyes (Quinn *et al.* 1996). In *Drosophila*, flies with a mutation in their orthologous gene, called *eyeless*, are characterised by an absence of eyes (Gehring 1996). These data and others indicate that these two genes, *Pax6* and *eyeless*, both sit high up in a hierarchy that specifies the development of eyes, regardless of the obvious and substantial differences between the types of eye involved. This data was

compounded by the genetic rescue of the *eyeless* mutant fly by the introduction of a transgenic murine *Pax6* gene (Gehring 1996).

1.2 The lens

The vertebrate eye is a highly complex organ, which has evolved to process visual stimuli into images within the brain. Light is initially focused by the cornea, and then by the lens after it has passed through the anterior chamber and iris. The lens is a biconvex tissue consisting of fusiform fibre cells, encapsulated in an elastic capsule of epithelial cells. The lens grows throughout life by mitosis of the outer lens. Central lens cells lose their organelles. Light passes through the lens and into the vitreous humour, a gel that comprises 98% water as well as collagenous fibrils, which on the outer surfaces of the humour attach it to the surrounding tissue, including the lens capsule and retina (Bron *et al.* in *Wolff's Anatomy of the Eye and Orbit*, 8th Edition, 1997).

1.3 Morphology, the retina, RPE and cell types

The neural retina is a highly organised laminated three-layered tissue (see Figure 1.1), whose function is the capturing of photons and the subsequent processing of phototransduction to the brain. The outermost layer (i.e. furthest

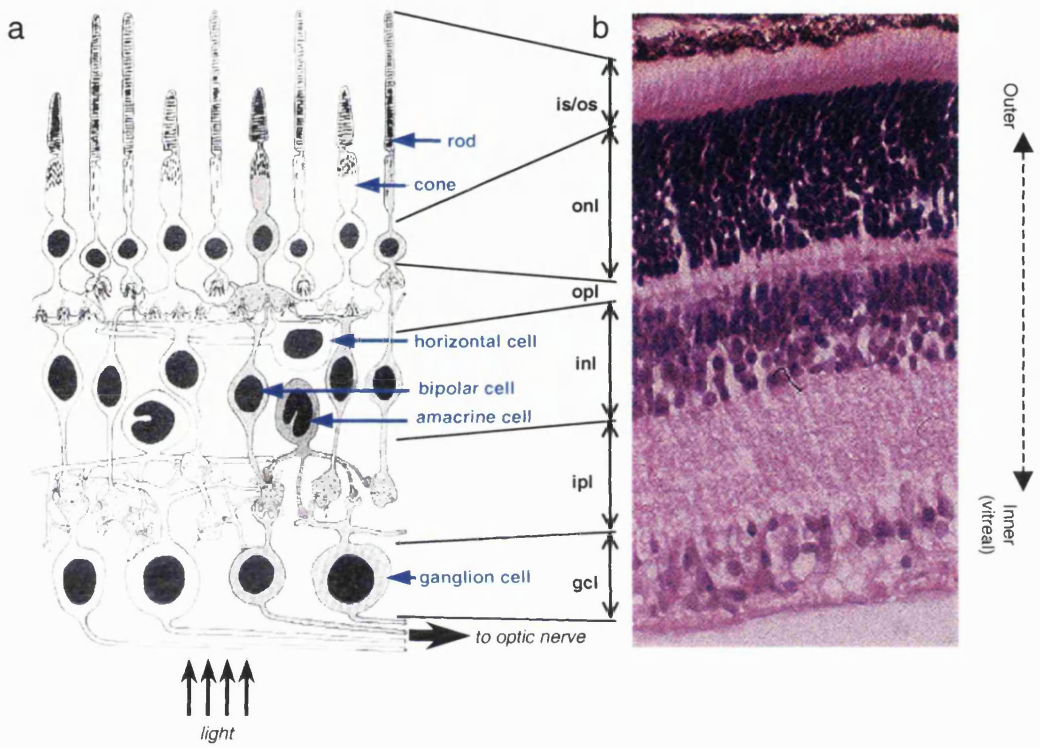

Figure 1.1. Histology of the adult retina. The mature murine retina is divided into three cellular strata, separated by two acellular plexiform layers, in which synaptic connections are made. (a) shows a cartoon schematic of the retina, and (b) a histological section stained with haematoxylin and eosin. The inner (is) and outer (os) segments of the photoreceptors are uppermost, connected via cilia to the photoreceptor cell bodies held within the outer nuclear layer (onl). The inner nuclear layer comprises three neuronal cells, bipolar, amacrine and horizontal cells. These in turn synapse in the inner plexiform layer (ipl) with cells in the ganglion cell layer (gcl). Axons from ganglion cells project via the optic nerve to the brain.

from the lens) of the neural retina consists of the photoreceptors, cells in which the process of phototransduction begins. The other cellular layers are the inner nuclear layer and the ganglion cell layer, which are discussed in 1.3.3 and 1.3.4.

1.3.1 Structure and function of photoreceptors and retinal pigmented epithelium

Photoreceptors are highly specialised light sensitive neuronal cells, capable of detecting individual photons (Hecht *et al.* 1942), comprising several cellular compartments (see Figure 1.2). These include the outer segment (os), which contains photoreceptor lamellae or discs, which resemble flattened membranous sacs, and these are the initial sites of the process of phototransduction. In broad terms, there are two types of photoreceptor, rods and cones. However, there are many subsets, including blue green and red cones. The distributions and relative proportions of the different subtypes are discussed below. Photoreceptors are embedded, via desmosomes and other anchoring junctions, in the non-neuronal layer of the retina, the retinal pigmented epithelium (RPE) – a highly pigmented monolayer of epithelial cells that prevent photons from escaping the eye, and also provides nurturing for the embedded photoreceptors. On the apical, photoreceptor side of the RPE, there are processes that extend into the photoreceptor layer. The matrix between the RPE and photoreceptors is crucial for the maintenance of disc regeneration, which is functional in the maintenance of circadian rhythms, as this regeneration occurs in a roughly 24-hr period (Young 1976, Ostroy 2001).

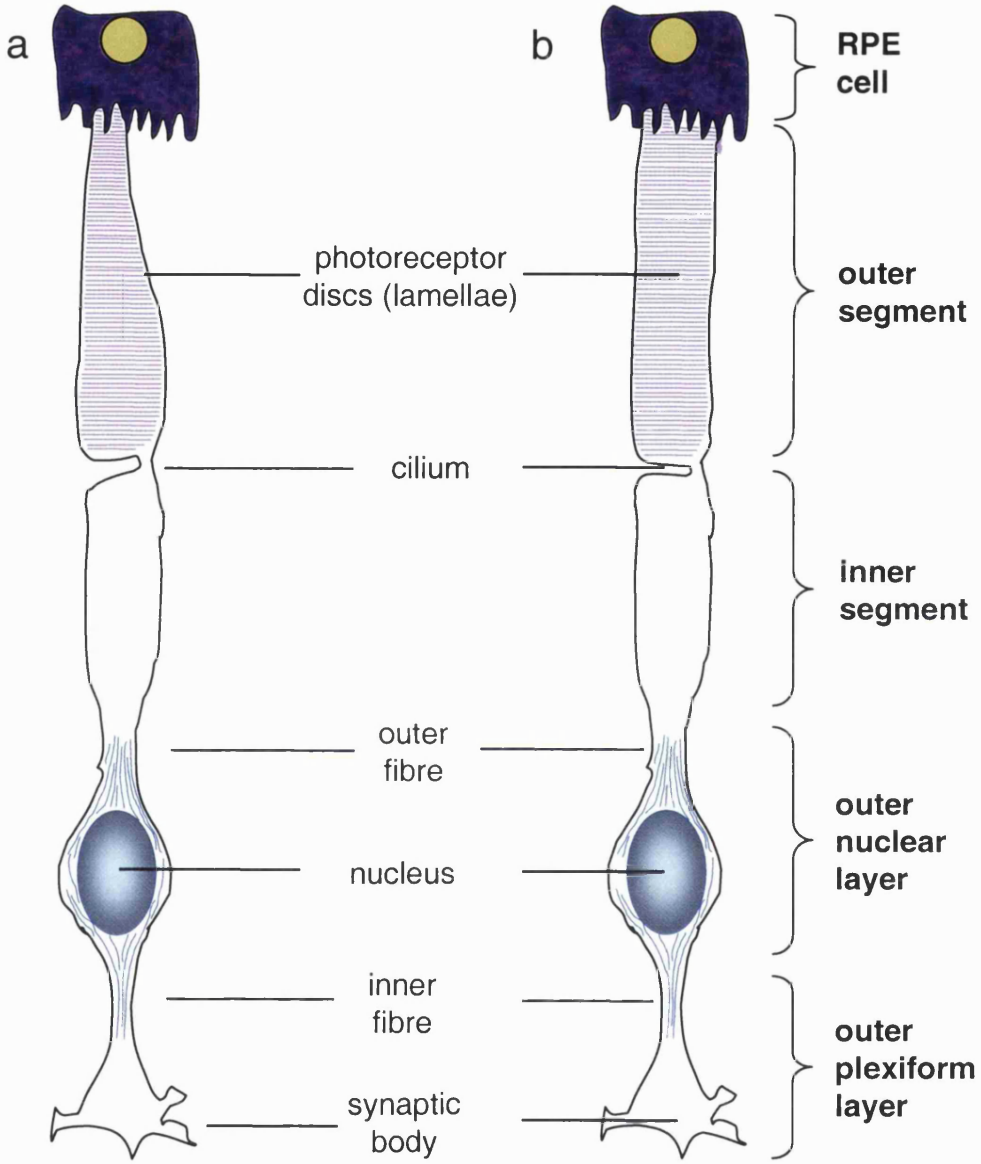

Figure 1.2 Diagram of generic cone (a) and rod (b) photoreceptor, showing how the components of the cell correspond to the layers of the retina. The outer segments, containing the lamellae, are embedded in the retinal pigmented epithelium (RPE), and connect to the inner segment via thin cilia. The nucleus is contained within the outer nuclear layer. Synaptic connections to interneurons in the inner nuclear layer are made in the outer plexiform layer.

The outer segment is connected by a cilium to the inner segment, which contains the components of the subcellular organelles, including the golgi apparatus, and several hundred mitochondria. This connects to the nucleus containing cell body, which makes up the outer nuclear layer. Axonal projections from the innermost tip of the photoreceptor make synaptic connections to other retinal cells within the outer plexiform layer.

1.3.2 A simplified model of phototransduction

The membranes of the discs contained in the outer segments of photoreceptors harbour seven-pass membrane bound molecules, rhodopsin (Figure 1.2). The structure of the helical portions of this molecule encloses the chromophore retinal, which is a light sensitive molecule capable of several stereoisomeric forms. The absorption of a photon by retinal in its dark state causes the conversion of rhodopsin into its activated state and the subsequent activation of the retina-specific G protein transducin, by the conversion of GDP to GTP. This activated form of transducin in turn activates the multi-sub-unit enzyme cGMP phosphodiesterase (PDE), which catalyses the molecule cGMP to 5'GMP. The disruption of the cationic flow through cGMP-gated Na^+ and K^+ channels caused by photonic stimulation results in the alteration of the membrane potential of these cells. The resultant hyperpolarisation of the photoreceptor initiates a decrease in the release of the molecule glutamate by vesicular exocytosis. The glutamate-signalling pathway allows the transduction of visual

information from photoreceptors to other neurons (reviewed in Oyster, The Human Eye, 1999).

1.3.3 Cells within the inner nuclear layer

The connections that photoreceptor cells make to other neurons are complicated. Horizontal cells of the inner nuclear layer, of which there are at least two distinct types, have a role in integrating input signals from multiple photoreceptors (Kolb 1997). Bipolar cells, of which there are a number of subtypes, are the prime system by which photoreceptors convey signals to the ganglion cells in the ganglion cell layer (Grünert and Martin 1991, Wassle *et al.* 1991). Of the subtypes that have been identified, there are cone on- and off-bipolar cells which have opposing sensitivities to glutamate signalling, midget bipolar cells, which process signals from red and green cones, blue cone bipolar cells, rod bipolar cells, which do not connect directly with ganglion cells, instead channelling through amacrine cells, and diffuse bipolar cells, which are non-specific. Bipolar cells are located on the outer aspect of the inner nuclear layer, in a similar position to horizontal cells. Amacrine cells are located on the opposite side of this layer, but also in the ganglion cell layer, at a frequency of ~3% in humans. Bipolar cell terminals are located in the inner nuclear layer at many different functional sub-levels, and signalling to ganglion cells is predominantly controlled by the glutamate, glycine and GABA signalling pathways (reviewed in Oyster, The Human Eye, 1999).

1.3.4 The ganglion cell layer

There are at least 20 types of ganglion cell described so far, but the majority can be classed as either midget or parasol ganglion cells. These are found throughout the ganglion cell layer of the retina, and project visual signals through to the primary visual-processing centres in the brain, such as the superior colliculus.

Müller glial cells make up the seventh cell type in the retina, but these are not directly involved in phototransduction and are not neurons, but rather have a structural supportive role in the retina. They are radial cell types, which span the entire depth of the retina, from the inner segments to the vitreous. The vitreal end-feet of these glia fasiculate the axons from ganglion cells to form the nerve fibre layer.

1.3.5 Spatial distribution of cells types across the human retina

The retina is not a homogeneous structure when viewed in the central to peripheral axes, although these variations are often species-specific. The fovea, although not the geometrical centre of the retina, contains the highest density of photoreceptors. It is located, as a depression in the retina, about 4mm temporally from the centre of the optic nerve head (Bron *et al.* in *Wolff's Anatomy of the Eye and Orbit*, 8th Edition, 1997). The cells in the centre of the fovea are almost all cones, with a complete absence of rods, and thus their bipolar cells have extended processes to account for that concentration. The density of cones across the rest of the retina is low. In the human, there are

approximately 20 times more rods than cones. The patterns by which cones tile the retina are poorly understood, but are neither regular nor random. Although rods and cones were initially distinguished from each other by morphological criteria, these two cell types have distinct roles in vision: rods are primarily adapted to register scotopic spectral sensitivity, i.e. the phototransduction of dark-adaptation; photopic spectral sensitivity, i.e. colour vision, is controlled by cones, the precise absorbance of whose photopigments determines perception of different colours.

Ganglion cell density steadily declines from the fovea to the periphery of the retina.

1.4 Embryological origins of the eye

1.4.1 Morphological model of eye development (see Figure 1.3)

Development of the major sensory organs of the head in vertebrates involves the formation of epidermal thickenings, the cranial ectodermal placodes, and their interactions with specific regions of the neural tube (Gilbert, in *Developmental Biology,* 4th Edition 1994). In the mouse, the optic vesicles evaginate as bilaterally symmetrical pouches from the forebrain at about embryonic day eight (E8). By E9, these evaginations have made contact with the overlying surface ectoderm, and this contact in turn causes this head ectoderm to thicken into the lens placode. Upon contact with the lens placode

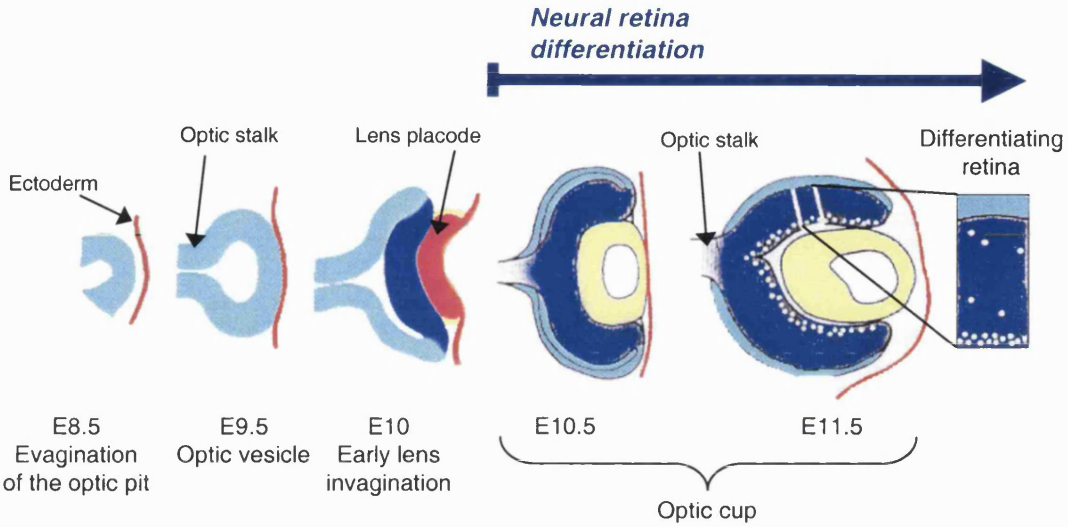

Figure 1.3. Early development of the murine eye. At around E8 two symmetrical evaginations from the forebrain emerge as the optic pits. As the optic vesicle forms, the evagination thins into the optic stalk. Upon contact with the surface epithelium (shown here in red), this tissue thickens to form the lens placode, which subsequently invaginates as the lens vesicle (shown here in yellow). The inner layer of the optic vesicle forms a pool of progenitor cells from which the neural retina develops (shown here in dark blue). The outer layer (shown here in light blue) differentiates into the retinal pigmented epithelium. By E10.5, the neural retina in the optic cup has begun to differentiate, with cells in migrating to their correct position during the rest of development, up until P12.

the optic vesicle invaginates back in on itself, forming the optic cup. This structure at E10 defines three of the major components of the mature eye: the lens placode has been invaginated into the optic vesicle as the presumptive lens; the neuroepithelium of the optic vesicle has folded back on itself causing the formation of a bilayered optic cup. These two layers form pools of (at this stage morphologically indistinguishable) cells, which will go on to form the (non-neuronal) RPE and neural retina respectively. Proliferation of the neural retina and RPE continues in the mouse until postnatal day 11 (P11). During this period the eye increases in size considerably, and the neural retina differentiates into the highly organised structure described above.

1.5 Comparative human eye development

The human retina is largely similar to that of the mouse; it is made up of the same sets of cells, arranged in the same three-layered strata. However, there are significant differences in cell distribution and development.

1.5.1 Developmental timing

Although the development of the human and mouse eyes follows the same overall pattern, the relative timings of development are very different, and do not correlate in a linear fashion (Table 1.1). These differences probably reflect the intrinsic differences in cellular distributions in the two retinae. The

development of the human retina is relatively shorter compared with that of the mouse, given the total length of gestation. Precise timings of eye and retinal development have been made experimentally in the mouse (Young 1985). Of course, equivalent timings in humans are not known with the same testable accuracy.

Mitosis continues in the murine retina until postnatal day 12 (Young 1985), and mice are born sightless with their eyelids not opening until P12–14 (Kaufman, in *Atlas of Mouse Development*, 1995). The human retina is largely postmitotic by the 15th week of gestation (Hollenberg and Spira 1972, 1973), and babies are born sighted.

The primitive components of the adult eye have formed by the sixth week of gestation. These include the lens vesicle, which has invaginated from the surface epithelium, and the bilayered optic vesicle, whose inner layer represent the multipotential progenitor pool of cells from which the retina will develop, and the outer layer which will develop as the RPE. The presence of these components is roughly equivalent to that of an E9 mouse eye. Within a few days, the neural retina can be divided into two layers, separated by the transient fibre layer of Chievitz. The morphologies of the cells in these two layers are distinct, with the outer layer containing more elongated cells, and the inner layer containing more spherical cells. This may reflect the presence of differentiating ganglion cells in the inner layer, and mitotic cells in the outer. By the 8th week of gestation, the nerve fibre layer is clearly visible, indicating that ganglion cells have projected their axons towards the optic nerve head. The

number of axons does not accurately represent the final number of ganglion cells: at 10–12 weeks about 1.9 million axons are present in the human optic nerve. This number rapidly increases to 3.7 million by the 16th week, reflecting the rapid increase in the ganglion cell pool. However, by the 33rd week of gestation, there are only 1.1 million axons in the optic nerve. Up to 70% are eliminated in the foetus, relating to the number of ganglion cells that are undergoing apoptosis during this period (Bron *et al.* in *Wolff's Anatomy of the Eye and Orbit*, 8th Edition, 1997).

By the 10th week, cells displaying cone-like morphology can be detected in the outermost layer of the neuroblastic retina. But it is not until the 5th month that outer segment formation can be detected. In the mouse, this occurs from P3 (Sanyal *et al.* 1980).

By the 22nd week, the fovea is formed in the central portion of the retina, as an elliptical disc of about 1.5mm diameter. At this stage, cells are present in all layers of the foveal retina, and only by the fourth postnatal year has the fovea taken its mature morphology comprising only cones.

Table 1.1 Comparative human and mouse retinal development

Developmental event	Human *(weeks post coitus)*	Mouse *(embryonic/postnatal day)*
Evagination of optic vesicle		E8
Contact with surface epithelium		E9
Formation of bilayered optic cup	5 wpc	E10
Formation of neural retinal progenitor cells	6 wpc	E10
Formation of bilayered neural retina	7 wpc (layer of Chievitz)	
Early born cells undergo terminal mitosis (formation of nerve fibre layer)	8 wpc	E10.5
Inner plexiform layer formed	9 wpc	E14 – 15
Tri-layered retina visible	12 wpc	E17–18
		P0: birth
Onset of outer segment formation	20	P3
Cessation of retinal mitosis	15	P12
	~ 40 wpc: birth	

Human data adapted from Hollenberg and Spira 1973, mouse data from Kaufmann (in The Atlas of Mouse Development. 1995), and Chapter 5.

Table 1.2 Glossary of terms for cellular development

Concept	Definition
Birth	Point of terminal mitosis, often indicating commitment or a reduction in potential
Cell fate	The cell type that an immature cell will eventually become
Commitment	State where a cell is irreversibly bound to become a specific cell type
Competence	The ability of a cell to adopt multiple fates, via response to intrinsic and extrinsic cues (see below)
Differentiation	The process during which time a maturing cell displays specific characteristics
Extrinsic factors	Secreted factors, e.g. signalling molecules
Intrinsic factors	Cellular or nuclear factors, e.g. transcription factors
Potential	The ability of a cell to adopt cell fates. Retinal progenitors are accepted to be multipotential
Progenitor	A cell with limited mitotic capability, which is capable of producing a range of mature cell types

Adapted from Livesey and Cepko, 2001.

1.6 Genes involved in eye development

The migration and differentiation of proliferating cells determines the correct development of the eye and retina. Many of the genes involved in these processes are known, as are some of the conceptual ideas that shape development and organisation of the highly complicated retina. Definitions of some important concepts are outlined in Table 1.2.

1.6.1 Order of cell birthing (Figure 1.4)

The order in which retinal cells are born, i.e. become postmitotic and migrate from the proliferating progenitor pool to their final destination is well documented, and appears to be heavily conserved across all vertebrate species. Cells leave the multipotential progenitor pool at specific and overlapping times (Young 1985). These and other data (Holt *et al.* 1988, Turner and Cepko, 1987, Turner *et al.* 1990) indicate that specification of retinal cell types is not lineage dependent, i.e. the fate of a daughter cell is not directly related to its mother cell. However, other evidence suggests that restricted potentiality of retinal progenitors exists as the retina develops, and that artificially altering cell fates *in vitro* does not necessarily permit the reassignment of a cell to any other retinal fate (Cepko *et al.* 1996) (this is discussed in further detail in 1.6.2). The non-linearity of retinal fate is further indicated by the overlapping periods of time that spawn the various different types (see Figure 1.4). The important study by Young (1985) demonstrated by

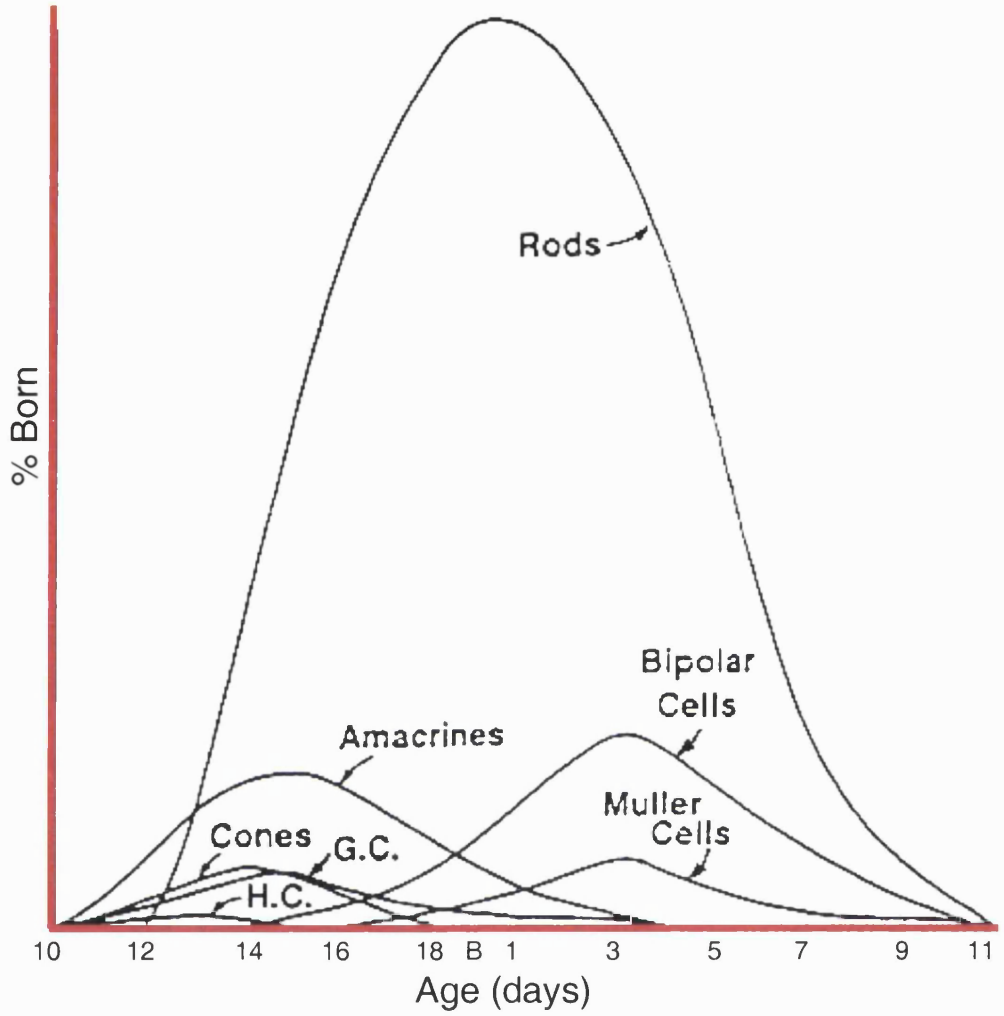

Figure 1.4. Order of cell birthing in the developing murine retina (adapted from Cepko *et al* 1996). During the terminal mitosis by a cell, ^{3}H-thymidine is taken up and subsequently not diluted (as happens with cells that are still dividing). The mice were sacrificed when their retinae were mature, and processed for incorporated ^{3}H-thymidine. This experiment demonstrated the specific cells that were undergoing terminal mitoses at each specific time, with ganglion cells being the first cells to undergo terminal mitosis, starting at ~E10.5, closely followed by horizontal and amacrine cells and cones. Cells that differentiate late include rods, which make up the majority of cells in the murine retina, bipolar cells and Müller glia. The peak of the genesis of these cells occurs post-natally in the mouse.

^{3}H-thymidine incorporation the order in which cells of the retina undergo their terminal mitosis, and therefore are accepted to gain a specific cell fate. During the course of retinal development in the mouse, individual mice were injected with a dose of ^{3}H-thymidine on specific days. During the terminal mitosis by a cell, ^{3}H-thymidine is taken up and subsequently not diluted (as happens with cells that are still dividing). The mice were sacrificed when their retinae were mature, and processed for incorporated ^{3}H-thymidine. This experiment demonstrated the specific cells that were undergoing terminal mitoses at each specific time.

Ganglion cells are the first cells to undergo terminal mitosis, starting at ~E10.5, closely followed by horizontal and amacrine cells and cones. Cells that differentiate late include rods, which make up the majority of cells in the murine retina, bipolar cells and Müller glia. The peak of the genesis of these cells occurs post-natally in the mouse.

1.6.2 The competence model of retinal development (Figure 1.5)

The concept of competence of retinal neuroblasts (see Table 1.2) states that progenitor cells are capable of responding to molecular cues in a limited manner, and are thus capable of differentiating into in a subset of retinal cell types (Livesey and Cepko, 2001). Evidence suggests that competency is intrinsically determined, but for cells within a given competency, both intrinsic and extrinsic signals determine the cellular outcome.

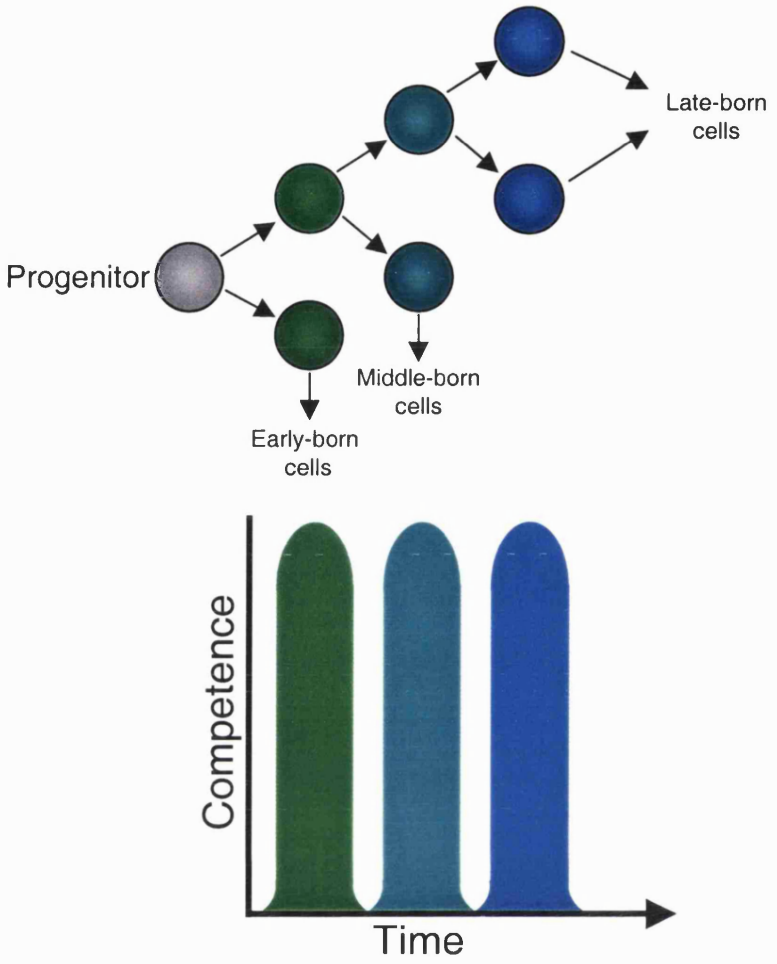

Figure 1.5. Competency model of retinal development. Multipotential progenitor cells pass through different stages of competence during development, indicated by the different colours. During each of these stages they are capable of generating a subset of retinal cells, regardless of the lineage of that cell. The first division of the progenitor cell produces two cells, one that is capable of differentiating into an early-born cell (such as a ganglion cell), and one that progresses to the next competency, and so on. The number of competencies is unknown, but here has been divided for convenience into early, middle and late. Adapted from Livesey and Cepko,(2001).

Central to the competency model of retinal development is the notion that progenitor cells are competent to generate different sets of retinal cells during the course of retinal development. This is in contrast to previous models that state that cells become progressively restricted in their potential, reflecting that late-stage progenitors give rise primarily to rods. Although a straightforward lineage-dependent relationship does not exist in the retina between progenitor cells and their progeny, some studies have shown that cellular determination is largely lineage independent (Turner, *et al.* 1990, Turner and Cepko, 1987, Holt *et al.* 1988).

1.6.3 Retinal development

The increasing limitations of a progenitor cell's potency as it progresses through development are determined by expression, or repression, of specific proteins, as regulated by the combination of intrinsic factors (cell autonomous factors), and extrinsic cues derived from long- or short-distance signalling from other cells. These events combine to reduce the potency of a cell until it is committed to a specific type, at which stage a differentiation pathway can be initiated and completed. As described in section 1.6, the retina contains many different cell types, which can be characterised by specific gene expression patterns, and are born and differentiate in very tightly regulated spatio-temporal patterns.

Several transcription factor genes have been identified that are involved in this process (Hanson and Van Heyningen 1995, Freund *et al.* 1996), and some significant ones for the intents of this thesis are discussed below, and

summarised in Table 1.3. Amongst the approaches used to identify key genes have been the analysis of a number of animal models. These include naturally occurring mouse mutations, such as *Small-eye* (discussed in 1.6.4), gene targeting involving retinal-specific genes, such as for *Crx*, (discussed in 1.6.11 and Chapter 5). In addition, the identification of mammalian homologues of genes involved in invertebrate eye development has provided a source of eye development genes, such as the Six family (Kawakami *et al.* 1996, Lopez-Rios *et al.* 1999).

Table 1.3 Transcription factors involved in retinal development

Protein	Species	Expression	Function	References
Chx10	M, Ch, H	Retinal neuroblasts, bipolar cells	Promotes proliferation and bipolar cell fate	Liu *et al.* (1994), Burmeister *et al.* (1996), Belecky-Adams *et al.* (1998)
Mash-1	M, X	Differentiating cells	Promotes differentiation of late-born cells	Guillemot and Joyner (1993)
MITF	M	RPE	RPE survival	Hodgkinson *et al.* (1998)
NeuroD	M, X	Neuronal differentiation	Neuron specification	Lee *et al.* (1995)
Otx2	M	RPE	Unknown	Bovolenta *et al.* (1997)
Pax6	M, H, X, Z, C	Neural retina, amacrine cells, GCL	Early optic field determination	Macdonald and Wilson, (1997)
Rax/rx	M, X	Neural retina	Early optic field determination, Müller glia specification	Furukawa *et al.* (1997)
Brn3b	M, C	GCL	Ganglion cell differentiation	Gan *et al.* (1999) Liu *et al.* (2000)
Hes1	M	Retinal progenitors	Prevents premature differentiation	Tomita *et al.* (1996)
Six-2, -3, -5	M	GCL, INL,	Unknown	Kawakami *et al.* (1996)
Crx	M, H	Photoreceptors	Promote photoreceptor differentiation	Livesey *et al.* (2000)

Abbreviations: C, chicken; GCL, ganglion cell layer; H, human; INL, inner nuclear layer; M, mouse; RPE, retinal pigmented epithelium; X, *Xenopus*; Z, zebrafish.

Adapted from Jean *et al.* (1998)

1.6.4 Specification of retinal fate

Expression of the homeo- and *paired*-domain containing transcription factor Pax6 is widespread through the developing brain (Grindley *et al.* 1995). In terms of eye development, its expression pattern within the developing telencephalon defines the regions that evaginate to form the optic vesicles, and for this reason is thought to be one of several genes at the top of the genetic hierarchy that regulates vertebrate eye development. Pax6 expression continues throughout eye development, and becomes restricted to particular cell types later on (discussed in 1.6.8) (Hitchcock *et al.* 1996). The expression pattern of Pax6 is largely indistinguishable in both humans and mice (Nishina *et al.* 1999). Dosage of *Pax6* is critical for ocular organogenesis. The *Small eye* mouse is caused by mutations in the *Pax6* gene; heterozygous mice develop smaller eyes by mid-gestation (Hill *et al.* 1991), and humans suffer from eye malformations in the disease aniridia (discussed below), both as a result of haplo-insufficiency. Homozygous mice largely fail to develop forebrains and thus optic cups, and are neonatally fatal owing to CNS defects (Grindley *et al.* 1997). However, as the defects that occur as a result of mutations in *Pax6* occur predominantly before retinal neurogenesis, it renders further analysis of Pax6 function in later development difficult without the generation of conditional knockout mice. Recently, a Cre-mediated conditional Pax6 knockout mouse was generated (Marquardt *et al.* 2001), and is discussed in detail in the Chapter 7, Discussion.

Several other genes appear to be involved as well as *Pax6* in the specification of the different cell types of the eye.

A number of proteins (particularly transcription factors) have been identified that are expressed in retinal progenitor cells. However the precise roles that these molecules play in specifying a retinal fate is poorly understood. Mash1, Math3 and 5, and NeuroD are all expressed in retinal progenitor cells, but are not detectable before the onset of ganglion cell differentiation (Brown *et al.* 1998). Targeted deletion of *Mash1* does not, however, result in a retinal phenotype. Hes1 appears to be essential for retinal development, as targeted deletion of the gene encoding it results in reduced optic cup size by E10.5. *Math5* and *Hes1* are targets of Pax6 (whether this interaction is direct or not is unknown) (Brown *et al.* 1998), again indicating Pax6's role high up in the ocular organogenesis hierarchy.

Perron *et al.* (1998) use the *Xenopus* ciliary marginal zone (CMZ) as a model for the genes expressed during the course of retinal development. Unlike in higher vertebrates, the retina of the frog continues to grow throughout its life, in a periphero-central gradient, i.e. cells in most peripheral retina are most multipotent, expressing Pax6, Rx1 and Six3. Similarly, in the mouse, retinal progenitor cells express Pax6, Rx, Six3 and Six6 (Jean *et al.* 1999, Marquardt *et al.* 2001). The subsequent steps in *Xenopus* towards specific retinal cell fate include the onset of neurogenic gene expression (Notch, Delta), before the onset of expression of specific cell markers, such as Chx10 [bipolar cells, (Liu *et al.* 1994)], *Brn3b* [ganglion cells (Gan *et al.* 1996)], and so on. The use of

Xenopus as a model for retinal development is profound, as the CMZ provides a "snapshot" of gene expression for the various stages of potential and commitment (Perron *et al.* 1998).

1.6.5 Genetic specification of the neural retina and RPE

The RPE and neural retina are both derived from neuroepithelial cells, and both are initially bipotential. Genes involved in the distinction between neural and non-neural retina are known to include the leucine-zipper transcription factor mitf (Nguyen and Arnheiter, 2000). Expression of *mitf* is maintained in the RPE, but downregulated in response to expression of the Chx10 transcription factor. Furthermore, *mitf* mutant mice continue to express neuroretinal markers in RPE progenitor cells. Conversely, removal of the surface ectoderm results in a maintenance of *mitf* expression in the neuroretinal progenitor pool, loss of Chx10 expression, and subsequent conversion of this pool into a pigmented monolayer. These data indicate that the maintained expression of mitf, and repression of Chx10 (and *vice versa*) is critical for the formation of the RPE and neural retina, respectively. Interestingly, mutations in the *mitf* gene cause microphthalmia in mice, although the onset of expression in mice does not occur until around E13.5 (Freund *et al.* 1996) (see Table 1.4).

1.6.6 Cell-specifying genes

Recently, several genes have been identified that appear to be essential for the differentiation of specific cell types in the retina. It seems that the expression profile of specific combinations of genes during precise windows of time can determine the fate of a cell. Many of the genes identified are transcription factors, and thus are capable of regulating downstream targets. This class of protein is particularly interesting in terms of questions of fate-specification, as it is an attractive idea to suggest that the complex process of differentiation, which involves cascades of different genes, has a controlling factor at the top of the hierarchy. Some of the genes that make good candidates for this type of protein are discussed below.

1.6.7 Brn3b

Brn3b (also referred to in different species as Pou4F) is a POU-domain transcription factor that is expressed in the retina in a subset of ganglion cells. It is also expressed in regions of the superior colliculus that are known to be involved in the processing of sensorimotor inputs to control eye movement, and receives afferent fibres from ganglion cells (Xiang 1998). The fact that Brn3b is only expressed in a subset of cells reflects the diversity of ganglion cells that have been identified morphologically. So far, few other genes have been identified that have such potential as ganglion cell differentiation molecules. Targeted deletion of *Brn3b* results a loss of most (70%) of these cells in homozygous mice (Gan *et al.* 1996). Furthermore, ganglion cells in knockout

mice fail to project their axons at the correct time and place (Gan *et al.* 1999). However, it remains one of the earliest genetic markers of ganglion cells development.

1.6.8 Amacrine cells

Belliveau and Cepko (1999) investigated the mechanisms by which an amacrine fate is determined *in vitro.* By co-culturing postnatal rat retinal cells with embryonic retinal cells, they found that inhibition of amacrine cell genesis was derived from postnatal amacrine cells, suggesting that amacrine cell number is controlled by feedback inhibition. However, the molecules involved in this inhibition remain elusive.

1.6.9 Müller glia

Müller glial cells are the only non-neuronal cell-type located within the neural retina. Their function includes providing structural support for the retina, and fasciculation of the ganglionic axons with their end-feet. Furukawa *et al.* (2000) demonstrated by retroviral transduction of retinal progenitor cells in culture that the homeobox gene *rax*, the basic helix-loop-helix gene *Hes1*, and *notch1*, a transmembrane receptor gene were all capable of inducing Müller cell genesis. These genes are all expressed in retinal progenitor cells, indicating that expression of these genes is necessary but not sufficient for Müller glia differentiation. Evidence also suggests that the cyclin-dependent kinase (CDK) and Notch signalling pathways are involved in gliogenesis in the retina and

other parts of the central nervous system (Vetter and Moore, 2001) (see Figure 1.6).

1.6.10 Horizontal cells

In experiments to determine genes involved in cell fate, Alexiades and Cepko (1997) demonstrated that the expression in a subset of retinal progenitor cells of the epitope VC1.1, a marker of horizontal and amacrine cells, coincided with the birthday of horizontal cells. VC1.1-positive cells in cultures of early progenitor cells generated a high percentage of horizontal (and amacrine) cells, at the expense of cones. However, VC1.1-positive cells in late progentior cell cultures (late embryonic and early post-natal) resulted in an increase in amacrine cells and rods, but not horizontal cells. This indicates that VC1.1-positive cells have a temporally regulated and distinct set of biases in the fates of their progeny, and highlights the significance of the cellular milieu that dictates the strict temporal regulation and order for cell birthing in the retina (see Figure 1.6).

1.6.11 Crx

Crx is a *paired*-type homeobox gene, which is photoreceptor specific, and is the earliest known marker for photoreceptor differentiation (Furukawa *et al.* 1997). In humans, mutations in *CRX* result in a spectrum of retinal degenerations including cone-rod dystrophy and Lebers congenital amaurosis (Freund *et al.* 1997, Freund *et al.* 1998, Traboulsi 1998). Crx is first detected in the murine

retina at E12.5, roughly the onset of cone differentiation, but earlier than rod generation. Targeted deletion of this gene in mice, however, does not result in the absence of photoreceptors. Rather photoreceptors are present but morphologically abnormal, in that their inner and outer segments are severely truncated or absent. Identification of the putative preferred binding site of Crx in the upstream regions of a number of photoreceptor-specific genes suggests a regulatory role for Crx in the expression of these genes. Indeed, using microarray analysis on the *Crx*$^{-/-}$ knockout mouse, expression of several of these genes was reduced or absent, confirming their (at least partial) regulation by Crx (Livesey *et al.* 2000). These data indicate that Crx, although not required for the genesis of photoreceptors, is certainly necessary for the correct differentiation of photoreceptors, particularly the inner and outer segments.

1.6.12 Chx10

The cell-specifying capabilities of the homeobox gene *Chx10* are discussed in detail in 1.9 and Chapter 5, and are the central theme of this thesis.

1.7 Extrinsic factors involved in retinal fate decisions

The complexities of the factors involved in retinal fate specification are exemplified in experiments in which fate can be altered *in vitro*. The majority of these experiments focus on the fates of photoreceptor cells, in particular on

rods (possibly because these are by far the most abundant cell type in the retinae of most model organisms, but also because these are the primary cells lost in retinal degenerations). Watanabe and Raff (1992) demonstrated that rat retinal embryonic cells cultured in the presence of postnatal retinal cells resulted in a 40-fold increase in the numbers of (opsin-positive) photoreceptors generated, and that the cue from the postnatal cells was a short-range signalling molecule. Levine *et al.* (2000) formalised this into an analysis of fate-altering molecules. Retinoic acid (RA), which is known to regulate many aspects of development (Ross *et al.* 2000), is produced is large quantities in the developing vertebrate retina, although its role is poorly understood (Drager *et al.* 2001). Kelley *et al.* (1994) showed that in concentration-dependent manner, addition of RA to retinal progenitor cells resulted in an increase in rod photoreceptors, mostly at the expense of amacrine cell, which are born *in vivo* at roughly the same time (Young 1985), and that the action of RA was on progenitor cells. These data were corroborated by *in vivo* experimentation on zebrafish, in which RA injection during development caused precocious rod development, this time at the expense of cone maturation (Hyatt *et al.* 1996). Furthermore, targeted deletion in mice of two of the RA receptor genes, RARβ and RARγ, leads to the absence of rhodopsin in areas of the retina (Grondona *et al.* 1996).

Taurine, which is critical for photoreceptor survival (Lombardini *et al.* 1991), has also been shown to promote rod development in the retina (Altshuler *et al.* 1992). Specific blockage of the fibroblast growth factor receptor (FGFR)

using a dominant negative form in *Xenopus* leads to a 50% reduction in photoreceptors and amacrine cells, but a concurrent increase in Müller glia. Conversely, use of a receptor that blocks non-FGF ligand binding to FGFR leads to the opposite effect, with a 50% increase in photoreceptors, and a 67% decrease in Müller glia. These data suggest that photoreceptor and Müller glia generation are finely balanced using a FGFR signalling pathway that is determined by FGF and non-FGF ligands (McFarlane *et al.* 1998).

Inhibition of photoreceptor differentiation has also been demonstrated, for example with transforming growth factor (TGF) α, which was shown to have an inhibitory effect on rod genesis (Lillien and Cepko, 1992), possibly with a mitogenic effect.

The cytokine ciliary neurotrophic factor (CNTF) has a profound effect on retinal development *in vitro*. CNTF has a regulatory role on the regulation of photoreceptors, but confoundingly, this role appears to be opposite in rat and chicks. Ezzedine *et al.* (1997) showed that addition of CNTF to retinal explanted cultures dramatically reduced the numbers of (rhodopsin-positive) rods being formed, and a corresponding increase in the numbers of bipolar cells. These data suggest a bipotentiality to the precursors of these cell types that can be regulated by CNTF. Furthermore, despite the evidence that suggests that retinal neurons (and indeed all neurons) became committed to a specific fate during or after the terminal mitosis (Young 1985), cells putatively fated to become rods that were postmitotic could also be respecified into bipolar cells. Resistance to the respecification of postmitotic rods by CNTF coincided with the expression of

rhodopsin, a period of several days in many species, emphasising the difference between the birth of rod progenitors (marked by the terminal mitosis) and commitment to a rod fate (marked by rhodopsin expression). Levine *et al.* (2000) suggests that this is a mechanism to delay rod maturation until other retinal components have reached an apposite functional state.

The issue of rod genesis is further complicated by the discovery of two phases of rod genesis (Morrow *et al.* 1998), which may support Levine *et al.*'s (2000) suggestion. Again using the rat as a model animal, studies demonstrated that rods born after E19 experienced a 5.5–6.5 day delay before the onset of rhodopsin expression. Rods born before this time experienced an 8.5–12.5 day delay before expression of rhodopsin, and this did not correlate with terminal mitosis. Therefore, expression of rhodopsin was synchronised between the two phases of rod genesis. Co-culture of early-born cells with late-born cells did not affect their fate, indicating that the early-born cells were intrinsically programmed.

1.8 Schematic diagram of genes involved in cell fate determination (Figure 1.6)

The current information about some of the genetic signals that specify cell types and differentiation from the multipotential pool of retinal neuroblasts is summarised schematically in Figure 1.6, incorporating the data discussed

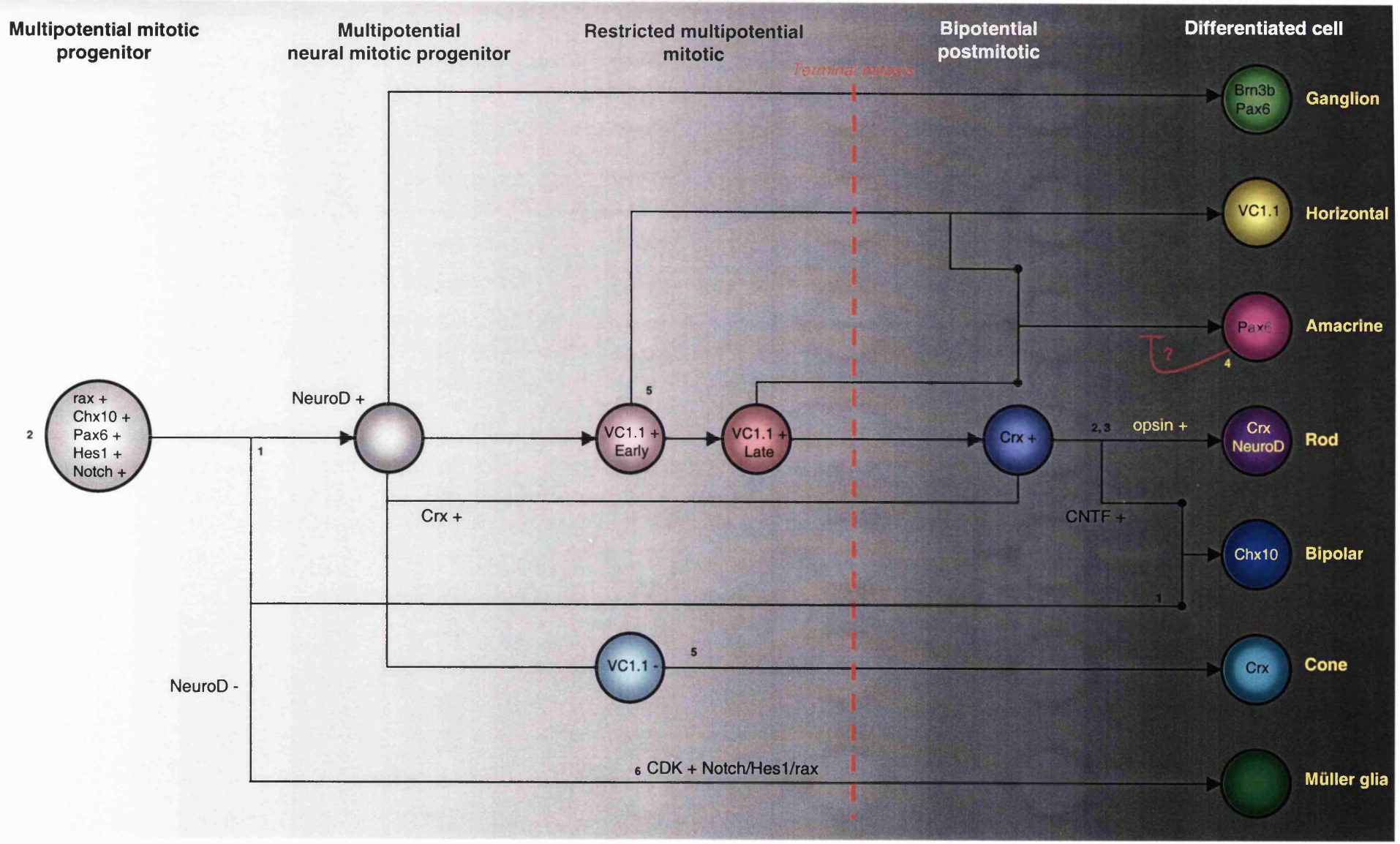

Figure 1.6. Schematic representation of some of the genes involved in retinal fate determination and differentiation. See text for details. References: 1. Morrow E.M. *et al* (1999), 2. Morrow E.M. *et al.* (1998), 3. Ezzeddine Z.D. *et al.* (1997), 4. Belliveau M.J. and Cepko C.L. (1999) 5. Alexiades M.R. and Cepko C.L. (1998), 6. Vetter and Moore, (2001).

above. The scheme indicates the genes that characterise mature retinal cells, as well as those involved during their development from multipotential progenitor cells.

1.9 The role of Chx10 in retinal development

Chx10 is a homeodomain-containing transcription factor, first identified by Liu *et al.* (1994) in a human retinal-specific library screen. Liu *et al.* (1994) focused on analysis of the murine homologue of this novel gene, which encodes a 361 amino acid, 39-kDa protein. Sequence analysis of a 1089bp transcript indicated that it was a homeobox containing gene, defined by the possession of sequence encoding a 60 amino acid highly conserved DNA binding motif, called the homeodomain. Further analysis indicated that *Chx10* was a member of the sub-family, *paired*-type homeobox genes, named after the first discovered in this family, the *Drosophila* gene, *paired* (*prd*) (see Figure 1.7). *Chx10* was named on the grounds that its homeodomain shared the highest amino acid sequence identity with that of the *Caenorhabditis elegans* gene, *Ceh10* (Hawkins *et al.* 1990), and hence Ceh10-like HomeoboX. Members of this subfamily include the Pax proteins, Orthodenticle-like proteins. The homeobox is typically encoded by 3 exons in *prd*-type genes, and consists of a helix-loop-helix tertiary structure (Latchman, in Eukaryotic Transcription Factors, 1998).

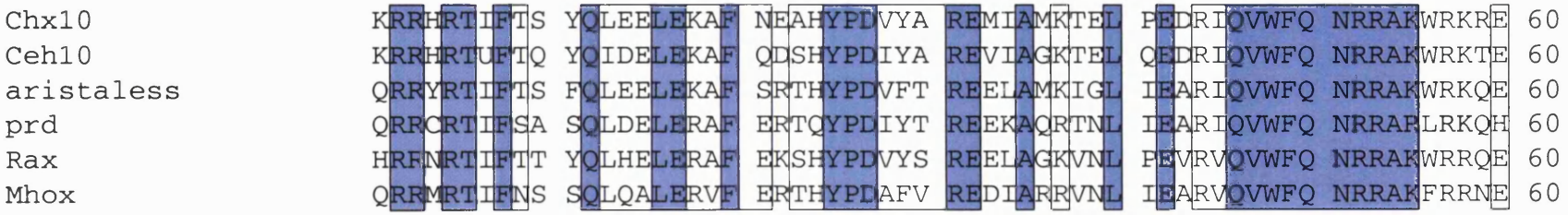

Figure 1.7. Comparison of the predicted amino acid sequences of various *prd*-type homeodomains. Shading indicates conservative changes, boxes indicate sequence identity.

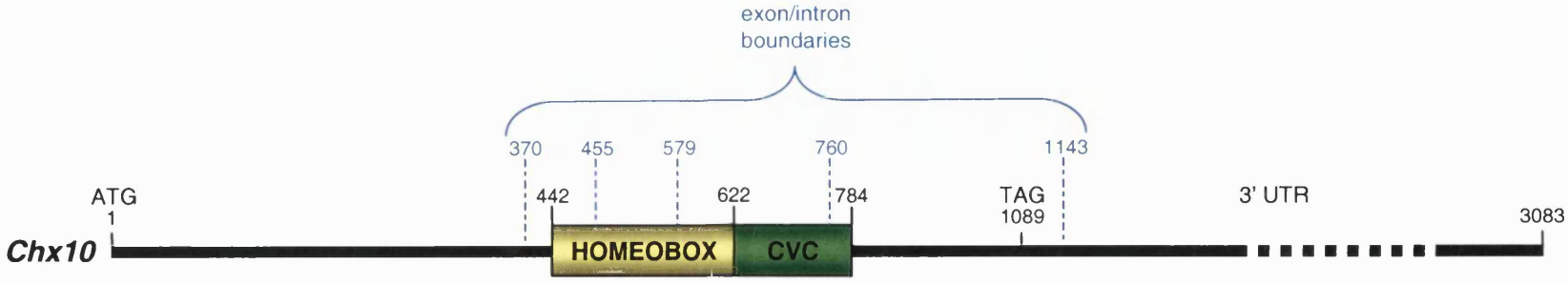

Figure 1.8. Structure of the *Chx10* cDNA. Chx10 is encoded by a 1089bp coding sequence, consisting of several conserved domains.

Sequence comparison with other homeobox genes indicates that Chx10 has several other conserved domains, which therefore may be functionally significant (Liu *et al.* 1994). Immediately 3' to the homeobox there is a 180bp region that appears to be highly evolutionarily conserved between *Chx10*-like genes in several different species, including goldfish, zebrafish, and chicken (see below). This region is termed the CVC domain [after the genes in the species in which it was initially identified, *Ceh10* (*C. elegans*), *Vsx1/2* (goldfish), *and Chx10* (mouse)]. However, no function has yet been associated with this motif.

1.9.1 Structure of Chx10 *(Figure 1.8)*

The structure of *Chx10* is given in the schematic diagram Figure 1.8. The coding sequence spans 1089bp and features several putative functional domains. These include the homeobox (442–622), the CVC domain (623–784), the function of which is yet unknown.

1.10 Expression of Chx10 in mouse

Liu *et al.* (1994) reported the developmental expression pattern of Chx10 in the mouse and rabbit. Retinal expression is discussed in section 1.10.1 and Chapter 5 in more detail. Expression is found in the ventral posterior neural tube, more specifically the developing rhombencephalon, spinal cord and

thalamus from E10.5. In the adult, extra-ocular expression of Chx10 appears to be limited to a subset of motor neurons in the spinal cord, specifically the V2 interneurons. No functional significance of extra-ocular Chx10 expression has been described (Burmeister *et al.* 1996).

1.10.1 Chx10 expression in the murine retina

Northern blot analysis shows that *Chx10* transcripts are abundant in the retina, and faintly detectable in the pons, medulla and spinal cord as discussed in section 1.10, but in no other tissue examined (Liu *et al.* 1994). *In situ* hybridisation data suggests the importance of Chx10 in the developing and adult retina, and are further discussed in Chapter 5.

1.11 Microphthalmia, and the microphthalmic mouse, *ocular retardation*

The human condition known broadly as microphthalmia [which is now accepted to reflect a spectrum of conditions, including anophthalmia and nanophthalmia (Ferda-Percin *et al.* 2000)], and the congenital blindness that accompanies it, is a clinically and genetically heterogeneous developmental disorder that is characterised by a small eye and other ocular abnormalities. To date, five loci have been identified in the human genome that co-segregate with microphthalmia (Bessant *et al.* 1998, Ferda-Percin *et al.* 2000).

There are a number of animal models, in which a small eye or microphthalmia is a central phenotype. Details of some of these models are summarised in Table 1.4.

Truslove (1962) identified a spontaneous natural mutation in a colony of mice that were severely microphthalmic and blind. This mutation was named *ocular retardation* (*or*), and displayed fully recessive Mendelian inheritance patterns, with no phenotype in heterozygotes. The phenotype of this mouse has subsequently been shown to be restricted to the eye, and is characterised by microphthalmia, a thin hypocellular retina, an absent optic nerve, morphologically abnormal photoreceptors, cataractous lens, and an absence of bipolar interneurons (Burmeister *et al.* 1996). Developmental analysis of this mutant revealed that by E12 *or/or* embryos had smaller eyes than normal. Truslove noted that the choroid fissure prematurely closed in the *or/or* mice during development, and erroneously attributed the reduction in size of the eye to the reduction in blood flow through the hyaloid vessels.

Because the microphthalmia was deemed to be similar, Konyukhov and Sazhina (1964) investigated the interactions between *or* and *microphthalmia* (*mi*), a recessive microphthalmic mouse mutation with a similar microphthalmic phenotype to *or*. *or/or/mi/mi* mice displayed a phenotype that was less severe than either of the single mutants, showing a smaller degree of microphthalmia (Rod McInnes, personal communication). The gene causing the *mi* phenotype was subsequently shown to be *mitf*, and interactions between mitf and Chx10

are critical for the definition of the RPE and the neural retina, as discussed in section 1.6.5.

In 1976 a new mutation on the inbred mouse strain 129/Sv-*Sl*^{J} was identified in the Jackson laboratories that was shown to be allelic to *or*, and was named *or*^{J} (Theiler *et al.* 1976). The *or* allele was subsequently lost, and all further work on this mutant has been carried out on *or*^{J}. Theiler *et al.* (1976) also focused on the apparent constriction of the blood vessels that flow through the choroid fissure during development, but more specifically identified a reduction in morphogenetic cell death, (described as "necrosis" there, in fact this cell death was almost certainly apoptotic, as it was not caused by injury) on the lateral edges of the choroid fissure, causing it to thicken and prematurely close. Silver and Robb (1979) expanded on this by noting that the edges of the choroid fissure abut squarely in normal mice during development, but in the *or*^{J}, due to the reduced apoptosis, the edges overlap, and cause the premature and total fusion of this fissure. Analysis by Robb *et al.* (1978) re-interpreted this phenomenon, as well as the observed absence of optic nerves and cataractous lens, as being a secondary to an underlying cellular defect, which manifests itself as a "failure of retinal precursors to differentiate beyond a rudimentary level". This study noted that the developing *or*^{J} eye was in fact heavily vascularised, despite the constriction of the hyaloid artery. The absence of the optic nerve had been noted in many of these studies. Silver and Robb (1979) performed detailed microscopic analysis and observed that ganglion cells were present in the retina, and indeed projected axons. These axons fail to exit the

globe, and instead form whorls in between the retina and the RPE, and this causes or adds to the observed retinal detachment. The suggested explanation for this is that axons face a mechanical barrier in the fused choroid fissure, rather than the possibility of an inherent biochemical defect within the ganglion cells.

Table 1.4 Animal models with small eye or microphthalmia phenotypes

Model	Species	*Gene*	Description	References
Ocular retardation	M	*Chx10*	Point mutation causing premature stop codon causes reduction of retinal proliferation from E10.5	Burmeister *et al.* 1996
Small eye	M	*Pax6*	Homozygotes fail to form forebrain structures (neonatally lethal); heterozygotes have small eyes and are blind.	Graw 1996
Aphakia	M	*Pitx3*	Bilateral microphthalmia due to a failure of lens morphogenesis: caused by large gene deletion	Rieger *et al.* 2001
Microphthalmia (mi)	M	*Mitf*	Microphthalmia in rats and mice.	Freund *et al.* 1996
Mib	R			Opdecamp *et al.* 1998
Cyclin D1	M	*Cyl-1*	Homozygous targeted deleted animals display severe retinopathy caused by impaired development of all layers of the retina	Fantl *et al.* 1995
Rx	M	*Rx*	Homozygous targeted deleted animals fail to develop eyes	Zhang *et al.* 2000

Abbreviations: M, mouse, R, rat.

1.12 A mutation in *Chx10* causes *or^{J}*

Following the identification of homeodomain transcription factor Chx10 (Liu *et al.* 1994), Burmeister *et al.* (1996) demonstrated that the *or^{J}* phenotype was caused by a mutation in *Chx10*, resulting in a null allele. Owing to the accepted terms of genetic nomenclature, the identification of the gene causing a mutation in a mouse requires the renaming of that mouse. The mutant mouse that harbours the *or^{J}* allele therefore is now officially known as *Chx10$^{or\text{-}J/or\text{-}J}$*. For the purpose of this thesis, I shall continue to refer to this mouse as *or^{J}*.

Sequence analysis of *Chx10* in *or^{J}* revealed a C→ A transversion that encodes a premature stop codon (tyrosine176stop) in the homeodomain. Electromobility shift assays have demonstrated that this reduces the DNA binding ability of Chx10 by up to 90%, and therefore this mutation can truly be considered a null (Rod McInnes, personal communication). This was confirmed by the absence of any detectable Chx10 protein when using an antibody raised to recognise the N-terminal 139 amino acids of the predicted protein. By contrast, Chx10 protein could readily be detected in the wild-type murine retina at E10.5 and E14.5.

Liu *et al.* (1994) and Burmeister *et al.* (1996) investigated the expression pattern of *Chx10* during development by *in situ* hybridisation. This is described in detail in Chapter 4. Broadly, initial ocular expression coincided at E9.5 with the morphological formation of the inner layer of the optic vesicle and continues to be expressed throughout development in dividing retinal neuroblasts. As cells

leave this pool and become postmitotic, *Chx10* expression is downregulated, apart from bipolar cells, in which expression is maintained throughout life.

Given this expression pattern of Chx10 during eye development, Burmeister *et al.* (1996) chose to focus on analysis of the retinal phenotype. The absence of expression of Chx10 in the choroid fissure or optic stalk, but the presence of a phenotype here (as discussed in the earlier work) suggests an interaction between Chx10 and downstream targets that have a longer range effect. This however, has not been investigated further.

Cell proliferation was assayed in the development of the mutant retina by bromodeoxyuridine (BrdU) incorporation at E11.5, which was reduced by up to 83% in the peripheral retina (though not significantly different in the central retina). However, by this stage the mutant retina contains 30–50% fewer less cells than the wildtype. Reduced proliferation in the peripheral retina continued until at least E18.5. Given *Chx10*'s expression pattern throughout the undifferentiated neuroblastic retina during early development, and this reduced cell proliferation phenotype, Burmeister *et al.* suggest that Chx10 plays a major role in promoting cell proliferation in the developing neural retina.

1.13 Chx10 interacts with pRB family members

Further evidence that Chx10 is involved in cellular proliferation came from Wiggan *et al.* (1998). Their study reported that members of the family of

proteins termed pRB [(some of which cause the human ocular condition retinoblastoma, (Friend *et al.* 1986)] are capable of directly interacting with transcription factors that contain a *prd*-type homeodomain, including Chx10. Members of this family are known to act as negative regulators of cell cycle progression. Wiggan *et al.* (1998) demonstrated that the pRB family members p130, p107 and pRB itself bind *in vitro* to the homeodomain of Chx10. This may indicate a regulator of Chx10 whose expression may influence cell fate decisions. The authors speculate that the binding of Chx10 by its functional domain to a negative regulator of cell cycle progression might repress its function, indicating that Chx10 may support proliferation via this pathway. These data give biochemical credence to Chx10's putative role in the promotion of proliferation.

1.14 Chx10 is crucial for bipolar cell fate decisions

Liu *et al.* (1994) showed that expression of Chx10 in the adult retina was restricted to a band of cells within the inner nuclear layer. This band was restricted to cells in the outer aspect of the inner nuclear layer, which includes the location of bipolar cells. However, the band of expression appears wider than the bipolar layer, indicating that cells other than bipolar cells may weakly express Chx10. Chx10 expression in bipolar cells was confirmed by Burmeister *et al.* with immunocolocalisation of Chx10 and protein kinase C (PKC) proteins,

PKC being a bipolar-cell marker (Greferath *et al.* 1990). This expression pattern suggests a role for Chx10 in the maintenance of bipolar-cell function, but also in function of other inner nuclear layer cell-types.

Burmeister *et al.* also performed immunohistochemistry, using antibodies to cell specific antigens, to determine whether all retinal cell types were present in the *or*^{J} retina. Staining for the axon specific cell adhesion molecule L1 demonstrated the presence of ganglion cells at E14.5, indicating this cell type was present and differentiated, and confirmed that the axons formed whorls, or neuromas in the inter-neural retinal–RPE space. Ganglion cells are amongst the first cell type to become postmitotic and differentiate in the vertebrate retina (Young 1985), and these data indicates that their birthing is little affected by the absence of functional Chx10. Similarly, at P14 (when the retina is fully postmitotic and can be considered mature), cell types were identified by the positive observation of cell specific mature markers; Müller cells (vimentin-positive), amacrine cells (syntaxin-positive), horizontal cells (neurofilament-positive), and rod photoreceptors (rhodopsin-positive at P18) were all shown to be present in the mutant retina. Furthermore, all of these cell types appeared to be in strata that were approximately equivalent to that of the wild type, despite the absence of obvious lamination or stratification in the mutant retina. L1 positive cells were invariably seen in a layer closest to the lens, inner nuclear layer cells were seen in the single nuclear layer, and rod photoreceptor cells were seen mostly on the outer aspect of the neural retina, abutting (when not detached) the RPE.

By stark contrast, no immunoreactivity was detected for the bipolar cell markers PKC or RetB1, indicating that bipolar cells are absent in the adult *or*^{J} retina. Bipolar cells are amongst the last cell type born in the retina (Young, 1985). Two arguments present themselves here to address this phenotype. One is that as bipolar cells are born late, and there is a great reduction in proliferation and hence cell number in the mutant retina, that there are no cells remaining in the neuroblastic progenitor pool that can differentiate as bipolar cells. This would be supported by the reduced level of proliferation observed with BrdU labelling at later stages of retinal development (Burmeister *et al.* 1996). This argument is refuted however by the presence of Müller cells, which are born similarly late in retinal development. The second possibility is that Chx10 has a role in the specification and differentiation of bipolar cells, and that absence of a functional Chx10 results in the failure of these cell to develop normally or at all. This is reinforced by the high levels of expression of *Chx10* in bipolar cells seen in the adult retina, which indicates that, at least, Chx10 has a role on the maintenance of bipolar cell function.

Expression of Chx10, analysis of the phenotype of the *or*^{J} retina and biochemical analysis of Chx10–p130 interaction indicates that Chx10 has a number of distinct roles in the retina:

1. Chx10 is essential for correct levels of cellular proliferation of the neuroblastic retina, possibly by repressing the activity of a negative regulator of the cell cycle.

2. Chx10 is necessary for specification and differentiation of bipolar cells from the neuroblastic pool of retinal progenitor cells.
3. Continued expression of Chx10 in differentiated bipolar cells may indicate a role in the maintenance of these non-diving neurons, or at least as a regulator of bipolar-cell-specific function.

1.15 Other ocular phenotypes in the *or*^{J} mouse

There are several phenotypes in the *or*^{J} retina that are not addressed by these putative roles of Chx10. One is the absence of an optic nerve. Ganglion cells are present in the mutant, and they do project their axons, but these fail to leave the globe and fasiculate into a cohesive optic nerve. The optic stalk degenerates into a residual line of cells that are morphologically distinct from the surrounding mesenchyme (see Figure 1, Chapter 4). Chx10 is not expressed in postmitotic ganglion cells (Burmeister *et al.* 1996), leaving a number of possibilities to explain this phenotype. One is that the premature closure of the choroid fissure presents a physical barrier through which the axons cannot advance, and their guidance cues cause axons to form the observed whorls. Another is that, owing to the reduction in cell numbers during early development, there is a disruption in the microenvironment, which prevents ganglion cells from differentiating correctly. A third possibility is that the absence of Chx10 in mitotic cells that are fated to become ganglion cells

results in a ganglion cell phenotype upon differentiation. The failure of ganglion cells to aggregate into a nerve fibre layer, or to form an optic nerve head, suggests that the notion of a simple mechanistic physical barrier to axonal growth is not sufficient to explain this phenotype. If it were, then one might expect the formation of a fasiculated optic nerve head, which was then unable to leave the globe. As it is in the *or*^{J} retina, axons migrate away from ganglion cells through the retina.

As Chx10 is expressed only in the neural retina during development, it is perhaps surprising that the *or*^{J} phenotype displays such severe microphthalmia. One might speculate that as the reduction in proliferation in the neural retina is notable when the eye is at a very early stage of development, that this has a profound effect on total eye size rather than just on the retina itself. This phenotype indicates that signalling occurs between the retina and other areas of the eye to convey information about growth, and that these signals are inhibited or lost in the *or*^{J} retina owing to reduced proliferation, or inherent disruption of a relevant signalling pathway.

Lens development in the *or*^{J} eye is relatively normal (although the lens is proportionally smaller than in the wild type), but the lens invariably becomes cataractous in adulthood (Burmeister *et al.* 1996). The reduction in the size of the lens again may be attributable to disturbances in signalling between the retina and the lens, which have been shown to be essential for lens development (Grainger, 1992). Burmeister *et al.* (1996) suggest that the formation of cataracts in the *or*^{J} eye may be a secondary phenomenon, bearing

in mind the fact that Chx10 does not appear to be expressed in the lens at any stage.

Similarly, Burmeister *et al.* suggest that the morphologically abnormal photoreceptors seen in the mutant may be secondary effect, as Chx10 is not reported to be expressed in differentiated photoreceptors. The photoreceptors have reduced or absent inner and outer segments, shown by the juxtaposition of the outer nuclear layer (i.e. the cell bodies of the photoreceptors) to the RPE. In the normal retina, these layers are clearly separated by the inner and outer segments. This is investigated in depth in Chapters 4 and 5.

It is interesting that given strong Chx10 expression in V2 interneurons in the spine during development and adulthood (Sander *et al.* 2000) that no spinal phenotype has ever been associated with the *or*^{J} mouse. This has not been investigated yet, but it may be that other factors are capable of compensating for the loss of Chx10 in these cells, or that loss of these cells themselves result in a subtle phenotype that is not severe enough to be notable.

1.15.1 Chx10 interacts with ROR-β

Interactions with a member of the nuclear receptor family of transcription factors have been suggested (Chow *et al.* 1998). Co-localisation of *Chx10* and *RORβ* and a dramatic reduction in *RORβ* expression observed in the *or*^{J} mouse suggest a role for this protein in retinal proliferation, possibly by via Chx10.

1.15.2 Amelioration of the or^{J} *phenotype by genetic modifiers*

Bone-Larson *et al.* (2000) examined the offspring of back-crossed inbred *or*^{J} mice of the strain 129/Sv-*Sl*^{J} and sub-species *Mus musculus castaneus.* The ocular phenotype was ameliorated, although the eyes were not of normal size. Furthermore, the bipolar cell marker RetB1 was identified by immunohistochemistry, although the marker PKC was not. Optic nerves were present bilaterally, and electroretinograms indicated partial visual function. These data suggest that the presence of genetic modifiers, as found in a different genetic background, interact strongly with Chx10 during development, and have a profound effect on its function.

1.15.3 Identification of retinal stem cells

Recently, stem cells have been identified in various vertebrate organs and tissue types, including the liver and mesenchyme (Shafritz 2000). Tropepe *et al.* (2000) and Ahmad *et al.* (2000) both independently demonstrated the existence of neural progenitor cells from the adult mouse eye that display stem cell properties *in vitro.* These cells were capable of proliferation in culture, and showed subsequent differentiation into some of the cells of the retina including bipolar cells, rods and Müller glia. This finding opposes the dogma that the mature retina lacks regenerative capability, and contains no mitotic neurons. The putative stem cells expressed Chx10, reflecting their multipotentiality as neuro- retinal precursors.

1.16 Chx10 orthologous family members in other vertebrates

The gene with the highest sequence identity to *Chx10* in *Drosophila* is *aristaless*, which is predominantly involved in the establishment of the proximo-distal axis in leg and antennal imaginal discs (Pueyo *et al.* 2000). No evidence exists that suggests a role for this gene in ocular development, in the same way that *Pax6* and *eyeless* share genetic hierarchies. However, several orthologues of Chx10 have been identified in various species, in which it appears to have a similar role to that in the mouse.

Interestingly, the *C. elegans* gene, *Ceh10*, (Hawkins *et al.* 1990) with which Chx10 shares sequence identity is expressed in an interneuron that may connect to a photosensitive cell, perhaps suggesting an evolutionary history for this gene family.

Levine *et al.* (1994) and Passini *et al.* (1998) report the cloning of two *Chx10*-like genes, named *Vsx-1* and *-2*, in the goldfish (*Aurelius*). Both are expressed in the adult retina, in overlapping expression patterns that indicate bipolar cells. Vsx-2 is expressed at high levels in the retina during embryogenesis, but also in areas of the metacephalon–myencephalon border that suggest a role for Vsx-2 in specification and maintenance of specific neurons.

The goldfish retina is capable of limited regeneration following injury, and ablation studies (Levine *et al.* 1994) note an upregulation in Vsx-1 expression in cell in the inner nuclear layer, and *de novo* in cells outside this layer. The

authors speculate that this may reflect the stabilisation of differentiated cells, and the multipotentiality of new cells that are contributing to the regeneration. These functions are in accordance with the putative roles of Chx10 in the murine retina, if the regenerating retina is considered to be similar to the developing retina.

Orthologues of Chx10 have also been identified in chickens (*Gallus domesticus)*, Chx10 and Chx10-1 (Chen and Cepko 2000). Their sequences are most closely related to *Vsx-1* and *-2*, respectively. The embryological expression pattern of Chx10 is similar to that of the mouse, that is, in all retinoblasts in early development, and restricted to presumptive bipolar cells later, but Chx10-1 is expressed in a novel pattern on the naso–temporal border. Expression of both genes is maintained at low levels in mature bipolar cells. The function of Chx10-1 during development as delineated by the novel pattern of expression is unknown.

So far, no second highly related Chx10-like gene has been identified in mice or humans, as shown in chickens and goldfish. The separate functions of the two variants have not been fully explored, but may, at least in the goldfish, be specific to its regenerative retinal capabilities. The presence of a variant that is highly-related to goldfish *Vsx-2* in the chicken (which has extremely limited regenerative properties in the retina) suggests that this function has been lost in higher vertebrates (i.e. mice and humans, at least).

A Chx10-like orthologue has also been reported in the zebrafish, named *Alx* (Barabino *et al.* 1997). The expression pattern of this gene mirrors that of

Chx10 in the mouse, in that it is expressed throughout the neural retina during early eye development, and later and in the adult becomes restricted to the inner nuclear layer, presumably in bipolar cells. Inhibition of *Alx* using antisense oligonucleotides produced a phenotype that resembled *or*^{J} in its microphthalmia and retinal hypocellularity.

1.17 Aims of this thesis

Previous studies have shown that Chx10 is essential for eye development, and formation of bipolar cells in the inner nuclear layer.

In this thesis, I have attempted to address the following questions with regard to the current knowledge concerning the genes involved in human and murine retinal development:

1. What are the expression patterns of orthologues of *Chx10* and other transcription factor genes that are known to be essential for murine retinal development in the developing human eye?
2. How does the absence of Chx10 in the *or*^{J} retina affect the expression of other transcription factors that are known to be essential for retinal development?
3. How do interactions between Chx10 and other retinal genes confer the phenotype of the *or*^{J} mouse?
4. What factors are capable of altering the *or*^{J} phenotype, and thus may be viewed as having an involvement in the genetic cascade determined by Chx10?
5. Given the existence of multiple Chx10 orthologues in other vertebrate species, are there other *Chx10*-like genes that have a role in mammalian retinal development?

CHAPTER 2

METHODS AND MATERIALS

CHAPTER 2

METHODS AND MATERIALS

2.1 General reagents

All reagents apart from those listed below were supplied by either BDH Ltd (Poole, UK) or Promega (Promega Corp, Madison, WI, USA). Sigma–Aldrich Company Ltd (Poole, UK) supplied: β-glycerophosphate, bovine serum albumin (BSA), 5-bromo-4-chloro-3-indolyl-β-D-galactosidase (X-gal), bromophenol-blue, diethylprocarbonate (DEPC), dithiothreitol (DTT), ethidium bromide, formamide, hydrogen peroxide (H_2O_2), β-mercaptoethanol, orange G, paraformaldehyde (PFA), sodium dodecyl sulphate (SDS), Tri Reagent and Trizma base.

Restriction enzymes were also supplied by Promega, as were T3, T7 and SP6 RNA polymerases, RNase I and RNase-free DNase I.

2.1.1 Bacterial growth media

Lennox L Broth (LB Broth), Lennox L Agar (LB Agar) and ampicillin were from Gibco (Gibco BRL, UK).

2.2 General molecular biology solutions

Solutions were made in following methods described in Sambrook *et al. Molecular cloning: A Laboratory Manual*, 2nd Edition. (1989):

Phosphate buffered saline (PBS)	137mM NaCl, 2.7mM KCl, 4.3mM $Na_2HPO_4.7H_2O$, 1.4mM KH_2PO_4
2M Tris–HCl	pH adjusted to 7.6, 8.0 and 9. For RNA work, this was made up with DEPC-treated H_2O.
0.5M EDTA	pH adjusted to 7.5 and 8.0 with NaOH.
Tris–EDTA	10mM Tris–HCl, 1mM EDTA. For RNA work, this was made up with DEPC-treated H_2O.
3M Na Acetate	pH adjusted to 5.2 with glacial acetic acid.

10% SDS (Sodium dodecyl sulphate)	
	100 g SDS dissolved at 68°C in 900 ml H_2O, pH adjusted to 7.2 with HCl, volume adjusted to 1l with H_2O
TSS	10% PEG (MW 3500-8000), 5% DMSO, 50 mM $MgCl_2$, in LB

2.2.1 Electrophoresis buffers

10× TAE	0.8M Tris, 40mM EDTA
Ethidium bromide	10mgml^{-1} in TE

2.3 Animals used in this study

Ocular retardation mice (on the inbred strain 129/Sv-*Sl*) were kindly provided by Ray Lund (Institute of Ophthalmology, UCL, London). Wild-type mice used were either C57Bl-6 or 129/Sv-SL. Mice were kept in a 12hr light–dark cycle. Female mice were mated overnight with males, and the presence of copulation plugs was detected at 9am the following morning. Midday on this day was considered to be embryonic day (E) 0.5.

2.4 Micro-dissection and microscopy

Micro-dissection was carried out on a Zeiss SV6 stereomicroscope (Zeiss, Welwyn Garden City, UK), using fine-tipped watchmaker's forceps, numbers 3–5, and microscissors (Raymond Lamb, UK).

Brightfield, phase and fluorescence microscopy was generally performed on an Olympus BH2 microscope (Olympus, Southall, UK), using ×4, ×10 and ×20 magnification objective lenses. Digital imaging was performed with a Seiss Kontron ProgRes 3012 digital camera (Imaging Associates, Oxford, UK), using version 2.0 of their software. Images were processed using PhotoShop 3.1 or 5.0 (Adobe Systems Europe, Edinburgh, UK), and assembled and formatted in Microsoft PowerPoint 97.

2.5 Standard molecular biology techniques

2.5.1 Restriction digests

Diagnostic restriction digests were generally carried out in a volume of 10 µl using the appropriate buffer supplied by the manufacturer (Promega or Roche). For double digests, the volume was doubled to accommodate for the increased volume of glycerol in which the enzymes are stored.

2.5.2 Agarose gels

Gel electrophoresis for DNA separation was carried out using horizontal agarose gels of an appropriate concentration (0.8–2%), and run at an appropriate voltage (40–150v). Gels were made up in TAE with 0.5μgml^{-1} ethidium bromide, and run out in the same buffer. Gels were visualised by transillumination with ultra-violet light, and either photographed with Kodak Polaroid film, or digitally processed with AlphaImager 1200 (Alpha Innotech Corporation) software (version 3.3b). Fragment sizes were determined with standard DNA markers of known molecular weight, generally Promega 1kb ladder.

2.5.3 DNA extraction from agarose gels

Extraction of DNA fragments for further subcloning, manipulation or sequence analysis was carried out by electrophoresis on low percentage gels. The desired band was excised from the gel with a clean scalpel, being careful to expose the gel to the UV light for a minimum amount of time to avoid DNA degradation. The band was processed using the Qiagen Gel Extraction kit according to the manufacturer's instructions (Qiagen, West Sussex, UK), and eluted from their DNA clean-up column using an appropriate volume of either water or TE, usually 30 or 50 μl.

2.5.4 Maxipreps and minipreps

Recombinant plasmid DNA was generally recovered from its host bacteria by maxi- and mini-prep (depending on quantity of DNA required), using column kits from Qiagen (West Sussex, UK). For a maxiprep, 200 ml LB ampicillin culture, grown shaking overnight at 37°C, was spun at 2000 rpm for 15 min at 4°C in a Sorvall SS-34 rotor. The bacterial pellet was resuspended in 40 ml of resuspension buffer by vortexing. To lyse the cells, 40 ml of lysis buffer was added and mixed by inversion so as not to shear the DNA. The solution was neutralised by adding 40 ml of neutralising buffer and mixed by inverting the tube. Cellular debris and precipitated chromosomal DNA were removed by centrifugation at 10,000 rpm for 15 min at 4°C. The supernatant was then filtered through a Qiagen column, cleaned with ethanol and subsequently eluted from the resin into a clean tube. Plasmid DNA was recovered by precipitation with isopropanol. The mixture was centrifuged at 10000 rpm for 15 min at 4°C. The DNA pellet was dissolved in an appropriate volume of either TE or water (based on visibility of the pellet, normally ~200µl).

For minipreps, 5ml of LB ampicillin culture was inoculated with single-picked colonies and grown overnight at 37°C. The Qiagen Spin Miniprep protocol was followed, and recovered, eluted DNA was resuspended in 50µl of either TE or water.

To quantify the plasmid DNA, the preparation was diluted (×100) and light absorption at 260 nm was measured using a spectrophotometer. A reading of one unit at 260 nm corresponds to 50 $\mu g ml^{-1}$ of double stranded DNA, while

the A_{260}/A_{280} ratio is a measure of protein contamination of the DNA preparation. A ratio of 1.8 or more was accepted as sufficiently pure.

2.6 Cloning of gene fragments

2.6.1 Polymerase chain reaction (PCR)

Genes to be used for *in situ* hybridisation with digoxygenin labelled riboprobes were cloned from an E15.5 mouse retinal cDNA library (constructed by Adrian Hardy and Jane Sowden). Mass excision of the pBk-CMV phagemid vector from λZAP Express library phage stock (Stratagene) was used to generate a phagemid library. *Brn3b* cDNA plasmid was a generous gift from David Latchman (Institute of Child Health, UCL, London). Table 2.1 below shows the primer sequences used. 50μl PCR reactions were used containing PCR buffer, 1.5mM Mg^{2+}, one unit of *Thermus aquaticus* polymerase (Promega), 40μM combined dNTPs (all from Promega), 50pMμl^{-1} of each primer, and 1μg of cDNA library as template. PCR cycling was based on the following:

1. 5 min @ 94°C
2. 30 sec @ 94°C
3. 1min @T_A
4. 1min @ 72°C
5. repeat steps 2–4 29 times
6. 10min @ 72°C

where T_A is the annealing temperature for a primer pair, as calculated by the formula: $T_A = [69.3 + (0.41 \times GC\%) - (650 \div n)] - 2$. [where n = length of oligo primer, and GC% is the percentage of G and C content in the oligo, typically 55% (11/20)].

Oligonucleotides were designed using the Pubmed nucleotide enquiry facility (www.ncbi.nim.nih.gov/entrez/query.fgci?db=Nucleotide), and Amplify 1.2 software (William Engels, University of Wisconsin, WI, USA). Oligonucleotides were custom synthesised by Genosys (Cambridge, UK).

Table 2.1. Sequence of gene specific primers

Gene	Oligonucleotide sequence	Predicted length (bp)
Arrestin antisense	5' AAGACCTGGATGTACTGGGC 3'	523
Arrestin sense	5' ACTTGTACTGCGCGGTGCTA 3'	
Chx10 antisense	5' ATGACGGGGAAAGCGGGGGAAG 3'	343
Chx10 sense	5' CGCTCTGCCTAGTGGCTGCAAG 3'	
Crx antisense	5' TGCTTCAAGAATCGTAGGGC 3'	636
Crx sense	5' TGAAACTTCCAGGCACTCTG 3'	
Brn3b antisense	5' ATCGTCTCCCAGAGCAAGAG 3'	184
Brn3b sense	5' GACAGTGTGAGGGACTCGAAA 3'	
IRBP antisense	5' CCTGACAGTAAGTCTGCCTC 3'	576
IRBP sense	5' GTCCCAGGGAGCATTTTCTG 3'	
PGM1 antisense	5' GAAAAATCAAAGCCATTGGTGGG 3'	417
PGM1 sense	5' GGCACCGAGTTCTTCACAGAGGAT 3'	
Peripherin antisense	5' CAGATACGGCGGCCTAGATT 3'	644
Peripherin sense	5' CGTTGTTCCCACAGCACTTG 3'	
Pde-β antisense	5' GGGAAGAAGTTGAGCCCTGA 3'	512
Pde-β sense	5' TCACTGCCATGATCACAGCC 3'	
Rhodopsin antisense	5' CTTTACCTAAGGGCCTCCAC 3'	490
Rhodopsin sense	5' GCAGCTTCTTGTGCTGTACG 3'	

Primers were all designed to have a T_A of ~57°C, and therefore generally have a GC content of 55%.

Variations on this basic PCR reaction were performed according to annealing temperature, quantity of template and so on, as described below.

PCRs were run out on an appropriate percentage agarose gel (0.8–2%) (see above), and the product was cut out using a scalpel and extracted using the Qiagen Gel Extraction kit. Purified PCR product was ligated into pGemT or T-easy vector (Promega) (both of which contain the gene encoding the LacZ protein within their multiple cloning sites, thus allowing blue/white selection for recombinant plasmids) overnight at 14°C, using T4 DNA ligase and ligase buffer (Promega). Approximately 50ng of ligated plasmid was transformed into either JM109 (Promega) or DH5α competent *E. coli* cells and grown on ampicillin/X-Gal/IPTG-containing agar plates overnight at 37°C. Individual white colonies were picked and used to inoculate 5ml cultures of LB broth containing $50\mu gml^{-1}$ ampicillin overnight at 37°C, and plasmid extracted and purified using the Qiagen Miniprep kit (see above).

2.6.2 Colony PCR

Plasmids were checked to see if they contained the desired cDNA using diagnostic restriction enzyme digestions (see above) or colony PCR, with gene-specific primers. This process allows large-scale screening without having to prepare plasmids from large numbers of cultures. It involves inoculation of a 5ml culture with the same pipette tip used to inoculate a PCR mix. The PCR is performed, while the cultures are grown overnight, and recombinant colonies,

as identified by PCR, are prepared as normal, and non-recombinant cultures can be discarded.

The cycling for this PCR method is somewhat different from the cycle described above, and is modified to optimise amplification from whole bacteria, rather than naked DNA, by the inclusion of an extended denaturation step that also disrupts bacterial cells.

(Cycle 1)

- 90 sec at 94°C
- 30 sec at 50°C
- 3 min at 72°C

(Cycles 2–10)

- 20 sec at 94°C
- 20 sec at T_A
- 2 min at 72°C

(Cycles 11–30)

- 20 sec at 94°C
- 20 sec at T_A
- 3 min at 72°C

where T_A is the primer-specific annealing temperature.

2.6.3 Semi-quantitative RT-PCRs

A number of PCRs were performed to test whether the amount of product generated was within the linear range of the PCR reaction, and thus could be

deemed semi-quantitative. This involved doing a series of PCRs with increasing number of cycles ranging from 25 to 35 cycles for the analysis of a given gene. The samples were run on an agarose gel and the intensity of the bands were measured using spot densitometry with AlphaEase 3.3b software. The relationship between the number of cycles and the intensity of the bands was established by graphically representing the data so that the chosen number of cycles to be used for quantification could be determined within the linear range. The samples to be compared were run on the same agarose gel and the intensities of the bands were determined. Standardisation was carried out by comparison of band intensities for a ubiquitously expressed gene (*Pgm1*).

2.6.4 Somatic cell hybrid PCR

PCR was performed on somatic cell hybrid DNA, obtained from the Human Genome Mapping Project (Cambridge, UK). cDNA-specific primers were used in the same standard PCR mixture (as described above), and 1μl of template from each of 25 pools of DNA species. These contained individual human chromosomes together with complete hamster genomes, plus control genomes of hamster and mouse alone.

2.7 World-wide Web-based sequence analysis

Novel sequences were identified and analysed using freeware available on the world-wide web. Initial identification of sequences used the nucleotide-, protein- and genome-specific databases of the Entrez search tool (http://www.ncbi.nlm.nih.gov/entrez/query.fcgi). Sequence comparison and alignment was performed using the basic local alignment search tool (BLAST) algorithm software (Altshul *et al.* 1990) (http://www.ncbi.nlm.nih.gov/BLAST/) and its variants. These include BLASTX (translated sequence), BLASTN (standard nucleotide–nucleotide comparisons), BLASTP (standard protein–protein comparisons) and MEGABLAST (graphical output of various other BLAST algorithms) (all available at the same URL).

More complicated sequence analysis was performed using software available at the UK Human Genome Mapping Project Resource Centre (http://www.hgmp.mrc.ac.uk/). These are included in the NIX package (http://www.hgmp.mrc.ac.uk/Registered/Webapp/nix/), and include GAP and Bestfit (alignment tools), Translate and MAP (DNA–protein manipulation tools) and Seqed (sequence editing).

2.8 Bacterial transformation

Transformation is the process of inserting a plasmid into a bacterium. Methods to do this include electroporation, in which a pulse of a high voltage is applied to a suspension of bacteria causing their membranes to become permeable to exogenous DNA, or chemical transformation. In the latter case, cells become competent (permeable to DNA) in the presence of cations and dimethyl sulfoxide (DMSO).

2.8.1 Competent cells

E. coli XL1-Blue cells were grown overnight in 5 ml of LB with the appropriate antibiotic (usually 50 µg/ml kanamycin). One millilitre of this culture was added to 100 ml of pre warmed LB containing kanamycin and incubated at 37°C until the OD reached 0.3 – 0.4. The cells were centrifuged at 1500 rpm for 20 min at 4°C and resuspended in 10 ml of cold TSS. The competent cells were then either used immediately or aliquoted on dry ice, stored at -70°C, and thawed on ice when required.

2.8.2 Transformation

Generally, 3µl of ligation reaction were put into a chilled microfuge tube on ice and 50 µl of competent bacterial cells was added. The contents were gently mixed by tapping the tube, to avoid shearing the DNA and lysing the cells. The tube was placed on ice for 15 min, then heat-shocked in a 42°C waterbath for

90 seconds and placed immediately on ice for 2 min. One millilitre of LB without antibiotic was added and incubation was continued at 37°C for an hour to allow the cells to recover. The cells were spun at 2000 rpm for 3 min, most of the supernatant was removed and the pellet resuspended in the rest. Using a sterile spreader, transformed bacteria were plated onto warm LB-ampicillin-agar plates, and incubated inverted at 37°C overnight.

2.8.3 Screening for recombinant bacteria

Screening for recombinant bacteria was based on various methods and levels of screening. A first round of selection was generally assessed based on the presence of an antibiotic resistance gene in the vector, so that only transformed bacteria could grow on the ampicillin-containing medium. Presence of a DNA insert in the vector was confirmed using either of the following two methods. If the DNA fragment was long enough to be able to see a size shift on an agarose gel, the following method was frequently used. Colonies were inoculated into 1 ml of LB ampicillin and incubated for 5 h at 37°C. Half of the suspension was spun and bacteria were resuspended in 50 µl TE. DNA was extracted first with phenol then with chloroform. The samples were run together with the vector on agarose gels as described previously.

If the insert was too short to be detected in this way, standard minipreps were performed, followed by the appropriate digestions with restriction enzymes as described above.

2.9 Tissue preparation

2.9.1 Mouse sacrifices

Mice were paired in the evening, and when vaginal plugs were observed the following morning 12.00 p.m. was taken to be E0.5. Pregnant mothers were sacrificed at 12.00 p.m. on the appropriate day by cervical dislocation. Embryos were removed and dissected using watchmakers forceps (size 3–5, Raymond Lam, UK) in cold PBS before being fixed in 4% w/v paraformaldehyde in PBS overnight at 4°C. E18.5 embryos were decapitated, and postnatal eyes were enucleated before fixation, and the lens was removed.

2.9.2 Human tissue

Human tissue was received in dissection medium and washed in PBS before fixation. Adult human eyes were sometimes calloted to allow better penetration of fixative into the globe; this involves the removal of a lateral pole of the globe by sectioning through a plain parallel with the vertical axis of the eye. Large foetal eyes (e.g. 15 weeks post conception) were pierced with a hypodermic needle through the lens for the same reason. Foetal age was determined by anatomical measurements (foot or crown–rump length). Human tissue was obtained after informed consent from the MRC Tissue Bank, Royal Postgraduate Medical School Hammersmith Hospital, Imperial College, London).

2.9.3 Tissue embedding

Tissue was washed post fixation in PBS, dehydrated through a graded ethanol series with water (30% ethanol, 50%, 70%, 85%, 95%, 100%, 100%, and cleared in xylene. Tissue was then carefully placed in an appropriately sized mould, and submerged in molten parafin. Whilst still hot, the tissue was orientated to achieve the desired plain of section. Paraffin embedded tissue was sectioned, using a Sigma microtome into 6–8μm transverse sections on 3-aminopropyltriethoxy-silane (APES) (Sigma) coated microscope slides. These create a surface on the microscope slide to which the sections stick well, and were prepared by initially submerging slides in acid-alcohol (70% ethanol, 10 HCl), and then 100% ethanol. Slides were then left to dry, and when dry, submerged in 4% APES in acetone, and washed in acetone twice. Slides were then left to dry overnight at 37°C.

2.9.4 Histological staining

Glass staining troughs and racks, storage containers and all histological stains were obtained from BDH. Glass microscope slides, coverslips and paraffin wax, (Lambwax - melting point 57-58°C) were obtained from Raymond Lamb (UK). HistoClear was purchased from National Diagnostics (Atlanta, GA, USA). Dehydrated samples on slides were mounted in dextropropoxyphene (DPX, BDH). Citifluor aqueous mount and clear nail varnish was used to mount aqueous samples (Citifluor Scientific, Cambridge).

Section integrity and histology was assessed by staining with the nuclear and cytosolic stains (respectively) haemotoxylin and eosin, using the following

protocol. Sections were placed in a polythene rack and rehydrated and dewaxed by sequentially passing through HistoClear twice, for 10 minutes each and a graded alcohol series of 100% (×2), 95%, 85%, 70%, 50% and 30% each for 5 minutes. The slides were then washed in filtered water for 5 minutes to equilibrate the tissue. Nuclei were stained by immersing the slides in Erhlich's or Mayer's haematoxylin for 5 minutes followed by running tap water for 5 minutes to develop the blue coloration. The sections were dehydrated to 95% ethanol, (5 minutes in each grade), and dipped in 1% eosin in 95% ethanol for 5 minutes followed by a wash in 95% and 100% ethanol. Finally, the slides were immersed in HistoClear twice, for 10 minutes each before mounting in DPX and drying overnight in a fume hood.

2.10 *In situ* detection of mRNA

2.10.1 Synthesis of digoxygenin (dig)-labelled riboprobe

The plasmid to be transcribed was linearised with an appropriate restriction enzyme (see table 2.2), in a volume sufficient to yield ~1mgml^{-1} after the digest and purification. Linearised plasmid was purified and washed using phenol extraction (as described above). Transcription of labelled RNA was carried out as described in the Boehringer–Mannheim protocol for the labelling of riboprobes. In brief, nucleotide mix (containing Dig-UTP), 0.001 DTT, 1µg linearised plasmid, RNase-inhibitor and the appropriate RNA polymerase (T3,

T7 or SP6) and DEPC water were mixed to a volume of 20µl. This was incubated for one hour at 37°C, and 1µl removed. Then, 2µl of RNase-free DNase I was added and the mixture incubated for a further 15 minutes at 37°C. Pre-DNase-treatment and post-DNase-treatment samples were compared on a native gel, to assess the success of the RNA synthesis and the success of the DNA degradation. Labelled RNA was then precipitated by overnight suspension in 70% ethanol with 3M NaOAc at –20°C, and harvested by centrifugation for 15 minutes at 4°C. The consequent pellet was washed in 70% ethanol, allowed to air-dry for a few minutes (typically 5–10), and resuspended in 100µl of TE. This was stored at –20°C, until resuspension in hybridisation buffer (see below) for use *in situ*.

Table 2.2. Riboprobe synthesis conditions

cDNA	Plasmid vector	Linearised with:	RNA polymerase
Chx10 antisense	pBS KS	*Not*I	T3
Chx10 sense	pBS KS	*Eco*RI	T7
Crx antisense	pGEM T-easy	*Not*I	T7
Crx sense	pGEM T-easy	*Nco*I	SP6
Brn3b antisense	pGEM T-easy	*Not*I	T7
Brn3b sense	pGEM T-easy	*Nco*I	SP6
Pax6 antisense	pBS KS	*Not*I	T3
Pax6 sense	pBS KS	*Eco*RI	T7
Novel human cDNA antisense	Modified pBS KS	*Eco*RI	T7
Novel human cDNA sense	Modified pBS KS	*Not*I	T3

2.10.2 RNA in situ *hybridisation*

In situ hybridisation was performed using a protocol modified from Breitschopf *et al.* (1992). Most steps were performed in 400ml glass troughs, containing 250 ml of liquid. Sections were dewaxed in two changes of xylene and rehydrated through graded ethanol (100% (×2), 95%, 85%, 70%, 50% and 30% each for 2 minutes). Sections were then postfixed in 4% paraformaldehyde in PBS for ten minutes, washed for 15 minutes in three changes of Tris-buffered saline (pH7.5) (TBS), then partially denatured in 0.2M HCl for ten minutes, and washed as before in TBS. Sections were acetylated for ten minutes in 0.5% acetic anhydride in 0.1M Tris (pH8), by drizzling acetic anhydride over the sections in a glass rack, while the trough was being gently stirred by a magnetic stirrer. Following this, the slides were washed as before in TBS. The tissue was partially digested at 37°C with Proteinase-K for ten minutes at a concentration of 50 μgml^{-1} in a 30ml solution of TBS in a plastic Coplin jar (BDH) with 2mM $CaCl_2$, and again washed in two changes of TBS. Tissue was dehydrated again through graded alcohols, and left to dry for up to 2 hours. A ring was drawn around the sections using an hydrophobic wax pen (DAKO Ltd, High Wycombe, Bucks, UK) for later in the protocol.

Antisense and sense riboprobe was diluted in hybridisation buffer consisting of 2× SSC, 10% dextran sulphate (Sigma), $100\mu gml^{-1}$ sheared salmon sperm (Gibco) and 50% formamide (Sigma), and 100µl (approximately equivalent to 40µg of RNA, dilution of 1:20) was applied to sections overnight at 65°C underneath a glass coverslip. Unhybridised probe was washed off with

1×SSC 50% formamide at 60°C for 1 hr, then 20 minutes in 1×SSC and 10 min in 0.5×SSC at room temperature. Sections were then washed in 0.1M maleic acid buffer (pH7.5) with 0.3% Tween 20 for ten minutes, and blocked in 1% Blocking reagent (Boehringer, Germany) in maleic acid buffer for 30 minutes. Slides were incubated for 1 hr with 400µl of anti-digoxigenin alkaline-phosphatase-conjugated Fab fragments (Boehringer–Mannheim) at a 1 in 500 dilution in 1% blocking solution, and washed for 1 hr in maleic acid buffer. Probes were visualised by incubating in a 1:1 molar ratio of BCIP and NBT in Tris pH9.5 (the alkaline pH is critical for the colour reaction to proceed). The reaction was incubated for 10mins in the dark, and then closely observed until staining was visible. This could range from 10 mins to 24 hours for different probe preparations. The reaction was terminated by submerging the slides in tap water. Slides were dehydrated as described in section 2.9.4, and mounted in DPX (Sigma) or Citifluor. Images were digitally captured and processed using Adobe PhotoShop 3.1, or 5.0

2.11 Immunohistochemistry on paraffin embedded sections

Immunohistochemistry was performed on paraformaldehyde fixed, paraffin embedded tissue cut into 6–8µm sections. Several methods were tested to establish the best results for the antibodies against Chx10 (kindly provided by T. Jessell, Howard Hughes Medical Institute, Columbia University, New York), and

Crx (kindly provided by C. Gregory-Evans, Imperial College London). Sections were dewaxed and antigens unmasked by microwaving in Declere (Cell Marque, USA) at 60% power for 10 minutes. Endogenous peroxidase was blocked by treatment in 0.6% H_2O_2; this step prevents false signal, as the colour reaction for the tertiary detection of the antigen relies on exogenous H_2O_2. Tissue was permeabilised by incubation in 0.5% Triton ×100 in 0.05M Tris–HCl, and blocked for 1 hour in 10% foetal calf serum. Antibody at a range of dilutions (1/250–1/4000 were tested, and 1/1000 was found to generate the best results) in 1% foetal calf serum was applied to sections overnight at 4°C. Biotinylated goat anti-rabbit (Sigma) at a 1/600 dilution was applied to the sections for 1 hour at room temperature, and the signal amplified by incubation in ABC biotin/streptavidin amplification kit according to the manufacturers instructions (Vector Laboratories, USA). This process amplifies the immunolocalised signal by binding further biotinylated streptavidin complexes, thus providing more colour-reactive H_2O_2 molecules to interact with 3,3'-Diaminobenzidine (DAB) (Sigma/Vector Laboratories), which is a substrate for horseradish peroxidase and produce a brown water-insoluble precipitate. The colour reaction was sometimes modified to produce a darker signal by the addition of nickel to the DAB buffer.

2.12 Gene expression by RNA analysis

2.12.1 RNA extraction

All solutions for RNA work were made, where possible, from solids that were kept separate from the general chemicals in the laboratory, and using DEPC treated water. DEPC is a potent inhibitor of ribonuclease (RNase) and is broken down to ethanol and carbon dioxide by autoclaving. RNAse-free pipette tips were used throughout the procedure.

Total RNA was extracted from tissues and cultured cells using TRI-Reagent (Sigma) (or RNAzol) promotes the formation of RNA complexes with guanidinium and water molecules and inhibits hydrophilic interactions of DNA and proteins. As a consequence, DNA and proteins are excluded from the aqueous phase, leaving the RNA, which can then be purified. The RNA contains the whole range of cellular RNA molecules.

Tissues for RNA extraction were freshly dissected and were homogenised in 1 ml TRI-Reagent per 100 mg of tissue. Homogenates were transferred into a 1.5 ml microfuge tube and left at room temperature for 5 min to allow the complete dissociation of nucleoprotein complexes. The homogenate was supplemented with 0.2 ml of chloroform per ml of TRI-Reagent. It was then vortexed, and left to stand at room temperature for 10 min. The samples were centrifuged at 12,000 rpm at room temperature for 15 min. The homogenate separated into an upper clear aqueous phase containing the RNA, and a lower red coloured phase containing the DNA and protein,

separated by a thick interface of cellular debris and protein. The upper aqueous phase was carefully transferred to a new tube and 0.5 ml of isopropanol was added as well as 10 µl of a carrier, linearised polyacrylamide, if necessary. Samples were mixed, left to stand at room temperature for 10 min to precipitate the RNA and centrifuged at 12,000 rpm for 10 min. The white RNA pellet formed at the bottom of the tube was washed with 75% ethanol and resuspended in an appropriate amount of DEPC water depending on the size of the pellet. RNA was quantified by spectrophotometry and visualised on a denaturing gel (1% agarose, 1× MOPS, 5% v/v formaldehyde), and stored at –70°C until used.

2.12.2 RT-PCR

~1µg of RNA template was used in a 25µl reaction, using Promega reagents of 2µl oligo-dT, 5µl MMLV 5x buffer, 1.25µl 10mM dNTP, 0.75µl RNase-out, or other RNase inhibitor, and up to 15µl of DEPC dH_2O. This reaction was incubated at 65°C for 10 minutes, then quenched on ice. 1µl of Reverse Transcriptase was added, and the mix incubated at 42°C for 90 minutes. This cDNA was stored at -20°C indefinitely.

Equivalent amounts of cDNA were used in RT-PCR reactions, with 30 cycles for *Chx10*, *PGM1*, and *Crx*, and 34 cycles for *Brn3b*. A list of primers used in all experiments is given in Table 2.1.

2.13 Western blotting

2.13.1 Tissue lysis

Tissue was dissected in ice cold PBS, added to solubilisation buffer and kept on ice for 15 mins. Tissue was then triturated using a series (19-21-23 gauge) of needles attached to a syringe (Becton Dickinson). Retina was solubilised in either ice-cold PBS or ice-cold RIPA buffer (150mM NaCl, 1% Tergitol, 0.5% Sodium Deoxycholate, 0.1% SDS, 50mM Tris-HCL pH 8.0) containing protease inhibitor cocktail (Sigma) The lysed tissue was then centrifuged at 14,000 rpm for 2 mins and the supernatant mixed 1:1 with laemmli sample buffer.

2.13.2 Electrophoresis and labelling of proteins: Sodium Dodecyl Sulphate-polyacrylamide gel electrophoresis (SDS-PAGE)

SDS-PAGE was performed using 12cm $\times$ 10cm glass plates assembled according to manufacturers protocols (Biorad). The appropriate percentage separating gel was prepared (see Table 2.3 for constituents) and pipetted between the plates taking care to avoid air bubbles. The gel was pipetted to a height that left enough room for the stacking comb plus 1cm of stacking gel, and subsequently overlaid with distilled H_2O. The gel was left for 45mins to polymerise, the overlaying H_2O poured off and the stacking gel prepared (see Table 2.4 for constituents). The stacking gel was then pipetted on top of the separating gel and the comb inserted, again taking care not to trap air bubbles. The gel was again left for 45 mins to polymerise, at which point the comb was

removed and any unpolymerised acrylamide removed from the wells by rinsing with distilled H_2O and the resulting gel was mounted using a vertical slab gel unit and bathed in Laemmli running buffer (25mM Tris, 192mM glycine, 0.1% SDS). Protein samples were denatured by heating in a 100°C heat-block for 5 mins in Laemmli sample buffer (125mM Tris, 4% SDS, 20% glycerol, 5% β-mercaptoethanol). Samples were loaded into each well using a gel loading pipette tips (Biorad) and electrophoresis applied at 10mA (Amersham Pharmacia Biotech EPS-300 powerpack).

Table 2.3. Separating gel constituents for SDS-PAGE (18 ml)

	4%	6%	8%	10%	12%	15%
Monomers (ml)	2.4	3.6	4.8	6.0	7.2	9.0
1.5M tris-HCL pH 8.8 (ml)	4.5	4.5	4.5	4.5	4.5	4.5
10% SDS (µl)	180	180	180	180	180	180
Distilled H_2O (ml)	10.8	9.6	8.4	7.2	6.0	4.2
APS (µl)	110	100	100	90	90	80
TEMED (µl)	11	11	10	8	8	7

Table 2.4. Stacking gel constituents for SDS-PAGE (5 ml)

	4%
Monomers (vl)	651
0.5M tris–HCL pH 6.8 (ml)	1.25
10% SDS (µl)	50
Distilled H_2O (ml)	3.0
APS (µl)	25
TEMED (µl)	5

2.13.3 Semi-dry and wet transfer western blotting

For semi-dry transfer the following sandwich was assembled on the anode. Three layers of absorbent paper (Whattman 3 MM) were wetted in transfer buffer

(48mM Tris, 39mM glycine, 0.037% (v/v) SDS, 20% (v/v) methanol) followed by the nitrocellulose membrane (Schleicher & Schuell) soaked in distilled H_2O. The polyacrylamide gel was laid on top followed by a further three layers of absorbent paper wetted in transfer buffer. Air bubbles were removed by rolling the sandwich with a pipette, the cathode plate was placed on top and a current of 0.8 mA cm^{-2} of gel was applied for a period of 1.5 hours.

Following electrophoretic transfer the nitrocellulose membrane was removed from the sandwich and washed twice in PBS for 5 mins. To check for efficient transfer of proteins the membrane was stained with a 1 in 10 dilution of Ponceau S solution (Sigma) (20% Ponceau S dissolved in 30% trichloroacetic acid, 30% sulfosalicyclic acid) which was added to the nitrocellulose membrane for 3 mins before being rinsed off with distilled H_2O and the molecular weight ladder bands marked with pencil. The membrane was rinsed several times in PBS to remove all Ponceau S before being processed for either immunological detection of proteins or blot-overlays.

2.13.4 Immunological detection of immobilised proteins

Non-specific sites on the membrane were blocked by incubation of the membrane in 5% Marvell in PBS at 4°C overnight. The membrane was then removed from the blocking solution and washed once for 10 mins in PBS, 0.1% (v/v) Tween-20. The primary antibody was diluted to the appropriate concentration in 5% Marvell, 0.1% Tween-20 and incubation was performed in a heat-sealed bag for 1 hour with agitation at RT. The blot was subsequently

washed three times for 10 mins in PBS, 0.1% (v/v) Tween-20. The HRP-conjugated secondary antibody was diluted in 5% Marvell, 0.1% Tween-20 in PBS and again incubated with the membrane in a heat-sealed bag for 1 hour with agitation at RT. The blot was then washed three times for 10 mins in PBS, 0.1% (v/v) Tween-20, once in PBS for 5 mins and then processed using the enhanced chemiluminescence (ECL) (Amersham Pharmacia Biotech) method. ECL was achieved by performing the oxidation of luminol by HRP in the presence of chemical enhancers. The membrane was covered in detection buffer, a 50:50 mix of solution 1:solution 2 for exactly 1 min, subsequently drained, wrapped in SaranWrap and placed in a film cassette. The membrane was then exposed to blue-light sensitive autoradiography film (Kodak) and mechanically developed.

2.14 Primary cell cultures

Various forms of primary retinal cultures were investigated to test a number of different gene expression criteria.

Dulbecco's modified essential medium (HEPES buffered DMEM), F12 modification of Eagle's minimal essential medium with ribosides and deoxyribonucleosides (α-MEM), Leibovitz's medium (L-15 code number 11415) and Dulbecco's calcium-, magnesium- and sodium bicarbonate- free phosphate buffered saline, were all supplied by Gibco BRL (UK). Foetal calf serum (FCS) was purchased from Sigma-Aldrich (UK). Penicillin/streptomycin solution

(100,000 units per ml) was purchased from Sigma-Aldrich. Tissue culture grade petri-dishes and other plastics were supplied by Philip Harris (UK), Nunc Inc (IL, USA) and Helena Bioscience (UK).

P0 (new-born) pups were killed by cervical dislocation (typically by decapitation with a scalpel) and their heads transported from the animal laboratory to the procedures laboratory in ice cold L15 medium (typically 20 minutes), a minimal medium that does not promote cellular differentiation or proliferation. Eyes, and subsequently retina were carefully micro-dissected and placed in F12 medium, being mindful to remove lens, RPE and any other extra-retinal tissue. Typically, up to 30 individual eyes were used per experiment, and divided into 8 wells. However, this was variable, given the unpredictable fecundity of the *or*^{J} mouse.

A similar procedure was used for embryonic mice, although embryos were transported undissected and *in utero* before retinal dissection.

Retinal tissue was partially mechanically dissociated by titration through a fine-bore glass pipette up to 10 times, and then enzymatically dissociated by incubation in 0.025% Trypsin–EDTA for 4 minutes at 37°C. This reaction was halted by the addition foetal calf serum (FCS) to a final concentration of 10%. After gentle spinning down on a bench centrifuge (500 rpm for 5 minutes), cells were resuspended in a volume of F12 (containing 25mM HEPES, 100 units ml^{-1} penicillin, 100$\mu g ml^{-1}$ streptomycin, and 10% FCS) estimated to give a concentration in the culture wells of ~200–300 cells per µl, as calculated by cell-counting using a haemocytomter. Typically this volume was ~2ml. Adjustments

of volume were made by either adding medium, or gentle centrifugation (as above) and resuspension.

In order to aid adhesion of cells in culture, glass coverslips were placed in 24 well cell culture plates with a diameter of 102 mm, a 10% mixture of laminin and poly-L lysine used to coat them for up to 30 minutes. Coverslips were allowed to dry before application of cell-containing medium. Up to 200µl of culture was used per well, and this volume was adjusted according to the requirements of the experiment (see below).

Variations on several conditions of the culture medium were tried in order to optimise these settings.

After 6 hours the medium was changed to remove any dead cells and any cell debris. Cells were typically incubated in culture for up to 72 hours, and were checked regularly for vitality, before performing immunocytochemistry.

2.15 Immunocytochemistry

These experiments on cultured retinal cells were designed to investigate gene expression, and whether it could be altered in both the wild-type and *or*^{J} cultures. Therefore, immunocytochemistry was performed on cultured cells after a period in culture to assess the expression of specific epitopes. Medium was removed from cell cultures wells and wells were washed 3 times with PBS. Cells were then fixed with ice cold methanol for 20 minutes (which was found to

retain morphology better than PFA fixation), and again washed 3 times in PBS. Primary antibody was applied in goat serum in PBS at a concentration of 1/500 (Crx, Chx10), 1/1000 (H3 and PCNA). H3 rabbit polyclonal IgG was obtained from Upstate Biotechnology (New York, USA). The immunogen used for the antibody production was a KLH-conjugated peptide corresponding to amino acids 7-20 of the human histone H3. Anti-PCNA (PC10) (cell division marker) mouse monoclonal IgG_{2a} antibody was obtained from Santa Cruz Biotechnology, Inc (California, USA). This antibody was derived by the fusion of BALB/c mouse spleen cells with recombinant PCNA, with Sp2/0-Ag14 myeloma cells. After one hour, wells were washed with 3 changes of PBS, and secondary antibody was applied as required.

Double labelling experiments were attempted, but owing to the fact that both Chx10 and Crx antibodies were raised in the same animal (rabbit), an alternative detection system was investigated.

2.15.1 Biotinylation of Crx antibodies

Crx antibodies were biotinylated using the following technique. Anti-Crx was diluted to 2.0 mg ml^{-1} in 1 ml of 0.1M $NaCO_3$ pH9.5, and then dialysed against 2 litres of 0.1M $NaCO_3$ pH9.5 overnight at 4°C, at which point the solution had an optical density of 2 at 280nm. Biotin ss-NHS (Biotin 3-sulfo-N-hydroxy-succinimide ester [Sigma-Aldrich, UK], 20 mg ml^{-1} in DMSO) was added to a ratio of 0.2 $mgmg^{-1}$, and this was incubated for 2hrs rotating at room temperature, and further dialysed against 4 litres of Tyrode's solution (plus

10mM Hepes, pH7.2, without Mg^{2+}). Biotinylation allowed for the simultaneous detection of Chx10 (with a fluorescent secondary antibody), and Crx using HRP and DAB, as described above. However, results were disappointing (see Chapter 4), and non-specific staining was observed. Therefore, this strategy was not pursued.

2.15.2 Fluorescent immunocytochemistry

Secondary antibodies used for immunocytochemistry were either goat anti-rabbit (TRITC) or rabbit ant-goat (FITC) (depending on the animal in which the primary antibody was raised), combined with a 1/500 dilution of Hoescht stain (which is a vital sub-nuclear marker) for 20 minutes in the dark (cells were kept in the dark from this point onwards). In double-labelling experiments, secondary antibodies were mixed and applied simultaneously. Wells were washed again three times in PBS, medium was removed without allowing the cells to dry, and then the coverslips were removed from the culture dishes using a bent hypodermic needle, and mounted inverted on microscope slides in a non-fluorescent aqueous mountant (either Aquamount, Citifluor, or 50% glycerol in water). Coverslips were sealed with nail varnish, and viewed on a fluorescent microscope with the appropriate filters. Photographs were either taken using Fujichrome100 Provia film, or using the digital imaging AlphaEase 3.3 software. Images were processed, and composite, superimposed images created in Adobe PhotoShop 5.0.

2.15.3 Culture conditions for altering gene expression

Experiments described in Chapter 4 aim to alter gene expression by various culture conditions. A co-culture system was used, in which *or*^{J} cells were exposed to secreted factors from wild-type cells. Transwells with a membrane pore size of 0.4 μm were purchased from Corning Costar (New York, USA). Mutant cells were placed on the membrane and wild-type cells in the well and cultured for 24 hrs. However, mutant cells did not survive longer than 24 hours in two experiments, and this technique was not pursued.

A second technique used was to expose *or*^{J} cells to medium that had itself been exposed to wild-type cells for 48 hours, and thereby contained all of the factors secreted by the wild-type cells during that period (conditioned medium). Wild-type E12.5 retinal cells were cultured as described above in F12 medium, which was removed after 48 hours, and this medium was diluted by half with fresh F12 (in order that there was a ready supply of fresh nutrients), and *or*^{J} cells were cultured for a further 48 hours.

Cultured *or*^{J} cells were also exposed to retinoic acid (RA) as a means of inducing photoreceptor gene expression (see Chapter 4). All-trans RA was resuspended in DMSO as a 50mM stock, and added to F12 culture at a concentration of 100nM. Control experiments containing equivalent amounts of DMSO without RA were also cultured. When culturing for 48 hours medium was replaced with fresh medium with 100nM RA after 24, in order to ensure a ready

supply of RA. As before, after 48 hours these cells were harvested for immunocytochemistry (as described above).

CHAPTER 3

ANALYSIS OF THE DEVELOPMENT OF THE HUMAN RETINA

CHAPTER 3

ANALYSIS OF THE DEVELOPMENT OF THE HUMAN RETINA

3.1 Introduction

Over 25% of the conditions listed in the Online Mendelian Inheritance in Man (OMIM) database feature an ocular phenotype (Gregory-Evans and Bhattacharya 1998, Ferda-Percin *et al.* 2000). This statistic indicates the high number of disease causing genes that are involved in development and maintenance of the eye.

Mutations in 14 transcription factor genes to date have been shown to cause human ocular diseases, thus indicating the significance of this class of protein in human retinal development (Freund *et al.* 1996). As in the mouse however, very few retinal cell fate-specifying genes have been identified. Although histological analysis is well established (Hollenberg and Spira 1972), few studies have been performed analysing transcription factor gene expression in the human retina.

I analysed the developmental expression patterns of three transcription factors in human retinal development, using tissue obtained with informed consent from terminated pregnancies. The transcription factors analysed are known to be essential for normal retinal development in the mouse, and two of them (CHX10 and PAX6) are ocular disease causing genes in humans (Ferda-Percin *et al.* 2000, Glaser *et al.* 1992, Wehr and Gruss 1996). These genes are all thought to mark specific cell types at early stages of their differentiation. This

study aims to compare the timing of retinal development in humans and mice. The period of time during which the retina develops in humans is condensed relative to total gestation time compared with the mouse. No mitotic cells are present in the human retina after 16 weeks post-conception (wpc) (Hollenberg and Spira 1972), whereas murine retina development continues until 12 days after birth (Young 1985). Although the order of cell birthing in the retina is thought to be conserved, the relative numbers of the various cell types differ considerably between human and other species, so analysis of patterns of cell specification will provide information about human retinal development as compared to murine eye development.

3.2 *CHX10* expression in the developing human retina

The human homologue of the mouse gene *Chx10* has recently been cloned and characterised. Mutations in *CHX10* have been shown to cause isolated microphthalmia, a condition that is very similar to the phenotype of the *or*^{J} mouse (Ferda-Percin *et al.* 2000, Burmeister *et al.* 1996).

I investigated the developmental expression pattern of *CHX10* in human foetal eyes as a means of establishing its function in human development. This was achieved by performing *in situ* hybridisation on wax embedded human tissue from 8 wpc up to 15 wpc, and in the adult retina. The protocol was performed as described in Chapter 2.10, Methods.

A 3kb plasmid containing the entire *CHX10* cDNA was kindly given by Rod McInnes (Hospital for Sick Children, Toronto, Canada), from which antisense and sense riboprobes were generated. These riboprobes contained the *CHX10* coding sequence (1.089kb), and a 1.9kb 3'UTR.

The earliest human tissue available was at 8 wpc. At this stage eye development is well under way, as shown in Figure 3.1, which is a transverse section through a foetal face. The section runs through the central retina on the right eye, shown by the presence of the optic nerve and optic nerve head on adjacent sections. On the left eye, the plain of section is dorsal retina, shown in Figure 3.1a, and does not cut through the vitreous.

The developing lens and cornea are present, as is the retinal pigmented epithelium, and neural retina. The retina is divided into two layers, inner and outer, separated by the layer of Chievitz, which is a transient acellular layer derived from the migration of cells into the inner layer (Hollenberg and Spira 1972). A nerve fibre layer (nfl) is visible, and forms the optic nerve head (onh) in the central retina. These observations indicate that the human retina is at a stage of development that is (in some aspects) approximately equivalent to E13.5 in the murine retina (Kaufman 1995 in *The Atlas of Mouse Development*). The presence of a nerve fibre layer, optic nerve head and an optic nerve indicates that post-mitotic ganglion cells are projecting axons.

CHX10 expression in the 8wpc foetal head was only detected in the neural retina and not in surrounding tissue, shown in blue/purple from the NBT/BCIP precipitate generated from the detection of digoxygenin labelled

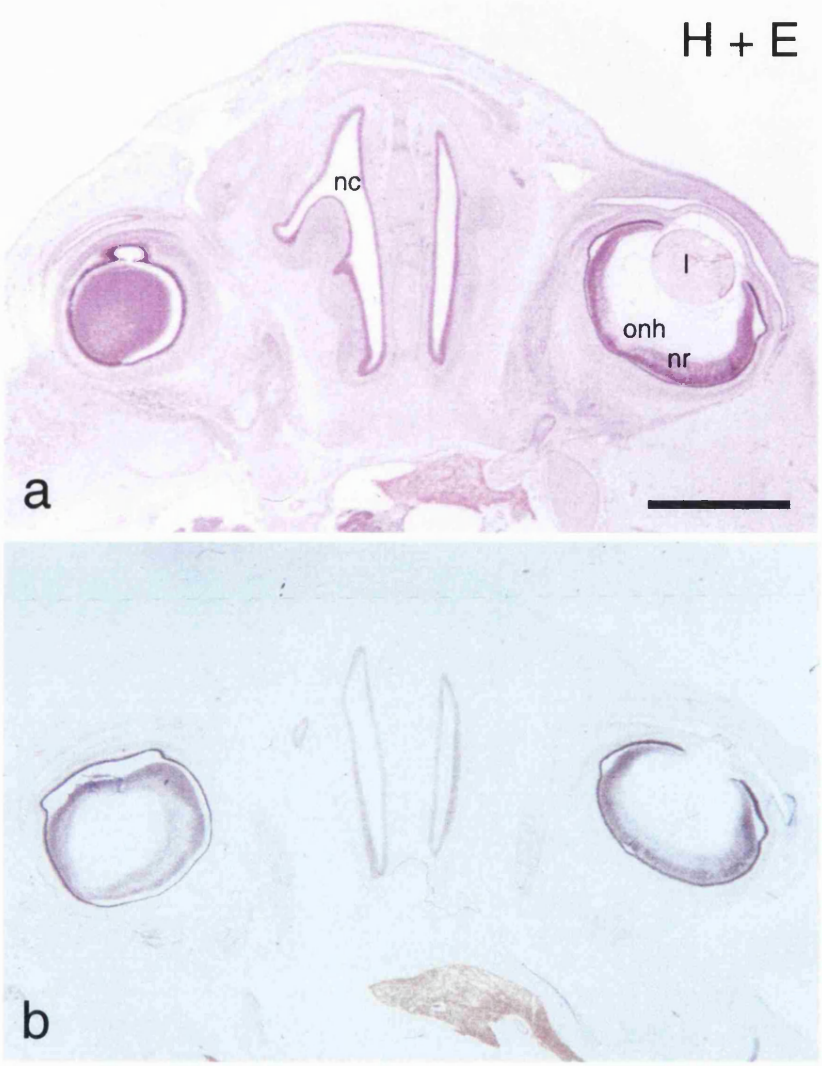

Figure 3.1. Transcription factor gene expression in the 8 wpc human retina by *in situ* hybridisation. In the 8wpc human retina (a), *CHX10* expression by *in situ* hybridisation (b). At this stage the retina is dived into two layers, and while *CHX10* expression can be readily detected in both, it is certainly expressed at lower levels in the inner layer. This may reflect the presence of differentiating ganglion cells in the inner layer, which do not express *CHX10*. Abbreviations: nc, nasal cavities; l, lens; nr, neural retina; onh, optic nerve head. Scale bar: 1mm.

riboprobe (Figure 3.1b). Figure 3.1b shows a low magnification image of this expression pattern. Although expression is detected throughout the retina, it is clearly more concentrated in the outer layer. This corresponds with the hypothesis that CHX10 is expressed in retinal neuroblasts, but not in postmitotic ganglion cells. The inner layer is the site of developing ganglion cells, (see below), and lower levels of CHX10 expression are detected here. CHX10 expression is most concentrated in the outer retina, but is certainly detectable in the inner, either in fewer cells, or at lower levels. This indicates one of two possibilities;

(1) The inner layer consists of dividing cells expressing CHX10, as well as postmitotic ganglion cells;

(2) Ganglion cells express CHX10 at low levels during this phase of development.

Data shown below indicates that ganglion cell markers and CHX10 do not co-localise at later stages in development, and certainly not in the adult retina. Therefore it seems more likely that this inner layer consists of ganglion cells, and mitotic cells that are expressing CHX10. The more concentrated expression in the outer layer indicates that this layer is predominantly neuroblastic, and fewer postmitotic cells are present.

At 10wpc (Figure 3.2c), the inner and outer layers are morphologically distinct, and the layer of Chievitz is no longer present (Hollenberg and Spira 1972). Cells within the inner layer are round compared with the more elongated and densely packed cells in the outer layer, possibly indicating that these cells

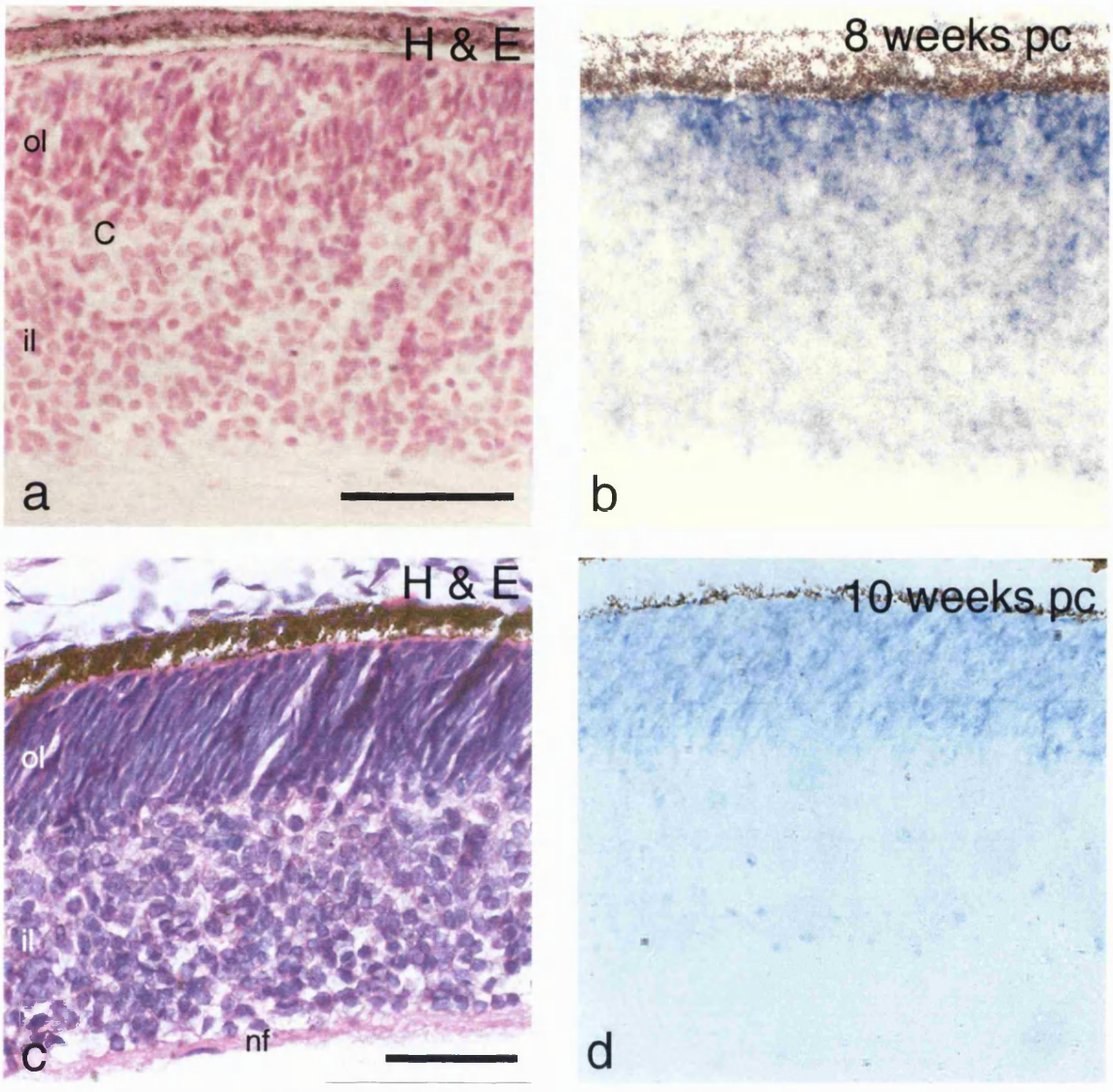

Figure 3.2. *CHX10* expression in the developing human retina by *in situ* hybridisation. (a) shows a high magnification image of Fig. 3.1, an 8 week post conception (pc) human retina. Two distinct cellular layers can be resolved, and *CHX10* expression (b), although present in both, is reduced in the inner layer (il). By 10 weeks (c), the inner layer has expanded considerably, and the outer layer remains densely packed. CHX10 is by this stage only significantly expressed in the outer layer, reflecting both the mitotic nature of cells within this layer, and the presence of postmitotic ganglion cells in the inner. Abbreviations: C, layer of Chievitz; nf, nerve fibre layer. Scale bars 100μm.

are migratory. The nerve fibre layer is clearly present (nf). The expression domain of *CHX10* is now restricted to the outer layer, and a very few individual cells in the inner layer. This is consistent with the evidence that *CHX10* is not expressed in ganglion cells (Burmeister *et al* 1996). The concentration of *CHX10* expression in the outer layer suggests that the majority of cells are dividing progenitor cells.

The ganglion cell layer is the first to form, and is largely postmitotic by 10 wpc (Hollenberg and Spira 1972, Oyster, The Human Eye, 1999). However, other discrete retinal layers have not yet been formed, indicating that many cells divisions and cell differentiation has to take place in order for the rest of the cells and layers of the retina to develop.

By 13wpc, lamination is well under way in the retina (Figure 3.3a). The ganglion cell layer has become separated from the rest of the retina by the presumptive inner plexiform layer. Cells in the neuroblastic layer are morphologically indistinguishable, indicating that the human retina is roughly equivalent to the E18.5–P2 murine retina (Kaufman 1995 in *The Atlas of Mouse Development*). The expression domain of *CHX10* is restricted entirely to the neuroblastic layer (Figure 3.3b), and no Chx10 expressing cells can be detected in the ganglion cell layer. However, *CHX10* expression is restricted to the inner aspect of the neuroblastic layer, and cells in the outer-most aspect are not expressing *CHX10.*

Foetal tissue is obtained with informed consent from terminated pregnancies, ethical approval was not granted for tissue older than 13 weeks,

and was not available for analysis. Figure 3.3c shows the histology of the adult human retina. The characteristic three cellular layers are clearly visible (ganglion cell, inner nuclear, and outer nuclear), separated by the two plexiform layers (inner and outer), and the inner and outer segments of the photoreceptors are fully developed and embedded in the retinal pigmented epithelium. In the adult retina, *CHX10* expression is restricted to cells within the inner nuclear layer. Furthermore, these cells are located on the outer aspect of the inner nuclear layer. The location of CHX10-positive cells corresponds with the location of bipolar cells, although as in the murine retina, the band of *CHX10* expressing cells is probably wider than just the bipolar cell layer, indicating that *CHX10* expression may persist in other cells within the inner nuclear layer, particularly horizontal cells, whose location is similarly in the outer aspect of the inner nuclear layer. Due to their location on the inner aspect of the inner nuclear layer these cells are unlikely to include amacrine cells (see below).

These data suggest that the postulated functions of Chx10 in the murine retina are indistinguishable to those of its human orthologue from in the human retina, i.e., *CHX10* is expressed in retinal neuroblasts during early development, but later its expression is restricted predominantly to bipolar cells (but possibly to other cells within the inner nuclear layer).

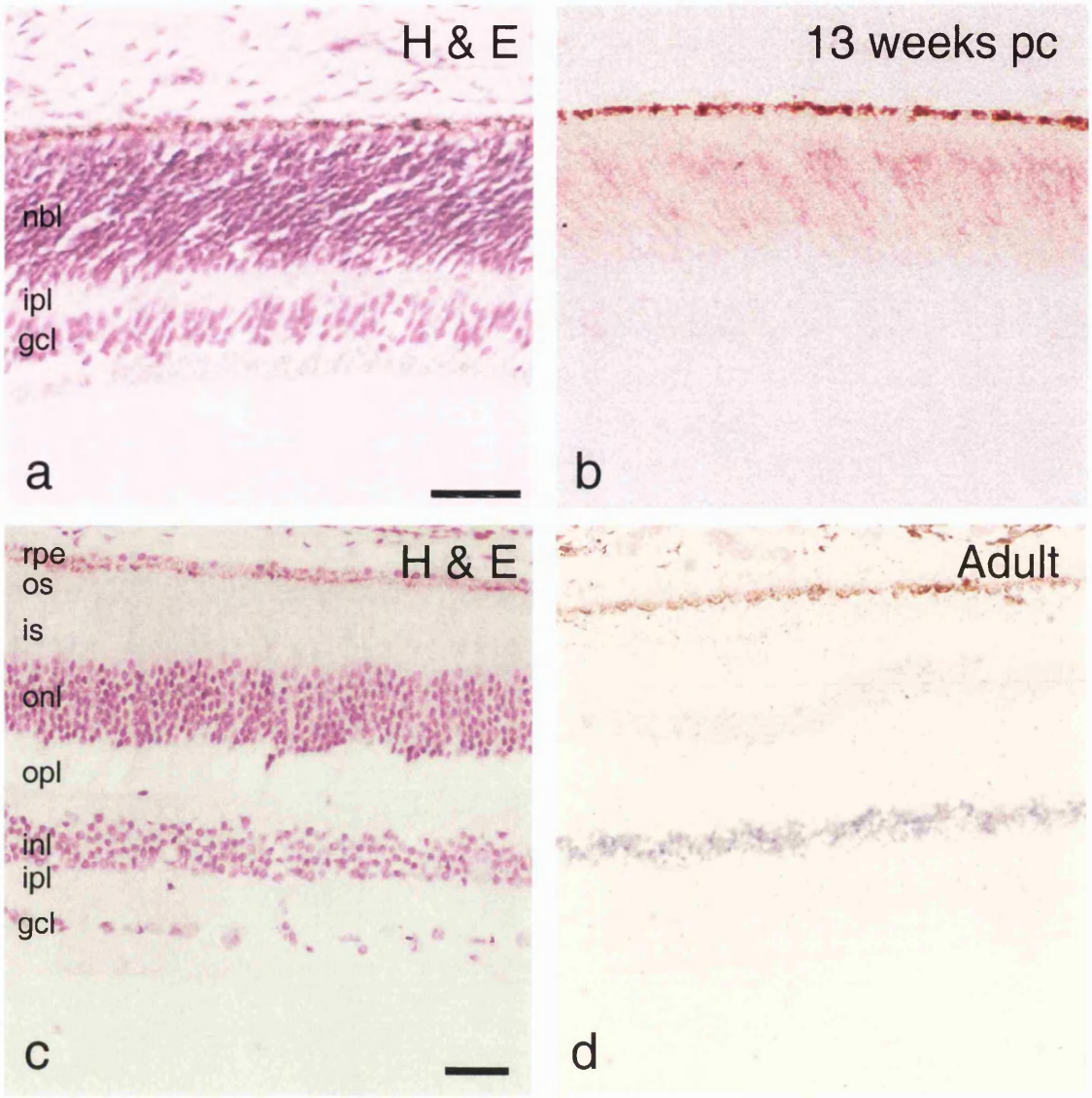

Figure 3.3. *CHX10* expression in the developing and adult human retina by *in situ* hybridisation. At 13 weeks, the retina is partially stratified, with a clear ganglion cell layer (gcl) and inner plexiform layer (ipl). *CHX10* expression is restricted to the neuroblastic layer (nbl), but a sharp demarcation of expression exists in the outer aspect of this layer. This may reflect the presence of cells differentiating as photoreceptors, which do not express Chx10. In the adult retina *Chx10* expression is restricted top cells within the outer aspect of the inner nuclear layer (inl). Abbreviations: rpe, retinal pigmented epithelium; os, outer segments; is, inner segments; onl, outer nuclear layer; opl, outer plexiform layer. Scale bars = 100μm.

3.3 Expression of *BRN3b* and *PAX6* in the developing retina

Plasmid containing a 200bp fragment of the mouse *Brn3b* gene was kindly donated by David Latchman (Institute of Child Health, UCL, London). Over the length of this fragment, the sequence conservation between mouse and human is high enough to make a useful human riboprobe (Liu *et al.* 2000). In the mouse, *Brn3b* is expressed in the retina exclusively in a proportion of postmitotic ganglion cells, and is the first known marker of a ganglion cell fate (Xiang, 1998). Evidence from expression studies and analysis of mice containing targeted deletion of *Brn3b* indicate that it is not required for ganglion cell fate specification, but is required for correct differentiation and maintenance of this cell type (Gan *et al.* 1999).

PAX6 is involved in the earliest stages of eye development, but in the adult retina in both humans and mice expression is maintained in a proportion (~30%) of ganglion cells (Graw 1996, Nishini *et al.* 1999), and in amacrine cells of the inner nuclear layer. Expression patterns for *BRN3B* and *PAX6* were generated by *in situ* hybridisation as described above and in Chapter 2, Methods.

At 8wpc, expression of *BRN3B* expression (Figure 3.4b) can be seen throughout the neural retina, but is more concentrated in the inner layer. This expression pattern may reflect the developing ganglion cell layer; the punctate and lower levels of *BRN3B* expression in the outer retina may reflect the migration of postmitotic ganglion cells into the presumptive ganglion cell layer.

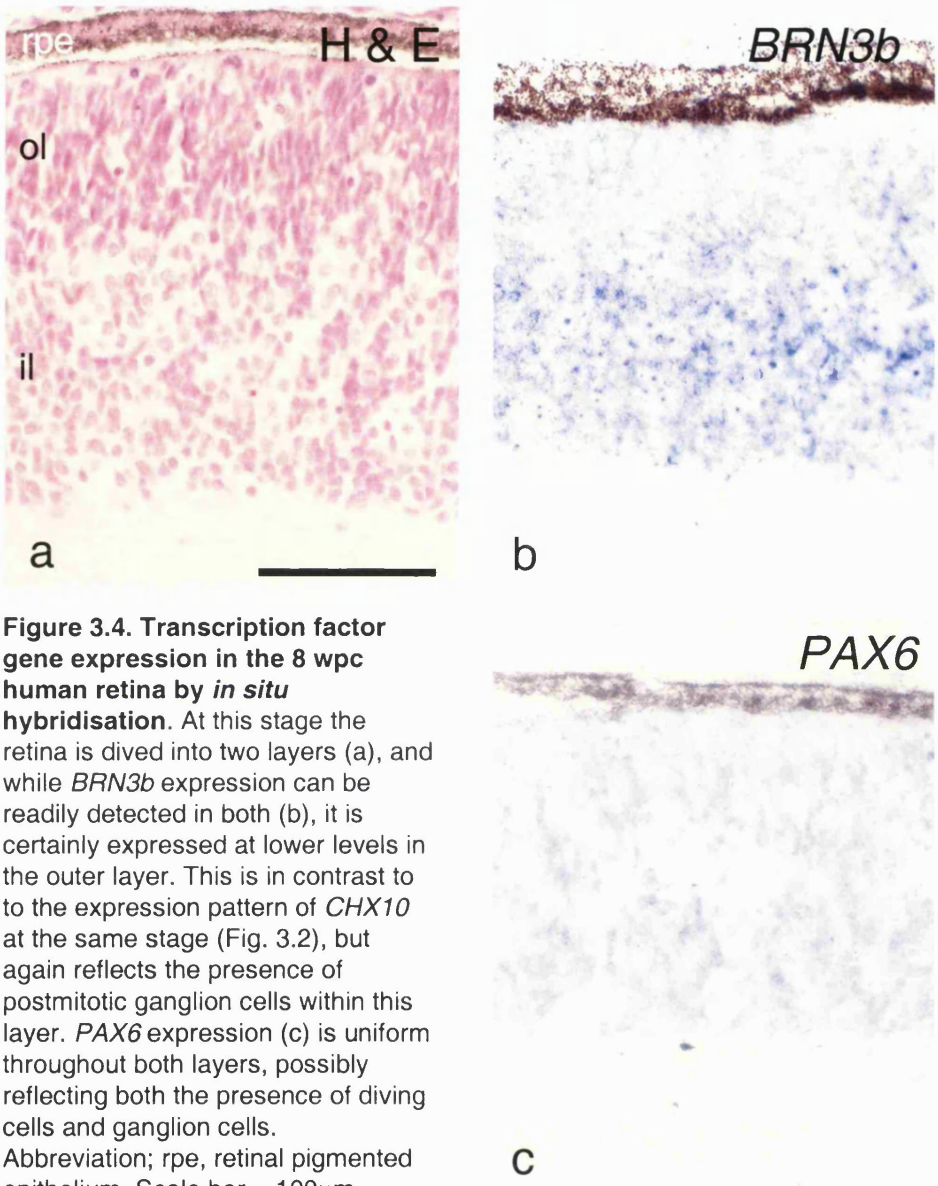

Figure 3.4. Transcription factor gene expression in the 8 wpc human retina by *in situ* hybridisation. At this stage the retina is dived into two layers (a), and while *BRN3b* expression can be readily detected in both (b), it is certainly expressed at lower levels in the outer layer. This is in contrast to to the expression pattern of *CHX10* at the same stage (Fig. 3.2), but again reflects the presence of postmitotic ganglion cells within this layer. *PAX6* expression (c) is uniform throughout both layers, possibly reflecting both the presence of diving cells and ganglion cells. Abbreviation; rpe, retinal pigmented epithelium. Scale bar = 100μm.

The expression gradient observed is complementary to that observed for *CHX10* (Figure 3.2).

In contrast to the gradients of expression seen at 8wpc for both *CHX10* and *BRN3B*, *PAX6* expression (Figure 3.4c) is seen uniformly throughout the retina. As *Pax6* in mice is expressed in retinal neuroblasts and ganglion and amacrine cells, it is difficult to dissect this expression pattern at this stage of development with reference to specific cell types. Judging from intensity of staining, cells are either expressing *PAX6* at lower levels, or not every cell is *PAX6*-positive. However, single-cell resolution is not visible. Given that *PAX6* is only expressed in a relatively small proportion of ganglion cells, the lower levels of expression seen in the inner layer may reflect *PAX6* expression in ganglion cells.

In the 10wpc retina, the morphological distinction between the inner and outer retina is far clearer (Figure 3.5a), and as discussed above, *CHX10* expression is maintained only within the outer (neuroblastic) layer (Figure 3.2d). Expression of *BRN3B* (Figure 3.5b), by contrast, is almost entirely restricted to the inner layer. This suggests that by 10wpc the majority of ganglion cells are found within a single layer of the retina. There are a very few *BRN3B*-positive cells within the outer layer, which may reflect late born ganglion cells within this layer as they migrate towards the putative ganglion cell layer.

PAX6 expression at this time (Figure 3.5c) is similarly restricted to the inner layer, with a few individual cells expressing in the outer layer. The intensity of *PAX6* expression is higher than that of *BRN3B* within this inner

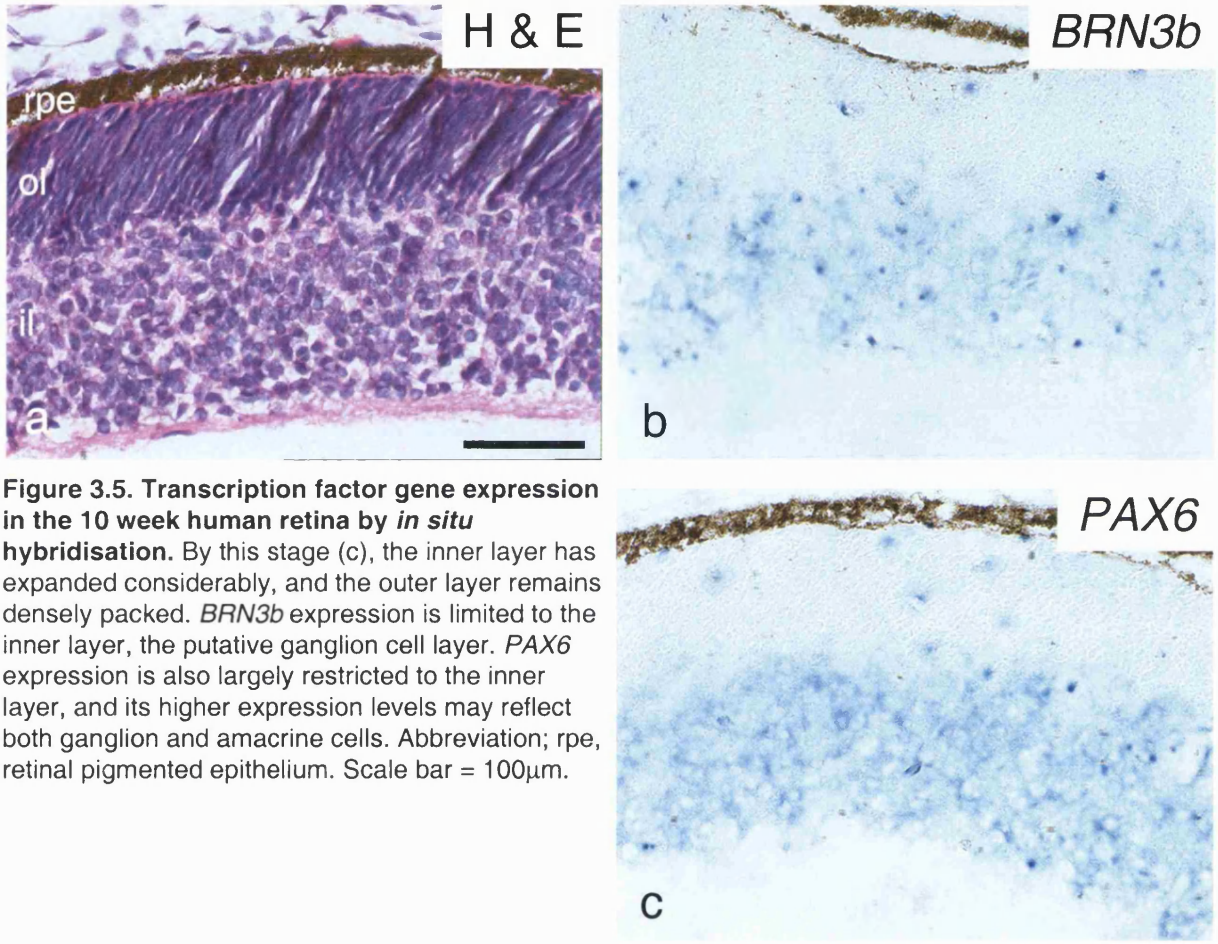

Figure 3.5. Transcription factor gene expression in the 10 week human retina by *in situ* hybridisation. By this stage (c), the inner layer has expanded considerably, and the outer layer remains densely packed. *BRN3b* expression is limited to the inner layer, the putative ganglion cell layer. *PAX6* expression is also largely restricted to the inner layer, and its higher expression levels may reflect both ganglion and amacrine cells. Abbreviation; rpe, retinal pigmented epithelium. Scale bar = 100μm.

layer. Although *PAX6* is expressed in proportionally fewer ganglion cells than *BRN3B*, this increased intensity of staining may reflect development of amacrine cells within the inner retina at 10wpc.

In the adult retina, *BRN3B* expression (Figure 3.6b) is weakly detected in the ganglion cell layer, suggesting that this gene has a role in the maintenance of this cell type. Expression appears to be in the majority of cells within this layer, consistent with the expression pattern seen in the mouse, and the loss of 70% of ganglion cells within the *Brn3b* targeted deletion mouse (Gan *et al.* 1996, 1999).

PAX6 expression in the adult human retina (Figure 3.6c) is seen in the ganglion cell layer in the majority of cells. This is in contrast to the 30% of *Pax6* expressing cells within the ganglion cell layer observed in the mouse. Although the differential gene expression patterns for the many different classes of ganglion cells has not been established, this may reflect differences in the relative proportions of distinct ganglion cell classes between mouse and human.

Expression of *PAX6* is also readily detected in the inner nuclear layer, in a discreet band on the inner aspect. This position is consistent with the location of amacrine cells (Hollenberg and Spira 1972). In comparison to the expression of *CHX10* in the inner nuclear layer there is no overlap between *CHX10* and *PAX6* expression domains, indicating that the cells expressing *CHX10* are certainly not amacrine cells.

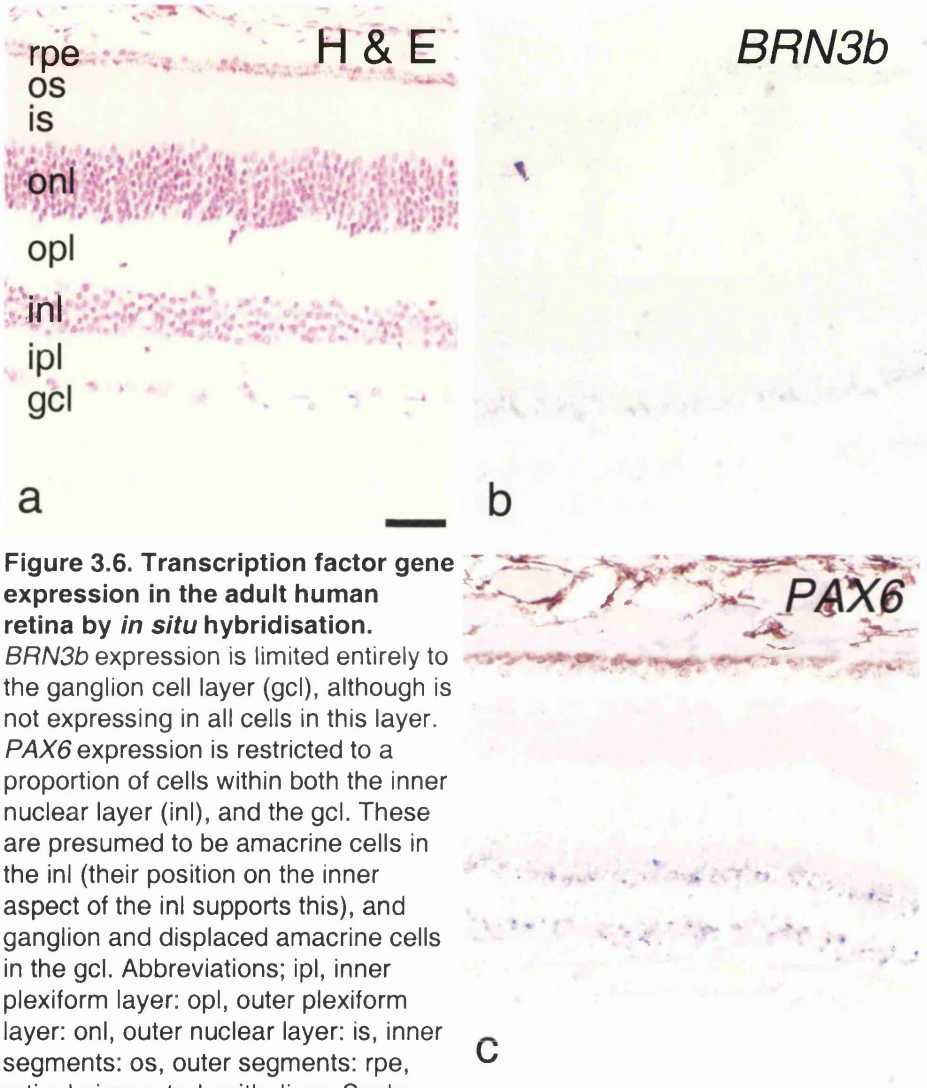

Figure 3.6. Transcription factor gene expression in the adult human retina by *in situ* hybridisation. *BRN3b* expression is limited entirely to the ganglion cell layer (gcl), although is not expressing in all cells in this layer. *PAX6* expression is restricted to a proportion of cells within both the inner nuclear layer (inl), and the gcl. These are presumed to be amacrine cells in the inl (their position on the inner aspect of the inl supports this), and ganglion and displaced amacrine cells in the gcl. Abbreviations; ipl, inner plexiform layer: opl, outer plexiform layer: onl, outer nuclear layer: is, inner segments: os, outer segments: rpe, retinal pigmented epithelium. Scale bar, 100μm.

3.4 Discussion

The data presented here suggest that the expression patterns, and possibly the functions of Chx10 in the murine retina are indistinguishable to those of its human orthologue from in the human retina. *CHX10* is expressed in retinal neuroblasts during early development, but later its expression is restricted predominantly to cells within the inner nuclear layer, predominantly bipolar cells.

The reduction in levels of *CHX10* expression in the inner retina at 8wpc corresponds with ganglion cell differentiation, which is marked by an upregulation in *BRN3B* expression at the same developmental stage. Expression of *PAX6* at 8wpc is uniformly throughout the retina. These last two pieces of data reflect the same expression patterns seen in the mouse at E13.5 (see Figure 4.3).

The restriction of *CHX10* expression at 13wpc may be an indication that photoreceptor genesis has begun, and these CHX10-negative cells are in fact postmitotic photoreceptors. This supports the evidence that *CHX10* is not expressed in postmitotic photoreceptors (Furukawa *et al.* 1997). This expression restriction has not been reported in any other species, including the mouse, chick and goldfish (Liu *et al.* 1994, Burmeister *et al.* 1996, Chen and Cepko 2000, Passini *et al.* 1998).

Expression patterns of *BRN3B* is largely the same as in the mouse, and this suggests that they are functional as well as structural homologues.

CHAPTER 4

ANALYSIS OF THE DEVELOPMENT OF THE RETINA OF THE *OCULAR RETARDATION* MOUSE

CHAPTER 4

ANALYSIS OF THE DEVELOPMENT OF THE RETINA OF THE *OCULAR RETARDATION* MOUSE

4.1 Introduction

The recessive mouse mutant *ocular retardation* (or^J) has a C→A transversion, which causes a tyrosine→ stop mutation at amino acid position 176 (Y176Stop) within the homeodomain of the transcription factor gene *Chx10* (Burmeister *et al.* 1996). The phenotype resulting from this mutation includes microphthalmia, blindness, an absent optic nerve, short, truncated photoreceptors and an absence of bipolar interneurons. Expression patterns of *Chx10*, coupled with analysis of the phenotype of the or^J retina suggests that Chx10 has a number of distinct roles in the developing eye, including as a promoter of proliferation in retinal neuroblasts, and also as a gene involved in establishing a bipolar cell fate.

Of the seven cell types found in the retina, immunohistochemical markers for all, bar bipolar cells, were found in the mature post-natal (P)14, P18 (or in the case of ganglion cells E14.5) or^J retina (Burmeister *et al.* 1996). This indicates that all cell types apart from bipolar cells are capable of differentiating in the absence of Chx10. Although the cellular composition of the mature or^J retina has been investigated, no studies have attempted to establish how development of distinct cell types differs in or^J from the wild type retina. Here, I

aimed to investigate how the timing of birthing and onset of differentiation of the various cell types of the retina was affected by the absence of Chx10, and whether alterations in differentiation patterns explains the disorganisation of the *or*^{J} retina.

The precise order and times at which the cell types leave the multipotential progenitor pool in the wild-type retina is well established through ^{3}H-thymidine incorporation studies (Young 1985). I chose to analyse the expression of cell specific markers (for the times investigated), which are known to be involved in cell specification at the earliest stages of cellular differentiation. All the genes analysed initially were transcription factor genes, and are the earliest known markers for each specific cell type. Homeodomain transcription factors, through their DNA binding and homo-/hetero-dimer forming capacity, are capable of regulating the expression of cascades of downstream target genes (Wilson *et al.* 1993), and therefore can play significant roles in cellular differentiation.

Gene expression was initially investigated using *in situ* hybridisation on paraformaldehyde fixed, paraffin wax embedded tissues, using a protocol modified from Breitschopf *et al.* 1992 (see Chapter 2 for details), looking at the transcription factors *Pax6*, *Chx10*, *Brn3b* and *Crx*. Expression patterns were examined at several stages during development; E12.5 and E13.5, when the retina is predominantly neuroblastic); E18.5, when lamination is well under way, and several strata can be observed, including the ganglion cell layer (gcl) and

the inner plexiform layer (inl); and P12, when all cells are postmitotic, and the retina can be considered mature.

4.2 Histological analysis of the *or^{J}* retina during retinal development

At E13.5, the wild-type murine retina comprises two layers, and a distinctive optic nerve (Figure 4.1a). The cells within these two layers are morphologically distinct from each other. The inner layer consists of presumptive ganglion cells, which project axons to the optic nerve head and nerve, and fasciculate to form the nerve fibre layer. In the *or^{J}* mouse at E13.5 the eye is noticeably microphthalmic, with all aspects of the eye being considerably smaller than the wild-type mouse (Figure 4.1b). The retina is hypocellular, comprising only one discernible layer. The nerve fibre layer is apparently absent, and sectioning throughout the eye reveals that the optic nerve head and nerve are completely absent (b shows a section through the central retina). Figure 4.1c shows a high magnification image of the tissue behind the retina in the region of the optic tract. A thin line of cells can be seen (arrow) in several sections around the central retina, which corresponds to the position of the now-degenerated optic stalk. In sections from several embryos (n=3), nerve fibres were never seen in this remnant optic stalk, indicating that either the *or^{J}* retina fails to develop an optic nerve, or it rapidly degenerates, such that by E13.5 no axons are present.

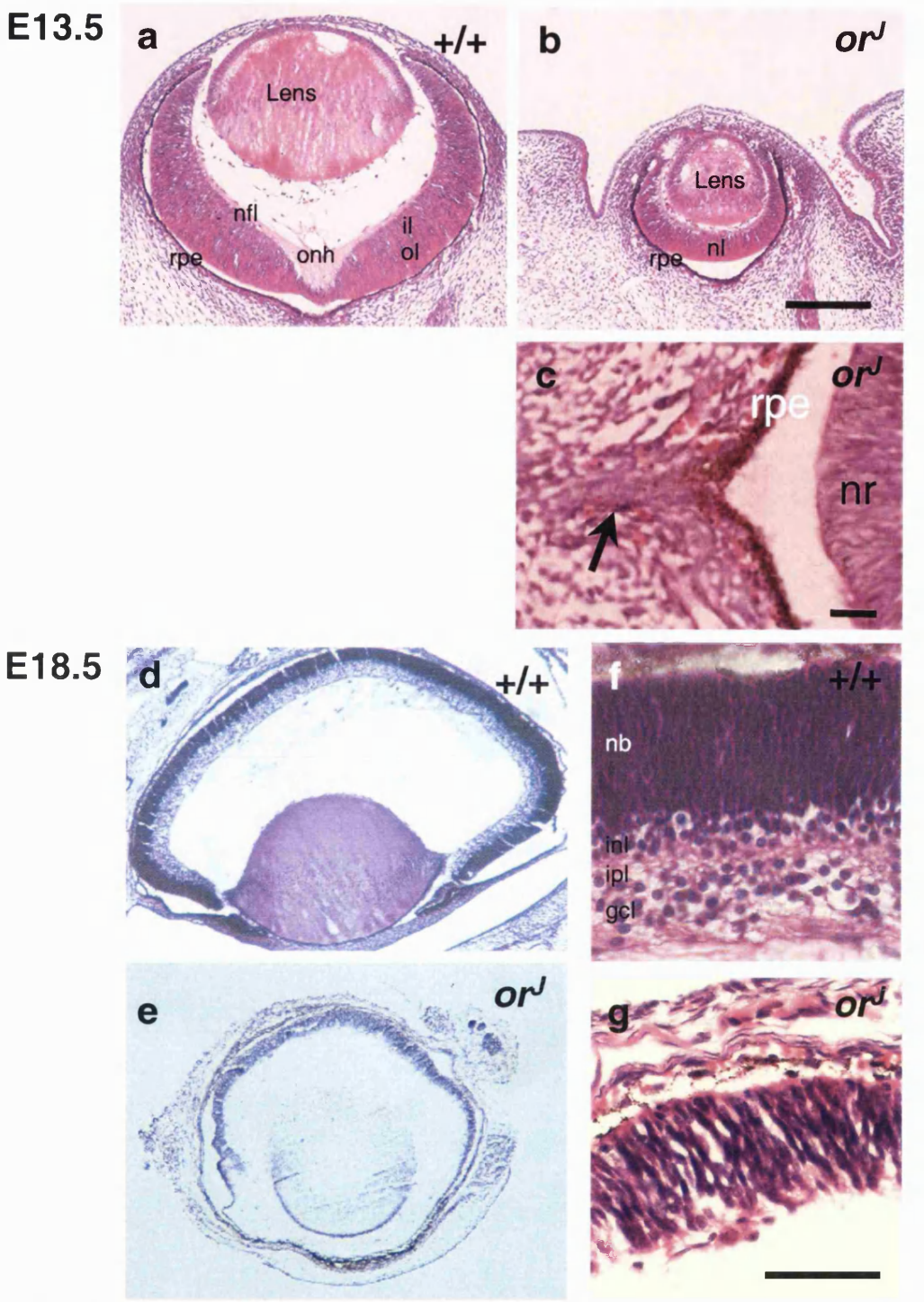

Figure 4.1. Histological analysis of the *or^J* and eye retina. At E13.5, the wild-type (+/+) retina (a) comprises the outer (ol) and inner (il) layers. The nerve fibre layer (nfl) is developed, indicating the presence of differentiated ganglion cells. These aggregate at the optic nerve head (onh). The *or^J* eye (b) at the same stage is considerably smaller, and the retina comprises only one discernible nuclear layer (nl). There is no nfl and no onh. (c) shows a high magnification view of the midline of the *or^J* eye. The optic nerve is absent; instead there is a thin line of cells indicated with an arrow. At E18.5 the wild-type eye (d) is notably larger than the *or^J* eye (e). The lens in the wild type is connected at the ciliary margins, and is flush with the front of the eye. In the mutant, the lens appears to be free floating within the vitreous. The E18.5 wild-type retina (f) is developing into a stratified tissue, comprising a neuroblastic layer (nb), an incomplete inner nuclear layer (inl), an inner plexiform layer (ipl) and a ganglion cell layer. By contrast, the *or^J* retina (g) is thin and unstratified, with no discernible plexiform layers. rpe, retinal pigmented epithelium; ch, choroid. Scale bars: 100μm, except (c): 300 μm.

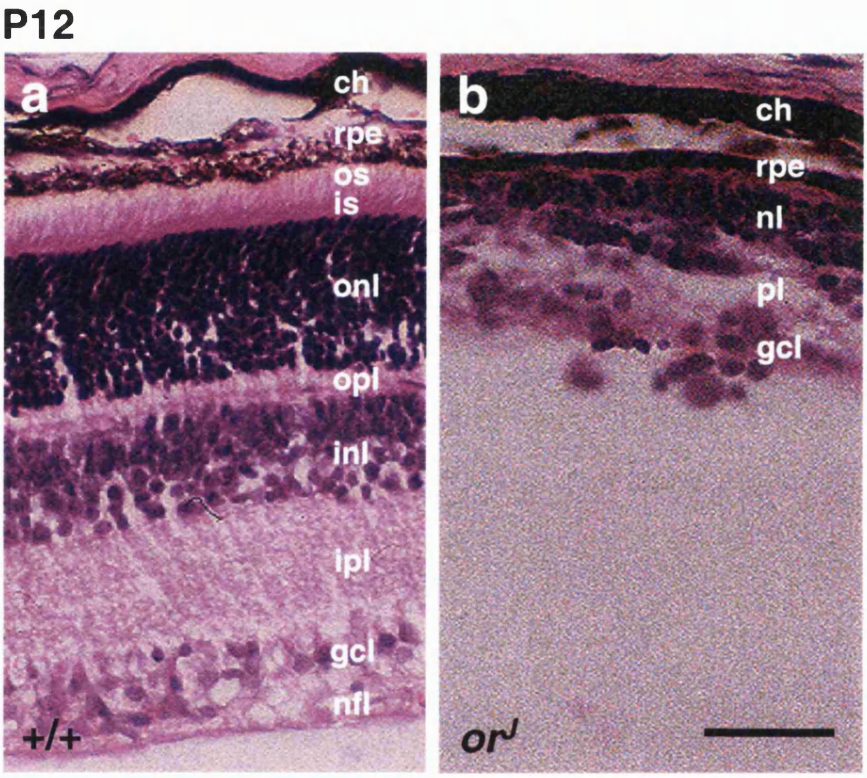

Figure 4.2. Histological analysis of the adult *or*^{J} and eye retina. At P12, the wild-type retina is mature (a), and consists of the characteristic three cellular layers: outer nuclear layer (onl) with inner (is) and outer segments (os); inner nuclear layer (inl); and ganglion cell layer (gcl). These are separated by the inner (ipl) and outer plexiform layers (opl) The *or*^{J} retina is now severely hypocellular and partially stratified with two discernible layers (b), a gcl and a nuclear layer (nl) separated by an interrupted plexiform layer (pl). rpe, retinal pigmented epithelium; ch, choroid. Scale bar: 100μm.

By E18.5, the wild-type retina is developing into a stratified tissue, with a neuroblastic layer, an incomplete inner nuclear layer, and a ganglion cell layer, separated from the rest of the retina by a presumptive inner plexiform layer (Figure 4.1d). By contrast, (Figure 4.1e) the mutant retina is hypocellular and unstratified, comprising only 10–15 cells at its thickest point (~100μm, as compared with ~200μm in the wild-type retina). These cells are morphologically indistinguishable from each other, and the retina is clearly lacking organisation.

The wild-type retina at P12 (Figure 4.2a) is fully postmitotic and can be considered effectively mature (Young 1985). It is well organised into its characteristic three cellular and two plexiform layers, and cell types are morphologically distinct, for example with photoreceptors possessing inner and outer segments. The *or*^{J} retina is by this stage irregularly stratified, with one inconsistent plexiform layer, and at best two cellular layers (Figure 4.2b). No photoreceptor inner or outer segments are visible adjacent to the RPE, and cells in the ganglion cell layer at the inner aspect appear to be prolapsing through the inner limiting membrane, which itself is inconsistent. The thickness of the retina is consistently <20 cells deep at its thickest point. Compared with the *or*^{J} retina at E18.5, in which all of the cells appear to be homogeneous, the P12 *or*^{J} retina contains cells that have different morphologies to each other, implying that some differentiation has occurred.

4.3 Transcription factor gene expression analysis by *in situ* hybridisation

4.3.1 Pax6

The *paired*-type homeodomain transcription factor Pax6 is known to play roles in many aspects of eye development (Graw 1996, Freund *et al.* 1996). For the purpose of this study, I was interested in using *Pax6* expression as a marker of the development of ganglion and amacrine cells. Early in development, *Pax6* is expressed throughout the neural retina, but in the mature retina, its expression is limited to amacrine cells and a subset of ganglion cells (Hitchcock *et al.* 1996, Belecky-Adams *et al.* 1997, Nishini *et al.* 1999). Antisense and sense riboprobe were synthesised from a plasmid containing a 1.6kb fragment of *Pax6* cDNA.

At E12.5 the wild-type neural retina is largely undifferentiated [although early-born cell types have become postmitotic, such as ganglion cells, (Young, 1985)]. Figure 4.3 shows expression of *Pax6* throughout the retina, as well as in the anterior lens, and the overlying surface ectoderm. The distribution of *Pax6* mRNA within the neural retina appears to follow a centro-peripheral gradient, where there is a higher concentration of expression in the peripheral retina.

The expression pattern of *Pax6* in the *or*^{J} retina at E12.5 (Figure 4.3) is largely similar to that of the wild-type retina, despite the overall microphthalmia. Expression can be seen throughout the neural retina, in the lens and in the surface ectoderm. However, the gradient of expression seen in the wildtype is not apparent in the mutant retina.

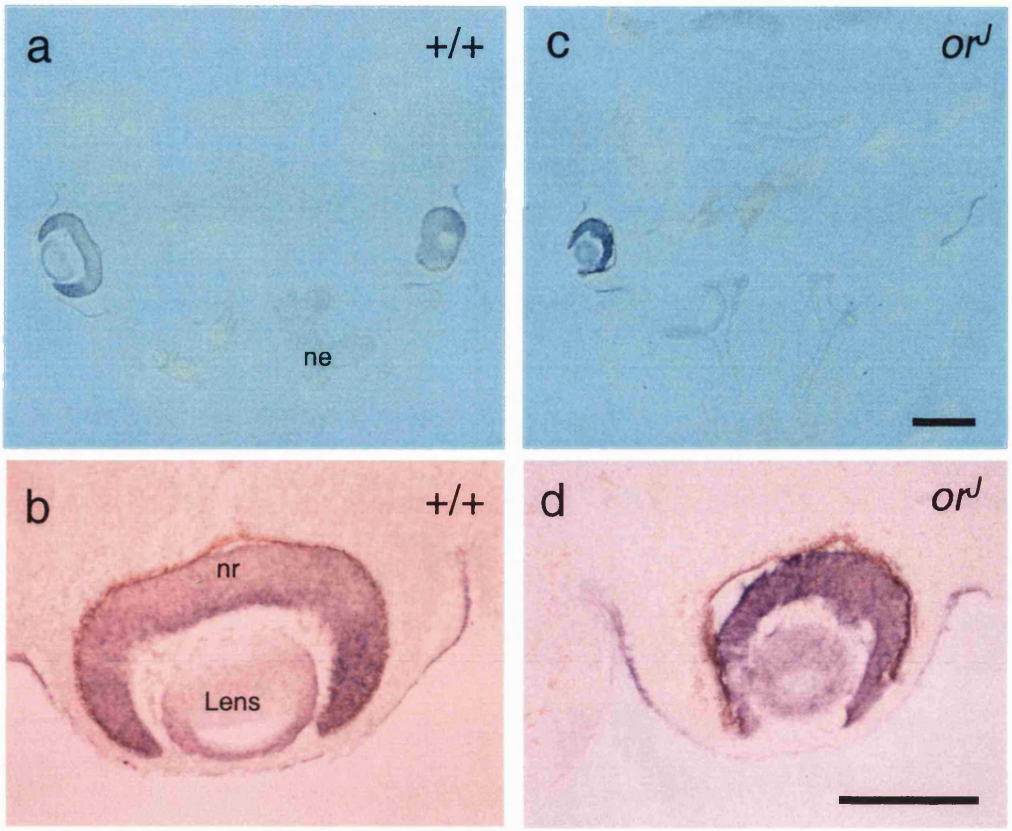

Figure 4.3. *Pax6* expression at E12.5. (a) and (b) show *Pax6* expression by *in situ* hybridisation in the wild-type (+/+) retina and surface epithelium. (c) and (d) show expression in the *or*^{J} retina. Although the eye is noticeably smaller, the expression pattern is similar, suggesting that *Pax6* expression is unaffected by the absence of Chx10. (b) and (d) are magnifications of (a) and (c). Abbreviations: ne, nasal epithelium; nr, neural retina. Scale bars: (a) and (c) 200 μm; (b) and (d) 100μm.

Pax6 expression at E13.5 (Figure 4.4c and d, pages 148–149) in both the wild-type and *or*^{J} retinae is still widespread, although the intensity of staining appears reduced, possibly indicating that Pax6 expression is becoming restricted to specific cell types. In the wild type, lowest levels of mRNA were detected in the outer retina. In the mutant retina, signal is noticeably more intense in the inner retina (despite the absence of any histological strata. The highest levels of mRNA correspond to cells expressing *Brn3b* (see below) and therefore are likely to be ganglion cells.

By E18.5, wild-type expression of *Pax6* (Figure 4.5e, pages 150–151) is abundant within cells of the developing inner nuclear layer and in the ganglion cell layer. These are presumed to be amacrine and ganglion cells, respectively. Expression has become downregulated in the majority of retinal cells. In the *or*^{J} retina at E18.5, *Pax6* (Figure 4.5f) expression has also become downregulated in approximately half of the retinal cells; however, these cells are distributed apparently randomly throughout the unstratified retina. This suggests that regulation of *Pax6* expression is maintained in the absence of Chx10, although these cells have thus far failed to migrate to an appropriate position across the laminae.

At P12 (Figure 4.6, pages 152–153) *Pax6* expression is limited to cells within the ganglion cell layer and to cells within the inner aspect of the inner nuclear layer. These are presumed to be ganglion and amacrine cells respectively, as previously reported. In the *or*^{J} retina at P12, *Pax6* expression is restricted to a layer of cells in the inner aspect of the neural layer. Based on

their location and *Pax6* expression, these are presumed to be ganglion and amacrine cells (Hitchcock *et al.* 1996). The presence of both of these cell types has been demonstrated previously in the *or*^{J} mouse using other cell specific markers (Burmeister *et al.* 1996). The contrast between the distribution of *Pax6* expressing cells at E18.5 and P12 is notable. Cells that were randomly distributed at E18.5 have migrated by P12 into a tight stratum corresponding to the position of the inner nuclear layer and the ganglion cell layer.

Several conclusions can be inferred from these expression data.

1) Early *Pax6* expression patterns are not significantly affected in the absence of Chx10. During early development expression patterns are similar (despite the microphthalmia). This almost certainly indicates that *Pax6* is upstream from Chx10 in the hierarchy of genes involved in eye development. This is perhaps unsurprising given that *Pax6* expression precedes *Chx10* expression. Moreover, it also indicates that onset of Chx10 within the neural retina is not needed for the continued expression of *Pax6* in this tissue.
2) Amacrine and *Pax6* expressing ganglion cell genesis is relatively unaffected by the *Chx10* mutation. It appears that at E18.5, developing amacrine and ganglion cells are expressing *Pax6* as in the wild type, but these cells are not organised into a layer. However, in the mature retina, these cells have migrated to a stratum that approximates that of the wild type.

4.3.2 Brn3b

A 200bp riboprobe was synthesised from a plasmid containing a fragment of the cDNA sequence for *Brn3b*, which was a kind gift from David Latchman (Institute of Child Health, UCL, London). Brn3b is a POU domain transcription factor whose retinal expression is restricted to post mitotic ganglion cells, and is the earliest known marker for this cell type (Gan 1996). *In situ* hybridisation with a *Brn3b* riboprobe at E13.5 (Figure 4.4e, pages 148–149) showed weak expression in cells in the inner layer of the neural retina indicating the presence of newly forming ganglion cells. Ganglion cell birthing spans from E10.5 until P3 (Young 1985), and by E13.5, the optic nerve is clearly visible on different sections of the same specimen. At E13.5 in the or^J, expression of *Brn3b* was detected in the otherwise unstratified retina (Figure 4.4e) in a thin band of cells in the innermost aspect of the retina. This expression pattern appears to overlap with that of a high concentration of *Pax6* (see above). These data indicate the presence of ganglion cells in the mutant retina although the optic nerve is apparently absent in any specimen analysed (see Figure 4.1). Although the neural retina is disorganised at this stage and later, this result suggests that ganglion cell birthing is relatively unaffected by the absence of Chx10, and also that these cells migrate to their appropriate location, as is observed in the wild-type retina. However, the absence of an optic nerve or a nerve fibre layer in the or^J retina indicates that these cells are not projecting their axons correctly.

Expression of *Brn3b* at E18.5 (Figure 4.5g, pages 150–151) in the wild-type retina is restricted to the forming ganglion cell layer. The cells expressing

Brn3b are no longer as densely packed as in the earlier retina, and axonal projections can be seen, as in the mature ganglion cell layer. Weak expression in the mutant retina is restricted to a thin layer of cells on the innermost aspect of the still apparently disorganised and unstratified retina (Figure 4.5h). Upon close inspection of histological stains of the *or*^{J} retina this layer of *Brn3b*-positive cells are not morphologically distinguishable from cells in the rest of the retina, perhaps indicating that these ganglion cells are not undergoing normal differentiation. This is a possibility that reflects the inability of these cells to project their axons to form an optic nerve.

Despite repeated independent experiments (n=3), expression of *Brn3b* was not detected at P12 in the *or*^{J} retina by *in situ* hybridisation. This may reflect a retinal degeneration where *Brn3b*-positive ganglion cells have died.

The observed *Brn3b* expression pattern during development indicates that ganglion cell birthing is relatively unaffected by the absence of functional Chx10, as is the capacity of these cells to migrate to an appropriate location in the mutant retina. However, ganglion cell differentiation is abnormal, as demonstrated by the absence of an optic nerve.

4.3.3 Chx10

A 1.6Kb length of *Chx10* cDNA was amplified from a wild-type E15.5 mouse retinal library using primers that flank the position of the C $\rightarrow$ A mutation (Burmeister *et al.* 1996). A riboprobe was generated from this clone and was used in *in situ* hybridisation experiments on both wild-type and *or*^{J} retinae. The

aims of these experiments were to examine the distribution of cells expressing the defective mRNA during development. Expression was analysed in the wild type at E18.5 and P12.

At E18.5, expression of *Chx10* in the wild type is restricted to the neuroblastic retina (Figure 4.5c, pages 150–151), and appears to be present in all of the cells within this layer. This is similar to the expression patterns seen in the human at 10 wpc (see Figure 3.2). By this stage, the presumptive inner nuclear layer is apparent but incomplete, separated from the ganglion cell layer by the developing inner plexiform layer. Bipolar cells are amongst the last neuronal cells in the retina to be born, in a period that spans from E14.5 until P11 (Young 1985). At E18.5, Chx10 mRNA was detected in the neuroblastic layer and within the presumptive inner nuclear layer.

By P12 expression of *Chx10* (Figure 4.6c, pages 152–153), is restricted exclusively to cells within the inner nuclear layer, with a higher concentration on the outer aspect of this layer, corresponding to the location of bipolar cells. This is consistent with the role of Chx10 in bipolar cell specification and maintenance. The band of expression may be wider than just the bipolar cell layer, indicating that *Chx10* may be expressed at low levels in other cells of the inner nuclear layer. Liu *et al.* (1996) reported co-localisation of Chx10 and the bipolar marker PKC, indicating that Chx10 is expressed in bipolar cells. However, the co-expression of *Chx10* with other cell specific markers has not been investigated, either during development or in the mature retina.

Expression of mutant *Chx10* transcripts (here denoted *Chx10*$^{-/-}$) was investigated in the *or*^{J} retina by *in situ* hybridisation. At E18.5 mutant mRNA transcripts were readily detectable (Figure 4.5d), whereas hybridisation with a sense probe resulted in no discernible signal. This indicates that the mutant mRNA transcript is stable, and that the riboprobe used to investigate *Chx10* expression hybridises successfully with the *Chx10*$^{-/-}$ mutated transcript. It has been reported previously that mRNA transcripts containing mutations are often unstable and are degraded. By contrast, other reports (Carlson *et al.* 2000) indicate that point mutations do not affect the quantity of mRNA transcribed.

This analysis allowed the monitoring of levels of *Chx10*$^{-/-}$ transcription in the absence of functional Chx10 protein, where any autoregulatory mechanism would be absent. *Chx10*$^{-/-}$ transcripts were strongly detected at E18.5 throughout the disorganised retina, except, on closer inspection, in a very thin band of cells on the inner most aspect of the retina. These correspond to the layer of cells expressing *Brn3b* (Figure 4.5h) and are presumed to be postmitotic ganglion cells. This, again, reinforces the notion that Chx10 is not required for the differentiation of ganglion cells, and that developing ganglion cells are capable of downregulating *Chx10* expression in the absence of functional Chx10 protein. However, at this stage of development, when in the wild type many cells in the inner retina have downregulated *Chx10* expression, the vast majority of cells in the mutant retina are expressing *Chx10* at higher levels. This may indicate a number of possible explanations:

(1) the mutant retina is immature compared with the wild type, and there is consequently a much larger proportion of dividing cells that are strongly transcribing *Chx10*$^{-/-}$ mRNA;

(2) the mutant retina contains a number of cell types which are incapable of downregulating *Chx10*$^{-/-}$ expression in the absence of a Chx10 protein. These possibilities are investigated below.

In contrast to its expression pattern at E18.5, *Chx10* mRNA has become restricted by P12 to a layer of cells on the inner aspect of the *or*^{J} retina (Figure 4.6d). This indicates that the cells on the outer aspect are capable of downregulating *Chx10*$^{-/-}$ transcription independently of Chx10. The band of cells expressing *Chx10*$^{-/-}$ corresponds to cells in the inner aspect of the nuclear layer (and is distinct from the putative ganglion cell layer). The absence of PKC immunolocalisation in the mature *or*^{J} retina (Liu *et al.* 1996) indicates that differentiated bipolar cells are absent. *Chx10*$^{-/-}$ expression in the mutant at P12 is therefore marking other cell types of the inner nuclear layer i.e. amacrine cells, horizontal cells or Müller glia, or labelling postmitotic bipolar cells that are blocked in their differentiation by the absence of Chx10.

Here, I have shown that there is a pool of cells located in the inner aspect of the neural retina, but outer to the ganglion cell layer which maintain *Chx10*$^{-/-}$ expression, despite the absence of differentiated bipolar cells.

Two important points emerge from this finding. First, the size of the putative photoreceptor layer in the mutant, as indicated by the downregulation of *Chx10* mRNA, is approximately 30% of the width of the equivalent layer in

the wild type. Second, the relative proportion of cells expressing *Chx10*$^{-/-}$ in the mutant appears to be greater than in the P12 wild-type retina. This may indicate that several cell types in the inner nuclear layer are dependent on functional Chx10 protein to downregulate expression of *Chx10* mRNA. Given that the band of cells that is expressing *Chx10*$^{-/-}$ in the mutant retina is wider than, but fully overlaps with, the band of cells expressing *Pax6* (here assumed to be amacrine and a proportion of ganglion cells, see above), amacrine cells may be the cell types incapable of downregulating *Chx10* expression, and this may be consistent with the possibility that *Chx10* is expressed at low levels in other cell types in the inner nuclear layer.

4.3.4 Crx

A 637bp fragment of the photoreceptor-specific transcription factor gene *Crx* was cloned from an E15.5 mouse retinal cDNA library, and this was used to synthesise sense and antisense riboprobes. Expression of *Crx* was analysed by *in situ* hybridisation (see Chapter 2, Methods for details).

At E13.5 faint *Crx* expression could be detected in the outer layer of the neural retina (Figure 4.4g, pages 148–149). This layer corresponds to the location of the prospective photoreceptor layer, and expression of *Crx* at this stage indicates the presence of developing cone photoreceptors (albeit in small numbers) (Furukawa *et al.* 1997), whose birthing precedes that of rods (Young 1985). This expression pattern is complementary to that of Brn3b in adjacent

sections, which indicates that these two genes are not co-expressed in the same layer of the developing retina.

In experiments with appropriate wild-type positive controls, *Crx* expression could not be detected in the *or*^{J} retina at E13.5 (Figure 4.4h). The lack of signal was comparable to incubation with a sense riboprobe (data not shown). This result suggests that *Crx* mRNA transcripts are not present at this time in the mutant retina, indicating a delay of at least one day in the onset of expression of this gene. This result was reproduced in separate independent experiments (n=4).

Expression of *Crx* in the wild-type E18.5 retina is restricted to the neuroblastic layer, and is punctate (Figure 4.5i, pages 150–151). This pattern reflects the presence of developing rods and cones (Young 1985). There is more concentrated expression signal in the outer most aspect of the neuroblastic layer, and this corresponds to the zone in which photoreceptor differentiation is underway. The apparently punctate pattern of expression reflects the nature of the neuroblastic retina, which contains many newly-born photoreceptors and dividing cells (see section 4.3) that will contribute to the other non-photoreceptor late born cell types in the mature retina, e.g. bipolar cells (born during the period E 14.5–P12).

Again, mirroring the situation at E13.5, *Crx* expression could not be detected in repeated experiments by *in situ* hybridisation at E18.5 in the *or*^{J} retina (Figure 4.5j). Positive controls within these experiments (i.e. other riboprobes on adjacent sections, *Crx* antisense riboprobe on different

specimens) demonstrated the robustness of the protocol and the integrity of the mRNA in the tissue. These results lead to the conclusion that *Crx* expression is delayed by at least six days in the or^J retina.

Crx expression is not detectable by *in situ* hybridisation at either E13.5 or 18.5 in the or^J retina (Figures 4.4h and 4.5j). However, by P12 expression is readily detectable in a layer of cells on the outer aspect of the retina (Figure 4.6h, pages 152–153). The band of *Crx*-positive cells seen here are presumed to be photoreceptors. Previous work has reported the presence of rod photoreceptors at P18, based on detection of rhodopsin using antibody staining (Liu *et al.* 1994). Normal length inner and outer segments are not detectable in the or^J retina by light microscopy, suggesting that photoreceptor differentiation is disrupted. The expression pattern of *Crx* at P12 is complementary to that of *Chx10* on adjacent sections. This indicates that these cells that are capable of downregulating *Chx10* expression in the absence of a functional Chx10 protein are in fact photoreceptor cells. Furthermore, these data suggest that the downregulation mechanism is specific to photoreceptors.

Figure 4.4. Transcription factor gene expression by *in situ* hybridisation at E13.5. *Pax6* expression is distributed throughout the wild-type (+/+) and *or*^{J} retinae (c and d) at E13.5, as well as on the overlying surface epithelium. *Brn3b,* which is ganglion cell-specific, is expressed only in the il of the wild-type retina (e), and in a layer of cells in the inner aspect of the unstratified *or*^{J} retina (f). This indicates that ganglion cells are present in the absence of Chx10, and localise to the correct tissue aspect. By contrast, the photoreceptor transcription factor gene *Crx* is expressed in the ol of the +/+ retina (g), corresponding to the future photoreceptor layer. However, *Crx* could not be detected by *in situ* hybridisation in the *or*^{J} retina at E13.5 (h). Scale bar: 100 μm

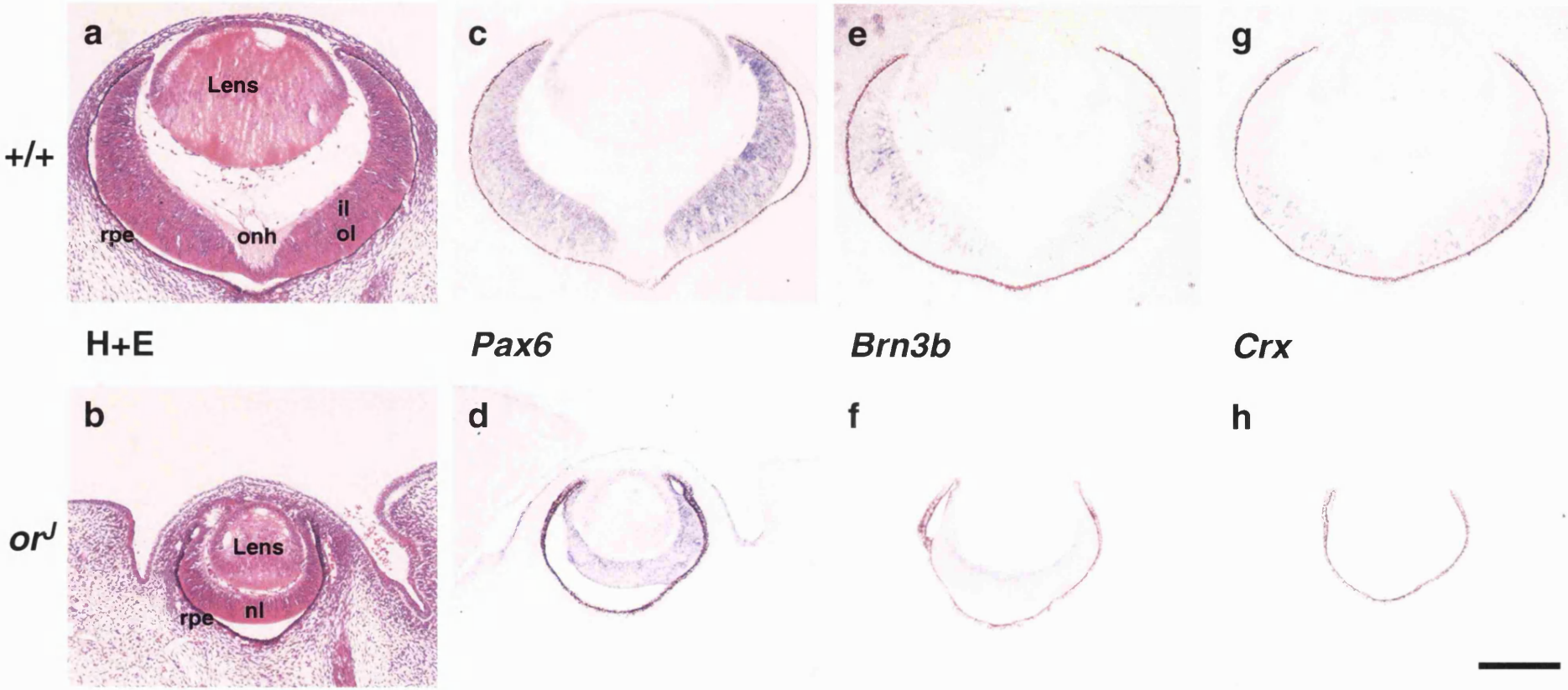
a
Lens
+/+
rpe
onh
il
ol
H+E
c
Pax6
e
Brn3b
g
Crx
b
Lens
or^J
rpe
nl
d
f
h

Figure 4.5. Transcription factor gene expression by *in situ* hybridisation at E18.5. The characteristic stratified retina is beginning to form in the wild-type (+/+) retina (a), but is notably retarded in the mutant retina (b). Mutant *Chx10* expression is readily detectable throughout the *or*^{J} retina (d) at this stage, implying that there may be an autoregulatory mechanism that downregulates expression into a subpopulation of cells in the wild-type (c). Expression of *Pax6* (f) is in a proportion of cells in the *or*^{J} retina, indicating that it has been downregulated as in the wild-type retina (e), but organisation of these *Pax6*-positive cells is absent. Brn3b expression is detected in the *or*^{J} and wild-type retinae (g and h). *Crx* expression is restricted to the outer, neuroblastic layer in the wild-type (i), but remains undetectable in the absence of Chx10 (j). Scale bar: 100μm.

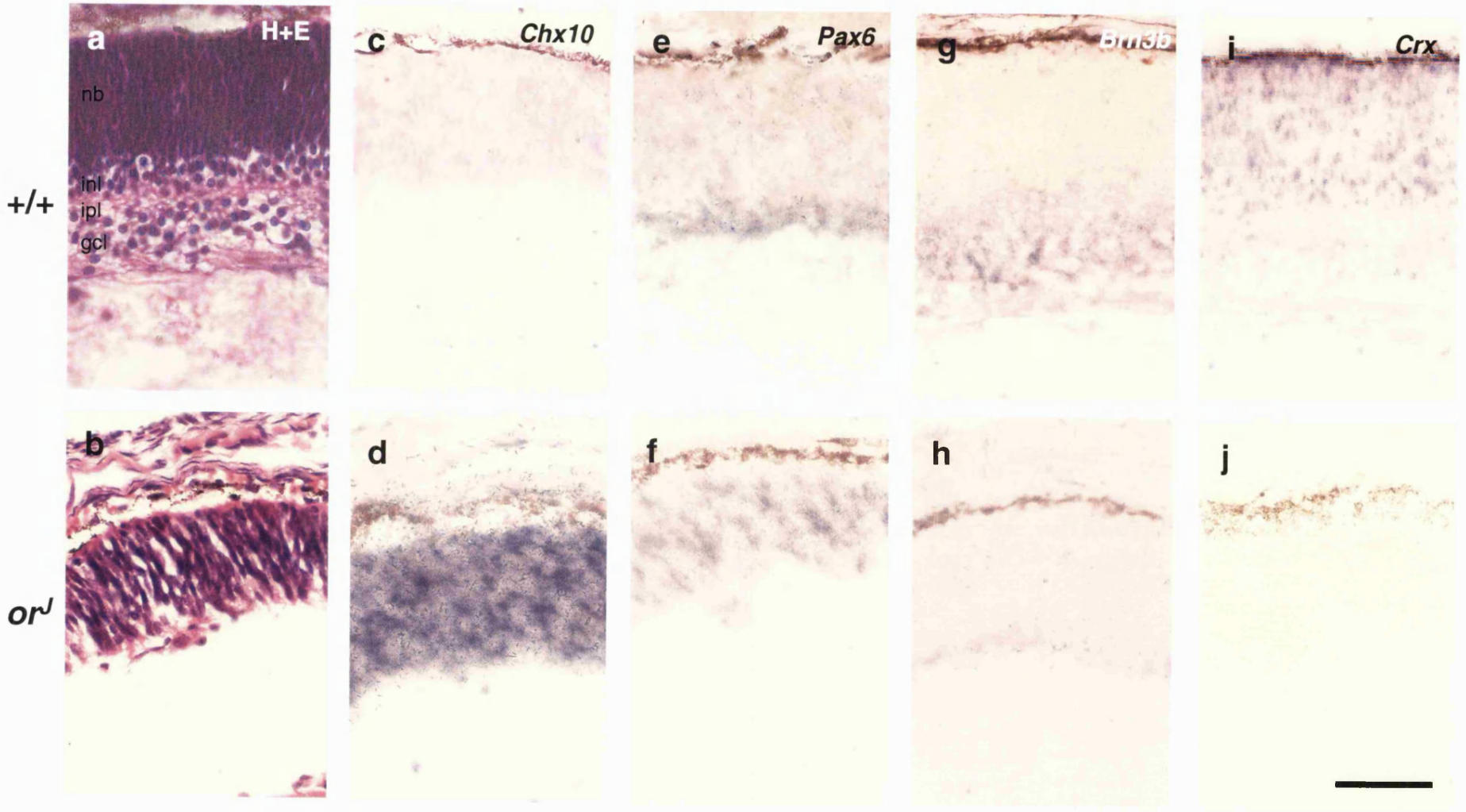
a
H+E
nb
inl
ipl
gcl
+/+
b
or^J
c
Chx10
d
e
Pax6
f
g
Brn3b
h
i
Crx
j

Figure 4.6. Transcription factor gene expression by *in situ* hybridisation at P12. (a) shows the characteristic mature retina, with its three cellular and two plexiform layers. (b) The mutant retina is hypocellular and disorganised. *Chx10* expression in the wild-type *(+/+)* (c) is restricted to cells within the inner nuclear layer (inl), presumed to be bipolar cells. *Chx10* expression in the mutant (d) is restricted to cells within the inner aspect, in contrast to its global expression at E18.5, suggesting that cells within the outer aspect have a Chx10-independent mechanism for the downregulation of *Chx10*. *Pax6* expression is restricted in both the wild-type (e) and mutant retina (f) to cells within the inner layers, presumed to be amacrine and ganglion cells. *Crx* expression, while absent at E18.5, is present in cells within the outer aspect of the mutant (h), indicating a delay in onset of expression in the absence of Chx10. Wild-type expression (g) is within the outer nuclear layer (onl). Scale bar: 100μm.

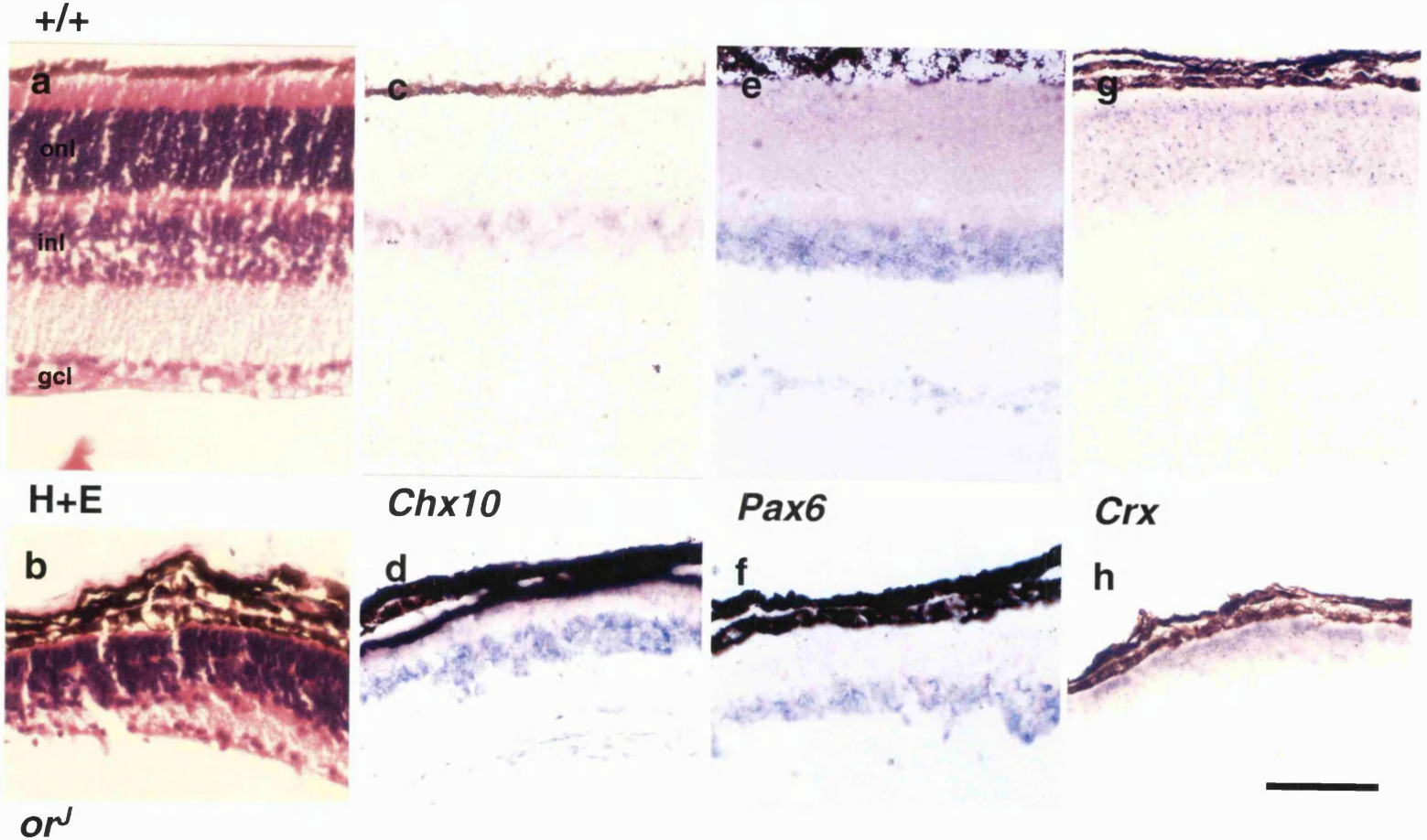
+/+
a
onl
inl
gcl
c
e
g
H+E
Chx10
Pax6
Crx
b
d
f
h
or^J

4.4 Transcription factor gene expression analysis by RT-PCR

Reverse transcriptase polymerase chain reaction (RT-PCR) was used as an alternative and more sensitive method of detecting gene expression in the *or*^{J} retina. The aim was to compare expression of the genes examined by *in situ* hybridisation using a different and independent technique. Moreover, RT-PCR is a very sensitive technique that would provide closer analysis of the apparent absence of *Crx* transcripts in the *or*^{J} retina.

Eyes (or separate dissected retinae from P12 eyes) from whole litters at the same stages as used in the *in situ* hybridisation experiments were dissected and total RNA extracted as described in Chapter 2, Methods. This RNA was quantified both by spectrophotometry and on denaturing ethidium bromide-stained agarose gels. Equivalent amounts were used as templates to synthesise cDNA pools, and these were used as templates for gene-specific PCR.

Primers were designed to amplify multiple exon spanning fragments from *Brn3b*, *Chx10*, *Crx* and phosphogluco-mutase1 (*Pgm1*) (Figure 4.7). This was to avoid any possible contamination of PCR product by amplification of genomic DNA. *Pgm1* is a ubiquitously expressed gene, whose expression was used as a positive control to demonstrate the integrity of the RNA extracted and cDNA quality (Putt *et al.* 1993). PCR was performed for each of these genes at each time point, using 30 amplification cycles (35 in the case of *Brn3b*). Quantification of PCR products amplified from mRNA for *Pgm1* and *Crx* at 24,

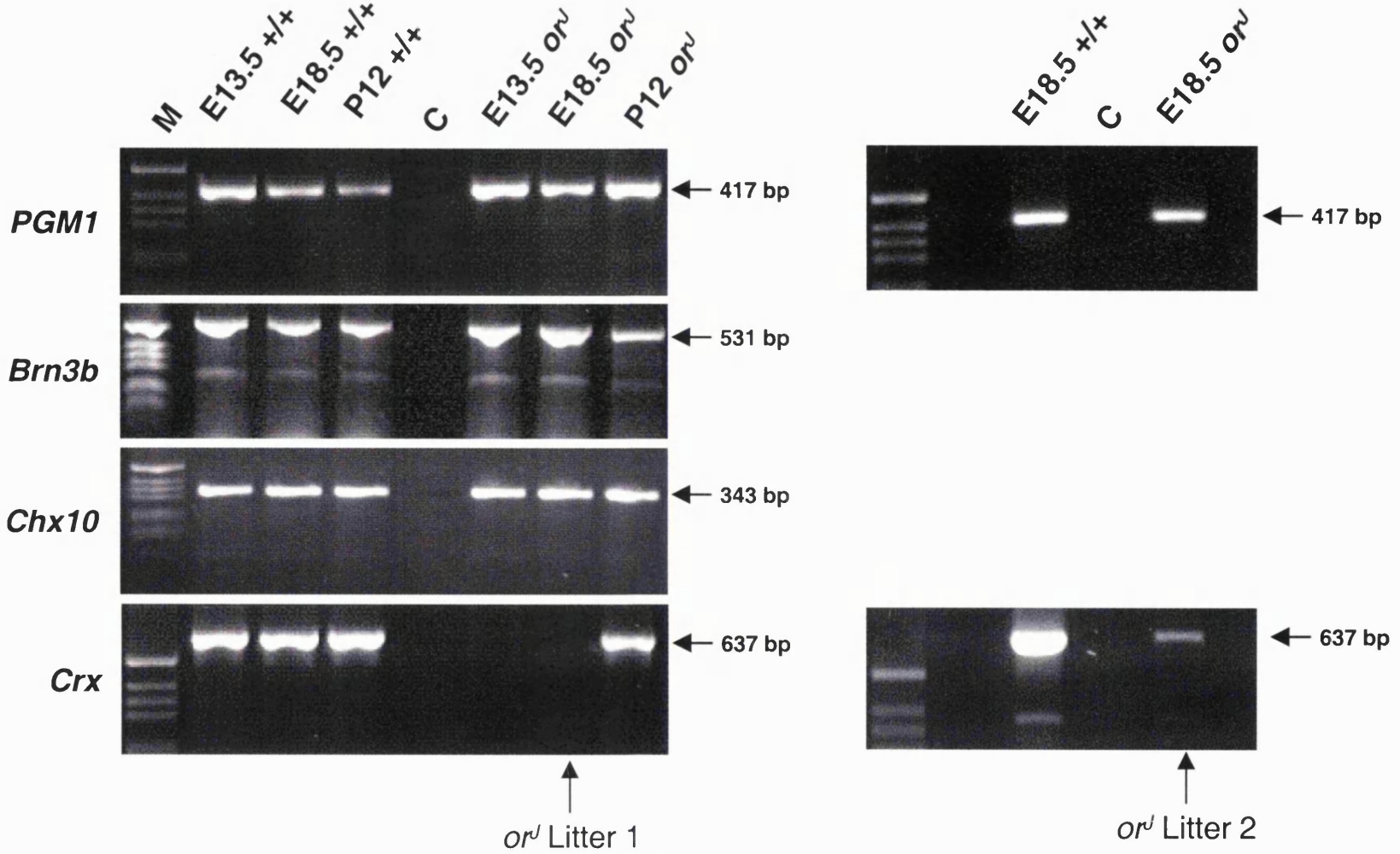

Figure 4.7. Transcription factor gene expression in the *or*^{J} retina during development was assessed by RT-PCR at the same developmental stages as had been investigated for *in situ* hybridisation (see Figs 4.3, 4.4 and 4.5). *In situ* data were confirmed, in that both *Brn3b* and *Chx10* were readily expressed in the wild-type (+/+) and *or*^{J} retina at all stages investigated, as was the ubiquitously expressed gene *PGM1*, but *Crx* was not detected at E12.5 and E18.5 in one litter, and was only faintly detected at E18.5 in a second (suggesting recent onset of expression). This indicates that expression of *Crx* is delayed in the absence of Chx10.

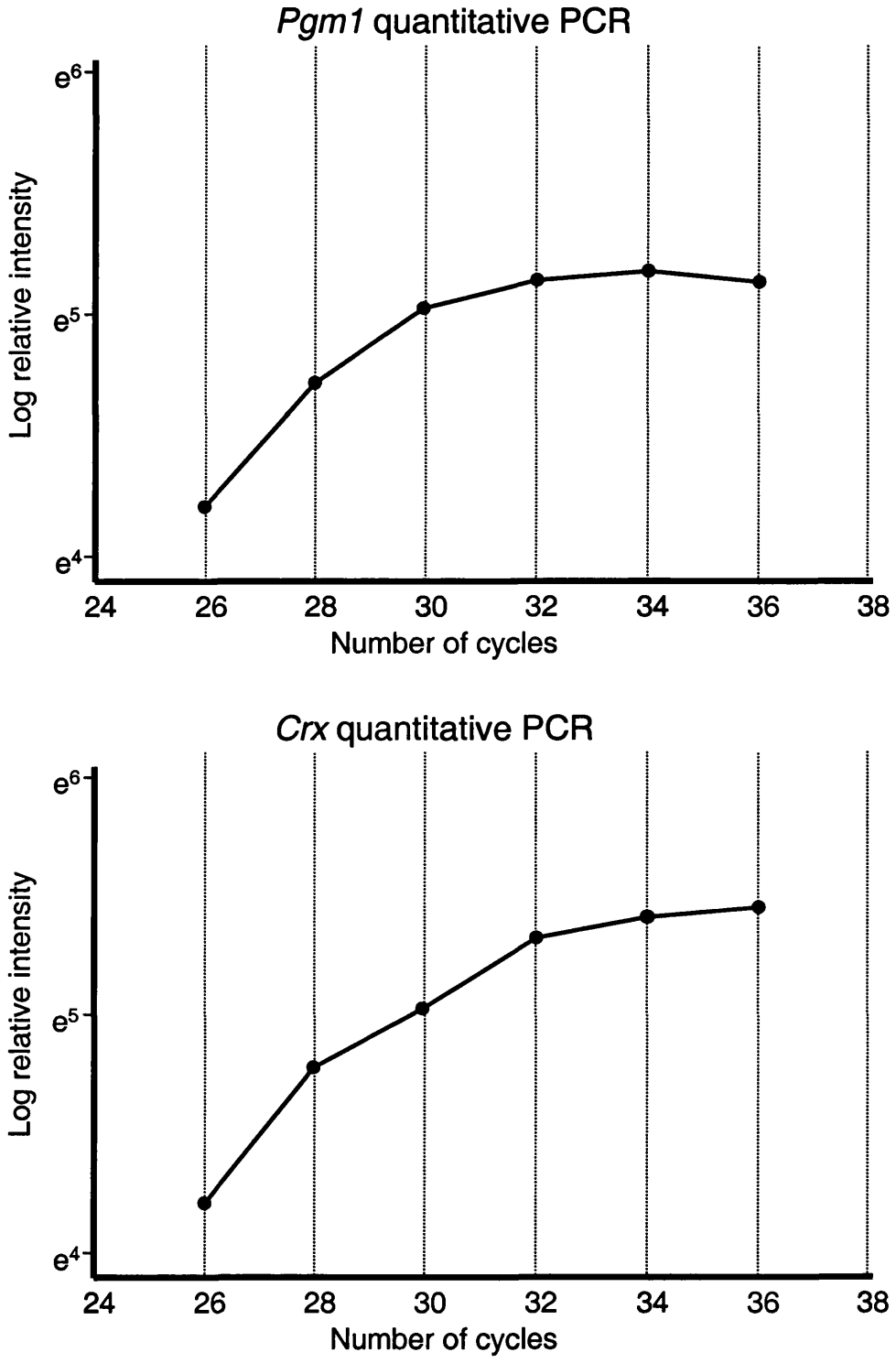

Fig. 4.8. Quantitative analysis of RT-PCR for *Crx* and *Pgm1* demonstrates that 30 PCR cycles is within the linear range of the reaction.

26, 28, 30 and 32 cycles demonstrated that 30 cycles was within the linear range of the PCR, and thus these data could be considered semi-quantitative (Figure 4.8).

Figure 4.7 shows gene expression of these genes, comparing wild-type samples at E13.5, E18.5 and P12 with *or*^{J} at the same stages. Expression of *Pgm1* at approximately equal levels in all samples demonstrates that RNA was successfully extracted. Negative controls (no mRNA template) show that amplification was not caused by cDNA contamination.

Expression of *Brn3b* was detected at all time points analysed, with a 531bp band clearly visible. This suggests that *Brn3b* expression is little affected at the time points analysed by the absence of Chx10, and is consistent with the *in situ* hybridisation data.

Expression of *Chx10* similarly was readily detectable at all times analysed. Primers used in this reaction did not flank the mutation site. This result demonstrates that the *Chx10* mRNA transcripts are stable, and this confirms the result of the *in situ* hybridisation. Furthermore, these results suggest that *Chx10*$^{-/-}$ transcription occurs independently of Chx10 protein, and thus rules out a model of *Chx10* expression that is dependent on a self-regulatory feedback loop for continued expression at later stages.

Crx expression was analysed by the same methods, and was readily detectable at E13.5, E18.5 and P12 in the wild-type eye, in accordance with the *in situ* hybridisation and published data (Furukawa *et al.* 1997). In the *or*^{J} eye

Crx transcripts were undetectable at E13.5, although other cDNA species were readily amplified, confirming the *in situ* hybridisation result.

At E18.5 or^J *Crx* expression was investigated in two litters. In Litter 1, no *Crx* expression could be detected. However, a faint band at the corresponding size was detected in Litter 2. Equivalent amounts of RNA were used in the synthesis of wild-type and mutant cDNA, and equivalent amounts of cDNA were used in each PCR. The intensity of the band showing *Crx* expression in Litter 2 is significantly less intense than that of the wildtype. This can be interpreted as showing very low levels of expression, indicating onset of expression at around E18.5 (see below). This suggests a six-day delay in *Crx* expression in the or^J mouse retina.

Crx expression was readily detectable at P12 in the or^J retina. The intensity of the band is equivalent to that of the wild type, and this suggests that levels of expression per milligram of total RNA are comparable with that of the wild-type retina. These data indicate that the low levels of expression detected in Litter 2 at E18.5 reflect the onset of *Crx* expression being around E18.5, rather than generally lower levels than the wild type.

4.4.1 Onset of Crx *expression*

RT-PCR was performed on RNA extracted from or^J retinae from newborn pups at P1, 2, 3, 4 and 5. Tissue was dissected from both eyes of single mice on each of these days. *Pgm1* expression was again used as a positive control to ensure the integrity of the RNA extracted, and this is shown in Figure 4.9. *Crx*

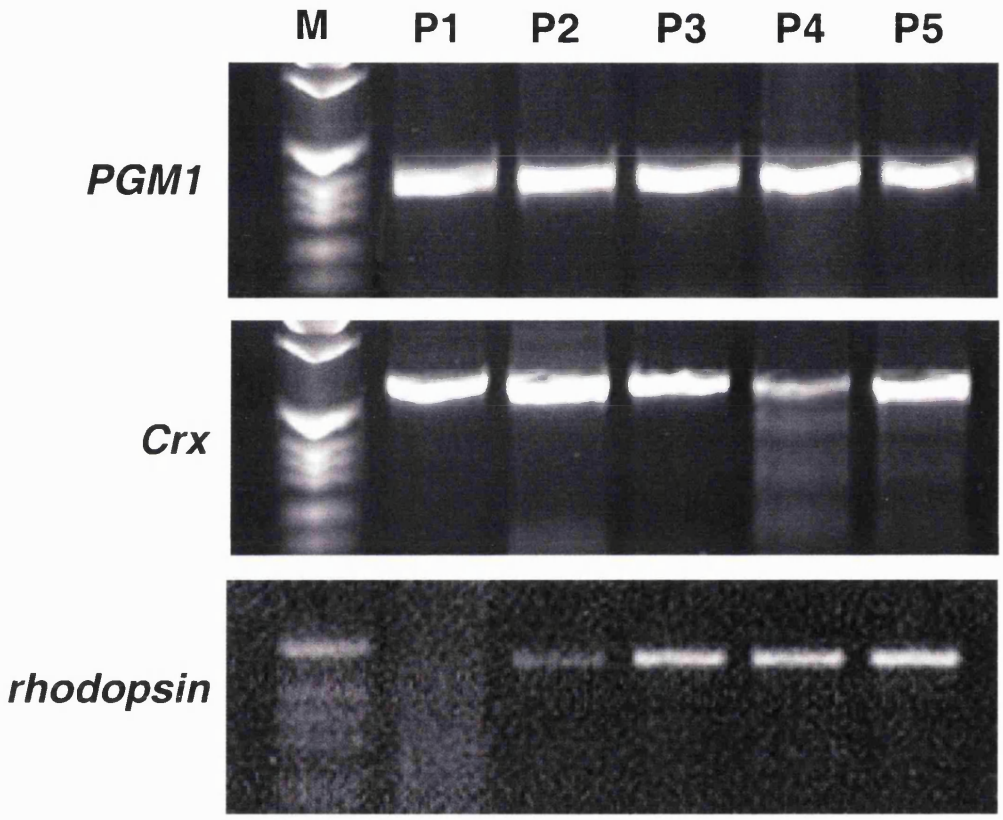

Figure 4.9. Onset of expression of *Crx* in the *or*^{J} retina was investigated, and was shown by RT-PCR to be readily detected at postnatal day (P) 1. Onset of *rhodopsin* expression, a putative downstream target of Crx, was shown to begin at P2, thus reinforcing the notion that it may be regulated by Crx.

expression was detected using the same primers as in Figure 4.7 at all times from P1–5. Mice are born (P0) at approximately 19.5 days post coitum (dpc). These combined data suggest that in the retina of the *or*^{J} mouse *Crx* mRNA transcripts are first detectable within a 48-hour period between E18.5 and P1. In the wild-type mouse Crx expression begins at E12.5 (Freund *et al.* 1997). Therefore, in the absence of Chx10, *Crx* expression is delayed by approximately seven days.

4.5 Cell proliferation in the developing *or*^{J} retina

The observed delay in *Crx* expression in the *or*^{J} retina might be the result of one of a number of causes. As *Crx* is expressed only in developing and mature photoreceptor cells (Furukawa *et al.* 1997), one possibility might be that a Chx10-dependent disruption of cell cycling in the mutant retina might be preventing the birth of photoreceptor cells. One of the most striking phenotypes of the *or*^{J} retina is its extremely hypocellular nature. Burmeister *et al.* (1996) reported a dramatic reduction (up to 85% in the dorsal peripheral retina) in cell proliferation of retinal neuroblasts at E11.5 by BrdU incorporation. This is described as the cause of the hypocellular retina, although cell proliferation in the central retina was comparable to that of the wild-type retina. The assay performed in their experiments does not take into account the length of time during which retinal proliferation is taking place, only that there is an absolute

reduction in the amount. Significantly, the number of cells in the mutant retina is already 30–50% lower than the wild-type retina by E11.5.

The immunolocalisation of a marker of mitosis was investigated at E13.5, E18.5 and at P12 in the wild-type and *or*^{J} retinae. Proliferation cell nuclear antigen (PCNA) is a protein involved in DNA replication, and is only expressed in mitotic cells (Hall *et al.* 1990). At E13.5 many mitotic cells are detected throughout the embryo (Figure 4.10c). Within the neural retina many PCNA-positive cells were observed in the outer, proliferative, layer, and only a very few cells within the inner layer. This reflects the early differentiation of ganglion cells relative to other cell types in the retina. Many of the cells that are PCNA-positive have the morphology of migrating cells. Within the *or*^{J} retina (Figure 4.10d) there are similar proportions of PCNA-positive cells. However the retina is much thinner, and there is no distinction between the two layers seen in the wild type retina.

At E18.5, many proliferative cells (PCNA-positive) can be observed throughout the wild-type retina (Figure 4.11b). By contrast, in independent repeatable experiments (n=4), no PCNA-positive cells could be seen in the *or*^{J} retina (Figure 4.11d). Extra-ocular tissue on the same sections showed immunoreactivity to the PCNA antibody, indicating a robust positive control (Figure 4.11e). Liu *et al.* (1996) suggested that the hypocellular retina observed in the *or*^{J} mouse is the result of a reduction in proliferation, shown by reduced BrdU labelling indices. This reduction was observed from E10.5 until E18.5, after which it was not recorded. The data presented here suggest that by E18.5,

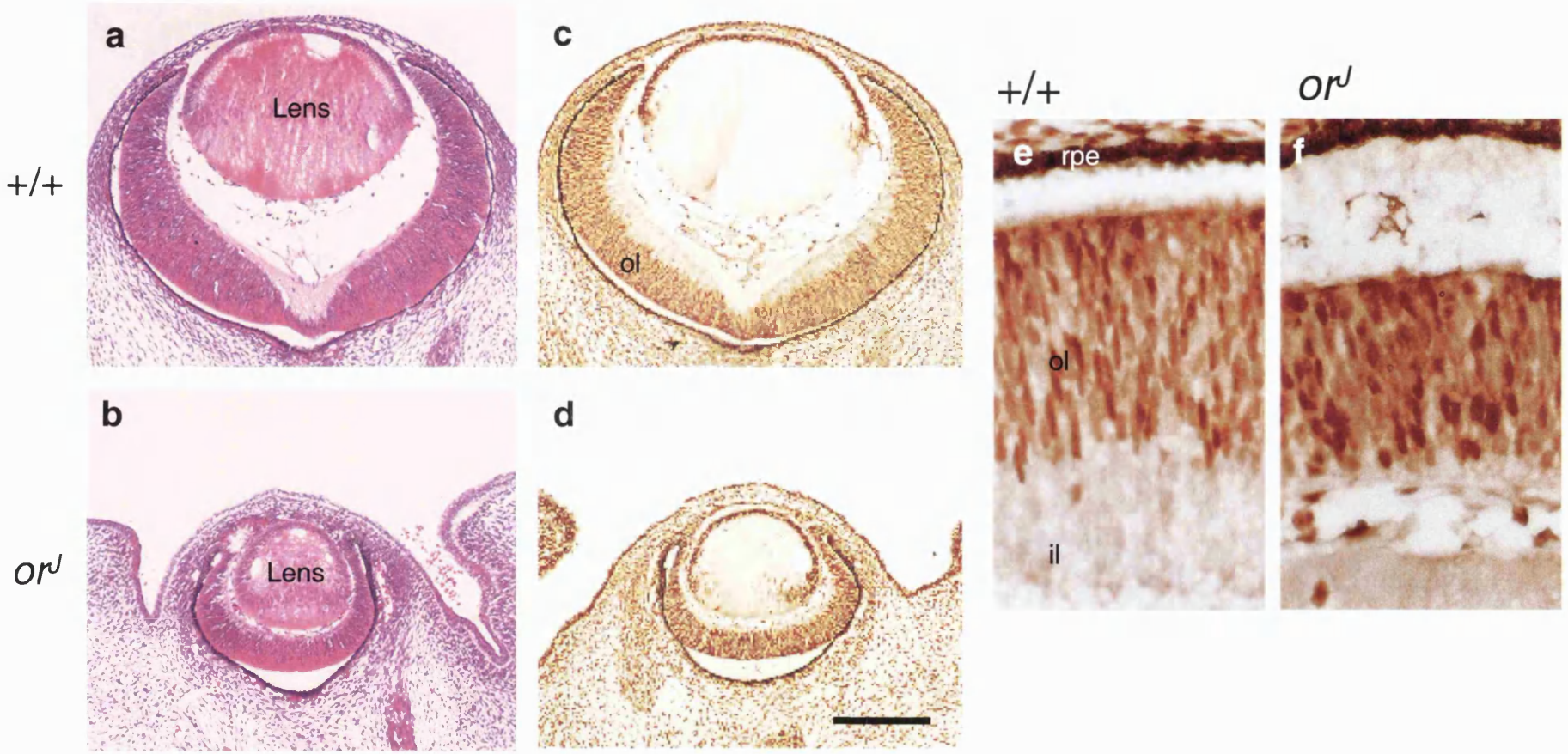

Figure 4.10. PCNA immunolocalisation in the *or*^{J} retina at E13.5. (a) and (b) show H and E stained wild-type and *or*^{J} retinae at E13.5. (c) and (d) show staining of cells that are positive for the mitotic cell marker PCNA. The majority of cells that are positive in the wild-type (+/+) are located within the outer layer (ol), but are distributed throughout the single layer of the mutant retina. (e) and (f) show high magnification images of (c) and (d). Abbreviations: il, inner layer; rpe, retinal pigmented epithelium. Scale bar: 100μm

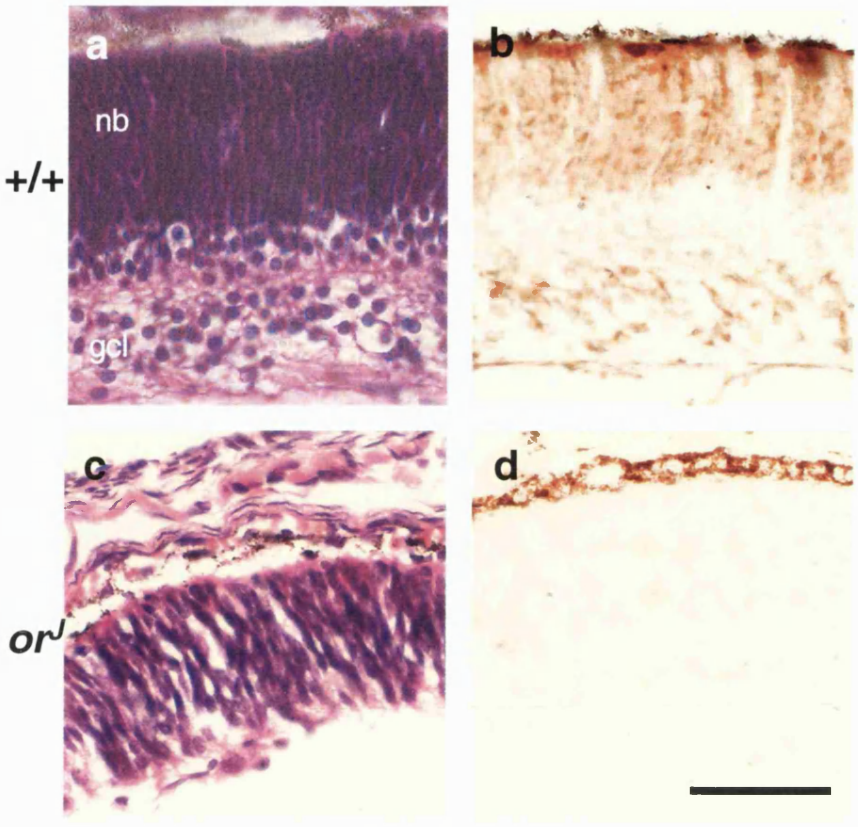

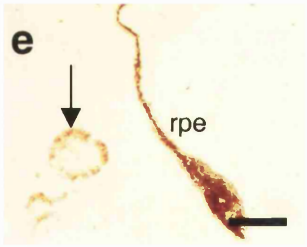

Figure 4.11. PCNA immunolocalisation at E18.5 in the *or*^{J} retina. (b) The majority of retinal dividing cells in the wild-type (+/+) are located within the outer, neuroblastic layer (nb). However, PCNA-positive cells were not detected within the retina of the *or*^{J} retina at E18.5 (d). These data suggest that the hypocellular retinal phenotype is at least in part caused by an early cessation of mitosis. (e) shows a positive staining of extra-ocular tissue on the same mutant section as (d). Scale bars: 100μm

no proliferating cells could be detected. Therefore, the hypocellular retina may be the result of a reduced period of proliferation, which stops approximately 12 days early, as well reduced proliferation *per se*. By P12 no PCNA-positive cells could be detected in either the wild-type or the *or*^{J} retinae (data not shown).

These data also suggest that as there are no dividing cells at E18.5 in the *or*^{J} retinae, all of the cells that are present in the mature retina are already postmitotic. The observed delay in *Crx* expression therefore cannot be caused by a failure of photoreceptor birthing, and suggests that differentiation of photoreceptors is disrupted. This is investigated in the following section, 4.6.

4.6 Photoreceptor-specific gene expression by RT-PCR

Expression of the photoreceptor specific transcription factor *Crx* is delayed by approximately seven days in the *or*^{J} retina. This is perhaps a surprising result, as Chx10 has not been reported to be expressed in photoreceptors, although the *or*^{J} mouse does have a photoreceptor phenotype, with an absence of normal sized inner and outer segments (Burmeister *et al.* 1996). The preferred binding site for Crx has been described, and during the course of this thesis, many photoreceptor genes have been shown to posses this motif in their 5' promoter regions (Livesey *et al.* 2000). These data indicate that Crx is (at least partially) responsible for the expression of several photoreceptor specific downstream targets.

Given this information, one prediction might be that expression of downstream targets of Crx would be similarly or further delayed in the *or*^{J} retina, and that disruption of this hierarchy is responsible for the observed photoreceptor phenotype. This prediction was addressed by examining the expression of a number of photoreceptor genes using RT-PCR on the same stages as before, E13.5, E18.5 and P12. Primers were designed to amplify short fragments of photoreceptor-specific genes.

The common factor for the choice of these genes was the presence of a Crx binding site in their 5' promoter regions (Livesey *et al.* 2000). Therefore, the prediction was that expression of these genes would be delayed in a similar manner to that of *Crx* in the *or*^{J} retina. Rhodopsin is a seven-pass membrane bound protein whose location is restricted to the outer segments of photoreceptors (Pepe 1999). Phosphodiesterase-β (Pde-β) is a sub-unit of the rod cGMP phosphodiesterase enzyme, and is part of the photo-transduction pathway. Mutations in *Pde-β* are known to cause autosomal recessive retinitis pigmentosa, and autosomal dominant stationary night blindness (Gal *et al.* 1994). Arrestin is a protein whose function contributes to the regulation of G-protein-mediated photo-transduction (Dolph *et al.* 1993). Peripherin (rds) plays an essential role in the maintenance of photoreceptor rod cell disk membrane structure. Mutations in peripherin in mice cause the *retinal degeneration slow* (*rds*) phenotype, and retinitis pigmentosa in humans (Kajiwara *et al.* 1991).

Interphotoreceptor retinoid binding protein (IRBP) is a secreted glycolipoprotein that is localised to the interphotoreceptor matrix surrounding

the inner and outer segments (Liou *et al.* 1994). There is evidence that the function of IRBP is to transport vitamin A across the hydrophilic subretinal space. Expression is first detected as early as E11, and thus may precede onset of *Crx* expression, which is first recorded at E12.5. Furthermore, there is some evidence that IRBP co-localises with BrdU incorporation in dissociated P2/3 retinal cultures (Liou *et al.* 1994). This suggests that IRBP may be a pre-terminal mitosis marker of photoreceptor fate. The 5' promoter region of *IRBP* also contains a Crx preferred binding site (Livesey *et al.* 2000), suggesting that Crx is involved with transcription of this photoreceptor specific gene.

As in section 4.3, primers to *Pgm1* were used again to test the integrity of the RNA. *Crx* expression was shown to be absent at E13.5 and E18.5 in the *or*^{J} retina (Figure 4.9), as was expression of rhodopsin (see above). Figure 4.12 shows that expression of *Pde-β* was weakly detected at E13.5, and readily at E18.5 and P12 in the wild-type mouse. This may reflect the low number of photoreceptors present at E13.5 (Young 1985), or photoreceptors at early stages of differentiation. However, no *Pde-β* expression by PCR could be detected in *or*^{J} retina in separate independent experiments at any time examined (n=3). This absence is likely to be an indirect result of the *Chx10* mutation, and may reflect the absence of outer segments, as this is where Pde-β is located. While *Crx* expression is delayed rather than totally absent in the *or*^{J} retina, this result indicates that mis-timing of a regulatory factor of Pde-β results in its complete absence.

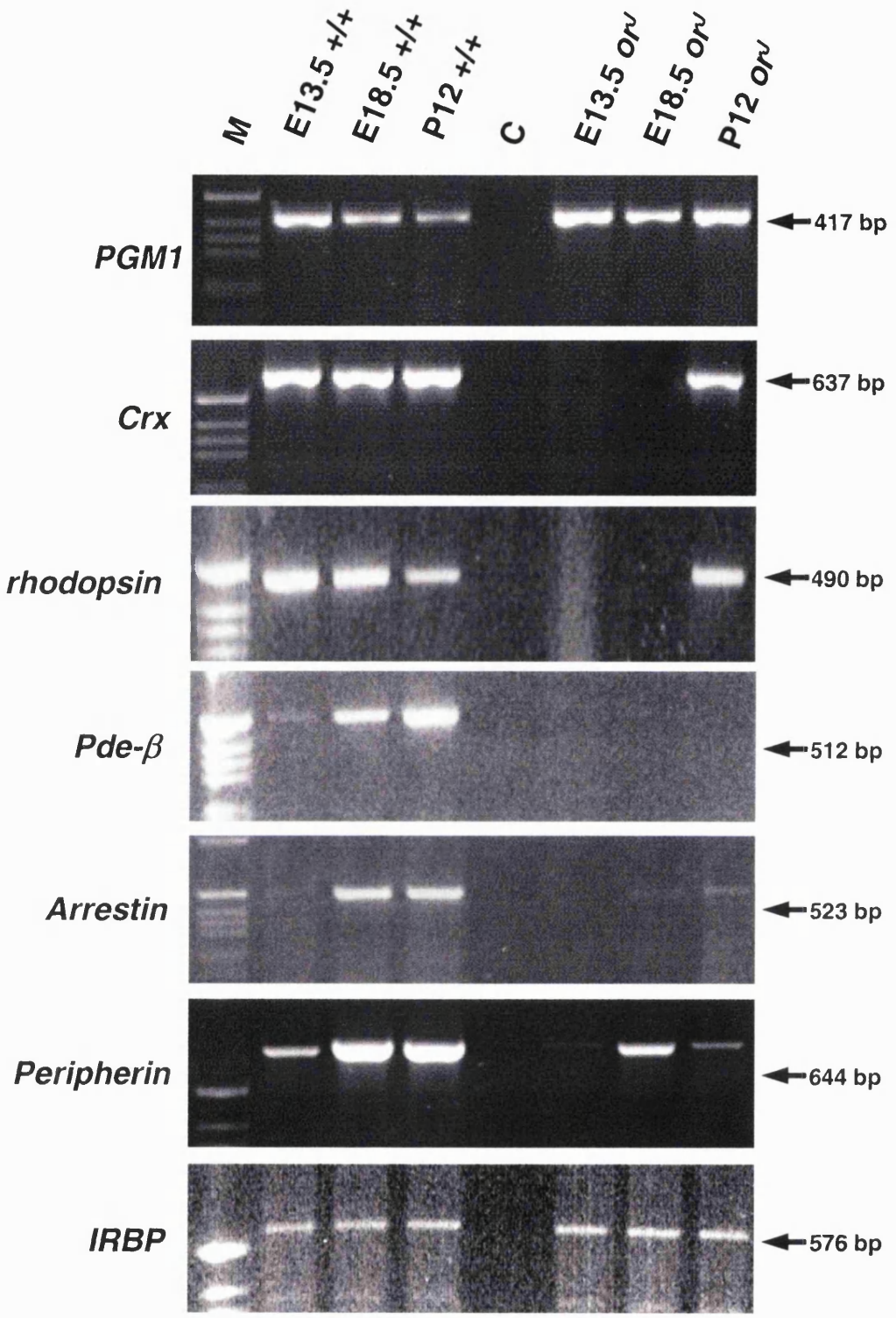

Figure 4.12. Photoreceptor gene expression in the *or*^{J} retina. Given the observed delay in *Crx* expression in the *or*^{J} retina, expression of other photoreceptor specific genes was investigated by RT-PCR at the same developmental stages. All of these genes have Crx consensus binding motifs in their promoter regions, and therefore are putative targets of Crx regulation. Comparative expression patterns fell into two groups: onset of expression of arrestin, peripherin and *IRBP* preceded that of *Crx* in the *or*^{J} retina, whereas *rhodopsin* and *phosphodiesterase (Pde)-β,* were similarly delayed to *Crx*. This suggests that the former set are not dependent upon Crx for their expression, despite their possessing a Crx binding site. Wild-type is shown on the left.

Expression of arrestin was very faintly detected at E13.5, and readily detected at E18.5 and P12 in the wild-type retina. At E13.5 in the *or*^{J} retina arrestin transcripts were undetectable. A very faint band was present at E18.5 and similarly low levels of expression were present at P12. The absence of expression at E13.5 is indicative of a delay as compared with the wild type. However, transcripts were detectable when Crx was absent, albeit at low levels. The low levels do not represent the hypocellular nature of the retina, as equivalent amounts of RNA were used in each cDNA synthesis reaction. This suggests that arrestin expression is partially regulated by Crx, as it is affected profoundly by the *Crx* delay, but is present before the onset of Crx expression.

Expression of peripherin was found to be readily detectable at all stages examined in the wild-type retina, although the intensity of the band at E13.5 was lower than that at E18.5 and P12. Again, this may reflect the low numbers of photoreceptors present, or photoreceptors at early stages of differentiation. Expression is strong at E18. the *or*^{J} retina, although the intensity of the band is much less than that of the wildtype at the same stage, again suggesting a reduction in expression levels, but not an absence. By P12 expression of peripherin is reduced back to very low levels. One possible explanation for this is that the absence of other factors caused by the mis-timing of *Crx* expression causes the subsequent downregulation of peripherin by P12.

IRBP expression was analysed at E13.5, E18.5 and P12, and was found to have comparable levels of expression at all stages. Surprisingly, expression of *IRBP* in the *or*^{J} mouse was also found to be indistinguishable from that of the

wild type. These data indicate that expression of *IRBP* is neither affected by the mutation in *Chx10*, nor by the consequent delay in the expression of *Crx*.

Further to the examination of the expression of these photoreceptor genes during development, I examined the precise onset of expression of rhodopsin by RT-PCR in the or^J mouse retina at P1, 2, 3, 4 and 5 (Figure 4.9). Expression was not detected at P1. Faint expression was detected at P2, and at P3, 4 and 5 transcripts were readily detectable. Although, as before, the amount of product amplified form these PCRs was not quantified, the absence of expression at P1, weak intensity at P2 and strong intensity at P3 indicates that the onset of rhodopsin expression in the or^J retina is on P2. This delay of at least one day after the onset of *Crx* expression certainly reinforces the possibility that Crx directly regulates rhodopsin expression.

4.7 Mouse background strain differences

The or^J mutation is present on the *Mus musculus musculus* strain sv129. Owing to ease of availability, mice of the C57Black6 × CBA were used as wild type in all experiments described. sv129, C57Black6 and CBA are inbred strains, i.e. are derived from more than 20 brother–sister matings, and are effectively homozygous at all genetic loci (Hogan *et al.* in *Manipulating the Mouse Embryo* 2nd edition). Strain differences are fundamentally polymorphisms, which may affect gene expression or protein function. While the observed delay of seven

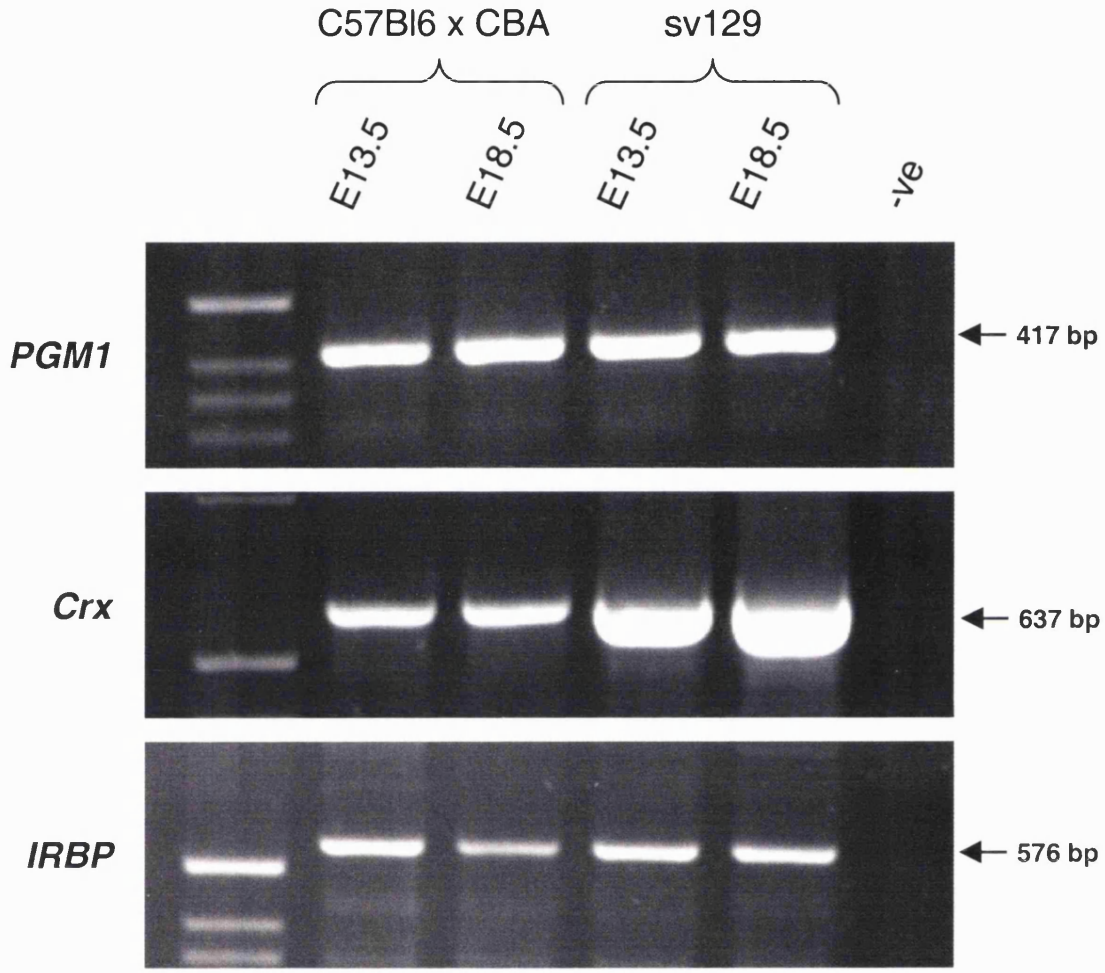

Figure 4.13. Demonstration by RT-PCR that *Crx* and *IRBP* expression is equivalent at E13.5 and E18.5 in two different strains of *Mus musculus*. The or^J phenotype is on the sv129 background, and this demonstrates that the observed phenotype of delayed *Crx* expression in t or^J retina is not caused by an affect of its strain.

days in *Crx* expression in the *or*^{J} mouse is almost certainly above the upper threshold of gene expression strain differences, expression of *Crx* and *IRBP* in the sv129 wildtype retinae at the time points examined was tested. RNA was extracted from retinal tissue of E13.5 and E18.5 eyes of both the C57Bl6 × CBA and sv129 strains.

cDNA was generated by reverse transcription of equivalent amounts of RNA, and this was used as template in a standard PCR reaction, with primers for *Pgm1* as a ubiquitously expressed gene as a positive control, and *Crx* and *IRBP* (Figure 4.13). Using 30 PCR cycles all three genes were shown to be expressed at E13.5 and E18.5 in both mouse strains. These data demonstrate that the validity of the result showing a delay in *Crx* expression in the *or*^{J} mouse is intact and this observation is not caused by differences in mouse background strain.

4.8 Discussion

The data presented here imply the significance of Chx10 on retinal development. There does not appear to be a profound effect on the genesis of ganglion cells and amacrine cells, which express differentiation markers appropriately. In terms of cellular location, ganglion cells appear least affected by the absence of Chx10, being in the innermost aspect of the mutant retina from the earliest time investigated. The complete absence of an optic nerve, however, suggests a defect that may reflect a disruption in the interactions between ganglion cells and the cellular milieu.

Amacrine cells appear to ultimately locate correctly, having previously been randomly distributed throughout the developing retina – a defect not seen in the developing wild-type retina.

The most profound effect that the absence of Chx10 confers, apart from on bipolar cells, appears to be on the differentiation of photoreceptors. A delay in the onset of *Crx* expression has a knock-on effect on a set of photoreceptor-specific *Crx* target genes. However, these data indicate that the photoreceptor-specific genes investigated here fall into two categories with respect to their expression in the *or*^{J} mouse:

1) those whose expression follows that of Crx, which is delayed in the mutant mouse, and,
2) those whose expression is not dependent on the presence of Crx.

All the genes investigated here have Crx binding sites in their promoter regions, suggesting that they are all (at least partially) regulated by Crx. However, these data indicate that at least for IRBP and peripherin, and possibly arrestin, absence of Crx is not enough to prevent expression, suggesting that expression of these genes is not simply regulated by Crx. Conversely, expression of rhodopsin and *Pde-β* is not detected before the delayed onset of Crx expression in the *or*^{J} mouse, suggesting that expression of these genes is principally regulated by Crx.

Mice with homozygous targeted disruption of *Crx* (Furukawa *et al.* 1999) show reductions in expression of rhodopsin, *Pde-β*, arrestin, and peripherin, indicating that Crx is required for expression of these photoreceptor specific genes, but is not the sole regulator. Kimura *et al.* (2000) demonstrated that high-level photoreceptor specific gene expression required the presence of photoreceptor conserved element 1 (PCE1)/Rx interactions as well as OTX element–Crx interactions. Levels of expression of IRBP in the Crx$^{-/-}$ mouse are normal (Furukawa *et al.* 1999). These data indicate that IRBP expression is independent of Crx *in vivo*, despite evidence that Crx is capable of transactivating the *IRBP* promoter (Furukawa *et al.* 1997). Co-transfection experiments show that human OTX2 as well as Crx activates the *IRBP* promoter (Bobola *et al.* 1999). The presence of *IRBP* mRNA in the *or*^{J} and *Crx*$^{-/-}$ mice may indicate that Otx2 is capable of compensating in the absence of Crx and thus directing photoreceptor specific IRBP expression. Expression of *Otx2* has not been investigated in the *or*^{J} mouse yet.

A requirement for expression of rhodopsin in a specific and discrete window of developmental time has been suggested as critical for normal retinal development in experiments in *Drosophila* rhodopsin mutants. Fly rhodopsin is encoded by the ninaE gene, and is expressed in the rhabdomere – a structure equivalent to the vertebrate outer segment. While abnormal rhabdomere development caused by mutated ninaE can be rescued by transgenic introduction of wild-type ninaE, delaying expression of the transgene fails to rescue the phenotype (Kumar *et al.* 1997).

It seems likely that the delay in expression of *Crx* in the or^{J} retina and a consequent delay in expression of other photoreceptor-specific genes disrupts outer segment morphogenesis and leads to the abnormal outer segments seen in the or^{J} retina.

The disruption in the Crx-dependent pathway caused by the absence of Chx10 suggests that there is an interaction between these two genes. The fact that onset of *Crx* expression is delayed, rather than completely absent, indicates that Chx10 does not directly regulate *Crx* expression, but is a key factor in the temporal regulation of expression of this gene.

Both Chx10 and Crx are homeobox transcription factors. This suggests that they are capable of dimerizing with each other (Wilson *et al.* 1993), or that one regulates gene expression by binding to the other's 5' promotor as a possible mechanism for interaction. However, data suggest that these two nuclear bound proteins are not expressed in the same cell at any stage (Burmeister *et al.* 1996, Furukawa *et al.* 1997). Other mechanisms for potential

interactions could involve a signalling pathway, utilising as yet unidentified molecules. These potential mechanisms are investigated in the following chapter.

CHAPTER 5

INVESTIGATIONS INTO INTERACTIONS BETWEEN CHX10 AND CRX DURING RETINAL DEVELOPMENT

CHAPTER 5

INVESTIGATIONS INTO INTERACTIONS BETWEEN CHX10 AND CRX DURING RETINAL DEVELOPMENT

5.1 Introduction

Data presented in Chapter 4 indicate that in the absence of Chx10, expression of the photoreceptor-specific transcription factor gene *Crx* is delayed by up to seven days. No evidence has yet been presented that suggests that these two genes ever co-express within the same cell, although their domains of expression overlap during development (Burmeister *et al.* 1996, Furukawa *et al.* 1997, Chapter 4, Figure 4.5). Indeed, the current understanding, based predominantly on expression data, is that Crx is only present in developing photoreceptors (Furukawa *et al.* 1997), and limited cells within the inner nuclear layer (Bibb *et al.* 2001), although these cells remain unidentified. By contrast, *Chx10* is expressed in mitotic retinal cells, and postmitotic bipolar cells. Therefore, the data presented in this thesis is somewhat surprising, that in the absence of Chx10, expression of a photoreceptor specific gene is disrupted. Given that both of these genes encode nuclear transcription factors there are two alternative possibilities as to how this delay in *Crx* expression could be explained. One is that Chx10 controls the instigation of *Crx* expression within photoreceptors indirectly through signalling pathways from nearby cells. The second possibility is that a direct interaction between Chx10 and Crx is involved

in photoreceptor development. For example, if Chx10 and Crx are transiently coexpressed in a progenitor cell, which has not yet started to differentiate as a photoreceptor, one might postulate an interaction where Chx10 directly regulates *Crx* expression by binding to its promotor, or where a Chx10–Crx protein–protein interaction is required for photoreceptor development.

There is some evidence to support the existence of a cell that may co-express Chx10 and Crx. Cepko *et al.* (1992) demonstrated the presence in culture of a postmitotic cell that was fated to express the photoreceptor marker rod opsin, whose fate could be altered by the addition of the secreted signalling molecule ciliary neurotrophic factor, (CNTF) to that of a bipolar cell, shown by expression of the cell specific marker PKC. In the adult retina, *Chx10* is expressed strongly within bipolar cells, and therefore may have a role in bipolar cell fate and differentiation (Liu *et al.* 1996). One possibility is that the re-specified bipolar cells maintain or re-instigate *Chx10* expression as a result of exposure to CNTF, and thus the photoreceptor differentiation pathway is blocked, and bipolar cell differentiation occurs. To test the hypothesis that Crx and Chx10 interact directly *in vivo*, I chose to investigate the possibility of the existence of a cell in which Crx and Chx10 could both be identified simultaneously *in vitro*.

5.2 Immunolocalisation of Crx and Chx10

The expression patterns of both *Crx* and *Chx10* at E13.5 and E18.5 indicate that they are expressed within the same domain (see Chapter 4, Figures 4.3 and 4.4). However, the resolution of the *in situ* hybridisation data is not sufficiently high to demonstrate co-expression within the same cell. By P2, the developing photoreceptors in the outer retina no longer express Chx10 (Figure 5.1). The aim of this section was to investigate whether any cells during development were Crx-positive and mitotic, and by extrapolation were Chx10-positive also.

In order to analyse the localisation of Crx and Chx10 in single cells, newborn (P0) wild-type retinae were dissected and mechanically dissociated into a single cell suspension in L15 medium, and transferred to 24 well culture plates, containing poly-L lysine coated coverslips (see Chapter 2, Methods for details). P0 pups were chosen because of availability, and as this point is close to the peak of rod genesis (Young 1985), and therefore a maximal number of putative co-expressing cells would be found. When these retinal cells had adhered to the coverslips, cells were either fixed or not, and immunocytochemistry was performed, using antibodies to Chx10, Crx, and to the cell proliferation markers PCNA and the phosphorylated histone H3 (Vermuru *et al.* 1992), individually and in certain combinations as double labelling. Two markers of proliferation were used to complement the secondary antibody used in double labelling experiments, i.e. PCNA was raised in mouse,

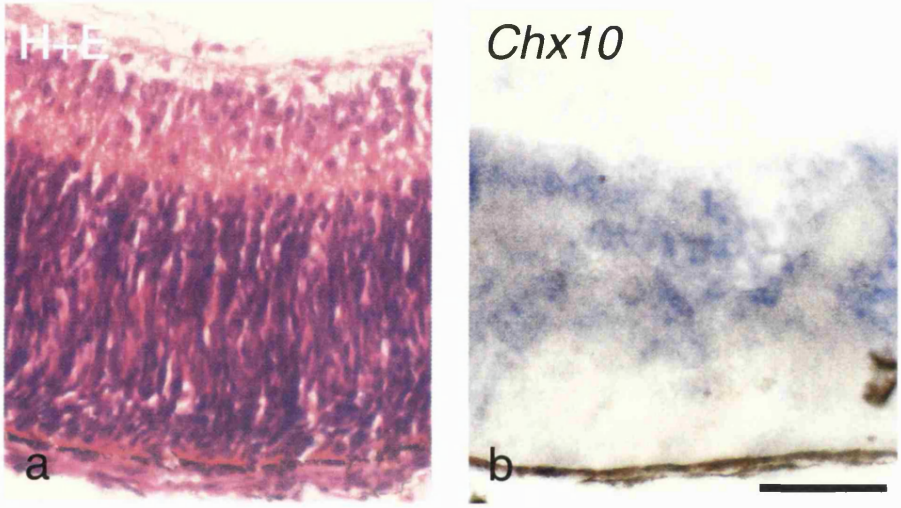

Figure 5.1. *Chx10* expression at P2. (a) shops H and E stained postnatal (P) day 2 retinal section. (b) Expression of *Chx10* by *in situ* hybridisation shows that cells on the outermost layer are now no longer *Chx10*-positive, suggesting that they are differentiating as photoreceptors. Scale bar: 100μm.

and H3 in rabbit, so H3 could not be used together with Chx10 or Crx, as these were both antibodies also raised in rabbit. Cell vitality and integrity was observed using the Hoescht nuclear stain (see Chapter 2, Methods).

Two Crx antibodies were used and these were raised to recognise part of the homeodomain and the N-terminus, respectively (provided by Cheryl Gregory-Evans, Imperial College, London). Before using for immunostaining on dissociated retinal cells in culture, these were tested by Western blotting using mouse retinal tissue, and showed binding to a protein of ~37kDa (Figure 5.2) (Bibb *et al.* 2001). Incubation with pre-immune serum did not detect this band. Higher affinity was observed in the homeodomain-specific antibody, and therefore this one was used in subsequent experiments. Immunolocalisation with the homeodomain-specific antibody was performed on adult paraffin embedded sections of mouse retina. Staining was seen in the bipolar layer (Chx10), and the outer nuclear layer (Crx) (Figure 5.3), both confirming published data (Liu *et al.* 1994, Furukawa *et al.*1997).

Immunocytochemistry on dissociated P0 retinal cells identified Chx10-, H3-Crx- and PCNA-positive cells. Cells expressing Chx10, H3, PCNA and Crx were each shown to be a proportion of the total number of cells (representative fields of view shown in Figures 5.4, 5.5, 5.6 and 5.7, respectively). Antibody and Hoescht staining have been superimposed to give a different colour. In Figure 5.4, ~50% of the total number of cell (n=64) in this field are expressing Chx10. In Figure 5.5, ~36% of the total number of cells (n=70) are expressing H3. In

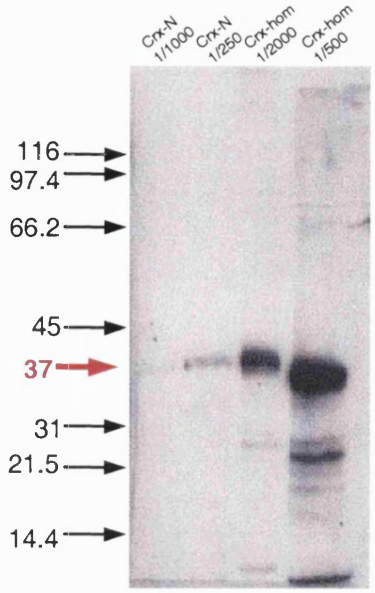

Figure 5.2. Western blotting to show antigen-specific affinity of antibodies raised against Crx homeodomain (hom), and Crx N- terminus (-N). Dilutions of primary antibody are indicated. The numbers indicate the size of each fragment in kDa, from a marker (not shown). Low-molecular-weight proteins are likely to be degradation products.

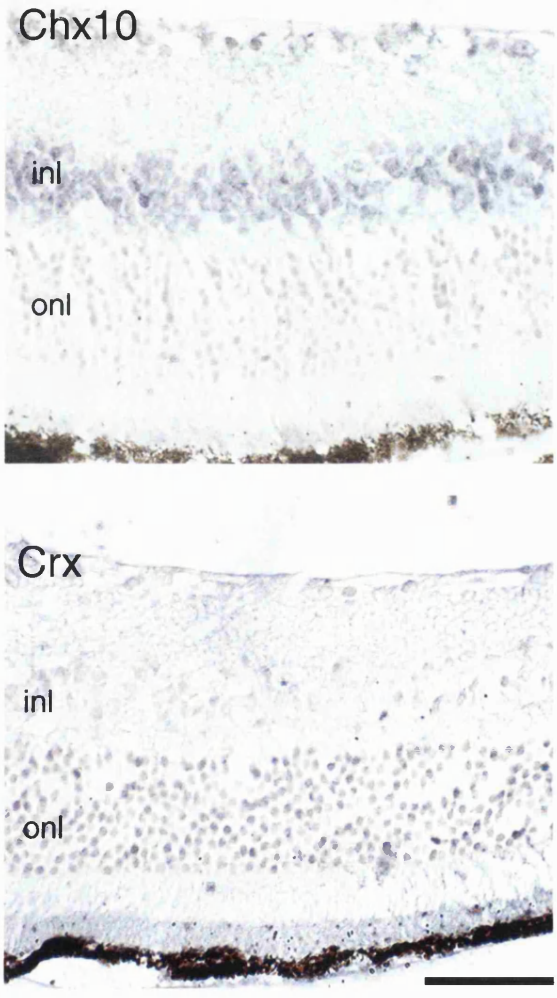

Figure 5.3. Immunolocalisation of Chx10 and Crx to the inner (inl) and outer (onl) nuclear layers of the adult mouse retina, respectively. These data, combined with immunoblotting (Figure 5.6) confirmed the specificity of the Chx10 and Crx antibodies. Scale bar: 100μm.

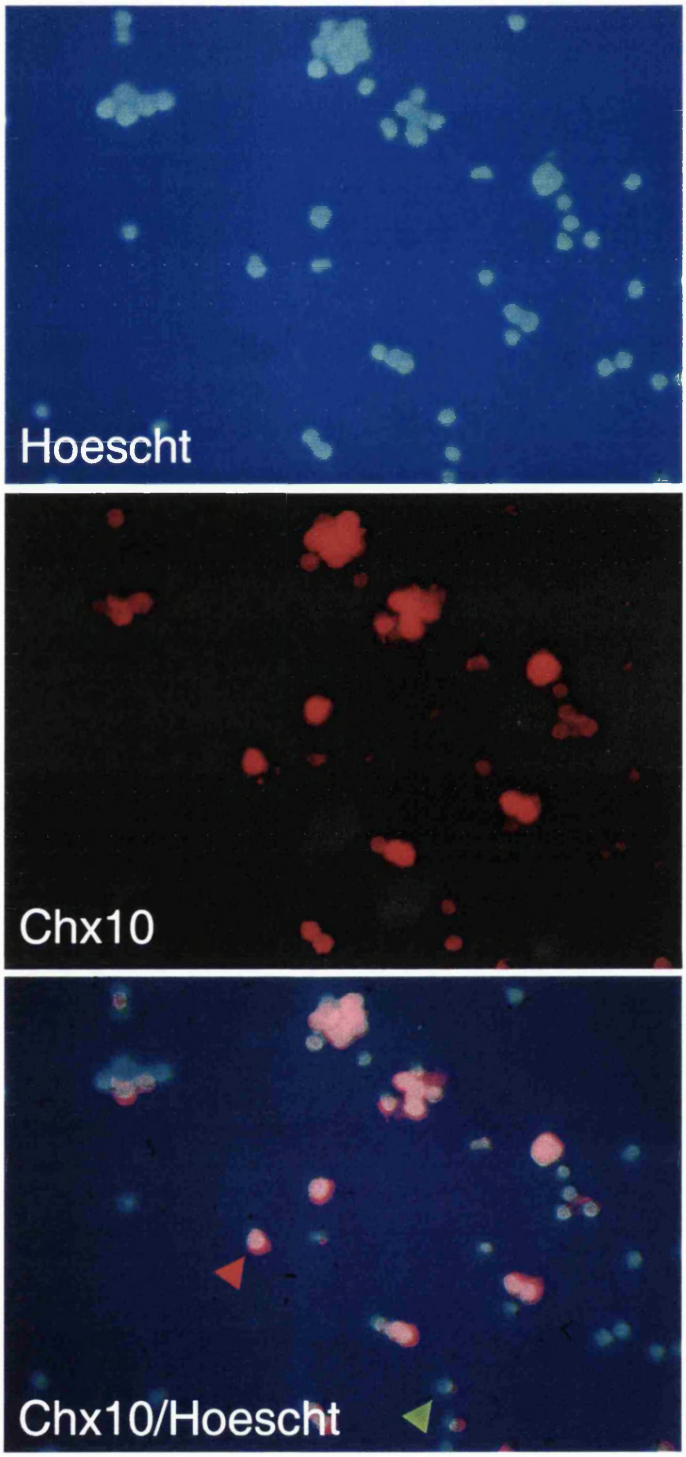

Figure 5.4. Immunocytochemistry of Chx10 to P0 retinal cells. Fluorescent staining of the vital marker Hoescht (blue), and Chx10 (red) shows that a proportion of retinal cells are expressing Chx10 at P2. The red arrow is indicating a cell which is both Hoescht- and Chx10-positive, whereas the green arrow shows a cell which is Chx10-negative.

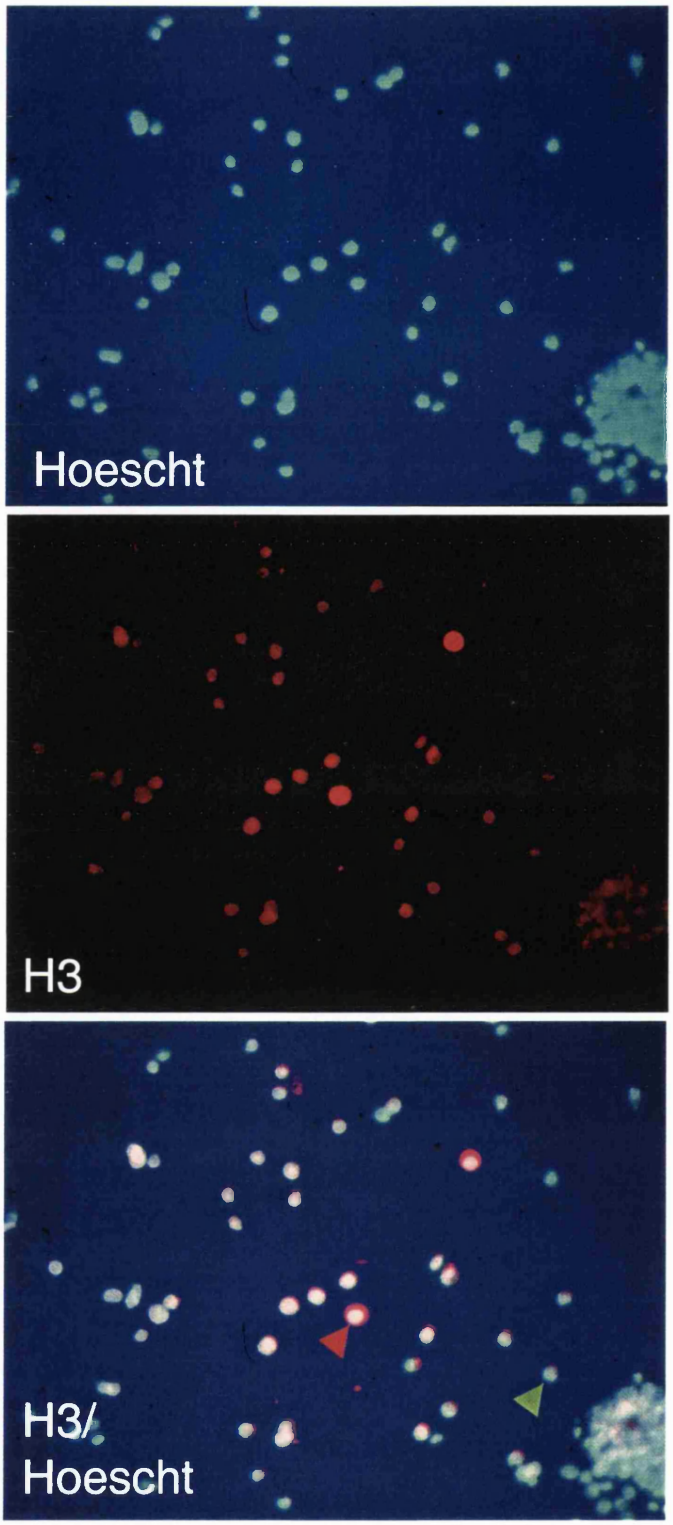

Figure 5.5. Immunocytochemistry of H3 to P0 retinal cells. Fluorescent staining of the vital marker Hoescht (blue), and H3 (red) shows that a proportion of retinal cells are dividing at P0. The red arrow is indicating a cell which is both Hoescht- and H3-positive, whereas the green arrow shows a cell which is H3-negative.

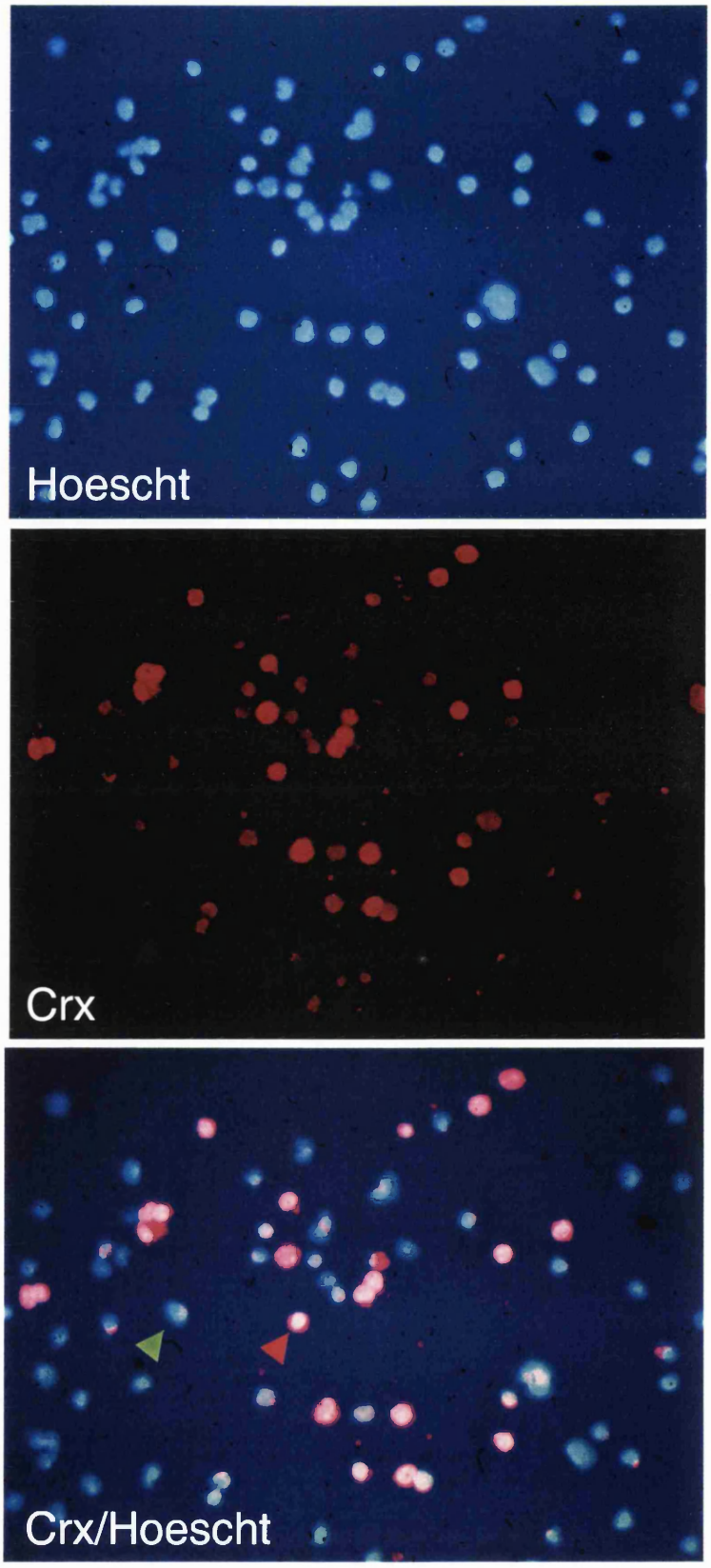

Figure 5.6. Immunocytochemistry of Crx to P0 retinal cells. Fluorescent staining of the vital marker Hoescht (blue), and Crx (red) shows that a proportion of retinal cells are expressing Crx at P0. The red arrow is indicating a cell which is both Hoescht- and Crx-positive, whereas the green arrow shows a cell which is Crx-negative.

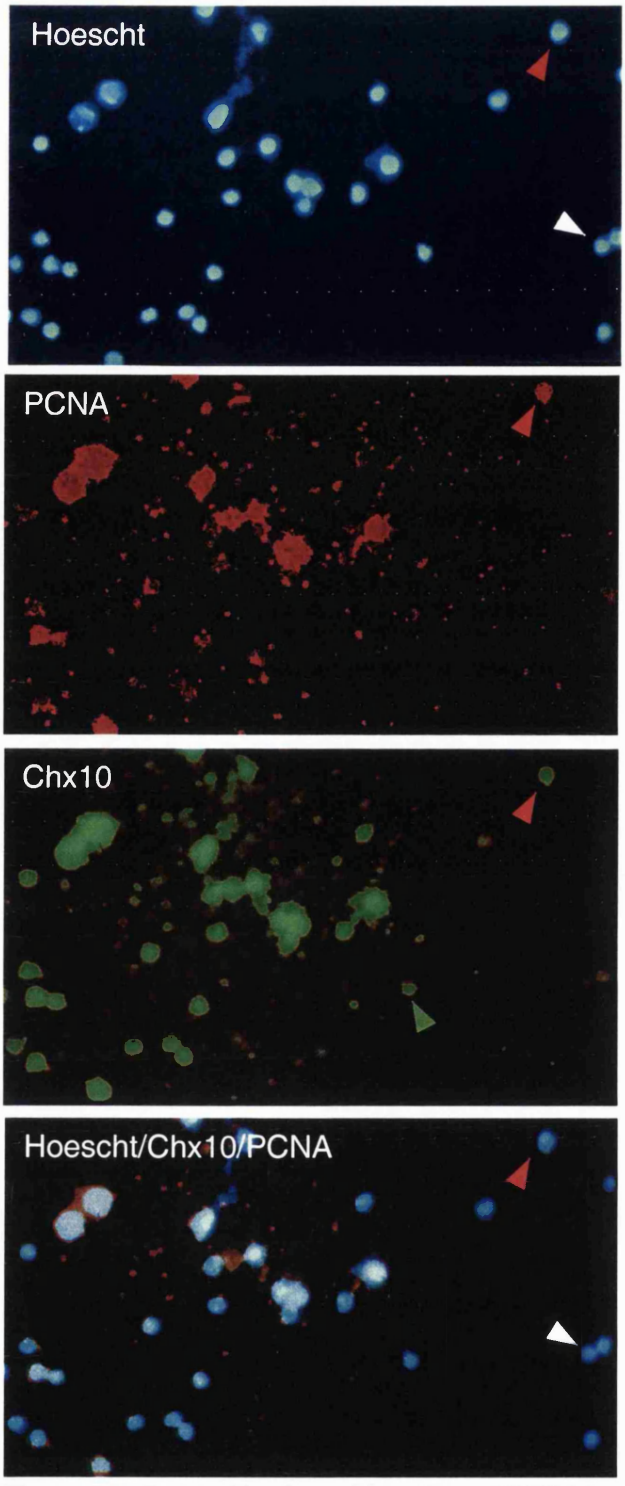

Figure 5.7. Co-localisation of Chx10 and PCNA by immunocytochemistry in P0 retinal cells.
Fluorescent staining of the vital marker Hoescht (blue), and Chx10 (green) shows that a proportion of retinal cells are expressing Chx10 at P0. PCNA (red) immuno-fluorescence shows that all PCNA-positive cells are also Chx10-positive, but some Chx10-positive cells are not PCNA-positive. The red arrows indicates a cell which is Hoescht- , Chx10- and PCNA-positive, whereas the green arrows show a cell which is Chx10-positive but PCNA-negative. White arrows indicate cells which are positive for neither Chx10 or PCNA, but are Hoescht stained.

Figure 5.6, Crx expressing cells make up ~24% of the total number (n=84). In Figure 5.7, PCNA immunostaining labelled ~30% of cells.

Double labelling with PCNA and Chx10 (Figure 5.7) indicated that a subset Chx10-positive cells expressed PCNA. This exemplifies dual roles of Chx10 in the developing retina, in that the Chx10-positive/PCNA-positive cells are dividing cells, whereas the Chx10-positive/PCNA-negative are presumed to be postmitotic cells. No Chx10-negative/PCNA-positive cells were observed in separate independent experiments (n=2). The postmitotic Chx10-positive cells are likely to be developing bipolar cells, as bipolar cell genesis is underway by P0. However, without co-labelling with a bipolar specific marker, these cells could represent other post-mitotic cells.

Several attempts were made to co-label cultures with antibodies to Crx and Chx10. Both antibodies were raised in rabbits (Bibb *et al.* 2001, Jessel *et al.* 1998), ruling out the possibility of straightforward double immunolocalisation, as a secondary anti-rabbit antibody would not be able to distinguish between the two primary antibodies.

The Crx antibody was conjugated with biotin to use in double labelling experiments with Chx10 antibody (see Chapter 2, Methods), to enable a separate detecting system. However, immunolabelling proved fruitless with the biotinylated antibody as it resulted in non-specific background staining. (Figure 5.8).

Double labelling was performed with Crx and PCNA, and these were shown to never co-localise (n=2) (Figure 5.9). Therefore, Crx is confirmed as

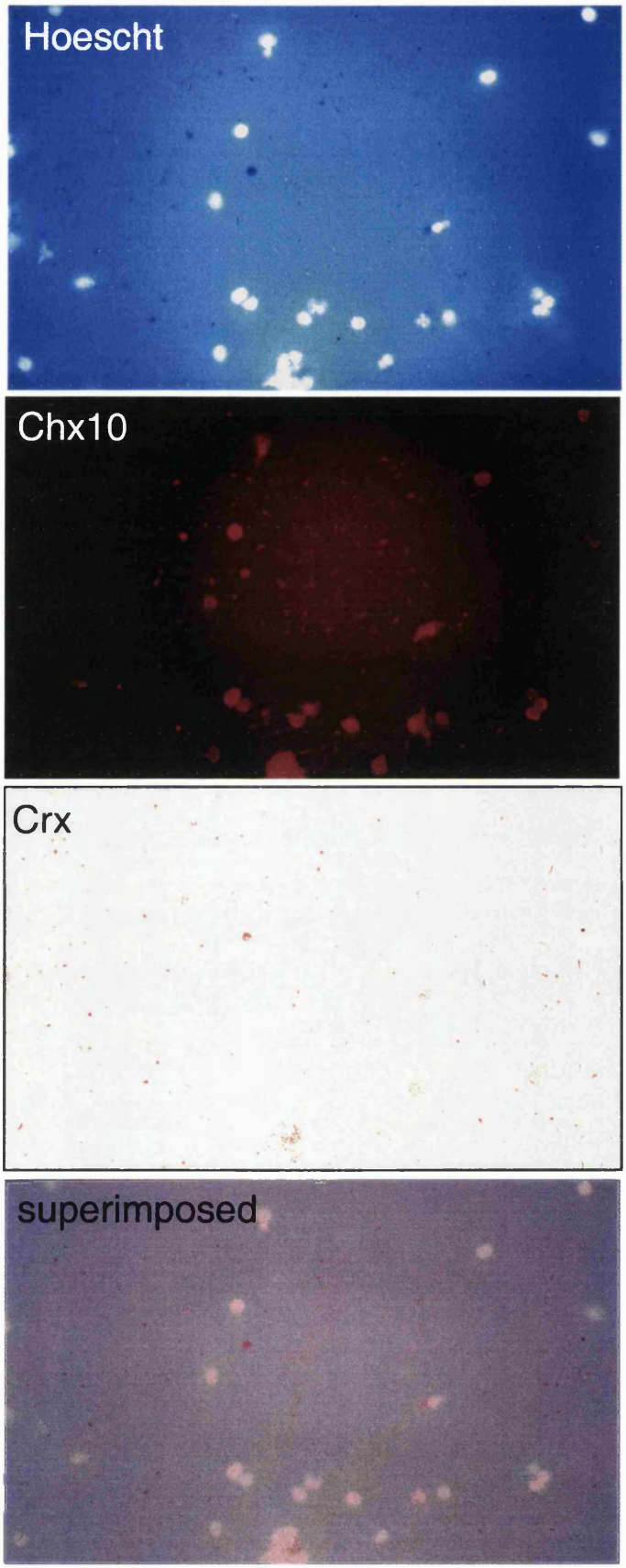

Figure 5.8. Attempted immunolocalisation of Chx10 (red) **and biotinylated-Crx** (visualised with HRP-DAB) resulted in weak signal that sometimes did not colocalise with Hoescht staining, indicating that it was false positive. This technique was not pursued further.

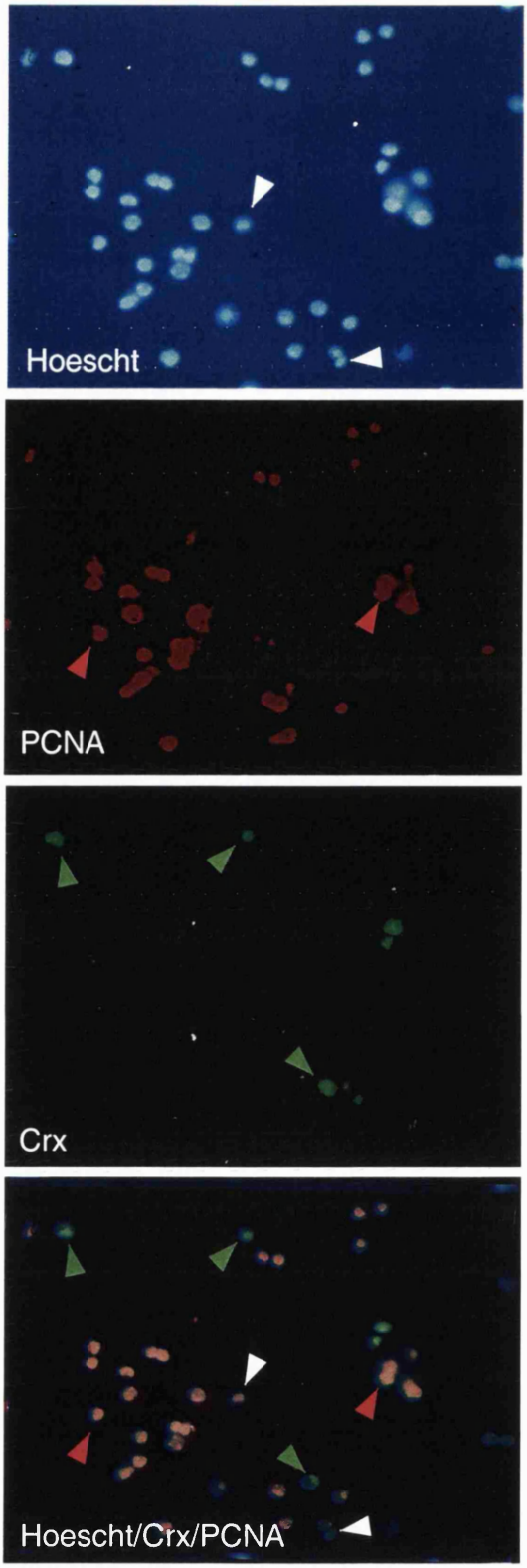

Figure 5.9. Crx and PCNA do not co-localise by immunocytochemistry in P0 retinal cells. Fluorescent staining of the vital marker Hoescht (blue), and Crx (green) shows that a proportion of retinal cells are expressing Crx at P0. PCNA (red) immuno-fluorescence shows that no PCNA-positive cells are Crx-positive. The red arrows indicates cells which are Hoescht- and PCNA-positive, whereas the green arrows show cells which are Crx-positive. White arrows indicate cells which are positive for neither Crx nor PCNA.

not being present in cells that are dividing, at least in these culture conditions. These data have not found any support for the hypothesis that Chx10 and Crx co-localise within the same cell. Thus any direct interaction, whether it be protein–protein or protein–DNA, seems unlikely.

One possibility that has not been ruled out here is that the cells that are Chx10-positive and PCNA-negative are in fact postmitotic photoreceptors, which were expressing Crx.

5.3 Cell–cell interactions of Chx10 and Crx

The possibility of an indirect interaction between Crx and Chx10 was investigated using a dissociated retinal cell culture system, based on the hypothesis that a secreted factor(s) causes the upregulation of Crx in presumptive photoreceptors, and this factor was absent in the *or*^{J} retina.

5.3.1 Retinoic acid cultures

Kelley *et al.* (1994, 1995) investigated the effect of the vitamin A derivative retinoic acid (RA) upon retinal cells in culture, based on the knowledge that all-*trans* RA was capable of altering cell fate decisions in the developing limb bud, hindbrain, and inner ear (Altaba and Jessell 1991, Kelley *et al.* 1994). RA has been shown to be important in a number of different aspects of eye development. All-*trans* RA and at least one of the RA receptors, RARα, have

been shown to be present in the developing retina (Drager *et al.* 2001). Furthermore, double knockout mice with targeted deletions in both *RARα* and *RARβ* display retinal hypoplasia and a shortening of the ventral retina (Ghyselinck *et al.*1997). Kelley and colleagues (1994) added all-*trans* RA at a concentration between 10 and 500nM to culture media that contained dissociated retinal cells from either E15 or E18 rats. In these cultures, disproportionately high numbers of rod photoreceptors differentiated from precursor cells, sometimes at the expense of bipolar cells. Their conclusions included that RA acted directly on a proportion of mitotic progenitor cells to steer their fate towards that of a rod photoreceptor, identified by immunocytochemistry with an antibody raised against rhodopsin.

In this study, I used a similar system to test whether all-*trans* RA was a factor capable of inducing expression of *Crx* in *or*^{J} retinal cultures, at a time point when these cells were not expressing *Crx*, but wild-type cells were. Kelley *et al.*'s (1994) use of rhodopsin as a marker for photoreceptor fate is in line with this test, as data presented here have already demonstrated that rhodopsin expression is similarly delayed to that of Crx in the *or*^{J} retina.

A culture system was used as described in Chapter 2, Methods, where dissociated E14.5 *or*^{J} retinal cells were cultured with Dulbecco's modified eagle medium (DMEM) for 48hrs on laminin and poly-L-lysine coated coverslips, this time with the medium containing 100nM all-*trans* RA. Previous studies have found that concentrations of 500nM have cytotoxic side effects (Kelley *et al.* 1994). Control experiments were carried out, with *or*^{J} cells being simultaneously

cultured without RA. Cells were checked after 6, 24 and 48 hours (Figure 5.10), by which stage, some cells had developed cellular processes. After 48hrs, cells were harvested for immunocytochemistry using an antibody for Crx.

Although cell survival was low in *or*^{J} retinal cultures, Crx expressing cells were detected by immunocytochemistry (Figure 5.11) in independent experiments (n=2), some of which displayed cellular processes, indicating that some level of differentiation had occurred. Untreated controls, or those with added DMSO but no RA showed no Crx immunoreactivity. These data suggest that addition of all-*trans* RA to culture medium was capable of inducing Crx expression in *or*^{J} retinal cells. Figure 5.12 shows immunoreactivity to Crx of wild-type cells cultured in untreated medium

5.3.2 Co-culture of wild-type and or^{J} *cells*

Two other approaches were used to examine induction of Crx expression, and to increase cell survival in *or*^{J} retinal cultures.

Based on the hypothesis that wild-type retinal neuroblasts are secreting RA, which is capable of inducing the expression of Crx in presumptive photoreceptor cells, but is absent or delayed in the mutant retina, retinal cells of these two genotypes were grown together in culture, under the possibility that RA or other signalling moleculeswas then introduced into the mutant cells. As these two genotypes are indistinguishable when dissociated, *in vitro* Corning Transwells were used to keep the two genotypes separate. This system allows the transfer, mediated by the size of the filter, of molecules between cells,

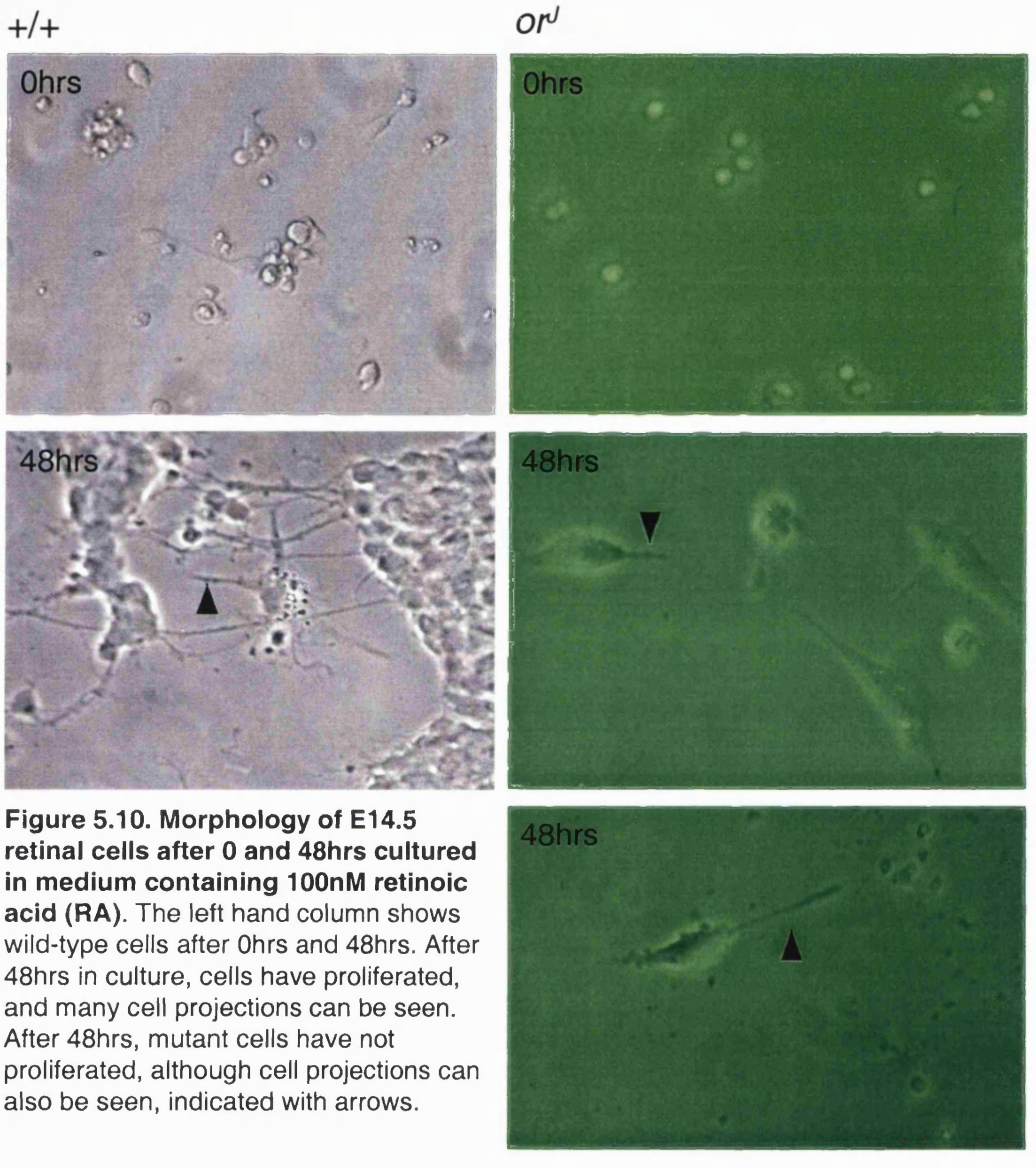

Figure 5.10. Morphology of E14.5 retinal cells after 0 and 48hrs cultured in medium containing 100nM retinoic acid (RA). The left hand column shows wild-type cells after 0hrs and 48hrs. After 48hrs in culture, cells have proliferated, and many cell projections can be seen. After 48hrs, mutant cells have not proliferated, although cell projections can also be seen, indicated with arrows.

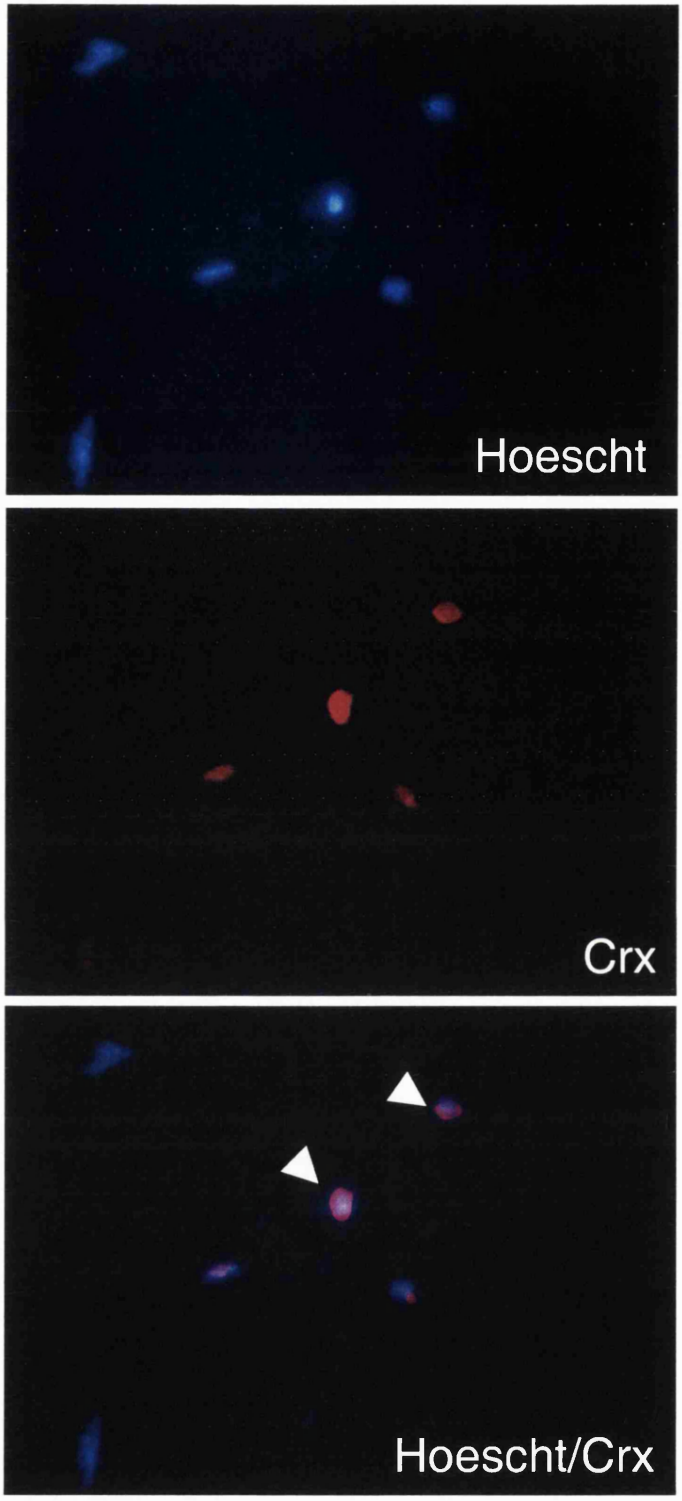

Figure 5.11. Immunoreactivity for Crx on E14.5 *or*^{J} retinal cells cultured for 48 hrs in medium with 100nM retinoic acid (RA). A small proportion of mutant cells expressed Crx, indicating that RA is capable of inducing Crx expression in the absence of Chx10. Cells cultured in medium without RA did not express Crx (data not shown). The digital combination of the blue Hoescht-stained and red Crx-stained cells gives a mauve colour (white arrows).

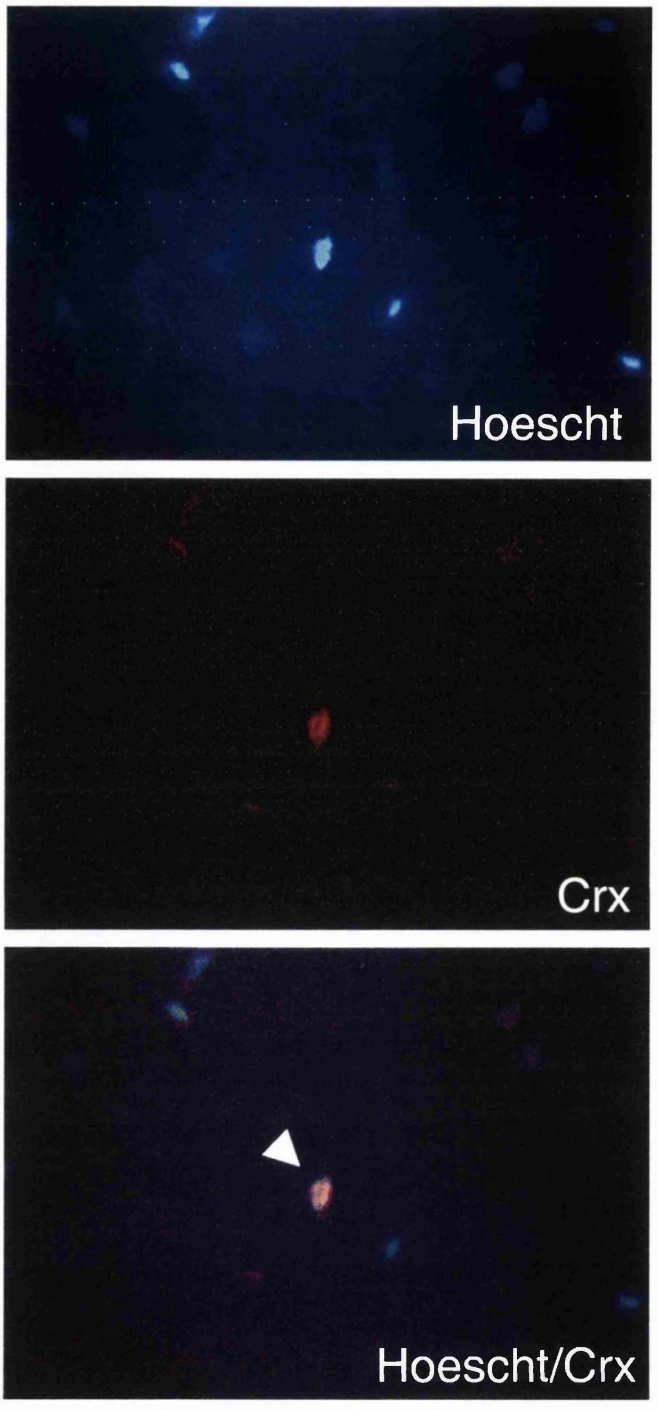

Figure 5.12. Immunoreactivity for Crx on E14.5 wild-type retinal cells cultured for 48 hrs in untreated medium. These data demonstrates that the Crx antibody immunostains a proportion of wild-type cells after 2 days in culture. Digital superimposition of the blue Hoescht-stained and red Crx-stained cells gives a mauve colour (white arrow).

without actually mixing the cells. E14.5 wild-type cells were harvested as described in Chapter 2, Methods, and allowed to adhere to coated coverslips in F12 DMEM medium. E14.5 *or*^{J} cells were also dissected in the same way and allowed to stick down to the Transwell membrane, with a filter size of 0.4μm. Repeated attempts of this method failed to generate cells that lived for 48hrs, and the medium was always full of cell debris, indicating the presence of dead cells. Therefore, this experiment was not pursued.

5.3.3 Conditioned medium

The second method used to increase the survival of *or*^{J} cells in culture was to culture mutant cells in medium that had been exposed to wild-type retinal cells ("conditioned medium").

Wild-type retinal cells were dissected from E12.5 mouse embryos and cultured with DMEM and 10% foetal calf serum, as described before, at a density of ~400 cells per 1μl. After 48hrs the medium from these cultures was collected, and added to an equal volume (200μl) of fresh DMEM. E14.5 retinae were dissected from *or*^{J} mice, and prepared as described above, and were incubated in the half-conditioned, half-fresh medium for 48hrs. Cells were observed and photographed after 4, 24, and 48hrs (Figure 5.13) to check their health, and differentiation status. After 48hrs, cells were harvested for immunocytochemistry.

Immunocytochemistry was performed as described previously, with antibodies to detect Crx. Effectively, these cell cultures were *or*^{J} retinal at E16.5,

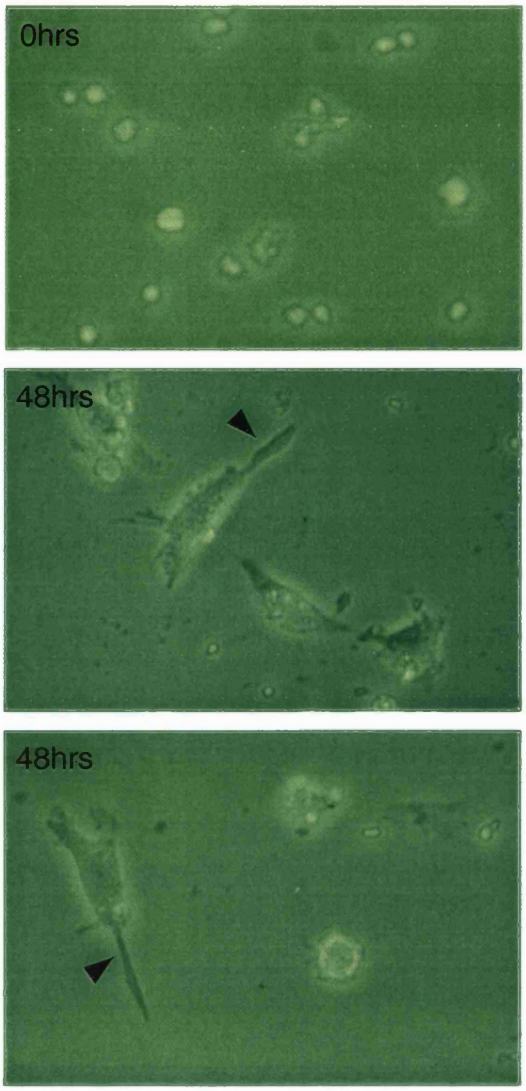

Figure 5.13. Morphology of E14.5 *or*^{J} retinal cells after 0 and 48hrs culture in conditioned medium. A small proportion of mutant cells displayed cellular processes, which are consistent with differentiation, indicated with arrows.

so, according to the data presented earlier (Chapter 4), would not be expressing Crx. Many of the cells displayed cellular processes (Figure 5.13), possibly indicating that cellular differentiation was progressing in these cultures. This is in agreement with the earlier data (Chapter 4.6), which showed that other photoreceptor genes were not delayed in their expression, and that only the Crx-dependent pathway was affected by the mutation in *Chx10*. In these cultures, where E14.5 *or*^{J} retinal cells had been cultured with wild-type-conditioned medium, cells expressing Crx were detected (Figure 5.14). This indicates that a secreted factor(s) induces Crx expression, and that it is not present in *or*^{J} retinae. Control experiments in which *or*^{J} were grown in medium which had not been exposed to wild-type cells, but had been treated in the same way (i.e. kept at 37°C for 48hrs, and diluted by half with fresh medium) did not show Crx immunoreactivity after 48hrs (data not shown).

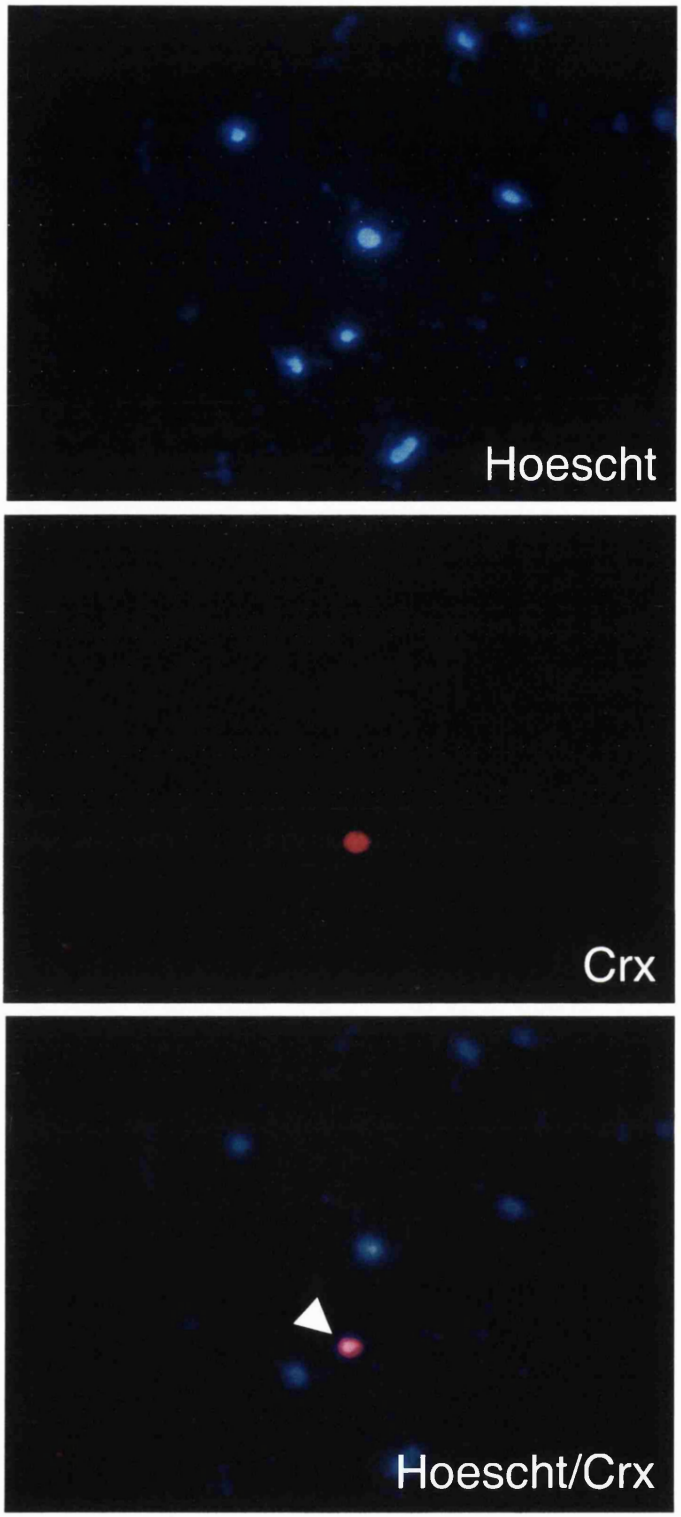

Figure 5.14. Immunoreactivity for Crx on E14.5 *or*^{J} retinal cells cultured for 48 hrs in conditioned medium. A small proportion of mutant cells expressed Crx, which indicates that a factor (s) in the medium was capable of inducing its expression despite the absence of Chx10.The digital superimposition of Hoescht-stained (blue) and Crx-stained (red) cell gives a mauve colour (white arrow).

5.4 Discussion

In the developing *or*^{J} retina, the molecular cascade that regulates the timing of *Crx* expression is defective. This fact invites the possibility that Chx10 and Crx interact during development, and that this interaction is disrupted in mutant retina. No evidence was found to support the hypothesis that Chx10 and Crx interact directly. All existing data indicates that these two are not co-expressed in the same cell at any stage of retinal development, leaving the possibility of a regulatory pathway that involves extrinsic factors.

Data presented here indicate that a factor, secreted by wild-type retinal cells at E12.5–14.5 is indeed capable of inducing *Crx* expression in cells in which it is absent, and that factor may be all-*trans* RA. The conditioned medium (5.3.3) itself was not examined to see whether it contained all-*trans* RA or not, but it is attractive to conclude that the unknown factor in the conditioned medium was in fact all-*trans* RA. Control experiments where *or*^{J} cells were grown in medium which neither was conditioned, nor contained RA showed that induction of Crx expression was not an artefact of culturing these cells in DMEM with FCS, and conversely, Crx immunoreactivity was detected in E14.5 wild-type cells cultured without treatment (Figure 5.12).

Difficulties with these experiments included the low level of cell survival for *or*^{J} cells in culture, regardless of the various combinations of medium used. The low levels of cell survival may reflect a number of factors, including the intrinsic lack of Chx10, as well as the very low numbers of cells in the *or*^{J} retina,

and therefore difficulty in culturing these cells in densities that mirrored that of the wild-type cells.

The fact that control cultures of wild-type cells showed survival, proliferation and apparent differentiation under the same culture conditions indicates that fragile nature and low survival is a property of the *or*^{J} cells. It will be important in future experiments to try a variety of different culture conditions including the addition of other growth factors to try to increase survival, proliferation and differentiation of the *or*^{J} cells in culture. This approach may provide a useful strategy for identifying conditions needed to promote photoreceptor development and proliferation from retinal progenitor cells.

Analysis of patterns of gene expression using *in situ* hybridisation of tissue sections has provided useful insights into the impairment of photoreceptor development in the *or*^{J} retina. Efforts to analyse photoreceptor development *in vitro* in dissociated cell culture have been hampered by low cell numbers and low survival, possibly caused by the reduced proliferation of *or*^{J} cells compared with wild-type retinal cells. An alternative strategy for future experiments could be the use of explanted whole *or*^{J} retinae. This approach would provide increased cell contact, which may allow an increased survival rate for *or*^{J} cells.

CHAPTER 6

IDENTIFICATION AND CHARACTERISATION OF A NOVEL *CHX10*-LIKE cDNA

CHAPTER 6

IDENTIFICATION AND CHARACTERISATION OF A NOVEL *CHX10*-LIKE CDNA

6.1 Introduction

At the onset of this thesis, a human homologue of the murine gene *Chx10* had not yet been identified or cloned. A search was instigated using the resources of the various genome databases available through the Internet for human DNA sequences that contained significant levels of identity to the mouse *Chx10* sequence. This involved using the programs available at the National Centre for Biotechnology Information (NCBI) (http://www.ncbi.nlm.nih.gov/), predominantly the various BLAST (basic local alignment search tool) tools (Altshul *et al.* 1990).

6.2 Identification of ESTs containing novel cDNA sequence

Using the 3.089kb sequence of mouse Chx10 cDNA (accession number L34808) as a search string in the basic BLAST program, covering all databases, identified several genes in different species which have been shown to be structural and functional homologues in diverse species. These include *Vsx1* and *Vsx2* from both the goldfish *Carassius auratus* (Levine *et al.* 1994, 1997) and zebrafish *Danio rerio* (Passini *et al.* 1998). Restricting the database searches to human sequence results in the identification of a number of cDNA

sequences that show high levels of sequence identity to mouse Chx10 over short fragments. These include a 30 bp stretch of 96% identity within the *Chx10* 3' untranslated region (UTR) to an unidentified fragment of genomic DNA, and several stretches of 90^{+}% identity over less that 30bp to the coding sequence of several homeobox genes including *Phox1*, *PMX1*, *SHOXa* and *b* and *Nkx6.1*. Given the high level of sequence conservation in the DNA binding domain between homeobox genes in general, these results are not surprising, and the significance of these regions of identity is not high enough to regard these genes as homologues of murine Chx10. Further restricting these searches to the database dbEST, which only contains human expressed sequence tags (ESTs), produced rather more limited results. A fragment showing 92% sequence identity over 520bp from a Stratagene ovarian cancer cDNA library has highest significance, although the region on *Chx10* where this identity lies is from 2135–2197bp, and therefore lies within the *Chx10* 3' UTR. Therefore, this was not considered for further investigation. Also significant was a 94% identical stretch of DNA identified as being from the human gene *CART1*. However, like *Chx10, CART1* is a *paired*-type homeodomain protein (Cai 1998), and this short stretch of sequence identity lies within *Chx10's* homeobox, which is heavily evolutionarily conserved. Furthermore, this EST was generated from a colon cDNA library, where Chx10 is not known to be expressed. Therefore this result did not warrant further investigation.

An 82% stretch of sequence identity with an expected value of $3e^{-7}$ over a 107bp region from an EST (H87757) was identified in this BLAST result (see

Figure 6.1), indicating a highly-related sequence. This identity ran from 433–545bp on *Chx10*. The homeobox of *Chx10* runs from 442–622bp, indicating that this sequence identity is almost exclusively within the homeobox. This EST was from an adult retinal cDNA library made from the RNA of a 55-year-old Caucasian man. As this cDNA was expressed in the retina it was investigated further as a candidate for the human homologue of *Chx10*, or a closely related gene. The total length of the EST H87757 was 264bp. However, significant numbers of "N" nucleotides were present in the last 50bp, which are unknown nucleotides caused by sequencing errors. Therefore the sequence was only reliable for 216bp. This sequence translates into a predicted protein with an open reading frame (ORF) from 1–230nt, and appears to encode an incomplete *prd*-type homeodomain from 100–222nt (see Figure 6.2). However, no significant nucleotide or protein identity with mouse *Chx10* was observed outside of the putative homeodomain, suggesting that this cDNA represented a novel *prd*-type homeobox gene, rather than the human *CHX10* homologue.

In order to generate more sequence for this cDNA, the EST H87757 was used to search the dbEST database using the BLAST algorithm (Altschul *et al* 1990) ("BLASTed") (http://www.ncbi.nlm.nih.gov/BLAST/). This identified another (362bp) EST from the same retinal library (H87056), which showed 90% sequence identity with H87757 over a 110bp stretch from 252–362bp. Although these ESTs are directionally cloned into specialised vectors, H87056 shared sequence identity in the reverse orientation to H87757 (see Figure 6.3). Because of the high level of sequence identity, the two ESTs were assumed to

```
Expect = 3e-07, Identities = 88/107 (82%)

Chx10 433 aagcgtaagaagcggcgacacaggacaatctttacttcctaccagctagaggagctggagaaagca 498
          ||| | ||||||||||||||||||||| | || ||| |  ||||||| || ||| ||||||| |||
EST   100 aagaggaagaagcggcggcacaggacagttttcactgctcaccagctggaagagttggagaaggca 165


Chx10 499 ttcaatgaagcccactacccagatgtctacgcccgggagatgctggc 545
          ||||| || |||||||||| ||||| || ||||| || ||||||||
EST   166 ttcagcgaggcccactaccctgatgtgtatgcccgagaaatgctggc 212
```

Figure 6.1. BLAST output following searching dbEST using the murine Chx10 sequence as a search string.

```
EST translation KRRHRTVFTA HQLEELEKAF SEAHYPDVYA REMIAVKTEL PEDRIQV--- ---------- 47
Chx10           KRRHRTIFTS YQLEELEKAF NEAHYPDVYA REMIAMKTEL PEDRIQVWFQ NRRAKWRKRE 60
Ceh10           KRRHRTUFTQ YQIDELEKAF QDSHYPDIYA REVIAGKTEL QEDRIQVWFQ NRRAKWRKTE 60
aristaless      QRRYRTIFTS FQLEELEKAF SRTHYPDVFT REELAMKIGL IEARIQVWFQ NRRAKWRKQE 60
prd             QRRCRTIFSA SQLDELERAF ERTQYPDIYT REEKAQRTNL IEARIQVWFQ NRRARLRKQH 60
Rax             HRRNRTIFTT YQLHELERAF EKSHYPDVYS REELAGKVNL PEVRVQVWFQ NRRAKWRRQE 60
Pax6            LQRNRTSFTQ EQIEALEKEF ERTHYPDVFA RERIAAKIDL PEARIQVWFS NRRAKWRREE 60
Mhox            QRRMRTIFNS SQLQALERVF ERTHYPDAFV REDIARRVNL IEARVQVWFQ NRRAKFRRNE 60
```

Figure 6.2. Comparison of the predicted amino acid sequences of various *prd*-type homeodomains, including the putative translation of the novel EST cDNA. Green shading indicates conservative changes, boxes indicate identity.

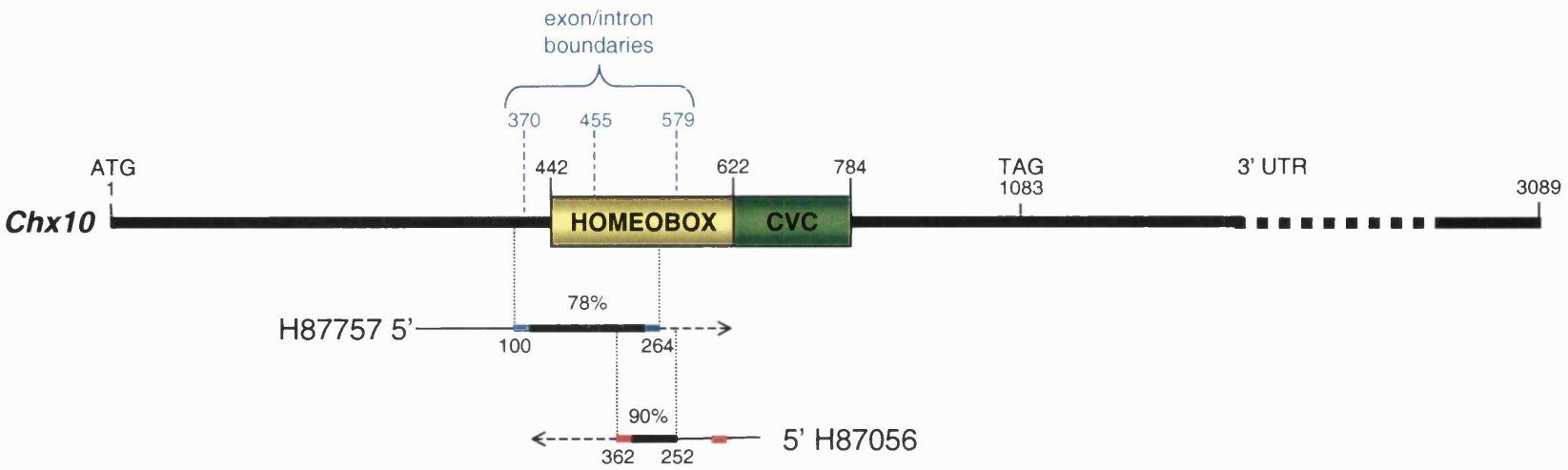

Figure 6.3. Diagram showing the ESTs displaying regions of sequence identity to *Chx10* identified by BLASTing murine *Chx10* sequence through the dbEST database. EST H87757 showed a 78% sequence identity to a 164bp stretch of *Chx10*, while EST H87056 showed a 90% sequence identity to a 110bp stretch of H87757. Sequence comparison indicates that these two ESTs represent the same cDNA species, and both are derived from the same adult retinal library. Slate-blue lines indicate the position of the cDNA primers (forward, F, to the left); red lines indicate the positions of the Genomic primers (forward, F, to the left).

be representative of the same cDNA species. H87056 predominantly only shared sequence identity with *Chx10* over the regions that it shared sequence identity with H87757. No ORF could be seen in either the forward or reverse orientation, and certainly no sequence identity with sequence of *Chx10*. Aligning these two ESTs and forming one sequence generated a 507bp fragment of putative cDNA, which encodes a putative 76 amino acid residue polypeptide, including a partial *prd*-type homeodomain (47 out of 60 residues, which is equivalent to ~90%), but no further ORF (see Figure 6.2). These two EST containing clones were obtained from the Human Genome Mapping Project as *Escherichia coli* plasmids, and were amplified and prepared in the standard way (see Chapter 2, Methods). Sequencing both of them failed to generate any further sequence, as the two clones overlapped considerably. It did however correct some of the database sequence, but not significantly enough to alter the identity comparisons presented above.

Three possibilities presented themselves at this point in the analysis;

1) The cDNA sequence represents a novel gene, which encodes a truncated homeodomain protein. This seemed unlikely, as no truncated homeobox proteins have yet been reported, and the last 10 amino acid residues of the homeodomain are heavily evolutionarily conserved (Purugganan 1998).

2) The cDNA represented a transcribed, but untranslated, non-functional pseudogene.

3) The sequence identity between the novel Chx10-like cDNA sequence and *Chx10* diverges in the last 13 amino acid residues in the homeobox (nt 579 in *Chx10*). At this point the ORF in the novel cDNA terminates. The equivalent point in mouse *Chx10* represents the junction between exons 3 and 4 in the genomic sequence. Therefore it was possible that the retinal cDNA library from which these clones originated was contaminated with unspliced RNA, and that this divergence represented an intron.

It is worth noting that an EST containing a fragment of a recently published novel gene, *Vax1*, was derived from the same retinal cDNA library, and certainly did contain intronic sequence (Jim Bellingham, personal communication, Hallonet *et al.* 1998), indicating that this library may be contaminated with unspliced RNA. Therefore this reinforced the notion that the cDNA represented a genuine homeobox gene. The insignificant levels of sequence identity outside the homeobox, coupled with the amino acid sequence identity within the homeobox being only 90% for the 47 encoded amino acids lead to the conclusion that this cDNA represented a novel gene, and not the human homologue of *Chx10*. This was confirmed when a plasmid containing the human *CHX10* gene was kindly provided by Rod McInnes for comparison. Sequence analysis indicated that the amino acid identity between *CHX10* and its murine homologue was 97% over the whole gene (Ferda-Percin *et al.* 2000), which is higher than the sequence identity of the novel cDNA sequence.

Sequence comparison thereby confirmed that he novel cDNA was not human *Chx10*.

6.3 The novel cDNA EST clones contain genomic sequence

A PCR based strategy was used to determine whether the non-ORF sequence in the EST was in fact genomic, intronic DNA. Two sets of primers were designed (see Figure 6.3 and 6.4), one pair that amplified a fragment solely from the putative ORF (dubbed cDNA primers), and another pair that flanked the putative intron–exon boundary (called genomic primers). PCR amplification was performed using adult human retinal cDNA generated from reverse transcription using RNA extracted from an adult retina. The genomic primers failed to generate a PCR product, whereas a PCR product of the predicted size was generated using the cDNA primers. These data suggest that the sequence to which the reverse genomic primer annealed (see Figure 6.3 and 6.4) was not present in the adult retinal cDNA, leading to the conclusion that it was genomic DNA, and the non-ORF sequence from the ESTs was indeed intronic. A positive control, demonstrating that the genomic primers successfully amplified a fragment of the predicted size from genomic DNA is shown in Figure 6.8.

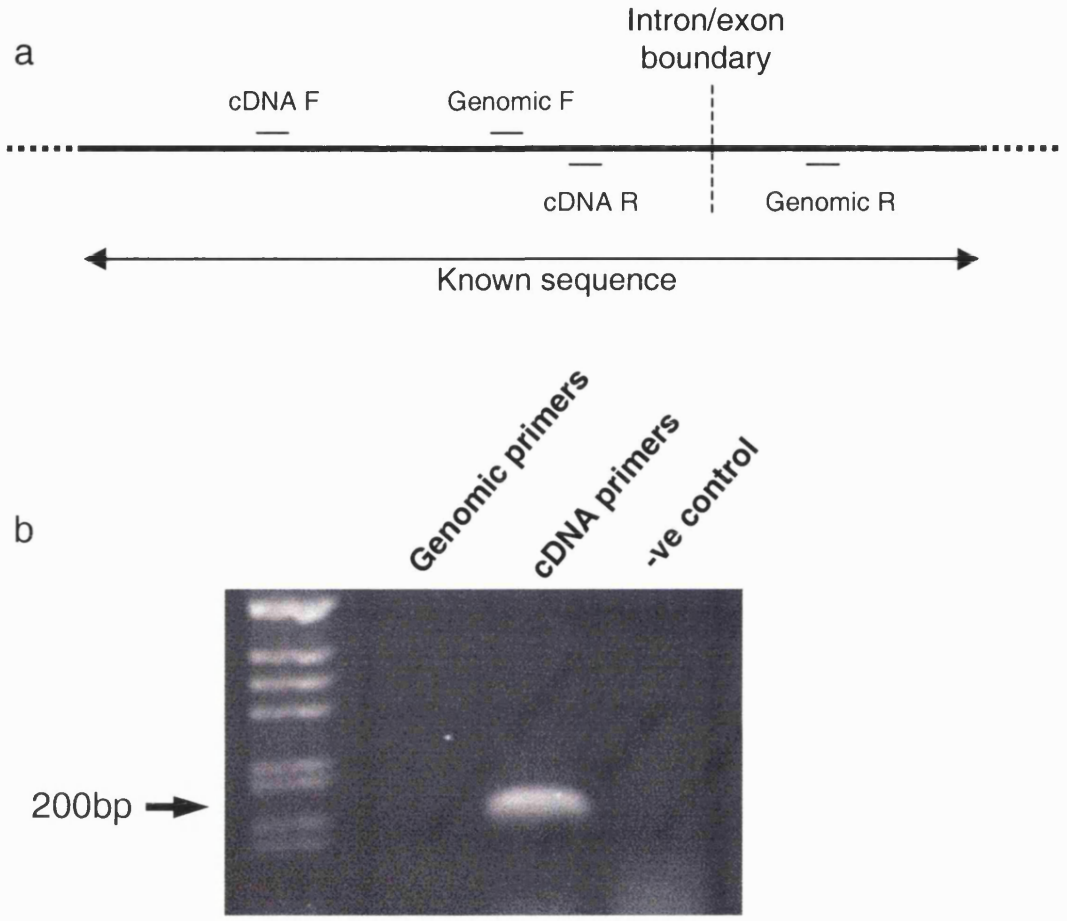

Figure 6.4. Scheme (a) for and results (b) showing a demonstration by PCR that EST containing clone contains unspliced genomic DNA, using adult retinal cDNA. Primers which flanked the putative intron/exon boundary, known to amplify a PCR product from the EST containing clone, would not amplify a product from adult retinal cDNA, indicating that this clone contained DNA which was not transcribed.

6.4 PCR-based amplification of novel cDNA

Primers were designed which were within the ORF of the novel cDNA sequence. These were used initially to determine whether a fragment of this cDNA could be amplified from various cDNA libraries, and also to determine using RT-PCR an expression profile for this putative novel Chx10-like gene.

Figure 6.5 shows that a 200bp fragment could be amplified from adult human retinal cDNA library (a generous gift from Jeremy Nathans) (this library was divided up into clones of length shorter than 1kb and more than 1kb, and the amplification was successful on both). Furthermore a band was amplified from an E15.5 retinal mouse cDNA library. No band was amplified from human adult genomic DNA. This is perhaps not surprising; the primers were designed to flank two intron/exon boundaries (see Figure 6.3, and 6.5) that are heavily conserved amongst a number of *prd*-type homeodomain genes. Introns 2 and 3 in *Chx10* (which is most similar in sequence to the novel cDNA) are both over 6kb in length, and therefore amplifying a fragment of DNA from genomic template would not be possible with these two primers, assuming that the genomic structure of this novel gene was similar to that of *Chx10*.

Based on the assumption that this novel cDNA was represented by clones in the various retinal libraries available, an "anchored" PCR strategy was employed to generate more sequence for this cDNA (see Figure 6.6). This method was unsuccessful using the human and mouse cDNA libraries on many attempts, despite the observation of a consistent pattern of PCR products when

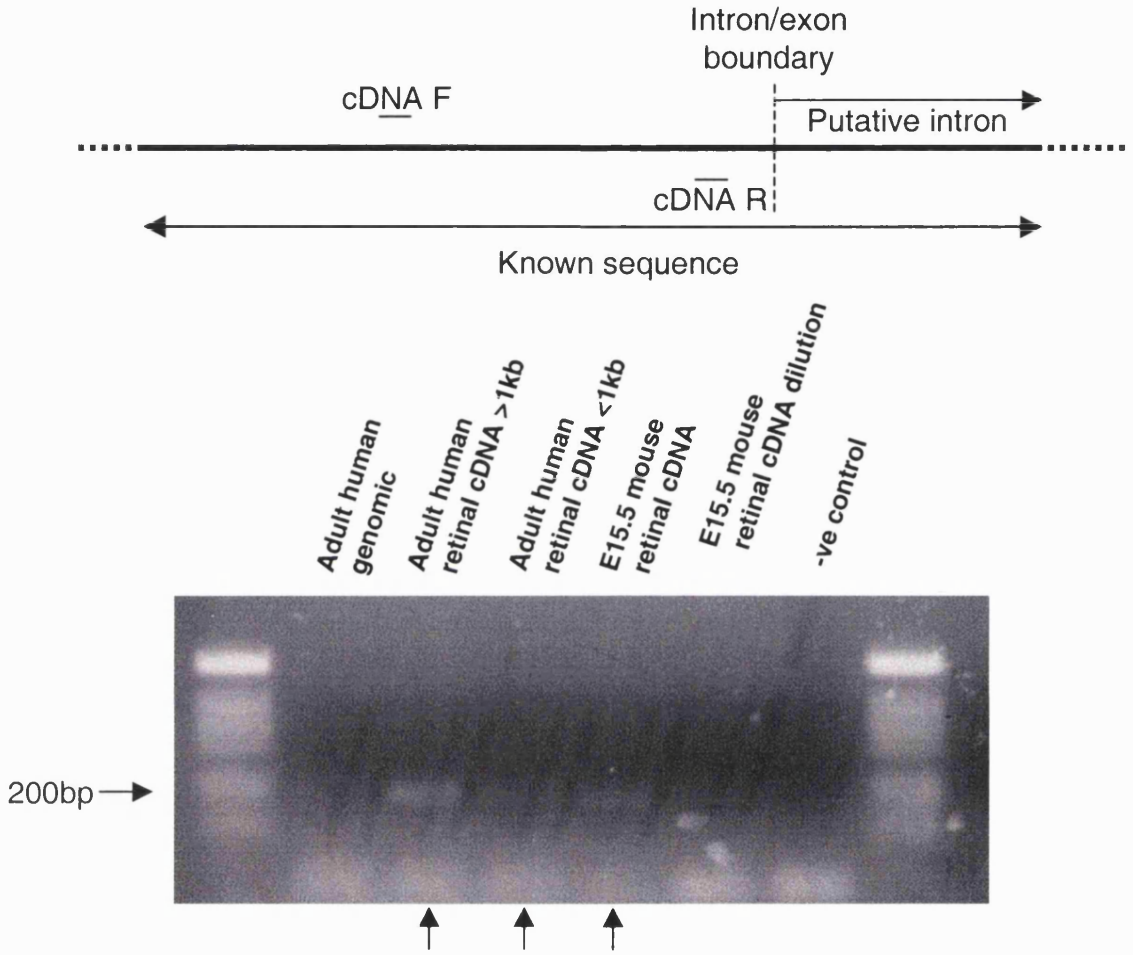

Figure 6.5. Novel cDNA is a genuine transcript. Using primers designed to the ORF of the putative novel cDNA, fragments were amplified from an adult retinal cDNA library, and a mouse E15.5 retinal library. No band was detected using genomic human DNA as a template.

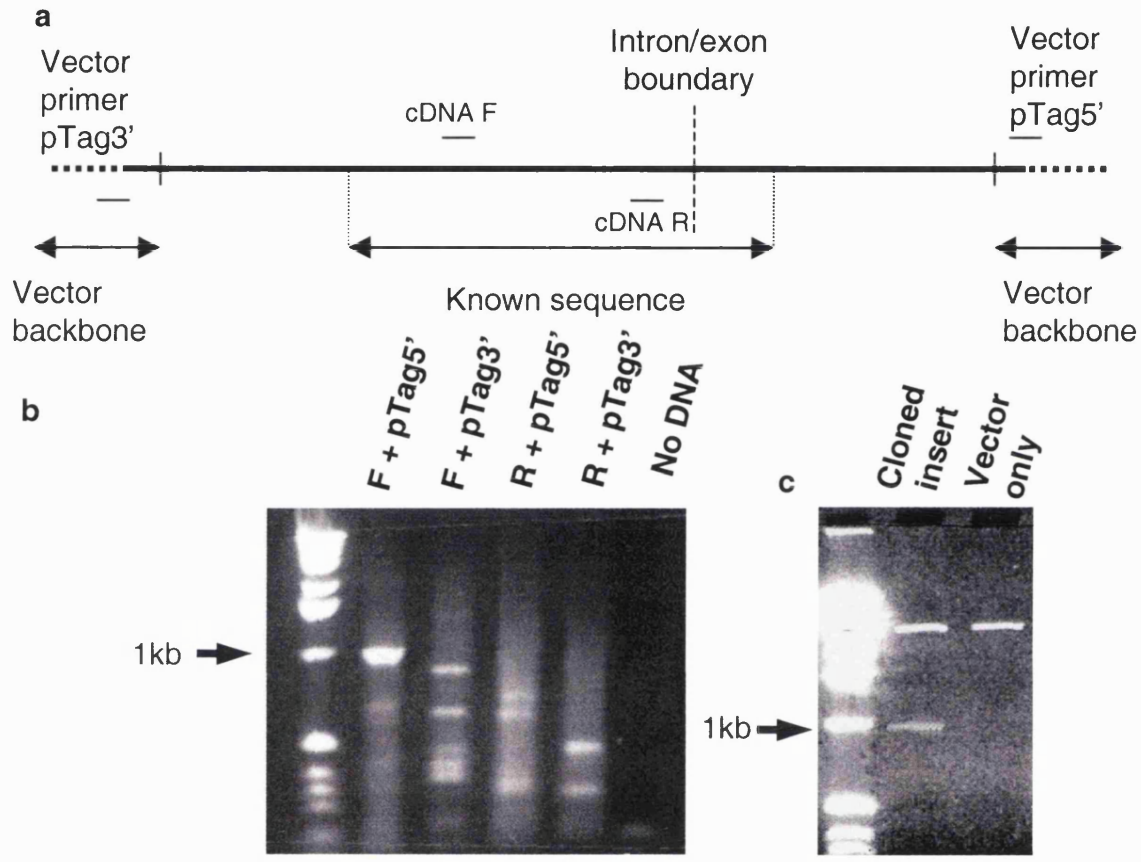

Figure 6.6. (a) Scheme for amplifying further sequence of novel cDNA from retinal cDNA library sources, using "anchored" PCR. EST specific primers were used in combination with vector specific primers to amplify fragments of the novel cDNA present in the E15.5 mouse retina cDNA library. A 1kb PCR product was consistently amplified (b) using the F sequence primer and the 5' vector primer. This product was excised from the gel and cloned into the plasmid vector pGEM T-easy (c) for sequencing.

performing this on the mouse E15.5 retinal library (see Figure 6.6). Of particular interest was a 1kb fragment using the F cDNA primer and the 5' vector primer, but upon cloning and sequencing it using the ABI 373 sequencing kit the clone showed no similarity to the known sequence of the novel cDNA, other that a fortuitous 15/20 stretch which corresponded with the sequence of the primer itself. Conventional library screening attempts were not successful, and it was concluded that the novel Chx10-like cDNA was either not present or present at very low levels in the human retinal library. Sequence differences between the mouse and human Chx10-like cDNAs may have also hampered isolation from the mouse library.

6.5 Tissue specific expression profile of novel cDNA

Using the primers designed to anneal to the ORF of the EST sequences described above, a tissue specific expression pattern was generated by RT-PCR. RNA was extracted (see Chapter 2, Methods) from the following human tissues: adult retina, 12wpc whole eye, 11wpc retina, embryonic brain, heart, kidney, limb, liver and spinal cord. RNA from these tissues was quantified and used as template for cDNA synthesis by reverse transcription. PCR was performed on cDNA from each of these tissues. Figure 6.7 shows that a strong PCR product was observed from the adult retina and very faint bands in the 12wpc eye and 11wpc retina. A PCR band was not detected in any other tissue

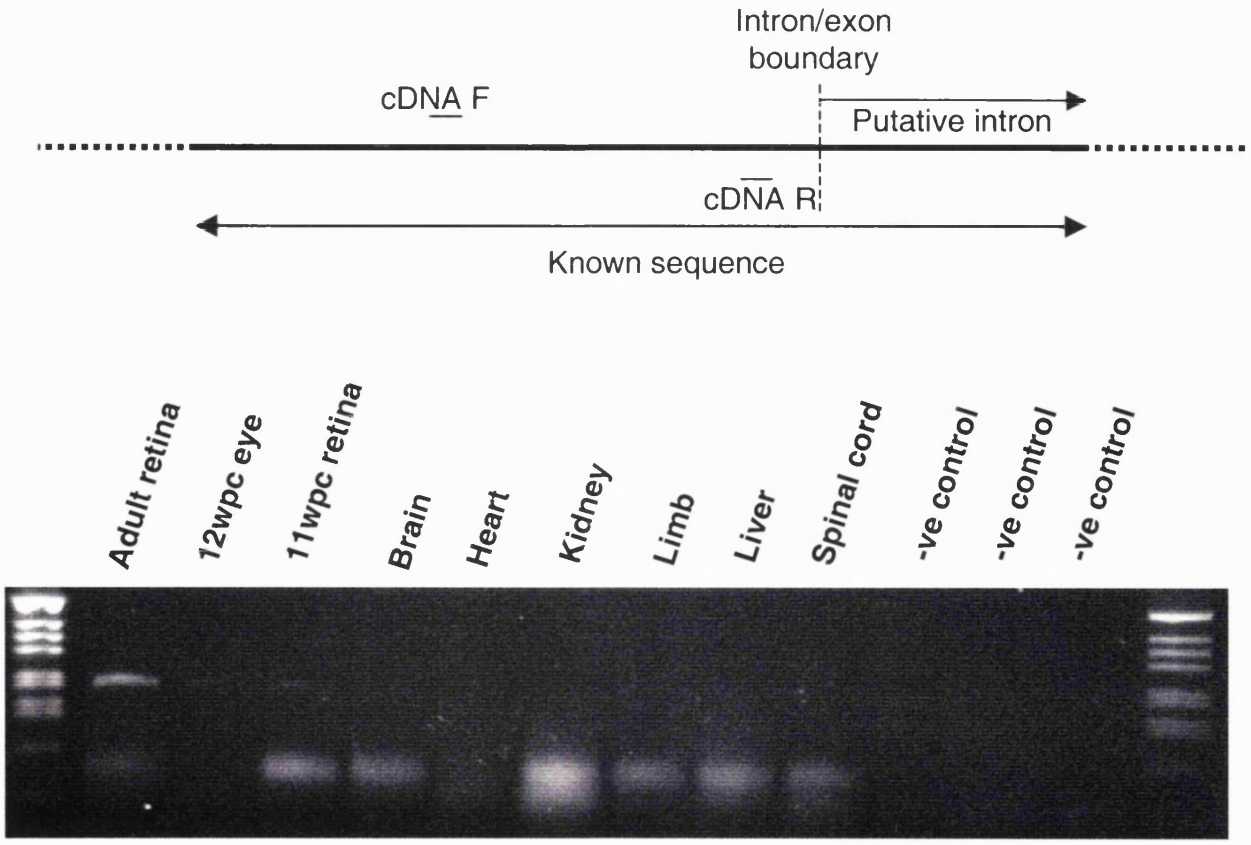

Figure 6.7. Expression profile of novel cDNA by RT-PCR. A strong band of the predicted size was observed, amplified from cDNA synthesised from RNA extracted from adult retina. Faint bands were seen in the 12wpc eye and 11wpc retina extracts, but not in any other tissue examined.

examined. Both ESTs were from an adult retinal cDNA library, and were not represented in any other EST library on dbEST. These results suggest that the novel cDNA is an eye-specific transcription factor, which may have a role in eye development, but is strongly expressed in the adult retina.

6.6 Chromosomal mapping

PCR primers that were specific to the genomic sequence (as described above, see Figure 6.4) were used to map the novel cDNA to a human chromosome (see Figure 6.8). A set of individual human chromosomes generated by somatic cell hybrid with either hamster or mouse cells was obtained from the Human Genome Mapping Project. These pools were used as templates for PCR. A PCR product was only detected from the chromosome 20 pool, and the total human pool, indicating that the novel cDNA is located on human chromosome 20. No fragments were amplified from either genomic hamster or mouse DNA indicating that the band for human chromosome 20 was indeed amplified from the human DNA and not the host cell genome.

There are several eye diseases that map to chromosome 20, including congenital hereditary endothelial dystrophy (CHED) and posterior polymorphous dystrophy (PPD) (Semina *et al.* 2000). This novel cDNA may stand a candidate for one such disorder.

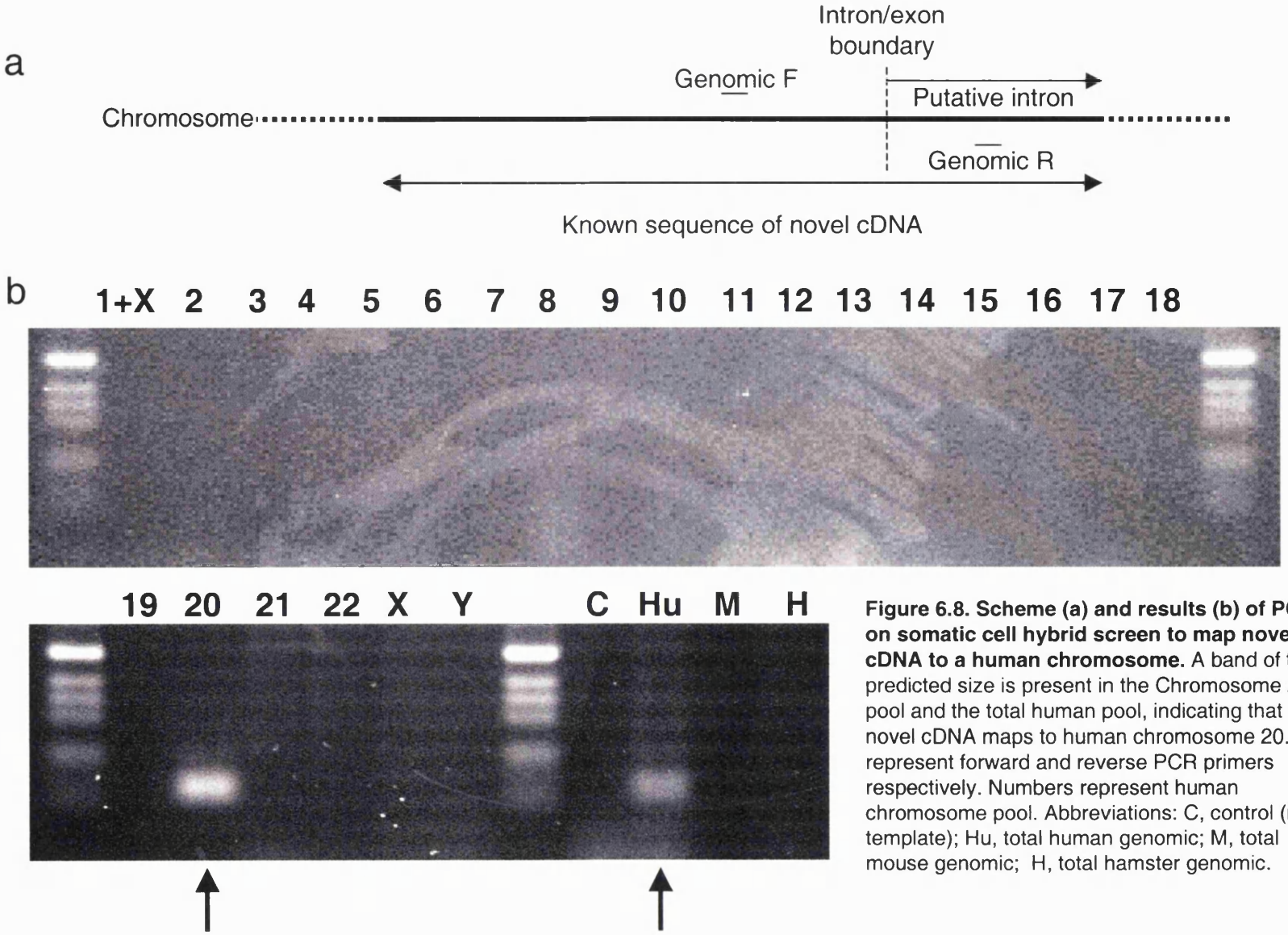

Figure 6.8. Scheme (a) and results (b) of PCR on somatic cell hybrid screen to map novel cDNA to a human chromosome. A band of the predicted size is present in the Chromosome 20 pool and the total human pool, indicating that the novel cDNA maps to human chromosome 20. F/R represent forward and reverse PCR primers respectively. Numbers represent human chromosome pool. Abbreviations: C, control (no template); Hu, total human genomic; M, total mouse genomic; H, total hamster genomic.

6.7 Tissue localisation by *in situ* hybridisation

In order to determine the location of expression of the novel cDNA within the adult retina, *in situ* hybridisation was performed on human tissues at various stages of development. A ~200bp riboprobe was generated using the previously described method (see Chapter 2, Methods), and was incubated with paraffin embedded, paraformaldehyde fixed human eyes, as described previously.

As predicted by the RT-PCR experiments described above, where fragments of the novel Chx10-like cDNA could not be amplified from developmental eye tissue from 9 to 15 weeks pc, no *in situ* hybridisation was observed in foetal eyes or retina (data not shown). These two results taken together support the hypothesis that this novel cDNA is not expressed in the eye during development.

However, expression was detected in the inner and outer nuclear layers of the adult human retina. Within the inner nuclear layer expression appeared to be restricted to the outer aspect, i.e. the location of bipolar and horizontal interneurons (Hollenberg and Spira 1972), as demonstrated by *CHX10* expression (see Figure 6.9). Expression within the outer nuclear layer, conversely, indicates expression within photoreceptor cells, an observation not seen with *CHX10*, but seen here with the photoreceptor marker gene *CRX*. Furthermore, expression was only observed in adult tissue (bearing in mind the paucity of range of human developmental tissue, which is restricted to 9–15

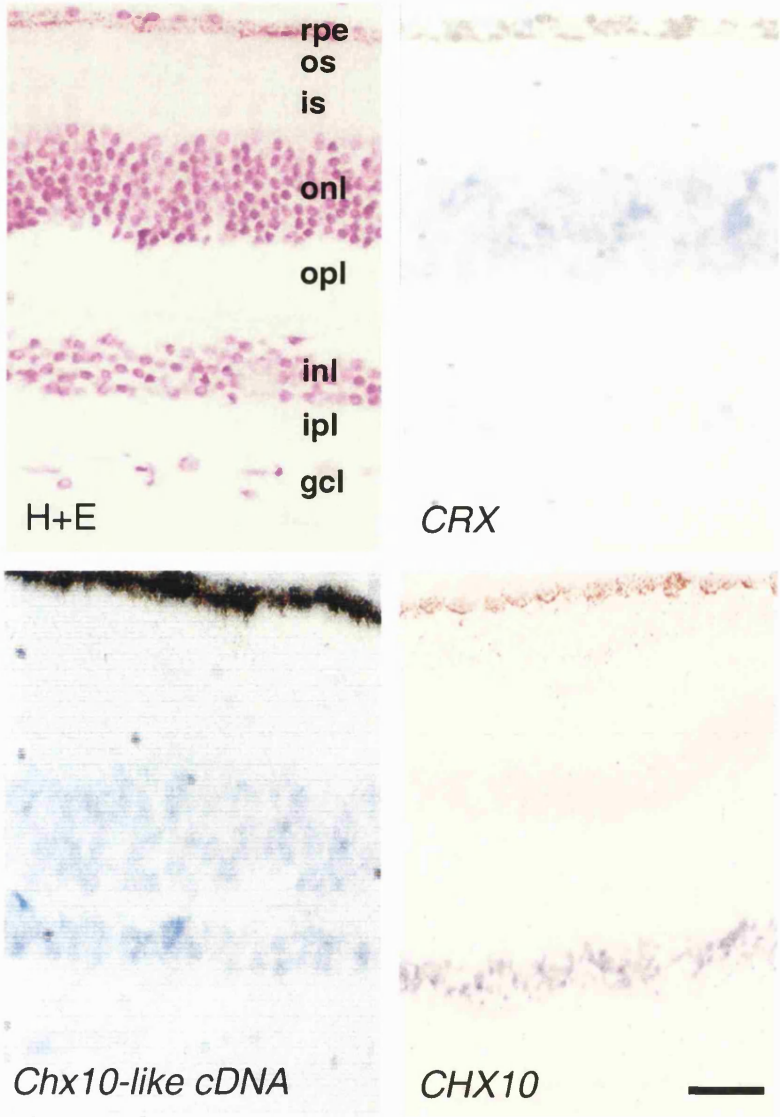

Figure 6.9. *In situ* hybridisation shows expression of *Chx10-like cDNA* is within the inner (inl) and outer nuclear (onl) layers of the adult human retina. By contrast, *CHX10* and *CRX* are expressed exclusively in the inner and outer nuclear layers, respectively. rpe, retinal pigmented epithelium; os, outer segments; is, inner segments; opl, outer plexiform layer; ipl, inner plexiform layer; gcl, ganglion cell layer. Scale bar: 100μm.

weeks), in stark contrast to the expression of *CHX10*, which is strongly expressed in the developing retina (for comparison see Figures 3.2 and 4.5).

These data indicate that the *Chx10*-like novel gene has a very distinct role from that of CHX10 in retinal biology. In the mouse, Chx10 is required for normal retinal development, and its developmental and maintained expression in bipolar cells indicates that it has a function in the development and maintenance neurons (Liu *et al.* 1994, Burmeister *et al.* 1996). Lack of detection by RT-PCR and by *in situ* hybridisation of the novel cDNA suggests that it is absent during development, and therefore is not required. Expression in the adult retina indicates that this gene may have a role in maintaining the function of the cells in which it is present, which, as observed by *in situ* hybridisation, appear to be bipolar cells and photoreceptors. As the novel cDNA almost certainly encodes a homeobox transcription factor, it seems likely that it regulates downstream targets that are involved in cellular function. Identification of these cell types needs to be confirmed by double labelling using known cell specific markers.

The identification of this putative novel transcription factor raises the strong possibility that it is a human retinal disease-causing gene. Of the retinal diseases that display Mendelian inheritance patterns, the majority involve degenerations of the photoreceptor layer, and these include the extensive group termed retinitis pigmentosa (RP) (Gregory-Evans and Bhattacharya 1998). A transcription factor that regulates cellular function in photoreceptors is therefore a good candidate gene for the cause of a retinal dystrophy disorder.

No RPs have been mapped to chromosome 20 however, so this gene is not immediately obvious as a specific candidate.

6.8 *VSX1/RINX1*

Since the discovery of the novel *Chx10*-like cDNA reported here, two papers have been published which simultaneously identified the gene represented by this cDNA, and named it *VSX1*, given its similarity to the goldfish homologue of *Chx10* (also called *Vsx1*) (Levine *et al.* 1997). The gene was cloned from a human embryonic craniofacial cDNA library (Semina *et al.* 2000) – a tissue type not examined in this thesis – and was shown to be a 1433bp cDNA, which encoded a predicted 365 amino acid homeobox transcription factor. The homeobox was demonstrated to be complete, and furthermore a complete CVC domain was also identified. The genomic structure was also characterised, and as predicted by results shown here, the intron–exon boundary within the homeobox was conserved with that of *Chx10*. These data suggest that the non-coding sequence shown in the EST database is indeed contaminating genomic DNA or unspliced RNA. By contrast though, the total genomic structure of *VSX1* spanned a length of only 6.2kb, compared to over 30kb for *Chx10* (Burmeister *et al.* 1996, Ferda-Percin *et al.* 2000). Chromosomal mapping also confirmed results presented here, and this region was narrowed to 20p11–q11. RT-PCR

confirmed that expression was maintained in the adult eye, and was present in the developing craniofacial region.

The second study (Hayashi *et al.* 2000) identified the same Chx10-like protein by employing a yeast one-hybrid screen, using the locus control region (LCR) of human red and green visual pigment genes, which are exclusively expressed in cone photoreceptors. Hayashi *et al.* found *VSX1* (which they named *RINX1*, for retinal inner nuclear layer homeobox) to be expressed only in the outer aspect of the inner nuclear layer of the adult retina (in contrast to results presented here, which reveal outer nuclear layer expression too). This study also further narrowed *VSX1*'s chromosomal location to 20p11.2, with which no retinal disease has yet been associated. Interestingly though, Hayashi *et al.* showed that *VSX1* encodes two splice variants, one of which lacks most or all of the homeodomain. How this splice variant behaves *in vivo* is unknown, and requires further investigation.

CHAPTER 7

DISCUSSION

CHAPTER 7

DISCUSSION

One of the primary aims of the field of developmental biology, especially with the relatively recent integration of embryological, molecular biological and genetic techniques, has been the identification of the molecular determinants of cellular fate.

In recent years, much research has been devoted to the identification of determinants of cellular fate of the cells in the retina, a large proportion of which has come out of the laboratory of Connie Cepko (Harvard Medical School, MA USA) (Livesey and Cepko 2000). This research has revealed that there are inscrutable complex networks of genes that play crucial roles in the determination of specific cellular fates. *Pax6* was thought to stand at the top of the hierarchy of factors that controlled the development of an eye, and was labelled a "master control gene" (Gehring 1996, Gehring and Ikeo 1999). The degree of evolutionary conservation in the regulation and function of Pax6 is profound, with the 5' regulatory regions being conserved, as well as the coding sequence between *Drosophila* and mice (Xu *et al.* 1999). Recent evidence suggests that the picture is more complicated. Members of vertebrate homologue families of the *Drosophila sine oculis*, *eyes absent* and *dachshund* gene families have been shown to be essential for eye development (Wawersik and Maas 2000).

Recently, new data has further enlightened the role of Pax6 in ocular and retinal development, with the creation of conditional Cre-mediate knockout mice (Marquardt *et al.* 2001). Pax6 functions in several capacities in eye development, with lack of early ocular Pax6 expression restricting growth of the optic vesicle, and a failure of the neuroectoderm to adopt identity of neuroretinal progenitor cells. The authors note that following ablation of neuroretinal expression of Pax6, progenitor cells maintain expression of early retinal determinants (Rx1, Six3, Six6 and Hes1) and lose their multipotency. In the normal retina, once the retinal progenitor identity is established, Pax6 function becomes dispensable in the differentiation of specific retinal cell types. This is exemplified by the absence of Pax6 expression in all but amacrine (and a proportion of ganglion) cells. However, in the mouse in which Pax6 expression was ablated after the establishment of a retinal progenitor pool, only amacrine cells differentiated, demonstrating the dispensability of Pax6 for the generation of this cell type.

The identification of *Chx10*, a gene that when mutated causes profound ocular defects in the *or*^{J} mouse (Burmeister *et al.* 1996) and similar defects in humans (Ferda-Percin *et al.* 2000), revealed another transcription factor that is essential in multiple stages of eye development. Its expression pattern and the phenotype suggest that Chx10 has several roles in retinal genesis, but the apparent absence of bipolar cells in the *or*^{J} retina suggested a determining factor for bipolar cell specification. However, crossing the *Chx10* mutation onto a different mouse strain resulted not only in the alleviation of the ocular

phenotype overall, but in the recovered expression of a bipolar-specific cell marker (Bone-Larson *et al.* 2000). Therefore, if one defines a specific cell type by the expression of a set of markers that are unique to that cell, then Chx10 cannot be regarded as the single molecular determinant of retinal bipolar cells. Indeed, Hatakeyama *et al.* (2001) suggest that Chx10 is crucial for the specification of the inner nuclear layer, rather than just bipolar cells. They note that in mice that are double mutants for the bHLH genes *Mash1* and *Math3*, although bipolar cells are absent, Chx10 expression is maintained in Müller glia. Moreover, *in vitro*, only the combined misexpression of Mash1 or Math3 with Chx10 results in a co-ordinated increase of bipolar cells.

Nevertheless, Ferda-Percin *et al.* (2000) (see Appendix 3) with data presented in Chapter 3 demonstrated the significance of CHX10 in human eye development, with the identification of mutations that cause congenital microphthalmia. These patients suffer a clinically heterogeneous developmental disorder featuring small eyes, iris colobomas or absent pupils, partial optic nerves, cataracts and blindness. Moreover, data presented in Chapter 5 regarding the reduced period of proliferation of Chx10-negative retinal progenitor cells adds to the existing data on the mechanisms that cause the observed retinal hypoplasia in the or^{J} mouse, and by extrapolation, in patients with microphthalmia.

In investigating the effect that lack of expression of Chx10 had on the expression of other transcription factors known also to be essential for retinal development, I observed a delay in the onset of expression of the

photoreceptor-specific gene *Crx.* This result was unexpected, given that Chx10 was not known to be expressed in photoreceptor cells. However, evidence presented here indicates that Chx10 does not co-express with Crx at any point, and that a signalling mechanism, possibly directed by Chx10 is crucial for the correct onset of Crx in developing photoreceptors. The fact that Crx expression is delayed, rather than absent, suggests that there may be two waves of Crx expression, and that the second is not dependent on Chx10. Nevertheless, without the initial phase of Crx expression, a crucial window is missed, and the cell cannot develop normally. This is reflected in the photoreceptors of the *or*^{J} retina, which are present but morphologically abnormal. Furthermore, part of the abnormality is short or absent inner and outer segments (Burmeister *et al* 1996). Data presented here and by Livesey *et al.* (2000) indicate that many of the genes whose expression is dependent on Crx are molecules expressed in the inner and outer segments. This model is summarised in Figure 7.1. Although there is no direct evidence for two waves of Crx expression during photoreceptor development, there is direct evidence that there are indeed two phases of photoreceptor development (Morrow *et al.* 1998) (discussed in Chapter 1.7).

CRX has revealed itself as a gene that can harbour many disease-causing mutations (Sohocki *et al.* 1998, 2001). In this thesis, I have presented data that suggest a previously unknown player in the regulation of *Crx* expression. Silva *et al.* (2000) describes a putative null mutation in *CRX* that is associated with both a Leber congenital amaurosis phenotype (in homozygotes)

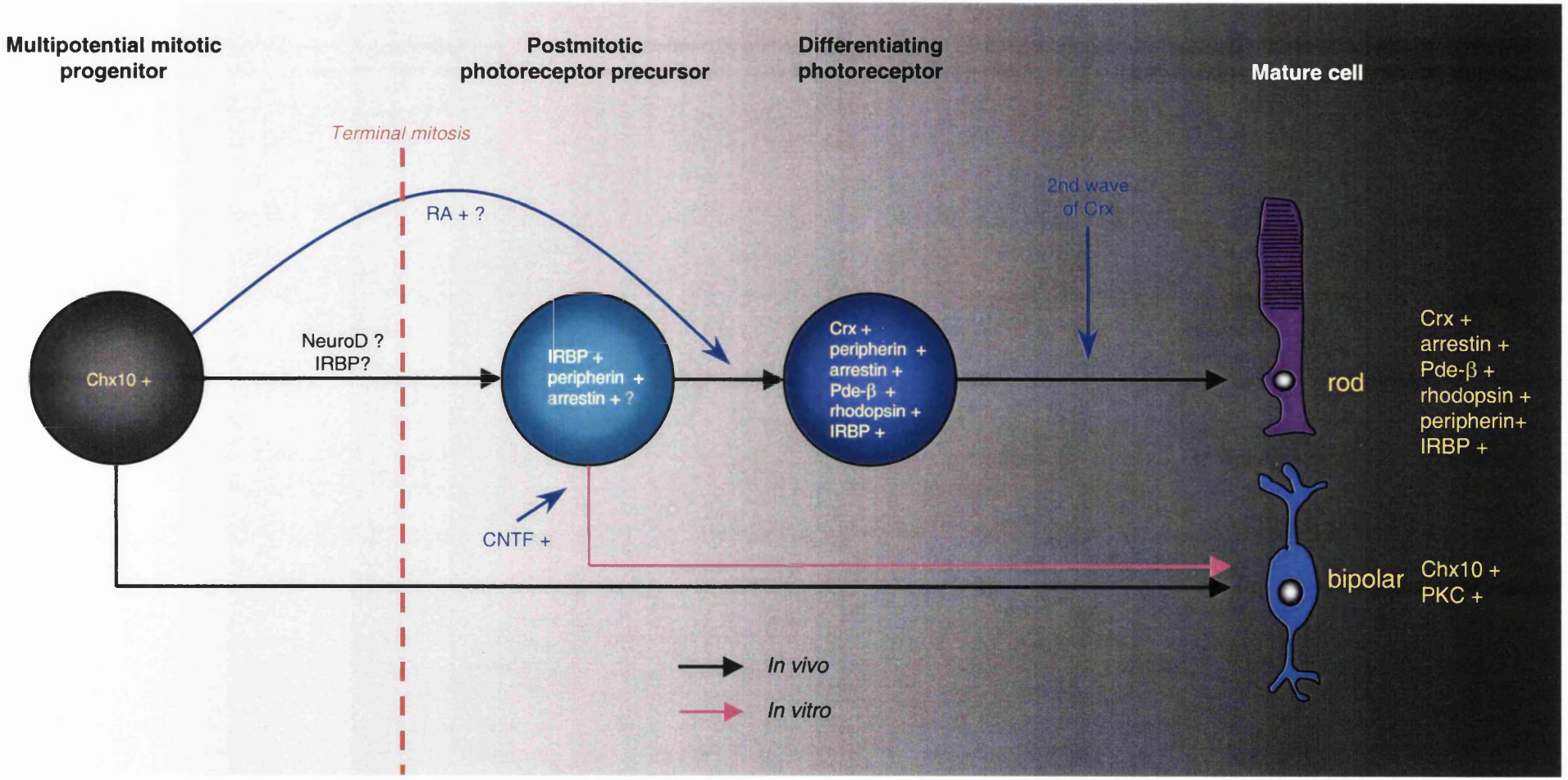

Figure 7.1. Model of Chx10-dependent photoreceptor and bipolar cell differentiation. Photoreceptor birthing (shown by expression of IRBP, peripherin and possibly arrestin) occurs in the absence of Chx10, but Crx expression is delayed. A signalling molecule, which is absent in the absence of Chx10 and may or may not be retinoic acid (RA), stimulates the expression of Crx, prompting Crx-dependent differentiation. Crx expression is delayed, not absent, without functional Chx10, suggesting that there is a second wave of Crx expression that is independent of Chx10. However, continuous Crx expression is required for correct differentiation. *In vitro*, addition of ciliary neurotrophic factor (CNTF) respecifies cells that would differentiate as rods into bipolar cells.

and a normal ocular phenotype (in heterozygotes), suggesting that haploinsufficiency is not a disease-causing mechanism in this case. This conclusion leads the authors to speculate that the disease mechanism is almost certainly multigenic. Therefore, information about the complex networks of regulatory pathways involving Crx will reveal important information about retinal disorders.

During the course of this thesis, retinal stem cells were identified (Tropepe *et al.* 2000 and Ahmad *et al.* 2000). Both of these studies isolated individual pigmented cells from the ciliary margins of the retina, which under specific culture conditions, formed spheres of undifferentiated retinal progenitor cells that expressed Chx10, and were capable of differentiating into a variety of retinal cells. Interestingly, despite the reduction in total number of retinal cells in the *or*^{J} retina, Tropope *et al* recorded a fivefold increase in the number of primary retinal stem cell cultures from the *or*^{J} mouse eye, although these spheres were significantly smaller than that of the wild-type cultures. The reduction in size of the cultures reinforces the role of Chx10 as a factor that promotes cellular proliferation in the retina. These data suggest that in the absence of Chx10, there are more retinal stem cells, although their proliferation and potential is restricted. The authors postulate that the numbers of neural retinal cells during development determines the numbers of retinal stem cells by inhibiting the expansion of the stem cell population. The identification of these cells has raised the possibility of stem cell therapy for retinal disorders, and indeed, Sakaguchi *et al.* (Iowa State University, USA) reported at the American

Society of Neuroscience annual meeting (New Orleans, November 2000) successful implantation, integration and differentiation of genetically modified stem cells in the eyes of postnatal Brazilian opossums. Young *et al.* (2000) also successfully integrated rat hippocampal cells into the retinae of rats with genetic retinal degeneration, which subsequently differentiated and expressed mature neuronal markers and showed synaptic profiles. This type of experiment introduces a real prospect for the treatment of retinopathies such as glaucoma and macular degeneration in the future.

Clearly, Chx10 has multiple roles in the development of the retina, and interacts with a number of other factors to implement these roles. Livesey *et al.* (2000) used microarray technology to identify downstream targets of Crx by comparing expression of retinal cDNAs in the wild-type and $Crx^{-/-}$ mouse. This technique unveiled several novel downstream targets, as well as many previously known photoreceptor genes, many of which are disease-causing genes. This same technique could easily be applied to the or^{J} mouse to identify bipolar specific markers that are regulated by Chx10 (if carried out using cDNA from retinal cells from late development, i.e. when bipolar cells are developing), or to identify the targets of Chx10 that regulate cellular proliferation during early development. The identification of the Chx10 preferred binding site (Ferda-Percin *et al.* (2000) will provide further evidence for the direct regulation of genes by Chx10. The finding that RA may be involved in the Chx10-dependent onset of Crx expression should be investigated using a system designed by Enwright and Grainger (2000). These authors used a transgenic mouse strain

harbouring retinoic acid response element (RARE) fused to β-galactosidase. By examining RARE transgene expression in the *sey* mouse (nullizygous for *Pax6*), levels of RA activity were examined. Reduction or absence of RA by analysing RARE transgene expression in the or^J retina during development would reinforce the notion that this signalling molecule has a role in this system.

The identification of novel homeobox transcription factor presented here, VSX1 (Semina *et al.* 2000 and Hayashi *et al.* 2000), also introduces another molecule into the complex network of genes involved in retinal development. Its expression pattern, in both the inner and outer nuclear layers, raises many possibilities for a role in cell specification, and putative interactions with Chx10 and Crx, as well as many other genes. Furthermore, mutations in *VSX1* may cause ocular disease. This field is yet to be explored.

One of the direct challenges following on from work presented here will be increasing the survival rates of or^J cells in culture. The low numbers of or^J cells renders cultures of equivalent density to that of wild-type cells difficult to establish, and therefore manipulation of these cells is similarly difficult. Nevertheless, data presented here does suggest that the absence of Chx10 lowers the survival rate of retinal cells in culture conditions in which wild-type cells thrive. One way round this problem would be to investigate the use of retinal explants in order to manipulate gene expression *in vitro*. Growth and subsequent manipulation of retinal cells has been successfully achieved at the early stages of murine eye development (E9–10.5) (Furuta *et al.* 1997, Furuta

and Hogan 1998), and could make the basis of experiments in which extrinsic factors alter the behaviour and fate of *or*^{J} retinae.

Furthermore, the transgenic experiment begun during the course of this thesis and described in Appendix A would provide valuable information about the ability of Chx10 expression to affect cellular fate while being driven by a photoreceptor-specific promotor. This experiment will help to unravel the complex pathways involving Chx10 that determines retinal growth and specific cell fates.

CHAPTER 8

REFERENCES

CHAPTER 8

REFERENCES

Ahmad, I., Tang, L., & Pham, H. Identification of neural progenitors in the adult mammalian eye. *Biochem.Biophys.Res.Commun.* **270**, 517-521 (2000).

Alexiades, M. R. & Cepko, C. L. Subsets of retinal progenitors display temporally regulated and distinct biases in the fates of their progeny. *Development* **124**, 1119-1131 (1997).

Altschul, S. F., Gish, W., Miller, W., Myers, E. W., & Lipman, D. J. Basic local alignment search tool. *J.Mol.Biol.* **215**, 403-410 (1990).

Altshuler, D. & Cepko, C. A temporally regulated, diffusible activity is required for rod photoreceptor development in vitro. *Development* **114**, 947-957 (1992).

Altshuler, D. & Lillien, L. Control of photoreceptor development. *Curr.Opin.Neurobiol.* **2**, 16-22 (1992).

Austin, C. P., Feldman, D. E., Ida, J. A., Jr., & Cepko, C. L. Vertebrate retinal ganglion cells are selected from competent progenitors by the action of Notch. *Development* **121**, 3637-3650 (1995).

Barabino, S. M., Spada, F., Cotelli, F., & Boncinelli, E. Inactivation of the zebrafish homologue of Chx10 by antisense oligonucleotides causes eye malformations similar to the ocular retardation phenotype. *Mech.Dev.* **63**, 133-143 (1997).

Belecky-Adams, T. *et al.* Pax-6, Prox 1, and Chx10 homeobox gene expression correlates with phenotypic fate of retinal precursor cells. *Invest Ophthalmol.Vis.Sci.* **38**, 1293-1303 (1997).

Belliveau, M. J. & Cepko, C. L. Extrinsic and intrinsic factors control the genesis of amacrine and cone cells in the rat retina. *Development* **126**, 555-566 (1999).

Belliveau, M. J., Young, T. L., & Cepko, C. L. Late retinal progenitor cells show intrinsic limitations in the production of cell types and the kinetics of opsin synthesis. *J.Neurosci.* **20**, 2247-2254 (2000).

Bessant, D. A. *et al.* A locus for autosomal recessive congenital microphthalmia maps to chromosome 14q32. *Am.J.Hum.Genet.* **62**, 1113-1116 (1998).

Bibb, L. C. *et al.* Temporal and spatial expression patterns of the CRX transcription factor and its downstream targets. Critical differences during human and mouse eye development. *Hum.Mol.Genet.* **10**, 1571-1579 (2001).

Boatright, J. H. *et al.* A major cis activator of the IRBP gene contains CRX-binding and Ret- 1/PCE-I elements. *Mol.Vis.* **3**, 15 (1997).

Bobola, N. *et al.* OTX2 homeodomain protein binds a DNA element necessary for interphotoreceptor retinoid binding protein gene expression. *Mech.Dev.* **82**, 165-169 (1999).

Bone-Larson, C. *et al.* Partial rescue of the ocular retardation phenotype by genetic modifiers. *J.Neurobiol.* **42**, 232-247 (2000).

Bovolenta, P., Mallamaci, A., Briata, P., Corte, G., & Boncinelli, E. Implication of OTX2 in pigment epithelium determination and neural retina differentiation. *J.Neurosci.* **17**, 4243-4252 (1997).

Breitschopf, H., Suchanek, G., Gould, R. M., Colman, D. R., & Lassmann, H. In situ hybridization with digoxigenin-labeled probes: sensitive and reliable detection method applied to myelinating rat brain. *Acta Neuropathol.(Berl)* **84**, 581-587 (1992).

Bron, A. J., Tripathi, R. C. & Tripathi B. J. *Wolff's Anotomy of the Eye and Orbit,* 8th Edition. 1997, Chapman and Hall, London, UK

Brown, N. L. *et al.* Math5 encodes a murine basic helix-loop-helix transcription factor expressed during early stages of retinal neurogenesis. *Development* **125**, 4821-4833 (1998).

Burmeister, M. *et al.* Ocular retardation mouse caused by *Chx10* homeobox null allele: impaired retinal progenitor proliferation and bipolar cell differentiation. *Nat.Genet.* **12**, 376-384 (1996).

Cai, R. L. Human CART1, a paired-class homeodomain protein, activates transcription through palindromic binding sites. *Biochem.Biophys.Res.Commun.* **250**, 305-311 (1998).

Carlson, S. J., Shanker, S., & Chourey, P. S. A point mutation at the *Miniature1* seed locus reduces levels of the encoded protein, but not its mRNA, in maize. *Mol.Gen.Genet.* **263**, 367-373 (2000).

Cepko, C. L. *et al.* Lineage analysis with retroviral vectors. *Methods Enzymol.* **327**, 118-145 (2000).

Cepko, C. L. The patterning and onset of opsin expression in vertebrate retinae. *Curr.Opin.Neurobiol.* **6**, 542-546 (1996).

Cepko, C. L. The roles of intrinsic and extrinsic cues and bHLH genes in the determination of retinal cell fates. *Curr.Opin.Neurobiol.* **9**, 37-46 (1999).

Cepko, C. L., Austin, C. P., Yang, X., Alexiades, M., & Ezzeddine, D. Cell fate determination in the vertebrate retina. *Proc.Natl.Acad.Sci.U.S.A* **93**, 589-595 (1996).

Cepko, C. L., Fields-Berry, S., Ryder, E., Austin, C., & Golden, J. Lineage analysis using retroviral vectors. *Curr.Top.Dev.Biol.* **36**, 51-74 (1998).

Cepko, C. Lineage versus environment in the embryonic retina. *Trends Neurosci.* **16**, 96-97 (1993).

Chen, C. M. & Cepko, C. L. Expression of Chx10 and Chx10-1 in the developing chicken retina. *Mech.Dev.* **90**, 293-297 (2000).

Chen, S. *et al.* Crx, a novel Otx-like paired-homeodomain protein, binds to and transactivates photoreceptor cell-specific genes. *Neuron* **19**, 1017-1030 (1997).

Chow, L., Levine, E. M., & Reh, T. A. The nuclear receptor transcription factor, retinoid-related orphan receptor β, regulates retinal progenitor proliferation. *Mech.Dev.* **77**, 149-164 (1998).

Dawkins, R. *The Blind Watchmaker* 1986 Penguin Books, UK

Dolph, P. J. *et al.* Arrestin function in inactivation of G protein-coupled receptor rhodopsin in vivo. *Science* **260**, 1910-1916 (1993).

Drager, U. C., Li, H., Wagner, E., & McCaffery, P. Retinoic acid synthesis and breakdown in the developing mouse retina. *Prog.Brain Res.* **131**, 579-587 (2001).

Dyer, M. A. & Cepko, C. L. p27Kip1 and p57Kip2 regulate proliferation in distinct retinal progenitor cell populations. *J.Neurosci.* **21**, 4259-4271 (2001).

Dyer, M. A. & Cepko, C. L. p57(Kip2) regulates progenitor cell proliferation and amacrine interneuron development in the mouse retina. *Development* **127**, 3593-3605 (2000).

Dyer, M. A. & Cepko, C. L. Regulating proliferation during retinal development. *Nat.Rev.Neurosci.* **2**, 333-342 (2001).

Dyer, M. A. & Cepko, C. L. The p57Kip2 cyclin kinase inhibitor is expressed by a restricted set of amacrine cells in the rodent retina. *J.Comp.Neurol.* **429**, 601-614 (2001).

Enwright, J. F. III & Grainger, R. M. Altered retinoid signaling in the heads of small eye mouse embryos. *Dev.Biol.* **221**, 10-22

Ezzeddine, Z. D., Yang, X., DeChiara, T., Yancopoulos, G., & Cepko, C. L. Postmitotic cells fated to become rod photoreceptors can be respecified by CNTF treatment of the retina. *Development* **124**, 1055-1067 (1997).

Fantl, V., Stamp, G., Andrews, A., Rosewell, I., & Dickson, C. Mice lacking cyclin D1 are small and show defects in eye and mammary gland development. *Genes Dev.* **9**, 2364-2372 (1995).

Fekete, D. M., Perez-Miguelsanz, J., Ryder, E. F., & Cepko, C. L. Clonal analysis in the chicken retina reveals tangential dispersion of clonally related cells. *Dev.Biol.* **166**, 666-682 (1994).

Ferda, P. E. *et al.* Human microphthalmia associated with mutations in the retinal homeobox gene CHX10. *Nat.Genet.* **25**, 397-401 (2000).

Fischer, A. J. & Reh, T. A. Identification of a proliferating marginal zone of retinal progenitors in postnatal chickens. *Dev.Biol.* **220**, 197-210 (2000).

Fong, S. L. & Fong, W. B. Elements regulating the transcription of human interstitial retinoid- binding protein (*IRBP*) gene in cultured retinoblastoma cells. *Curr.Eye Res.* **18**, 283-291 (1999).

Freund, C. L. *et al.* Cone-rod dystrophy due to mutations in a novel photoreceptor-specific homeobox gene (*CRX*) essential for maintenance of the photoreceptor. *Cell* **91**, 543-553 (1997).

Freund, C. L. *et al. De novo* mutations in the *CRX* homeobox gene associated with Leber congenital amaurosis. *Nat.Genet.* **18**, 311-312 (1998).

Freund, C., Horsford, D. J., & McInnes, R. R. Transcription factor genes and the developing eye: a genetic perspective. *Hum.Mol.Genet.* **5 Spec. No.**, 1471-1488 (1996).

Friend, S. H. *et al.* A human DNA segment with properties of the gene that predisposes to retinoblastoma and osteosarcoma. *Nature* **323**, 643-646 (1986).

Fuhrmann, S., Levine, E. M., & Reh, T. A. Extraocular mesenchyme patterns the optic vesicle during early eye development in the embryonic chick. *Development* **127**, 4599-4609 (2000).

Furukawa, T., Kozak, C. A., & Cepko, C. L. *rax*, a novel paired-type homeobox gene, shows expression in the anterior neural fold and developing retina. *Proc.Natl.Acad.Sci.U.S.A* **94** , 3088-3093 (1997).

Furukawa, T., Morrow, E. M., & Cepko, C. L. *Crx*, a novel otx-like homeobox gene, shows photoreceptor-specific expression and regulates photoreceptor differentiation. *Cell* **91**, 531-541 (1997).

Furukawa, T., Morrow, E. M., Li, T., Davis, F. C., & Cepko, C. L. Retinopathy and attenuated circadian entrainment in Crx-deficient mice. *Nat.Genet.* **23**, 466-470 (1999).

Furukawa, T., Mukherjee, S., Bao, Z. Z., Morrow, E. M., & Cepko, C. L. rax, Hes1, and notch1 promote the formation of Muller glia by postnatal retinal progenitor cells. *Neuron* **26** , 383-394 (2000).

Furuta, Y., Piston, D. W., & Hogan, B. L. Bone morphogenetic proteins (BMPs) as regulators of dorsal forebrain development. *Development* **124**, 2203-2212 (1997).

Furuta, Y. & Hogan, B. L. BMP4 is essential for lens induction in the mouse embryo. *Genes Dev.* **12**, 3764-3775 (1998).

Gal, A., Orth, U., Baehr, W., Schwinger, E., & Rosenberg, T. Heterozygous missense mutation in the rod cGMP phosphodiesterase β-subunit gene in autosomal dominant stationary night blindness. *Nat.Genet.* **7**, 551 (1994).

Gan, L. *et al.* POU domain factor Brn-3b is required for the development of a large set of retinal ganglion cells. *Proc.Natl.Acad.Sci.U.S.A* **93**, 3920-3925 (1996).

Gan, L., Wang, S. W., Huang, Z., & Klein, W. H. POU domain factor Brn-3b is essential for retinal ganglion cell differentiation and survival but not for initial cell fate specification. *Dev.Biol.* **210**, 469-480 (1999).

Gehrig, A. E., Warneke-Wittstock, R., Sauer, C. G., & Weber, B. H. Isolation and characterization of the murine X-linked juvenile retinoschisis (*Rs1h*) gene. *Mamm.Genome* **10**, 303-307 (1999).

Gehring, W. J. The master control gene for morphogenesis and evolution of the eye. *Genes Cells* **1**, 11-15 (1996).

Gehring, W. J. & Ikeo, K. Pax 6: mastering eye morphogenesis and eye evolution. *Trends Genet.* **15**, 371-377 (1999).

George, N. D., Yates, J. R., & Moore, A. T. X-linked retinoschisis. *Br.J.Ophthalmol.* **79**, 697-702 (1995).

Ghyselinck, N. B. *et al.* Role of the retinoic acid receptor β (RARβ) during mouse development. *Int.J.Dev.Biol.* **41**, 425-447 (1997).

Gilbert, S. F. *in Developmental Biology*, 4th Edition, (1994) Sinauer Associates Inc.

Glaser, T., Walton, D. S., & Maas, R. L. Genomic structure, evolutionary conservation and aniridia mutations in the human *PAX6* gene. *Nat.Genet.* **2**, 232-239 (1992).

Grainger, R. M. Embryonic lens induction: shedding light on vertebrate tissue determination. *Trends Genet.* **8**, 349-355 (1992).

Graw, J. Genetic aspects of embryonic eye development in vertebrates. *Dev.Genet.* **18**, 181-197 (1996).

Grayson, C. *et al.* Retinoschisin, the X-linked retinoschisis protein, is a secreted photoreceptor protein, and is expressed and released by Weri-Rb1 cells. *Hum.Mol.Genet.* **9**, 1873-1879 (2000).

Greferath, U., Grunert, U., & Wassle, H. Rod bipolar cells in the mammalian retina show protein kinase C-like immunoreactivity. *J.Comp Neurol.* **301**, 433-442 (1990).

Gregory-Evans, K. & Bhattacharya, S. S. Genetic blindness: current concepts in the pathogenesis of human outer retinal dystrophies. *Trends Genet.* **14**, 103-108 (1998).

Grimm, C. *et al.* Aphakia (ak), a mouse mutation affecting early eye development: fine mapping, consideration of candidate genes and altered *Pax6* and *Six3* gene expression pattern. *Dev.Genet.* **23**, 299-316 (1998).

Grindley, J. C., Davidson, D. R., & Hill, R. E. The role of Pax-6 in eye and nasal development. *Development* **121**, 1433-1442 (1995).

Grindley, J. C., Hargett, L. K., Hill, R. E., Ross, A., & Hogan, B. L. Disruption of PAX6 function in mice homozygous for the *Pax6*$^{Sey\text{-}1Neu}$ mutation produces abnormalities in the early development and regionalization of the diencephalon. *Mech.Dev.* **64**, 111-126 (1997).

Grondona, J. M. *et al.* Retinal dysplasia and degeneration in RARβ2/RARγ2 compound mutant mice. *Development* **122**, 2173-2188 (1996).

Grünert, U. & Martin, P. R. Rod bipolar cells in the macaque monkey retina: immunoreactivity and connectivity. *J.Neurosci.* **11**, 2742-2758 (1991).

Gualtieri, P., Pelosi, P., Passarelli, V., & Barsanti, L. Identification of a rhodopsin photoreceptor in *Euglena gracilis. Biochim.Biophys.Acta* **1117**, 55-59 (1992).

Guillemot, F. & Joyner, A. L. Dynamic expression of the murine Achaete-Scute homologue Mash-1 in the developing nervous system. *Mech.Dev.* **42**, 171-185 (1993).

Halder, G., Callaerts, P., & Gehring, W. J. New perspectives on eye evolution. *Curr.Opin.Genet.Dev.* **5**, 602-609 (1995).

Hall, P. A. *et al.* Proliferating cell nuclear antigen (PCNA) immunolocalization in paraffin sections: an index of cell proliferation with evidence of deregulated expression in some neoplasms. *J.Pathol.* **162**, 285-294 (1990).

Hallonet, M. *et al. Vax1* is a novel homeobox-containing gene expressed in the developing anterior ventral forebrain. *Development* **125**, 2599-2610 (1998).

Hanson, I. & van, H., V. Pax6: more than meets the eye. *Trends Genet.* **11**, 268-272 (1995).

Hatakeyama, J., Tomita, K., Inoue, T., & Kageyama, R. Roles of homeobox and bHLH genes in specification of a retinal cell type. *Development* **128**, 1313-1322 (2001).

Hawkins, N. C. & McGhee, J. D. Homeobox containing genes in the nematode Caenorhabditis elegans. *Nucleic Acids Res.* **18**, 6101-6106 (1990).

Hayashi, T., Huang, J., & Deeb, S. S. *RINX* (*VSX1*), a novel homeobox gene expressed in the inner nuclear layer of the adult retina. *Genomics* **67**, 128-139 (2000).

Hecht, S., Shlaer, S. & Pirenne, M. Energy, quanta and vision. *J.Gen.Physiol.* **25**, 819-840 (1942).

Hill, R. E. *et al.* Mouse small eye results from mutations in a paired-like homeobox- containing gene. *Nature* **354**, 522-525 (1991).

Hitchcock, P. F., Macdonald, R. E., VanDeRyt, J. T., & Wilson, S. W. Antibodies against Pax6 immunostain amacrine and ganglion cells and neuronal progenitors, but not rod precursors, in the normal and regenerating retina of the goldfish. *J.Neurobiol.* **29**, 399-413 (1996).

Hodgkinson, C. A. *et al.* Mutation at the anophthalmic white locus in Syrian hamsters: haploinsufficiency in the *Mitf* gene mimics human Waardenburg syndrome type 2. *Hum.Mol.Genet.* **7**, 703-708 (1998).

Hogan, B., Beddington, R. Constantini, F. & Lacy, E. *Manipulating the Mouse Embryo*: A Laboratory Manual. 2nd Edition. 1994, Cold Spring Harbor Laboratory Press

Holt, C. E., Bertsch, T. W., Ellis, H. M., & Harris, W. A. Cellular determination in the Xenopus retina is independent of lineage and birth date. *Neuron* **1**, 15-26 (1988).

Hyatt, G. A., Schmitt, E. A., Fadool, J. M., & Dowling, J. E. Retinoic acid alters photoreceptor development *in vivo*. *Proc.Natl.Acad.Sci.U.S.A* **93**, 13298-13303 (1996).

Hynes, M. *et al.* The seven-transmembrane receptor smoothened cell-autonomously induces multiple ventral cell types. *Nat.Neurosci.* **3**, 41-46 (2000).

Jean, D., Ewan, K., & Gruss, P. Molecular regulators involved in vertebrate eye development. *Mech.Dev.* **76**, 3-18 (1998).

Kajiwara, K. *et al.* Mutations in the human retinal degeneration slow gene in autosomal dominant retinitis pigmentosa. *Nature* **354**, 480-483 (1991).

Kaufman, M. H. *The Atlas of Mouse Development*. 1995 Academic Press, London, UK

Kawakami, K., Ohto, H., Takizawa, T., & Saito, T. Identification and expression of six family genes in mouse retina. *FEBS Lett.* **393**, 259-263 (1996).

Kelley, M. W., Turner, J. K., & Reh, T. A. Regulation of proliferation and photoreceptor differentiation in fetal human retinal cell cultures. *Invest.Ophthalmol.Vis.Sci.* **36**, 1280-1289 (1995).

Kelley, M. W., Turner, J. K., & Reh, T. A. Retinoic acid promotes differentiation of photoreceptors *in vitro*. *Development* **120**, 2091-2102 (1994).

Kelley, M. W., Williams, R. C., Turner, J. K., Creech-Kraft, J. M., & Reh, T. A. Retinoic acid promotes rod photoreceptor differentiation in rat retina *in vivo*. *Neuroreport* **10**, 2389-2394 (1999).

Kolb, H. Amacrine cells of the mammalian retina: neurocircuitry and functional roles. *Eye* **11 (Pt 6)**, 904-923 (1997).

Konyukhov, B. V. & Sazhina, M. V. Interaction of the genes of ocular retardation and microphthalmia in mice. *Folia.Biol.(Praha)* **12,**, 116-123 (1966).

Kumar, J. P., Bowman, J., O'Tousa, J. E., & Ready, D. F. Rhodopsin replacement rescues photoreceptor structure during a critical developmental window. *Dev.Biol.* **188**, 43-47 (1997).

Latchman, D. S., *Eukaryotic Transcription Factors* 3rd Edition 1998, Academic Press

Lee, J. E. *et al.* Conversion of Xenopus ectoderm into neurons by NeuroD, a basic helix- loop-helix protein. *Science* **268**, 836-844 (1995).

Levine, E. M., Fuhrmann, S., & Reh, T. A. Soluble factors and the development of rod photoreceptors. *Cell Mol.Life Sci.* **57**, 224-234 (2000).

Levine, E. M., Passini, M., Hitchcock, P. F., Glasgow, E., & Schechter, N. *Vsx-1* and *Vsx-2*: two *Chx10*-like homeobox genes expressed in overlapping domains in the adult goldfish retina. *J.Comp Neurol.* **387**, 439-448 (1997).

Lillien, L. & Cepko, C. Control of proliferation in the retina: temporal changes in responsiveness to FGF and TGFα. *Development* **115**, 253-266 (1992).

Liou, G. I. *et al.* Tissue-specific expression in transgenic mice directed by the 5'-flanking sequences of the human gene encoding interphotoreceptor retinoid-binding protein. *J.Biol.Chem.* **265**, 8373-8376 (1990).

Liu, I. S. *et al.* Developmental expression of a novel murine homeobox gene (*Chx10*): evidence for roles in determination of the neuroretina and inner nuclear layer. *Neuron* **13**, 377-393 (1994).

Liu, W. *et al.* All Brn3 genes can promote retinal ganglion cell differentiation in the chick. *Development* **127**, 3237-3247 (2000).

Livesey, F. J. & Cepko, C. L. Vertebrate neural cell-fate determination: lessons from the retina. *Nat.Rev.Neurosci.* **2**, 109-118 (2001).

Livesey, F. J., Furukawa, T., Steffen, M. A., Church, G. M., & Cepko, C. L. Microarray analysis of the transcriptional network controlled by the photoreceptor homeobox gene *Crx*. *Curr.Biol.* **10**, 301-310 (2000).

Lombardini, J. B. Taurine: retinal function. *Brain Res.Brain Res.Rev.* **16**, 151-169 (1991).

Lopez-Rios, J., Gallardo, M. E., Rodriguez, d. C., & Bovolenta, P. *Six9* (*Optx2*), a new member of the six gene family of transcription factors, is expressed at early stages of vertebrate ocular and pituitary development. *Mech.Dev.* **83**, 155-159 (1999).

Ma, C., Papermaster, D., & Cepko, C. L. A unique pattern of photoreceptor degeneration in cyclin D1 mutant mice. *Proc.Natl.Acad.Sci.U.S.A* **95**, 9938-9943 (1998).

Marquardt, T., Ashery-Padan, R., Andrejewski, N., Scardigli, R., Guillemot, F. & Gruss, P. Pax6 is required for the multipotent state of retinal progenitor cells. *Cell* **105**, 43-55 (2001)

Mathers, P. H., Grinberg, A., Mahon, K. A., & Jamrich, M. The *Rx* homeobox gene is essential for vertebrate eye development. *Nature* **387**, 603-607 (1997).

McFarlane, S., Zuber, M. E., & Holt, C. E. A role for the fibroblast growth factor receptor in cell fate decisions in the developing vertebrate retina. *Development* **125**, 3967-3975 (1998).

Morrow, E. M., Belliveau, M. J., & Cepko, C. L. Two phases of rod photoreceptor differentiation during rat retinal development. *J.Neurosci.* **18**, 3738-3748 (1998).

Morrow, E. M., Furukawa, T., & Cepko, C. L. Vertebrate photoreceptor cell development and disease. *Trends Cell Biol.* **8**, 353-358 (1998).

Morrow, E. M., Furukawa, T., Lee, J. E., & Cepko, C. L. NeuroD regulates multiple functions in the developing neural retina in rodent. *Development* **126**, 23-36 (1999).

Nguyen, M. & Arnheiter, H. Signaling and transcriptional regulation in early mammalian eye development: a link between FGF and MITF. *Development* **127**, 3581-3591 (2000).

Ninkina, N. N., Stevens, G. E., Wood, J. N., & Richardson, W. D. A novel Brn3-like POU transcription factor expressed in subsets of rat sensory and spinal cord neurons. *Nucleic Acids Res.* **21**, 3175-3182 (1993).

Nishina, S. *et al. PAX6* expression in the developing human eye. *Br.J.Ophthalmol.* **83**, 723-727 (1999).

Ohtoshi, A., Justice, M. J., & Behringer, R. R. Isolation and Characterization of *Vsx1*, a novel mouse CVC paired-like homeobox gene expressed during embryogenesis and in the retina. *Biochem.Biophys.Res.Commun.* **286**, 133-140 (2001).

Opdecamp, K. *et al.* The rat microphthalmia-associated transcription factor gene (*Mitf*) maps at 4q34-q41 and is mutated in the mib rats. *Mamm.Genome* **9**, 617-621 (1998).

Ostroy, S. E. Insights into the rod rhodopsin regeneration process using the excised mouse eye. *Prog.Brain Res.* **131**, 351-357 (2001).

Oyster, C. W. *The Human eye: Structure and Function.* 1999 Sinauer Associates, Massachusetts, USA

Passini, M. A. *et al.* Cloning of zebrafish *vsx1*: expression of a paired-like homeobox gene during CNS development. *Dev.Genet.* **23**, 128-141 (1998).

Passini, M. A., Levine, E. M., Canger, A. K., Raymond, P. A., & Schechter, N. *Vsx-1* and *Vsx-2*: differential expression of two paired-like homeobox genes during zebrafish and goldfish retinogenesis. *J.Comp Neurol.* **388**, 495-505 (1997).

Passini, M. A., Raymond, P. A., & Schechter, N. *Vsx-2*, a gene encoding a paired-type homeodomain, is expressed in the retina, hindbrain, and spinal cord during goldfish embryogenesis. *Brain Res.Dev.Brain Res.* **109**, 129-135 (1998).

Pepe, I. M. Rhodopsin and phototransduction. *J.Photochem.Photobiol.B* **48**, 1-10 (1999).

Perron, M., Kanekar, S., Vetter M. L. & Harris W. A. The genetic sequence of retinal development in the ciliary margin of the *Xenopus* eye. *Dev.Biol.* **199**, 185-200 (1998)

Plaza, S., Hennemann, H., Moroy, T., Saule, S., & Dozier, C. Evidence that POU factor Brn-3B regulates expression of Pax-6 in neuroretina cells. *J.Neurobiol.* **41**, 349-358 (1999).

Pueyo, J. I., Galindo, M. I., Bishop, S. A., & Couso, J. P. Proximal-distal leg development in Drosophila requires the apterous gene and the Lim1 homologue dlim1. *Development* **127**, 5391-5402 (2000).

Purugganan, M. D. The molecular evolution of development. *Bioessays* **20**, 700-711 (1998).

Putt, W. *et al.* Phosphoglucomutase 1: a gene with two promoters and a duplicated first exon. *Biochem.J.* **296 (Pt 2)**, 417-422 (1993).

Quinn, J. C., West, J. D., & Hill, R. E. Multiple functions for Pax6 in mouse eye and nasal development. *Genes Dev.* **10**, 435-446 (1996).

Rieger, D. K., Reichenberger, E., McLean, W., Sidow, A., & Olsen, B. R. A double-deletion mutation in the *Pitx3* gene causes arrested lens development in aphakia mice. *Genomics* **72**, 61-72 (2001).

Robb, R. M., Silver, J. & Sullivan, R. T. Ocular retardation (or) in the mouse. *Invest.Ophthalol.Vis.Sci.* **17**, 468-473 (1978).

Ross, S. A., McCaffery, P. J., Drager, U. C., & De Luca, L. M. Retinoids in embryonal development. *Physiol.Rev.* **80**, 1021-1054 (2000).

Sauer, C. G. *et al.* Positional cloning of the gene associated with X-linked juvenile retinoschisis. *Nat.Genet.* **17**, 164-170 (1997).

Saha, M. S., Servetnick, M., & Grainger, R. M. Vertebrate eye development. *Curr.Opin.Genet.Dev.* **2**, 582-588 (1992).

Salvini-Plawen, L. & Mayr, E. (1961) in *Evolutionary Biology,* (Vol. 10) (Hechct, M. K., Steere, W. C. & Wallace, B., eds) Plenum Press

Sambrook, J., Fritsch, E. F. & Maniatis, T. *Molecular cloning: A Laboratory Manual*, 2nd Edition. 1989 Cold Spring Harbor Laboratory Press

Sander, M. *et al.* Ventral neural patterning by Nkx homeobox genes: *Nkx6.1* controls somatic motor neuron and ventral interneuron fates. *Genes Dev.* **14**, 2134-2139 (2000).

Sanyal, S., De Ruiter, A., & Hawkins, R. K. Development and degeneration of retina in rds mutant mice: light microscopy. *J.Comp.Neurol.* **194**, 193-207 (1980).

Semina, E. V., Mintz-Hittner, H. A., & Murray, J. C. Isolation and characterisation of a novel human paired-like homeodomain- containing transcription factor gene, *VSX1*, expressed in ocular tissues. *Genomics* **63**, 289-293 (2000).

Silver, J. Robb, R. M. Studies on the development of the eyecup and optic nerve in normal mice and in mutants with congenital optic nerve aplasia. *Dev.Biol.* **68**, 175-190 (1979).

Shafritz, D. A. Rat liver stem cells: prospects for the future. *Hepatology* **32**, 1399-1400 (2000).

Silva, E. *et al.* A CRX null mutation is associated with both Leber congenital amaurosis and a normal ocular phenotype. *Invest Ophthalmol.Vis.Sci.* **41**, 2076-2079 (2000).

Sohocki, M. M. *et al.* A range of clinical phenotypes associated with mutations in *CRX*, a photoreceptor transcription-factor gene. *Am.J.Hum.Genet.* **63**, 1307-1315 (1998).

Sohocki, M. M. *et al.* Prevalence of mutations causing retinitis pigmentosa and other inherited retinopathies. *Hum.Mutat.* **17**, 42-51 (2001).

Soldati, T. & Perriard, J. C. Intracompartmental sorting of essential myosin light chains: molecular dissection and in vivo monitoring by epitope tagging. *Cell* **66**, 277-289 (1991).

Spira, A. W. and Hollenberg, M. J. Human retinal development: ultrastructure of the inner retinal layers. *Developmental Biology* **31**, 1-21

Sun, H. *et al.* Evolution of paired domains: isolation and sequencing of jellyfish and hydra Pax genes related to *Pax-5* and *Pax-6*. *Proc.Natl.Acad.Sci.U.S.A* **94**, 5156-5161 (1997).

Svendsen, P. C. & McGhee, J. D. The C. elegans neuronally expressed homeobox gene *ceh-10* is closely related to genes expressed in the vertebrate eye. *Development* **121**, 1253-1262 (1995).

Theiler, K., Varnum, D.s., Nadeau, J. H., Stevens, L. C. & Cagianut, B. A new allele of ocular retardation: early development and morphogenetic cell death. *Anat.Embryol.(Berl)* **150**, 85-97 (1976).

Tomita, K., Ishibashi, M., Nakahara, K., Ang, S. L., Nakanishi, S., Guillemot, F. & Kageyama, R. Mammalian hairy and Enhancer of split homolog 1 regulates differentiation of retinal neurons and is essential for eye morphogenesis. *Neuron* **16**, 723-734 (1996)

Traboulsi, E. I. Ocular malformations and developmental genes. *J.AAPOS.* **2**, 317-323 (1998).

Tropepe, V. *et al.* Retinal stem cells in the adult mammalian eye. *Science* **287**, 2032-2036 (2000).

Truslove, G. M. A gene causing ocular retardation in the mouse. *J.Embryol.Exp.Morphol.* **10**, 652-660 (1962).

Turner, D. L. & Cepko, C. L. A common progenitor for neurons and glia persists in rat retina late in development. *Nature* **328**, 131-136 (1987).

Turner, D. L., Snyder, E. Y., & Cepko, C. L. Lineage-independent determination of cell type in the embryonic mouse retina. *Neuron* **4**, 833-845 (1990).

Vemuru, R. P., Aragona, E., & Gupta, S. Analysis of hepatocellular proliferation: study of archival liver tissue is facilitated by an endogenous marker of DNA replication. *Hepatology* **16**, 968-973 (1992).

Vetter, M. L. & Moore, K. B. Becoming glial in the neural retina. *Dev.Dyn.* **221**, 146-153 (2001).

Wassle, H., Yamashita, M., Greferath, U., Grunert, U., & Muller, F. The rod bipolar cell of the mammalian retina. *Vis.Neurosci.* **7**, 99-112 (1991).

Watanabe, T. & Raff, M. C. Diffusible rod-promoting signals in the developing rat retina. *Development* **114**, 899-906 (1992)

Wawersik, S. & Maas, R. L. Vertebrate eye development as modelled in *Drosophila*. *Hum.Mol.Genet.* **9**, 917-925 (2000).

Wehr, R. & Gruss, P. Pax and vertebrate development. *Int.J.Dev.Biol.* **40**, 369-377 (1996).

Wiggan, O., Taniguchi-Sidle, A., & Hamel, P. A. Interaction of the pRB-family proteins with factors containing *paired*-like homeodomains. *Oncogene* **16**, 227-236 (1998).

Wilson, D., Sheng, G., Lecuit, T., Dostatni, N., & Desplan, C. Cooperative dimerization of paired class homeodomains on DNA. *Genes Dev.* **7**, 2120-2134 (1993).

Xiang, M. *et al. Brn-3b*: a POU domain gene expressed in a subset of retinal ganglion cells. *Neuron* **11**, 689-701 (1993).

Xiang, M. *et al.* The Brn-3 family of POU-domain factors: primary structure, binding specificity, and expression in subsets of retinal ganglion cells and somatosensory neurons. *J.Neurosci.* **15**, 4762-4785 (1995).

Xiang, M. Requirement for Brn-3b in early differentiation of postmitotic retinal ganglion cell precursors. *Dev.Biol.* **197**, 155-169 (1998).

Xu, P. X. *et al.* Regulation of Pax6 expression is conserved between mice and flies. *Development* **126**, 383-395 (1999).

Yan, R. T. & Wang, S. Z. neuroD induces photoreceptor cell overproduction *in vivo* and *de novo* generation *in vitro*. *J.Neurobiol.* **36**, 485-496 (1998).

Yanagi, Y., Masuhiro, Y., Mori, M., Yanagisawa, J., & Kato, S. p300/CBP acts as a coactivator of the cone-rod homeobox transcription factor. *Biochem.Biophys.Res.Commun.* **269**, 410-414 (2000).

Young, R. W. Visual cells and the concept of renewal. *Invest.Ophthalmol.Vis.Sci.* **15**, 700-725 (1976).

Young, R. W. Cell differentiation in the retina of the mouse. *Anat.Rec.* **212**, 199-205 (1985).

Young, M.J., Ray, J., Whiteley, S.J., Klassen, H. & Gage, F.H. Neuronal differentiation and morphological integration of hippocampal progenitor cells transplanted to the retina of immature and mature dystrophic rats. *Mol. Cell Neurosci.* **16**, 197-205

Zhang, L., Mathers, P. H., & Jamrich, M. Function of Rx, but not Pax6, is essential for the formation of retinal progenitor cells in mice. *Genesis.* **28**, 135-142 (2000).

Zhu, X. & Craft, C. M. Modulation of CRX transactivation activity by phosducin isoforms. *Mol.Cell Biol.* **20**, 5216-5226 (2000).

APPENDIX A

TRANSGENIC MANIPULATION OF *CHX10* EXPRESSION

A.1 Introduction

In chapter 4 of this thesis, it is described how the absence of Chx10 in the *or*^{J} mouse retina results in (amongst other things) expression of the photoreceptor specific transcription factor gene *Crx* and some of its putative downstream targets being delayed by up to seven days. *Chx10* is expressed neither in mature photoreceptors, nor in the photoreceptor layer during development.

As exemplified by the use of the *or*^{J} mouse for the understanding of retinal development, animal models are extremely useful in the analysis of developmental pathways. To further examine the role of Chx10 in the development of the retina, and more specifically to experimentally test the effect that Chx10 has on the development of photoreceptors, I instigated a project to manipulate *Chx10* expression by genetic manipulation using transgenic DNA constructs.

As described in Chapter 4.6, interphotoreceptor retinoid binding protein (IRBP) is a secreted glycolipoprotein that is localised to the interphotoreceptor matrix surrounding the inner and outer segments (Liou *et al.* 1994). There is evidence that the function of IRBP is to transport vitamin A across the hydrophilic subretinal space. Expression is first detected as early as E11, and thus may precede onset of *Crx* expression, which, first recorded at E12.5, is

presumed to be earliest known genetic marker for photoreceptors is Crx, first detectable at E12.5 (Freund *et al.* 1997). There is some evidence that IRBP co-localises with BrdU incorporation in dissociated P2/3 retinal cultures (Liou *et al.* 1994). This suggests that IRBP either is expressed in non-committed cells, or may be a pre-terminal mitosis marker of a photoreceptor fate. The 5' promoter region of *IRBP* also contains a Crx preferred binding site (Livesey *et al.* 2000), suggesting that Crx is involved with transcription of this photoreceptor specific gene. Results shown in Chapter 4.6 indicate that *IRBP* expression is unaffected by the absence of Chx10 and *Crx*, and therefore, although in possession of a Crx-binding site, is not dependent on its activity.

Photoreceptor genesis begins at approximately E10.5 in the mouse (Young 1985), according to studies of ^{3}Thymidine incorporation during development. Several studies have investigated the expression of IRBP during development, and have shown certain inconsistencies. *IRBP* mRNA has been detected as early as E11 by RNA protection assay (RPA), and Chloramphenicol acetyl transferase expression driven under the control of the human *IRBP* promoter is detectable at E13, in photoreceptors. Considered together, these data indicate that IRBP is one of the earliest expressed photoreceptor genes.

A.2 Transgenic *IRBP–Chx10* construct

A 1.329kb fragment of DNA from the 5' upstream region of the human *IRBP* coding sequence was isolated and characterised, and shown to contain a promoter for the *IRBP* gene that was capable of directing photoreceptor-specific gene expression in the mouse (Yokoyama *et al.* 1992). This promoter, cloned into pBluescript plasmid was a kind gift from Paul Overbeek (Baylor College of Medicine, Houston, Texas, USA).

The general hypothesis was that expression of *Chx10* in the mouse, under the control of a photoreceptor-specific promotor, would generate a retinal phenotype that would reflect aspects of the function of Chx10 during retinal development.

The initial idea was to ligate the human *IRBP* promoter to the coding sequence of murine *Chx10*, ligated to an *SV40* polyadenylation signal. In parallel, a transgene construct would be built that contains a genetic marker to enable visualisation of the exogenous *Chx10* expression, as distinct from the endogenous Chx10 (see Figures A.1 a and b). Use of both transgenes is important as a means of investigating how the presence of a fused marker sequence might affect expression of the transgene. To prepare the tagged gene construct, I used a *VSV*-tag (Soldati *et al.* 1991), by amplifying *Chx10* cDNA from a *Chx10* cDNA-containing plasmid, but using a *Chx10*-specific reverse primer with a *VSV*-tag (see Figure A.1b).

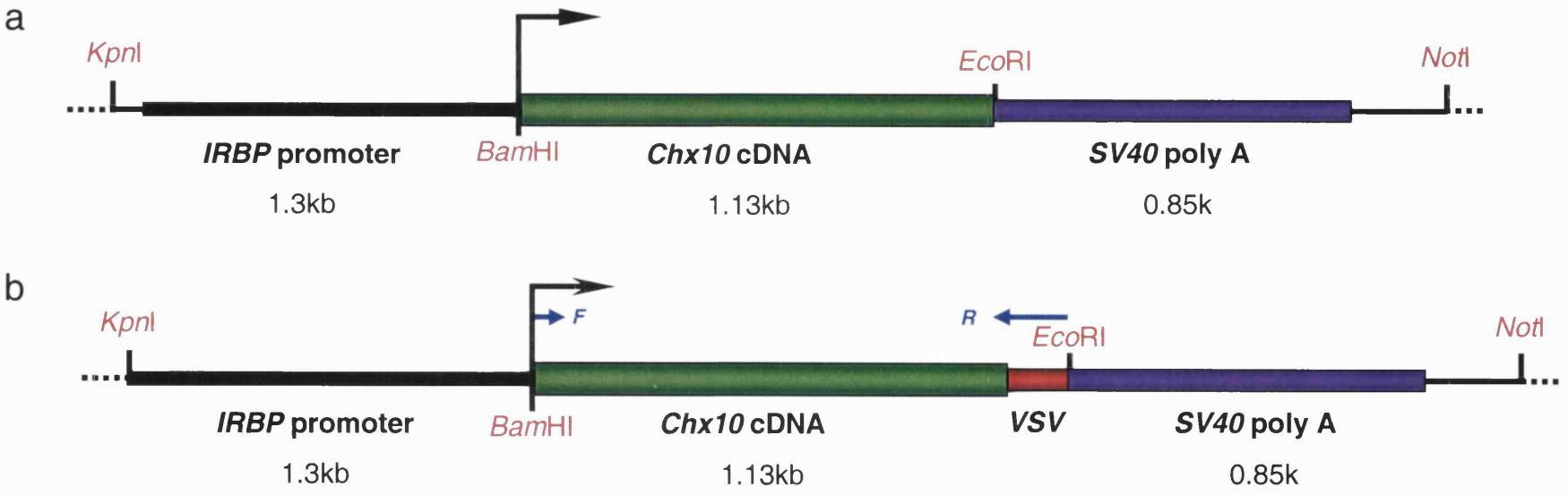

Figure A.1. *IRBP-Chx10* transgenic constructs. Constructs were made by ligating the human *IRBP* promotor to the coding sequence of murine *Chx10*, which in turn was ligated to the *SV40* polyadenylation signal. A second construct was made using Chx10 cDNA amplified by PCR with a *VSV*-tag on it 3' tail, using primers F and R.

Both constructs were to be micro-injected into single-cell fertilised mouse embryos, which were grown in culture, then re-implanted into pseudo-pregnant female mice. Founder offspring would be bred to establish transgenic lines, and any ocular phenotype in their offspring analysed using similar methods to those described in Chapters 4 and 5 of this thesis.

A.3 Speculative predictions of transgenic phenotype

Given the photoreceptor-specific nature of the *IRBP* promoter, and the understood expression and function of Chx10 in retinal development, several predictions can be made about the possible phenotype of a transgenic mouse carrying a construct in which Chx10 was driven by the IRBP promoter.

1. Due to the misexpression of Chx10, postmitotic fated photoreceptors are prevented from differentiating into mature photoreceptors, and thus fail to mature into a recognisable cell. This situation would preclude the presence of normal photoreceptors in the transgenic eye (but these cells may express both photoreceptor and bipolar cell markers).
2. Due to the continued or re-instigated expression of Chx10 past the terminal mitosis, transgene-expressing cells differentiate as bipolar cells. This presupposes a fulfilment of Chx10's role as a determinant of bipolar cell differentiation.

3. Postmitotic fated photoreceptors de-differentiate and return to a mitotic state, resulting in a hypercellular or undifferentiated retina.
4. Given the possibility of IRBP expression in a proportion of mitotic cells, a maintenance of Chx10 in these cells results in their sustaining mitosis, thus generating an over-proliferation of a small subset of cells.
5. Conversely, maintained Chx10 expression in the mitotic IRBP-expressing cells may result in a disproportionately high number of bipolar cells.
6. IRBP-driven expression of Chx10 in the pineal gland might generate a phenotype, given that Chx10 is not found in this tissue normally.

Both constructs were prepared by subcloning PCR amplified *Chx10* cDNA into a plasmid containing both the *IRBP* promotor and the *SV40* polyadenylation signal. Although high-fidelity Taq polymerase was used in amplifications, sequence analysis revealed a 3bp deletion that altered the *Chx10* reading frame. Efforts to remake these constructs were not completed within the time frame of this study.

APPENDIX B

Rs1, A GENE CAUSING RETINOSCHISIS, IS EXPRESSED IN THE INNER NUCLEAR LAYER

X-linked retinoschisis is a macular degeneration characterised by splitting of the inner retinal layers (the inner limiting membrane and nerve fibre layer) and lesions in the peripheral retina (George *et al.* 1995). This disorder presents in juvenile males with visual impairment progressing between 5 and 10 years of age, leading to vitreal haemorrhage, retinal detachment, retinal atrophy and blindness.

Linkage studies revealed that the gene causing X-linked juvenile retinoschisis maps to Xp22, and was identified by positional cloning in 1997 (Sauer *et al.* 1997). *RS1* was found to encode a retina-specific 224-amino acid protein of unknown function, predominantly comprising a discoidin domain. Discoidin domains are associated with extracellular or transmembrane proteins. Given that the location of the retinal splitting in retinoschisis is an acellular region of the retina, it has been suggested that retinoschisin acts as a secreted protein. This is supported by the presence of the discoidin domain (Grayson *et al.* 2000).

I examined the expression pattern by *in situ* hybridisation of *RS1* and its mouse orthologue in PFA-fixed, paraffin-embedded adult human and mouse retinal sections. Expression in the adult human retina was limited to the photoreceptor layer, in the outer nuclear layer and inner segments, and was absent from the inner plexiform layer – the site of the pathology. A similar

pattern was generated in the adult mouse retina (see Appendix C, Grayson *et al.* 2000).

Grayson *et al.* (2000) also performed immunohistochemistry using an antibody raised against retinoschisin. Immunolabelling was detected in the inner segments of the photoreceptors, the inner nuclear layer and in the ganglion cell layer. These data indicate that indeed retinoschisin is synthesised in photoreceptors, and is secreted to other layers in the retina.

Interestingly, sequence analysis of the upstream promotor region of the murine *Rs1* gene revealed a putative Crx binding site (Gehrig *et al.* 1999), suggesting that *Rs1* expression, like other genes investigated in Chapter 4, is regulated by Crx. Livesey *et al.* (2000) analysed the expression of a number of photoreceptor-specific genes in a mouse with targeted deletion of Crx, and found that although expression of *RS1* was not absent it was notably reduced in the $Crx^{-/-}$ homozygous knockout mouse. This suggests that expression of *Rs1* is at least partially regulated by Crx.

APPENDIX C – PUBLISHED RESEARCH PAPERS

1 Ferda-Percin, E., Ploder, L. A., Yu, J. J., Arici, K., Horsford, D. J., Rutherford, A., Bapat, B., Cox, D. W., Duncan, A. M., Kalnins, V. I., Kocak-Altintas, A., Sowden, J. C., Traboulsi, E., Sarfarazi, M. and McInnes, R. R. **Human microphthalmia associated with mutations in the retinal homeobox gene *CHX10*.** *Nat.Genet.* **25**, 397–401 (2000).

2 Grayson, C., Reid, S. N., Ellis, J. A., Rutherford, A., Sowden, J. C., Yates, J. R., Farber, D. B and Trump, D. **Retinoschisin, the X-linked retinoschisis protein, is a secreted photoreceptor protein, and is expressed and released by Weri-Rb1 cells.** *Hum. Mol. Genet.* **22**, 1873–1879 (2000).

3 Bibb, L. C., Holt, J. K. L., Tarttelin, E. E., Hodges, M. D., Gregory-Evans, K., Rutherford, A., Lucas, R. J., Sowden, J. C. and Gregory-Evans, C. Y. **Temporal and spatial expression patterns of the *CRX* transcription factor and its downstream targets. Critical differences during human and mouse eye development.** *Hum.Mol.Genet.* **10**, 1571–1579 (2001).

Human microphthalmia associated with mutations in the retinal homeobox gene *CHX10*

E. Ferda Percin[1,2*], Lynda A. Ploder[3*], Jessica J. Yu[3], Kemal Arici[2], D. Jonathan Horsford[3,5], Adam Rutherford[6], Bharati Bapat[7], Diane W. Cox[8], Alessandra M.V. Duncan[9], Vitauts I. Kalnins[10], Aysegul Kocak-Altintas[11], Jane C. Sowden[6], Elias Traboulsi[12], Mansoor Sarfarazi[1] & Roderick R. McInnes[3,4,5]

*These authors contributed equally to this work.

Isolated human microphthalmia/anophthalmia, a cause of congenital blindness, is a clinically and genetically heterogeneous developmental disorder characterized by a small eye and other ocular abnormalities. Three microphthalmia/anophthalmia loci have been identified[1-3], and two others have been inferred by the co-segregation of translocations with the phenotype[4,5]. We previously found that mice with ocular retardation (the *or-J* allele), a microphthalmia phenotype[6], have a null mutation in the retinal homeobox gene *Chx10* (refs 7,8). We report here the mapping of a human microphthalmia locus on chromosome 14q24.3, the cloning of *CHX10* at this locus and the identification of recessive *CHX10* mutations in two families with non-syndromic microphthalmia (MIM 251600), cataracts and severe abnormalities of the iris. In affected individuals, a highly conserved arginine residue in the DNA-recognition helix of the homeodomain is replaced by glutamine or proline (R200Q and R200P, respectively). Identification of the CHX10 consensus DNA-binding sequence (TAATTAGC) allowed us to demonstrate that both mutations severely disrupt CHX10 function. Human *CHX10* is expressed in progenitor cells of the developing neuroretina and in the inner nuclear layer of the mature retina. The strong conservation in vertebrates of the *CHX10* sequence, pattern of expression and loss-of-function phenotypes demonstrates the evolutionary importance of the genetic network through which this gene regulates eye development.

To evaluate the role of *CHX10* in developmental eye defects, we first cloned human *CHX10* cDNAs (ref. 8). The cDNA detected a 3.3-kb transcript in retinal RNA (data not shown), and encoded an ORF of 1,083 bp (for nucleotide and predicted protein sequences, see http://genetics.nature.com/supplementary_info/). The deduced human *CHX10* ORF encodes a polypeptide of 361 amino acids with a predicted mass of 39 kD. It is 97% identical to mouse *Chx10* (ref. 8) and is completely identical in the homeodomain and CVC domain. To allow genetic analysis of *CHX10* in humans, we determined the exon-intron structure of the gene from genomic clones (Fig. 1).

To determine the expression pattern of human *CHX10* and to compare it with that of other species, we first used polyclonal antibodies specific for CHX10 (ref. 8) to identify the CHX10-expressing cells in adult retina. CHX10 was restricted to nuclei of the inner nuclear layer (INL; Fig. 2*a*). Within this layer, as in mouse retina[8], a gradient of expression was apparent: the outer nuclei, where bipolar cells predominate, stained strongly; whereas the inner aspect, where amacrine cell nuclei are located, stained weakly. This expression pattern is identical to that in mouse, except that in mouse, staining of ganglion cell nuclei was occasionally observed[7,8].

We examined the developmental expression of *CHX10* by *in situ* hybridization of human fetal retinal sections (Fig. 2*b–g*). *CHX10* is expressed in retinal neuroblasts at all stages examined

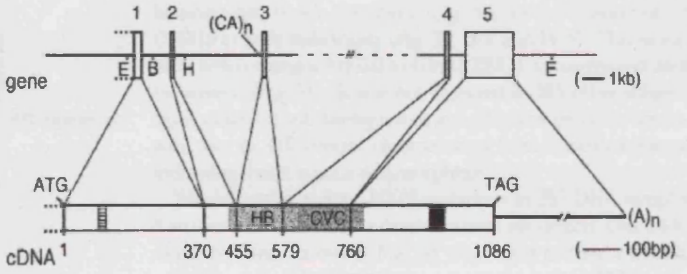

Fig. 1 The human *CHX10* gene and cDNA structure. The genomic organization of *CHX10* is identical to that of the mouse orthologue[7]. The five known exons are represented as numbered boxes, and the introns as lines. The exact location of the 5′ end of exon 1 is unknown (dotted lines), and it may not be the most 5′ exon. A restriction map was generated from the genomic *CHX10* inserts of λDASH clones 8 (22 kb) and 9 (22 kb): B, *Bam*HI; E, *Eco*RI; H, *Hin*dIII. The polymorphic CA repeat in intron 2 is indicated; 18 alleles were observed and 31 predicted, with 86% observed heterozygosity. Intron 3 was not fully characterized (dashed line). The exons are projected onto the schematic of the *CHX10* cDNA. Coding sequences are shown as large, open boxes. The HD is encoded by exons 2, 3 and 4, and is represented as a light grey box. The CVC domain is shown as a dark grey box, the octapeptide as a hatched box, and the OAR domain as a black box. The numbers below the cDNA refer to the nucleotides of the coding sequence (1 indicates the translation start, 1086 the translation stop; the number at the end of each exon is the last bp of the exon). The position of the 5′ end of the transcribed sequence is unknown, and is represented by a dotted line.

[1]*Molecular Ophthalmic Genetics Laboratory, Surgical Research Center, Department of Surgery, University of Connecticut Health Center, Farmington, Connecticut, USA.* [2]*Departments of Medical Biology, Genetics and Ophthalmology, Cumhuriyet University, Sivas, Turkey.* [3]*Programs in Developmental Biology and Genetics, The Research Institute, Hospital for Sick Children, Toronto, Ontario, Canada. Departments of* [4]*Pediatrics and* [5]*Molecular and Medical Genetics, University of Toronto, Toronto, Ontario, USA.* [6]*Developmental Biology Unit, Institute of Child Health, University College London, London, UK.* [7]*Samuel Lunenfeld Research Institute, Mt. Sinai Hospital, Toronto, Ontario, Canada.* [8]*Department of Medical Genetics, University of Alberta, Edmonton, Alberta, Canada.* [9]*Departments of Pathology and Human Genetics, McGill University Hospital Centre, Montreal Children's Hospital, Montreal, Canada.* [10]*The Department of Anatomy and Cell Biology, University of Toronto, Toronto, Ontario, Canada.* [11]*Ophthalmology Clinics, Ankara Hospital, Ankara, Turkey.* [12]*Department of Pediatrics, The Center for Genetic Eye Diseases, Division of Ophthalmology, The Cleveland Clinic Foundation, Cleveland, Ohio, USA. Correspondence should be addressed to M.S. (e-mail: mansoor@neuron.uchc.edu) or R.R.M. (e-mail: mcinnes@sickkids.on.ca).*

(Fig. 2*b–i*, outer layer). The lighter staining in the inner layer of retinas obtained 8–10 weeks post-conception (Fig. 2*c,e*) reflects the presence of post-mitotic ganglion cells (identified by a cell-specific marker; data not shown) in this population; mature ganglion cells do not express *CHX10* (Fig. 2*a,i*). At 13 weeks post-conception (Fig. 2*g*), the cells in the outer aspect of the outer layer, which are morphologically indistinguishable from other cells of this layer, did not express *CHX10*, in contrast with the cells on the inner aspect of this layer. This pattern of cellular heterogeneity in the developmental expression of *CHX10* has not been reported in other vertebrates. The outermost cells may represent a mitotic or immediately post-mitotic population committed to photoreceptor cell fate, consistent with the fact that *CHX10* is not expressed in mature photoreceptors (Fig. 2*a,i*). Because of the similarity of both the CHX10 protein sequence and the pattern of expression of the gene between vertebrates[8,9–12], we initiated a search for *CHX10* mutations in humans with developmental eye phenotypes similar to those seen in the *Chx10*$^{or\text{-}J/or\text{-}J}$ mouse[7] and zebrafish[10].

To examine the role of *CHX10* in genetic disease, we first mapped the gene to chromosome 14q band 24.3 (data not shown). This region has conserved synteny with the part of mouse chromosome 12 where *Chx10* is located[7]. To facilitate segregation analysis of *CHX10*, we identified a complex $(CT)_n.(CA)_n$ repeat in the second intron (Fig. 1). This repeat was analysed in CEPH families, indicating the order: centromere–*D14S71*–*CHX10*–*D14S273*–telomere. Radiation hybrid (RH) mapping of the CA-repeat positioned *CHX10* approximately 1.71 cR telomeric to *D14S71*. On the basis of this RH and linkage data, we determined that the order is cen–*D14S71*–*D14S1025*–*CHX10*–*D14S1047*–*D14S273*–tel.

We identified mutations in *CHX10* in two unrelated families (Fig. 3). Family 1 is a consanguineous kindred from Turkey (Fig. 3*a*), and we examined two microphthalmic family members; the phenotype of one is shown (Fig. 4*a–c*). The second proband, from family 2, was also the offspring of a consanguineous marriage (Fig. 3*b*). His phenotype (Fig. 4*d*) is similar to that of the affected members of family 1. All three subjects had microphthalmia, cataracts and iris colobomas or absent pupils. Notable, given the absence of optic nerves in *Chx10*$^{or\text{-}J/or\text{-}J}$ mice[7], was the presence of optic nerves in the one affected individual examined (Fig. 4*c*).

We used a candidate gene approach to determine whether genes associated with developmental eye defects in other mammals, or known to be expressed at early stages of eye formation, were associated with the microphthalmia of family 1 (Fig. 3*a*). We excluded co-segregation of the phenotype with the anophthalmia locus at 14q32 (ref. 3). Co-segregation of microphthalmia was observed only with DNA markers flanking *CHX10* on 14q24.3. Genotyping of the *CHX10* CA repeat and 18 markers in this location defined a critical region between *D14S77* and *D14S61*, within a genetic interval of 6.3 cM (Fig. 3*a*). We obtained a maximum lod score of Z=2.81 at θ=0.00 for the markers *D14S77*, the *CHX10* CA repeat and *D14S1047*. The next highest value, Z=2.51, was observed with marker *D14S1025*. The evidence of linkage did not improve when several markers were analysed together in a multi-point analysis. Eight markers (Fig. 3*a*), including the *CHX10* CA repeat, showed complete homozygosity in the affected subjects.

To identify mutations in *CHX10*, we used single-stranded conformational polymorphism analysis. Analysis of genomic DNA from the two affected subjects of family 1 revealed a single, homozygous, G→A transition (Fig. 5*a*) in the homeobox of *CHX10* in both individuals (Fig. 3*a*, II-3 and IV-5). This mutation, which changes Arg200 to Gln (R200Q), co-segregated with the disease (Fig. 3*b*). It was not observed in 365 other subjects from various ethnic backgrounds and with a range of eye anomalies, nor in 110 control chromosomes from Turkish subjects, indicating that it is not a polymorphism.

We also screened for *CHX10* mutations in 365 DNA samples from patients with various developmental eye defects. One additional proband (family 2; Fig. 3*c*) was found to have a *CHX10* mutation, a G→C transversion converting arginine 200 to pro-

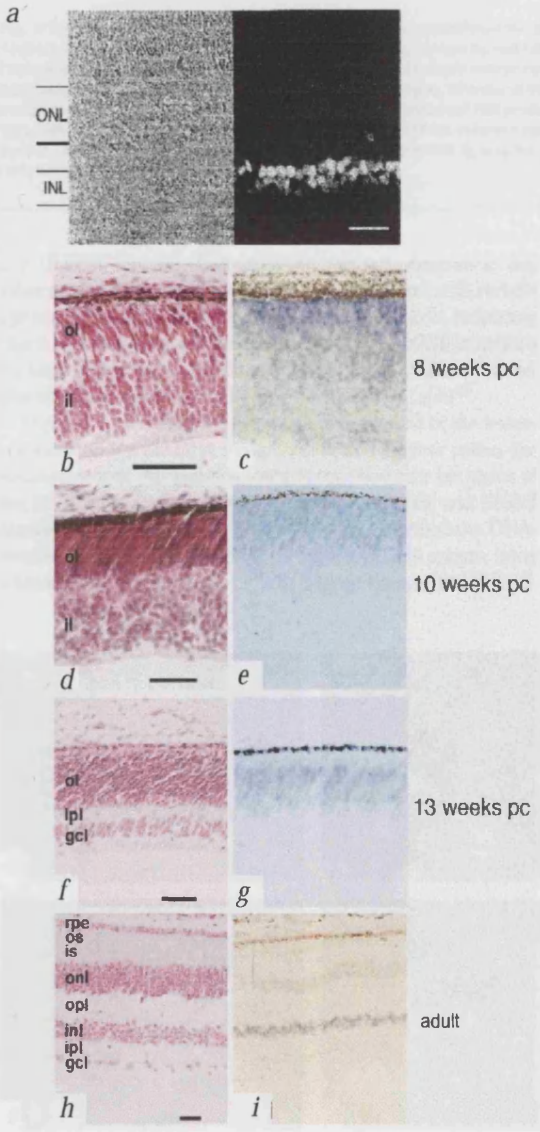

Fig. 2 *CHX10* is abundantly expressed in the inner nuclear layer of human adult retina, and in retinal neuroblasts during eye development. ***a***, Micrograph of a cryostat section of adult human retina showing immunofluorescent labellin of the inner nuclear layer with affiinity-purifiied antibodies to CHX10. Labelli was examined by laser confocal microscopy (right). The corresponding phase contrast micrograph is shown on the left. The preimmune sera did not show any retinal staining (not shown). ONL, outer nuclear layer; INL, inner nuclear layer. Bar, 30 μm. *b–i, CHX10 in situ* hybridization of developing and mature human retina. ***b,d,f,h,*** Haematoxylin and eosin stained sections. ***c,e,g,i,*** Sections hybridized with an antisense digoxygenin-labelled *CHX10* riboprobe. Fetal ages are shown as weeks post-conception (weeks pc). ol, Outer layer; il, inner layer; ipl, inner plexiform layer; gcl, ganglion cell layer; rpe, retinal pigmented epithelium; os, outer segments; is, inner segments; onl, outer nuclear layer; opl, outer plexiform layer; inl, inner nuclear layer. Scale bars, 100 μm.

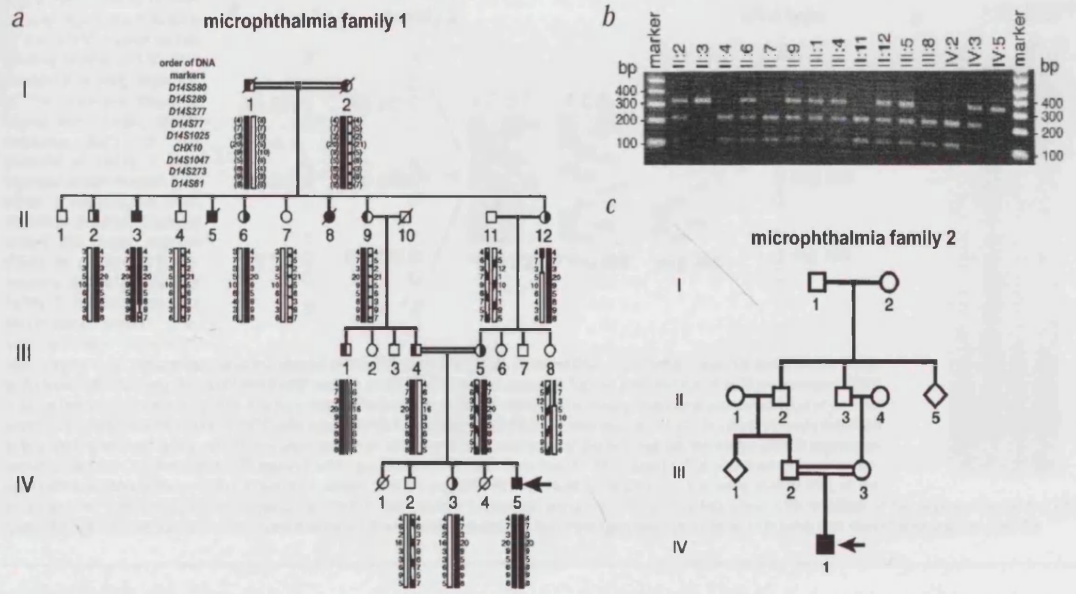

Fig. 3 Pedigrees of two families with autosomal recessive microphthalmia. ***a***, The Turkish kindred (family 1), in which the disease mapped to chromosome 14q24.3. Affected subjects are identified by filled symbols, carriers by half-filled symbols, and the d-type allele by open symbols. Individuals shown without haplotypes were not examined or tested, but were reported to have normal eyes and vision. The order of markers used is shown at the top left. The solid vertical bars below each subject indicate the disease-carrying haplotype, whereas all other vertical bars indicate the haplotypes of unaffected individuals. ***b***, The R200Q mutation was identified in members of family 1 by *TaqI* digestion of PCR products, as the mutation abolishes a *TaqI* site. In controls, digestion of a 329-bp wild-type DNA PCR product generated fragments of 105 bp and 224 bp; in heterozygous carriers, both the undigested fragment (329 bp) and digested fragments (224 bp and 105 bp); and in the two microphthalmic subjects (II-3 and IV-5), only the 329-bp fragment. ***c***, Family 2, a consanguineous family from the United Arab Emirates with one affected individual (filled square)

line (R200P; Fig. 5*a*). This mutation was not observed in 365 other subjects from diverse ethnic backgrounds and with various eye anomalies, nor in 220 alleles from normal subjects, indicating that it is not a polymorphism. That both of the *CHX10* mutations we identified occur in the same CGA codon may reflect the fact that the CG doublet is a well-known mutation hot spot[13].

Arginine 200 of the CHX10 protein is residue 53 of the homeodomain, within the DNA recognition helix[8]. In other paired-like homeodomains, this arginine contacts the phosphate backbone of the DNA (ref. 14). To determine whether the R200P and R200Q mutations confer a loss of function, we first identified the DNA-binding site preferentially used *in vitro* by the CHX10 protein, using a binding site selection assay[15,16]. An 8-bp consensus, TAATTAGC, was identified: the first 6 bp had an occurrence of greater than 90% in the selected oligonucleotide pool, whereas the last 2 bp, GC, had occurrences of 80% and 68%, respectively. The TAATTAGC target differs from that of other paired class homeodomains[14,17]. Because the TAAT sequence is present in many homeodomain binding sites, it may be the core recognition element for CHX10, with further specificity being conferred by the bases TAGC.

We used gel mobility shift assays to demonstrate that the R200Q and R200P substitutions impaired the binding of the mutant CHX10 proteins to the consensus binding site. We first established that wild-type and mutant proteins were present at comparable concentrations by immunoblot analysis (Fig. 5*b*, top). The c-myc–tagged wild-type and mutant proteins each migrated to a position consistent with a molecular weight of approximately 55 kD, whereas no protein was detected on blots using unprogrammed lysate (Fig. 5*b*, top). In gel mobility shift assays, binding of CHX10 to the consensus oligonucleotide was detected by the indicated band shift, but no specific binding was obtained with either R200Q or R200P mutant CHX10

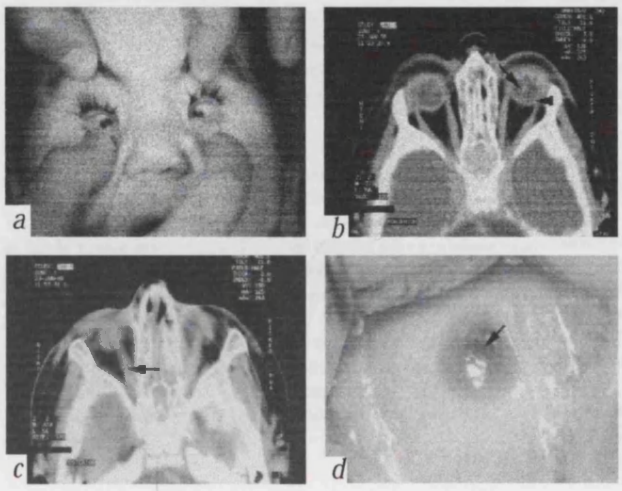

Fig. 4 Clinical presentation of patients with *CHX10* mutations. *a–c*, The phenotype of the proband of family 1 with the R200Q mutation. ***a***, Bilateral microphthalmia at 1 y; the cataract in the right eye is visible. ***b***,***c***, Computerized tomography of the eyes of the R200Q proband at 1 y, showing the microphthalmia in both images, in (*b*) the dislocated lenses (arrow) and increased thickness of the sclera (arrowhead) and in (*c*) the normally sized optic nerves (arrow). ***d***, The left eye of the patient with the R200P mutation at age 2 months, showing a poorly defiined limbus an conjunctivalization of the corneal epithelium. There was no pupillary aperature. The dark brown circular structure in the upper part of the cornea is the iris (arrow). A funnel-shaped retinal detachment inserted into the optic disc was observed OD, and a lesion compatible with a dislocated lens with surrounding membrane formation or localized retinal detachment was noted OS.

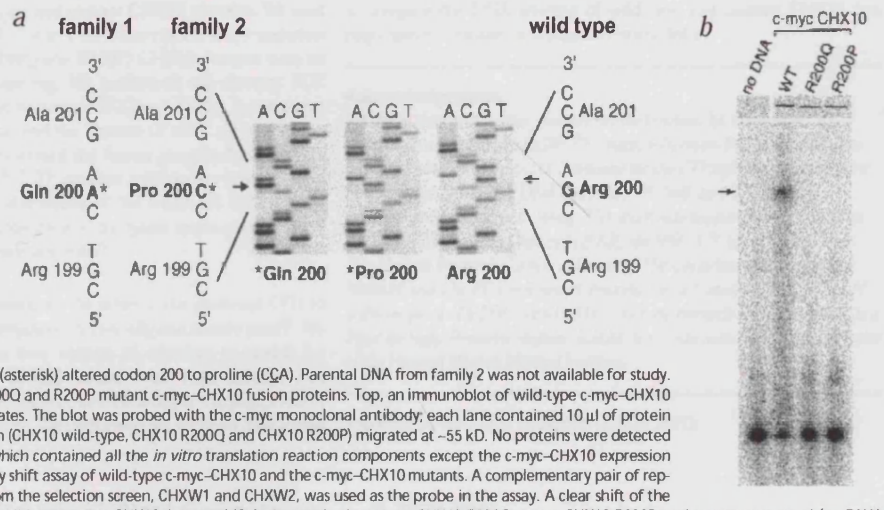

Fig. 5 Two missense homeodomain mutations in Arg200 of the CHX10 protein reduce binding to the CHX10 DNA consensus binding sequence. ***a***, The wild-type sequence (right) and mutant *CHX10* sequence (left) of the proband of family 1 were identical except in exon 4, in which a homozygous G→A transition (asterisk) changed codon 200 from arginine (CGA) to glutamine (CAA). Similarly, in the proband of family 2, the only sequence abnormality (second from left) was in exon 4, in which a homozygous G→C transversion (asterisk) altered codon 200 to proline (CCA). Parental DNA from family 2 was not available for study. ***b***, Reduced DNA binding by R200Q and R200P mutant c-myc–CHX10 fusion proteins. Top, an immunoblot of wild-type c-myc–CHX10 and the two mutant protein lysates. The blot was probed with the c-myc monoclonal antibody; each lane contained 10 µl of protein lysate. Each c-myc fusion protein (CHX10 wild-type, CHX10 R200Q and CHX10 R200P) migrated at ~55 kD. No proteins were detected in the unprogrammed lysate, which contained all the *in vitro* translation reaction components except the c-myc–CHX10 expression construct. Bottom, a gel mobility shift assay of wild-type c-myc–CHX10 and the c-myc–CHX10 mutants. A complementary pair of representative oligonucleotides from the selection screen, CHXW1 and CHXW2, was used as the probe in the assay. A clear shift of the probe (arrow) is observed with wild-type c-myc–CHX10, but no shift is detected using c-myc–CHX10 R200Q, c-myc–CHX10 R200P or the unprogrammed (no DNA) lysate. Background bands seen in the mutant lanes are the same as ones seen in the unprogrammed lysate lane, indicating that these bands are non-specific

proteins (Fig. 5, bottom). These results demonstrate that both mutations at residue 200 disrupt the binding of CHX10 to DNA.

We have demonstrated that *CHX10* is the gene at a fourth non-syndromic microphthalmia/anophthalmia locus, making it the only microphthalmia gene identified so far. *CHX10* mutations accounted for only approximately 2% (2/117) of the patients with non-syndromic microphthalmia studied. Although the ocular expression of *CHX10* is limited to the neuroretina in human (Fig. 2, and data not shown) and mouse[8], the loss of CHX10 function is panocular in its effects: the growth of the eye and the integrity of the lens and iris, in addition to the retina, are all disrupted. These non-retinal phenotypes suggest that the developing neuroretina may produce a *CHX10*-dependent factor essential for eye formation.

The eye abnormalities we observed probably result from a loss of *CHX10* function. The R200Q and R200P *CHX10* alleles are likely to be null alleles because their DNA binding is greatly impaired (Fig. 5*b*); position 53 of the homeodomain is almost always (344/346 in one survey[18]) an arginine[14], reflecting its role in contacting the DNA phosphate backbone[14]; and an R53C substitution in the *HESX1* paired-like homeodomain also ablates DNA binding[19]. Thus, a severe loss of CHX10 function leads to virtually orthologous phenotypes in human, mouse[7,20] and zebrafish[10]. Because the CHX10 loss-of-function phenotype is restricted to the eye in mouse[7] and human, CHX10 appears not to be essential for the development of the other—largely neural—tissues in which it is expressed[8].

Methods

Case reports. Family 1 consists of 35 subjects, with 4 affected individuals (2 are deceased). The proband's parents were clinically normal. The abnormalities of the proband at 9 months of age, and of the other affected subject at age 49 y, were strictly ocular. Both had bilateral microphthalmia, congenital cataracts and bilateral inferior colobomas of the iris; neither had light perception. By ultrasound, the proband's eyes had an axial length of 12.0 OD and 10.0 mm OS (<1th%; ref. 21).

In family 2, the proband was the only child of clinically normal parents. At two months of age, he had bilateral small globes (axial lengths: 10.9 mm OD and 13.6 mm OS by ultrasonagraphy, <1th%; ref. 21). Other eye phenotypes were noted. His only non-ocular abnormalities were undescended testes.

Linkage analysis and genotyping of family 1. The pedigree provides a maximum of 30 potentially informative meioses. We performed genotyping and linkage analysis as described (see http://genetics.nature.com/supplementary_info/). The order of markers we identified was consistent with a PAC clone (AC005519) which contains *CHX10*; this clone is part of a contig containing the *D14S1047* marker.

***CHX10* cDNA and genomic cloning.** We isolated *CHX10* clones from an adult human retina λgt10 cDNA library as described[8]. To identify *CHX10* genomic clones, we screened a human genomic library (made from a *Sau*3A1 partial digest) in the λ DASH vector with the *CHX10* cDNA using standard methods. We generated restriction maps of clones 8 and 9, identified exon-containing fragments with the cDNA probe, and compared sequences with those in GenBank[22].

Chromosome, RH and microsatellite mapping. We first mapped *CHX10* using autoradiographic *in situ* hybridization with a tritium-labelled *CHX10* cDNA probe on blood lymphocytes as described[23]. We performed RH mapping of the *CHX10* intron 2 CA repeat using the GeneBridge 4 RH panel. We used standard methods[24] to identify the CA repeat in the gene. The methods we used for amplification of the *CHX10* CA repeat are described (see http://genetics.nature.com/supplementary_info/).

Immunoblot analysis, immunofluorescent labelling and *in situ* hybridization of *CHX10* in human retina. We fixed human eyes obtained within 24 h of death in 2.5% paraformaldehyde for 2 h at 4 °C and stored them overnight in 30% sucrose. We prepared retinas and performed immunoblots, immmunofluorescence labelling[8] and *in situ* hybridization[25] as described. We generated *CHX10* riboprobes from a linearized pBluescript KS plasmid containing the *CHX10* cDNA. We determined fetal age by measurement of the foot- or crown-rump length. We obtained human tissue after informed consent from the MRC Tissue Bank, Royal Postgraduate Medical School, Hammersmith Hospital.

Mutation screening. We screened for *CHX10* mutations in the DNA of 88 patients with microphthalmia, 28 with anophthalmia, 10 with microphthalmia with systemic phenotypes, 8 with optic nerve aplasia or hypoplasia, 71 with Leber congenital amaurosis, and 160 patients with a range of other eye defects, including 39 with anterior segment anomalies. We amplified *CHX10* in five fragments spanning the coding and flanking intonic sequences as described (see http://genetics.nature.com/supplementary_info/). We performed SSCP analysis and direct sequencing of PCR products as described[26]

In vitro translation of wild-type and mutant CHX10 proteins. We used the plasmid pT7tagN (ref. 16) for *in vitro* transcription and translation of wild-type and mutant (R200Q and R200P) CHX10 proteins with an amino-terminal c-myc epitope tag. We performed site-directed PCR mutagenesis[27] to generate the mutants R200Q and R200P, documented the presence of each mutation and the absence of other changes in the cDNA by sequencing, and expressed the fusion proteins from *CHX10* plasmid (1 μg) using the TNT T7 coupled reticulocyte lysate system (Promega). To examine the abundance of the translated CHX10 proteins, we performed immunoblotting of the lysate reaction (see http://genetics.nature.com/supplementary_info/)

CHX10 DNA-binding site selection. We selected the preferred CHX10 binding site from a random sequence 26-mer oligonucleotide pool[28]. We used the CHX10 protein in four rounds of selection to enrich for oligonucleotides to which CHX10 bound with high affinity, and sequenced 31 oligonucleotide inserts from the selected transformants to identify a consensus binding site. We performed gel mobility shift assays to compare the DNA binding of wild-type and mutant CHX10 (see http://genetics.nature.com/supplementary_info/).

Acknowledgements

We thank the participating members of the families; M. Hankin for the description of the iris of Chx10$^{or\text{-}J/or\text{-}J}$ mice; J. Nathans for the adult human retina λgt10 cDNA library; D. Zarkower for the PT7tagN vector and advice; M. Ozguc for facilitating DNA extraction; W. Shih and L. Collins for technical assistance; and L. Wong. This study was supported by grants from the TUBITAK, Ankara, Turkey to E.F.P., the MRC UK to J.C.S., and from The Medical Research Council of Canada, The Canadian Genetic Disease Network and The RP Eye Research Foundation of Canada to R.R.M. D.J.H. is the recipient of a FFB Canada/MRC doctoral research award, and A.R. is a Fight for Sight Research Student. R.R.M. is an International Research Scholar of the Howard Hughes Medical Institute.

Received 29 February; accepted 15 May 2000.

1. Graham, C.A., Redmond, R.M. & Nevin, N.C. X-linked clinical anophthalmos. Localization of the gene to Xq27–Xq28. *Ophthal. Paediatr. Genet.* **12**, 43–48 (1991).
2. Othman, M.I. *et al.* Autosomal dominant nanophthalmos (NNO1) with high hyperopia and angle-closure glaucoma maps to chromosome 11. *Am. J. Hum. Genet.* **63**, 1411–1418 (1998).
3. Bessant, D.A. *et al.* A locus for autosomal recessive congenital microphthalmia maps to chromosome 14q32. *Am. J. Hum. Genet.* **62**, 1113–1116 (1998).
4. Al-Gazali, L.I. *et al.* Two 46,XX,t(X;Y) females with linear skin defects and congenital microphthalmia: a new syndrome at Xp22.3. *J. Med. Genet.* **27**, 59–63 (1990).
5. Yokoyama, Y., Narahara, K., Tsuji, K., Ninomiya, S. & Senio, Y. Autosomal dominant congenital cataract and microphthalmia associated with a familial t(2;16) translocation. *Hum. Genet.* **90**, 177–178 (1992).
6. Truslove, G.M. A gene causing ocular retardation in the mouse. *J. Embryol. Exp. Morph.* **10**, 652–660 (1962).
7. Burmeister, M. *et al. Ocular retardation* mouse caused by *Chx10* homeobox null allele: impaired retinal progenitor proliferation and bipolar cell differentiation. *Nature Genet.* **12**, 376–384 (1996).
8. Liu, I.S.-C. *et al.* Developmental expression of a novel murine homeobox gene (*Chx10*): evidence for roles in determination of the neuroretina and inner nuclear layer. *Neuron* **13**, 377–393 (1994).
9. Belecky-Adams, T. *et al. Prox-1, Pax6* and *Chx10* homeobox gene expression correlates with phenotypic fate of retinal precursor cells. *Invest. Ophthalmol. Vis. Sci.* **38**, 1293–1303 (1997).
10. Barabino, S.M., Spada, F., Cotelli, F. & Boncinelli, E. Inactivation of the zebrafish homologue of *Chx10* by antisense oligonucleotides causes eye malformations similar to the ocular retardation phenotype. *Mech. Dev.* **63**, 133–143 (1997).
11. Chen, C.-M.A. & Cepko, C.L. Expression of *Chx10* and *Chx10-1* in the developing chick retina. *Mech. Dev.* **90**, 293–297 (2000).
12. Passini, M.A., Levine, E.M., Canger, A.K., Raymond, P.A. & Schechter, N. *Vsx-1* and *Vsx-2*: differential expression of two *paired*-like homeobox genes during zebrafish and goldfish retinogenesis. *J. Comp. Neurol.* **388**, 495–505 (1997).
13. Cooper, D. & Krawczak, M. The mutational spectrum of single basepair substitutions causing human genetic disease: patterns and predictions. *Hum. Genet.* **85**, 55–74 (1990).
14. Wilson, D.S., Guenther, B., Desplan, C. & Kiriyan, J. High resolution crystal structure of a paired (pax) class cooperative homeodomain dimer on DNA. *Cell* **82**, 709–719 (1995).
15. Pollock, R. & Treisman, R. A sensitive method for the determination of protein-DNA binding specificities. *Nucleic Acids Res.* **18**, 6197–6204 (1990).
16. Zarkower, D. & Hodgkin, J. Zinc fingers in sex determination: only one of the two *C. elegans* Tra-1 proteins binds DNA *in vitro*. *Nucleic Acids Res.* **21**, 3691–3698 (1993).
17. Wilson, D., Sheng, G., Lecutt, T., Dostatni, N. & Desplan, C. Cooperative dimerization of paired class homeodomains on DNA. *Genes Dev.* **7**, 2120–2134 (1993).
18. Duboule, D. (ed.) *Guidebook to the Homeobox Genes* (Oxford University Press, Toronto, 1994).
19. Dattani, M.T. *et al.* Mutations in the homeobox gene *HESX1/Hesx1* associated with septo-optic dysplasia in human and mouse. *Nature Genet.* **19**, 125–133 (1998).
20. Bone-Larson, C. *et al.* Partial rescue of the ocular retardation phenotype by genetic modifiers. *J. Neurobiol.* **42**, 232–247 (2000).
21. Isenberg, S.J. Physical and refractive characteristics of the eye at birth and during infancy. in *The Eye in Infancy* (ed. Isenberg, S.J.) 36–51 (C.V. Mosby, St. Louis, 1994).
22. Altschul, S.F., Gish, W., Miller, W., Myers, E.W. & Lipman, D.J. Basic local alignment search tool. *J. Mol. Biol.* **215**, 403–410 (1990).
23. Duncan, A.M.V., Chow, W. & Robinson, G.H. Localization of the human 75 Kd Fe-S protein of NADH-Coenzyme Q Reductase gene to 2q33–34. *Cytogenet. Cell Genet.* **60**, 212–213 (1992).
24. Dib, C. *et al.* A comprehensive genetic map of the human genome based on 5264 microsatellites. *Nature* **380**, 152–154 (1996).
25. Breitschopf, H., Suchanek, G., Gould, R.M., Colman, D.R. & Lassmann, H. *In situ* hybridization with digoxigenin-labeled probes: sensitive and reliable detection method applied to myelinating rat brain. *Acta Neuropathol. (Berl)* **84**, 581–587 (1992).
26. Bascom, R.A., Liu, L., Heckenlively, J.R., Stone, E.M. & McInnes, R.R. Mutation analysis of the *ROM1* gene in retinitis pigmentosa. *Hum. Mol. Genet.* **4**, 1895–1902 (1995).
27. Cormack, B. Mutagenesis of cloned DNA. in *Current Protocols in Molecular Biology* (eds Ausubel, F.M. *et al.*) 8.5.7–8.5.9 (John Wiley & Sons, Boston, 1999).
28. Pollock, R.M. DNA-protein interactions. in *Current Protocols in Molecular Biology* (eds Ausubel, F.M. *et al.*) 12.11.11–12.11.17 (John Wiley & Sons, Boston, 1999).

Human Molecular Genetics, 2000, Vol. 9, No. 12 1873–1879

Retinoschisin, the X-linked retinoschisis protein, is a secreted photoreceptor protein, and is expressed and released by Weri–Rb1 cells

Celene Grayson, Silvia N.M. Reid[1], Juliet A. Ellis, Adam Rutherford[2], Jane C. Sowden[2], John R.W. Yates, Debora B. Farber[1] and Dorothy Trump[+]

Department of Medical Genetics, The Wellcome Trust Centre for Molecular Mechanisms in Disease, Cambridge Institute for Medical Research, University of Cambridge, Addenbrookes Hospital, Hills Road, Cambridge CB2 2QQ, UK, [1]Jules Stein Institute, UCLA School of Medicine, Los Angeles, CA, USA and [2]Developmental Biology Unit, Institute of Child Health, University College London, London, UK

Received 10 April 2000; Revised and Accepted 19 May 2000

X-linked retinoschisis is characterized by microcystic-like changes of the macular region and schisis within the inner retinal layers, leading to visual deterioration in males. Many missense and protein-truncating mutations of the causative gene *RS1* have now been identified and are thought to be inactivating. *RS1* encodes a 224 amino acid protein, retinoschisin, which contains a discoidin domain but is of unknown function. We have generated a polyclonal antibody against a peptide from a unique region within retinoschisin, which detects a protein of ~28 kDa in retinal samples reduced with dithiothreitol, but multimers sized >40 kDa under non-reducing conditions. A screen of human tissues with this antibody reveals retinoschisin to be retina specific and the antibody detects a protein of similar size in bovine and murine retinae. We investigated the expression pattern in the retina of both *RS1* mRNA (using *in situ* hybridization with riboprobes) and retinoschisin (using immunohistochemistry). The antisense riboprobe detected *RS1* mRNA only in the photoreceptor layer but the protein product of the gene was present both in the photoreceptors and within the inner portions of the retina. Furthermore, differentiated retinoblastoma cells (Weri–Rb1 cells) were found to express *RS1* mRNA and to release retinoschisin. These results suggest that retinoschisin is released by photoreceptors and has functions within the inner retinal layers. Thus, X-linked retinoschisis is caused by abnormalities in a putative secreted photoreceptor protein and is the first example of a secreted photoreceptor protein associated with a retinal dystrophy.

INTRODUCTION

X-linked juvenile retinoschisis is the leading cause of juvenile macular degeneration in males (1) and is characterized by schisis (splitting) of the inner retinal layers [inner limiting membrane (ILM) and nerve fibre layers] resulting in cystic degeneration 'retinoschisis' of the central retina (2,3). Peripheral retinal lesions are also present in ~50% of cases (3). Clinically the condition is variable, with most patients presenting with progressive visual impairment between 5 and 10 years of age, but a proportion of patients present in infancy with squint, nystagmus and bilateral and highly elevated bullous retinoschisis (4,5). In the later stages of retinoschisis complications include vitreal haemorrhage, choroidal sclerosis, retinal detachment and in rare cases, retinal atrophy resulting in blindness (6).

Previously it had been suggested that an underlying defect in the Müller cell, the retinal glial cell, could explain the combination of features (2,7–9). Histological reports describe the characteristic abnormality as a schisis within the superficial retinal layers, the ILM, the nerve fibre layer and the ganglion cell layer (2,10,11). The inner leaflet of the schisis consists of ILM, fragments of Müller cells and blood vessels and a thinned ganglion cell layer. Degeneration of the overlying photoreceptors is also observed (11). The schisis cavity and surrounding retina are described as containing an amorphous eosinophilic PAS-positive filamentous material thought to originate from Müller cells (2,11). The electroretinogram of patients affected with retinoschisis shows a reduced b-wave [suggesting an inner retinal abnormality (3)], consistent with a Müller cell abnormality. Furthermore, these patients exhibit the 'Mizou phenomenon', a change in colour of the dark-adapted retina from red to gold shortly after exposure to light, which is thought to be due to a potassium imbalance in the inner retina (9). Photoreceptor hyperpolarization occurs in response to light leading to a rise in extracellular potassium, which is distributed to the vitreous fluid via the Müller cells. Thus, an abnormality in these cells might lead to a build up of potassium ions in the extracellular space (9).

[+]To whom correspondence should be addressed. Tel: +44 1223 331139; Fax: +44 1223 331206; Email: dorothy.trump@cimr.cam.ac.uk

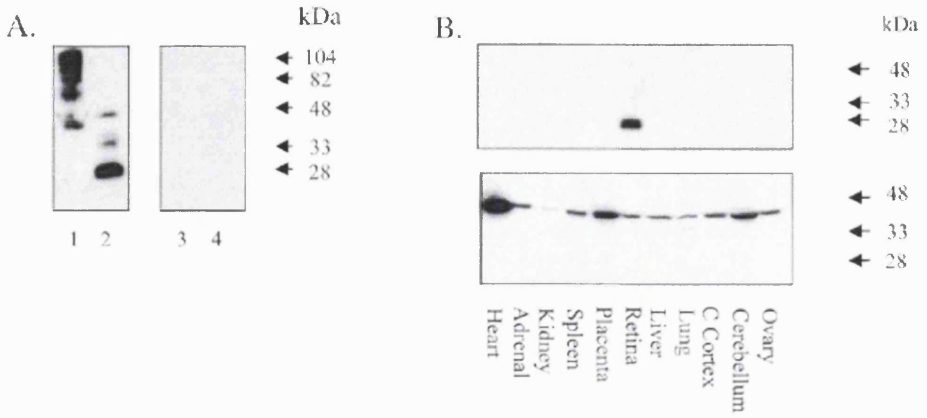

Figure 1. (**A**) Immunoblot of human retinal proteins reacted with antibody RS24–37. Lanes 1 and 2, samples without and with the addition of DTT, respectively. In the reduced samples the antibody recognizes a predominant band at ~28 kDa but in the non-reduced sample it recognizes multimers sized >40 kDa. None of these bands were detected when the antiserum had been adsorbed by the peptide prior to immunoblotting(lanes 3 and 4). (**B**) Immunoblot of proteins from different human tissues using RS24–37. This antibody recognizes a specific band in retina only (upper panel). An antibody against actin was used together with RS24–37, which had been previously adsorbed by the peptide that was used to generate it (lower panel). Actin is detected in all lanes and the specific retinal band is no longer detected by RS24–37.

The gene causing X-linked juvenile retinoschisis, *RS1*, maps to Xp22 and was identified recently (12) after an extensive positional cloning effort by several groups (13–15). The mouse orthologue gene has also been cloned (16). *RS1* has six exons and encodes a 224 amino acid protein, retinoschisin. The function of retinoschisin is unknown. Almost the entire protein consists of a discoidin domain, and disease-causing mutations are clustered in regions that encode this domain, suggesting that it is crucial for the normal function of retinoschisin (17). Discoidin domains are present in extracellular or transmembrane proteins implicated in cell adhesion or cell–cell interactions (18). These proteins include, for example: (i) neuropilin I and II (receptors for the semaphorin family of cell adhesion molecules) (19); (ii) neurexin IV/caspr (axon–glial interactions in septate junctions) (20); (iii) P47 (binding of sperm to the zona pellucida during fertilization) (21); (iv) del-1 (a ligand for the αVβ3 integrin receptor which induces integrin signalling and angiogenesis) (22); and (v) the receptor tyrosine kinases DDR1 and DDR2 (for which collagen acts as a ligand) (23). Therefore, it has been speculated that retinoschisin could be a secreted protein involved in either cell–cell interaction or adhesion and that with this function it could contribute to the maintenance of the cellular architecture of the retina (16). In mice the retinoschisis gene is expressed in the photoreceptors which are located far from the site of pathology (16). This cell expression needs to be confirmed in the human retina. Since the schisis occurs at a site other than the site of synthesis of retinoschisin, this suggests that the protein is secreted by the photoreceptors. The purpose of this study was to investigate these issues. Our results are consistent with the notion that retinoschisin is a secreted photoreceptor protein and that it performs a function within the inner retina.

RESULTS

Affinity-purified antibody against retinoschisin

Rabbit polyclonal antiserum was raised against peptide STEDEGEDPWYQKA (amino acid residues 24–37) conjugated to keyhole limpet haemocyanin (KLH) and affinity-purified (24). The resulting antibody RS24–37 was characterized against human, bovine and murine retinal tissues. In samples of human retinal proteins reduced with dithiothreitol (DTT), RS24–37 recognized a protein of ~28 kDa but under non-reducing conditions it bound multimers of >40 kDa (Fig. 1A). Pre-immune serum showed no cross reactivity (data not shown), and the band was not detected when RS24–37 was incubated with the peptide against which it was generated prior to immunoblotting (Fig. 1A). These results indicate that the bands detected by RS24–37 were specific. RS24–37 also reacted with specific proteins of similar sizes from reduced bovine and murine retinal samples with proteins of much higher molecular weight from non-reduced samples (data not shown). Immmunoblotting with RS24–37 against a panel of 10 other human tissues, including ovary, cerebellum, cerebral cortex, lung, liver, placenta, spleen, kidney, adrenal and heart, confirmed and extended this finding. RS24–37 detected a specific band only from retinal tissue (Fig. 1B). This confirmed previous analyses using cDNA *RS1* probes and multi-tissue northern blots which revealed mRNA expression in retina only (12,16).

Retinoschisin expression pattern within the retina

The expression pattern of the *RS1* mRNA and its encoded protein, retinoschisin, were investigated using retinal sections from adult human and mouse [the gene is first expressed at day 5 postnatally in mouse (16)]. Digoxigenin-labelled sense and antisense riboprobes were generated from the full-length RS1 cDNA (including the open reading frame of 642 bp). Consistent with previous findings in mice (16), staining in human retina was detected only within the photoreceptor cell layer and was most prominent within the inner segments of the photoreceptors (Fig. 2A). It was absent from the inner plexiform layers (where the retinoschisis pathology is most prominent) and the inner nuclear layer [which contains the cell bodies of the Müller cells, previously implicated in retinoschisis pathology (3–5,11)]. The pattern of expression was

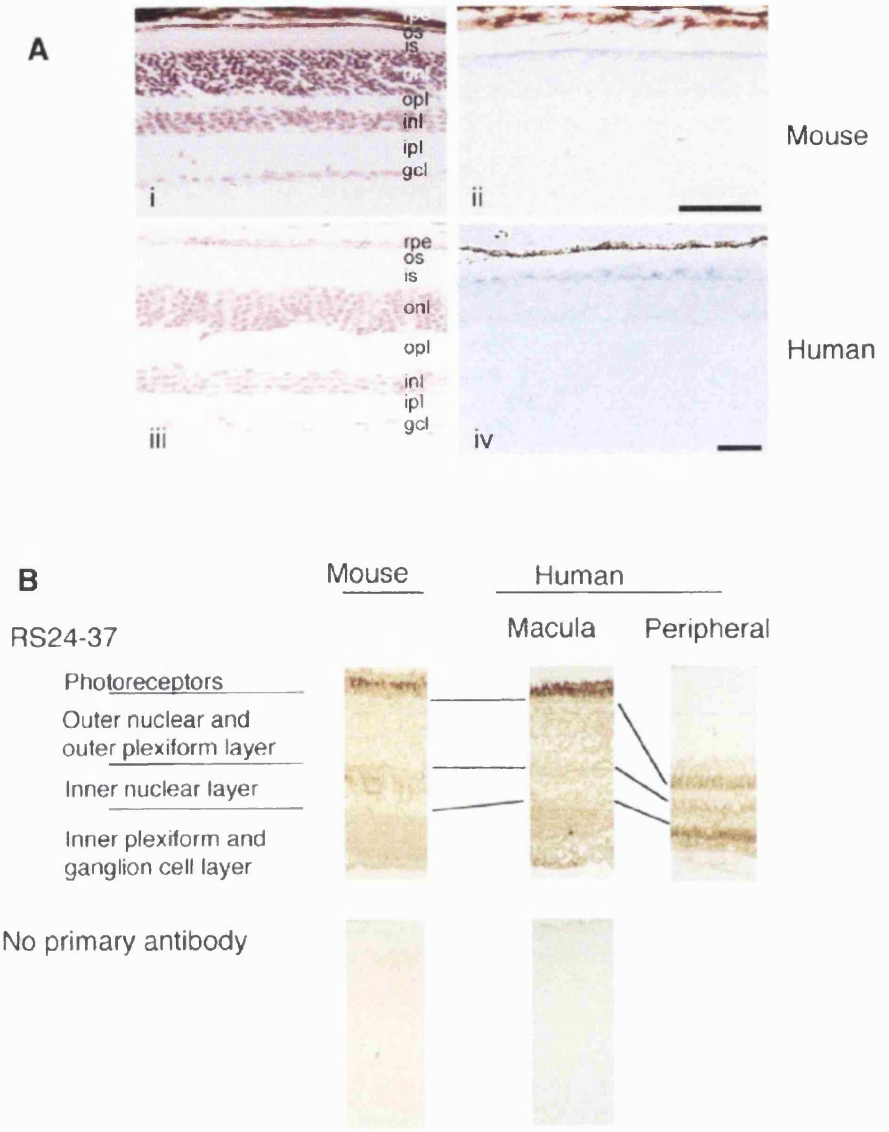

Figure 2. *In situ* hybridization of retina with digoxigenin-labelled antisense *RS1* riboprobes. (**A**) mRNA transcripts are readily detectable in the inner segments of the photoreceptors only in adult human (iv) and mouse (ii) (shown for comparison). (i) and (iii) are adjacent sections from the same specimens stained with haematoxylin and eosin to show the histology, and labelled as follows: rpe, retinal pigment epithelium; os, outer segment of photoreceptor; is, inner segment of photoreceptor; onl, outer nuclear layer; opl, outer plexiform layer; inl, inner nuclear layer; ipl, inner plexiform layer; gcl, ganglion cell layer. (**B**) Immunohistochemistry in mouse and human retina using RS24–37. Immunolabelling is found in the inner segment of the photoreceptors, the inner nuclear layer, the inner plexiform layer and the ganglion cell layer in both mouse and human peripheral sections. The staining in the inner nuclear layer is patchy. In the human macula, there is patchy staining in both nuclear layers and more homogeneous staining in the inner plexiform layer. The immunoreaction was not observed when the primary antibody was omitted, using pre-immune serum or the peptide-epitope pre-absorbed RS24–37.

similar in mouse and in human samples (Fig. 2A). No staining was detected with the sense riboprobe.

Immunohistochemistry

In mice, immunolabelling with RS24–37 was found in the inner segment of the photoreceptors, the inner nuclear layer, the inner plexiform layer and the ganglion cell layer. The staining in the inner nuclear layer was patchy (Fig. 2B). This pattern was also found in the peripheral portion of the human retina (Fig. 2B). At the macula, there was patchy immunoreactivity in both the outer and inner nuclear layers and more homogeneous staining in the inner plexiform layer (Fig. 2B). No reaction was observed when the primary antibody was omitted (Fig. 2B) or when pre-immune serum or serum pre-absorbed with the original peptide was used.

Expression of retinoschisin in Weri–Rb1 cells

Expression of retinoschisin was investigated in the Weri–Rb1 cell line using a combination of RT–PCR with exonic primers from within the *RS1* gene (designed so that the products would span introns) and immunoblotting with the antibody RS24–37 (to detect the presence of the protein within the Weri–Rb1 cells and/or in the media in which cells had grown). Retinoblastoma cells are precursors of photoreceptors and are an appropriate *in vitro* photoreceptor cell model since photoreceptor cell lines are not available (25).

RT–PCR using RNA from undifferentiated Weri–Rb1 cells and two sets of primers [RSPEP10 and RSPEP5 from exons 2 and 4, respectively (product size 262 bp), and RSPEP3 and RSPEP6 from exons 4 and 6, respectively (product size 406 bp)] gave products of the expected size. Figure 3 shows only the products from primers RSPEP10 and RSPEP5. These results indicate that the *RS1* gene is expressed in the Weri–Rb1 cell line.

Undifferentiated and differentiated Weri–Rb1 cells were investigated by immunoblotting with the RS24–37 antibody. Undifferentiated Weri–Rb1 cells were grown in suspension and differentiation was induced by coating culture dishes with poly-D-lysine and fibronectin to induce adhesion and adding di-butyryl cyclic AMP (DBcAMP) to the culture media. Differentiation was detected by a change in morphology of the cells. Antibody RS24–37 detected a specific band of ~28 kDa in both cell lysates and conditioned medium from differentiated and undifferentiated Weri–Rb1 cells (Fig. 3B) indicating that retinoschisin is secreted from these cells. A more intensely labelled band in the lanes loaded with proteins isolated from the differentiated cells showed that expression of retinoschisin appeared to be enhanced by cell differentiation (Fig. 3). The antibody detected a clean monomeric band in the Weri–Rb1 cells and the media which contrasts with the results from reduced retina in the same western blot showing additional bands of higher molecular weight and may indicate differences in oligomerization.

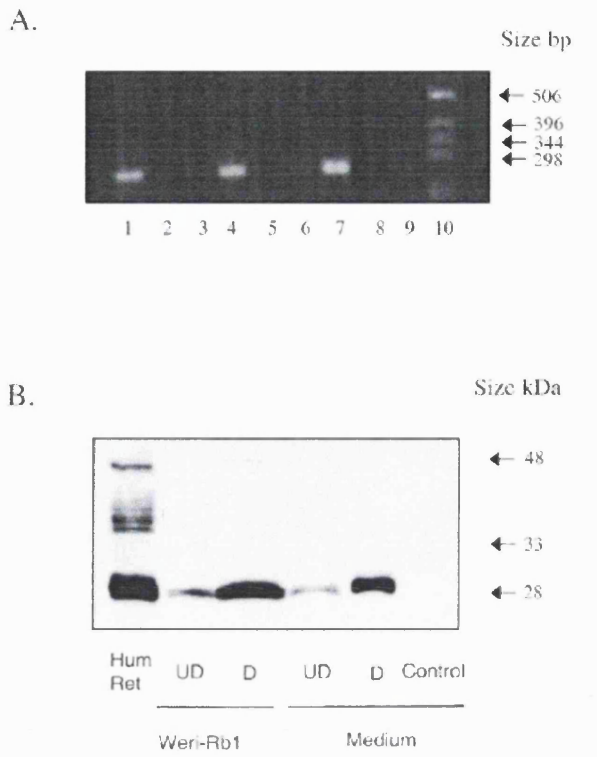

Figure 3. (**A**) RT–PCR of Weri–Rb1 cells using primers from *RS1* exons 2 and 4. Lanes 1–3, RT–PCR using oligo(dT) primers for the initial RT, Weri–Rb1 cells (lane1), water control (lane 2), Weri–Rb1 cells without RT 9 (lane 3); lanes 4–6, RT–PCR using random hexamer primers for RT, Weri–Rb1 cells (lane 4), water control (lane 5), Weri–Rb1 cells without RT (lane 6); lane 7, *RS1* cDNA; lane 8, genomic DNA; lane 9, water; lane 10, 1 kb ladder. Bands of the expected size (262 bp) were observed with Weri–Rb1 cells and the cDNA only, and not in any negative control, indicating that the cell line expresses the *RS1* gene. (**B**) Immunoblot containing proteins of theWeri–Rb1 cells reacted with RS24–37: results obtained with proteins of human retina (Hum Ret), Weri–Rb1 cells undifferentiated (UD) and differentiated (D), medium from Weri–Rb1 cells undifferentiated (UD) and differentiated (D), and unused medium used as control (control). RS24–37 recognizes a band of ~28 kDa in both undifferentiated and differentiated Weri–Rb1 cells and in medium from each. No band was observed in control medium. Thus, retinoschisin is present in both undifferentiated and differentiated Weri–Rb1 cells and is released from the cells into the medium.

DISCUSSION

The identification of the retinoschisis gene (12) enabled computer analysis of its sequence and of that of the predicted protein. These analyses suggested that retinoschisin could be a secreted globular protein. Moreover, they showed that its sequence contains: a putative signal peptide with an endopeptidase cleavage site; 10 cysteine residues which may form disulphide bridges (rare in intracellular proteins); and a discoidin domain which functions in the extracellular environment in other proteins (18). The disease-causing mutations described in the *RS1* gene are most commonly missense mutations and cluster within the discoidin domain residues (17) of retinoschisin, suggesting that this functional domain of the protein is responsible for interaction with other proteins.

The results of our studies confirm that the expression of the *RS1* gene is restricted to photoreceptors in human retinae. They also suggest that retinoschisin is produced by photoreceptors in adult retinae and that it is secreted by these cells. Thus, the intriguing result showing *RS1* expression within photoreceptors at some distance from the site of retinoschisis pathology can be explained by secretion of retinoschisin into these layers.

The role of retinoschisin within the inner retina has yet to be established. Proteins containing discoidin domains are thought to be involved with cell–cell interactions, and discoidin, in *Dictyostelium discoideum*, from which this class of proteins drives its name, is a lectin involved in cell aggregation (18,23,26). The discoidin domain is present in a variety of proteins but its interactions with ligands (either other protein domains or phospholipids) have not been fully elucidated. The discoidin domain receptors (DDR1 and DDR2), with extracellular discoidin domains and intracellular tyrosine kinase domains, are known to be activated by collagens, although the discoidin-binding domains within the collagen molecules are not yet defined (27,28). Blood coagulation factors V and VIII contain discoidin domains which are thought to interact with

phospholipids on the surface of platelets (29), and the secreted protein del1, which contains two discoidin domains, interacts with the αVβ3 integrin receptor (although this interaction is dependent on the RGD motif within an EGF repeat rather than the discoidin domain (30). Retinoschisin is a small protein consisting almost entirely of one discoidin domain (and no other recognized domains), and thus elucidating its interactions with cell surface receptors or the extracellular matrix may yield information applicable to the whole family of proteins about how this domain functions. The results we discuss here, which are consistent with secretion and interactions within the inner retina, are an important first stage of this work.

The pathological changes described in X-linked retinoschisis have previously been attributed to abnormalities in the Müller glial cell. The interaction of retinoschisin with a Müller cell receptor such as an integrin receptor would be in keeping with its discoidin domain and an abnormality in this interaction could account for all the recognized findings. Alternatively, the pathology could be occurring secondarily to architectural disruption within the inner retinal layers leading to abnormal Müller and bipolar cell function resulting in, for example, a reduced b-wave in the electroretinogram. This may be the case if retinoschisin interacts with components of the extracellular matrix and could explain the detection of the high molecular weight bands when immunoblotting retinal extracts but bands of the expected size of retinoschisin (in keeping with monomers) when investigating protein secreted by Weri–Rb1 cells. The high molecular weight bands detected in retinal extracts might represent protein complexes in which the other proteins originate from retinal cells distinct from photoreceptors (or Weri–Rb1 cells). Further investigation of these protein interactions may give insight into the processes leading to cell adhesion and architectural integrity within these retinal layers. Furthermore, investigation of mutant retinoschisin will determine firstly whether it is successfully secreted from photoreceptors and subsequently targeted appropriately within the retina, or secondly whether the different mutations interfere with crucial protein–protein interactions within the inner retinal layers by interfering with the structure of the discoidin domain.

In conclusion, retinoschisin, the protein causing X-linked retinoschisis, is the first example of a secreted protein leading to retinal dystrophy. Further evaluation of its function may give insight into the processes leading to cell adhesion and architectural integrity within the retina.

MATERIALS AND METHODS

In situ hybridization

Sections (8 μm) were cut from paraffin embedded mouse retina and mounted on glass slides. The sections were dewaxed with xylene (twice for 10 min at room temperature) and the following steps used for preparation of the sections. The sections were rehydrated for 2 min in each of seven ethanol solutions at decreasing concentrations (100 to 30%), washed with phosphate-buffered saline (PBS), fixed with 4% paraformaldehyde at room temperature for 20 min, treated for 10 min with 0.2 M HCl_2, rinsed in PBS, acetylated with 0.5% acetic anhydride (10 min at room temperature) rinsed with PBS, treated with proteinase K (50 μg/ml in PBS supplemented with 0.02 M $CaCl_2$ for 10 min at 37°C), washed in PBS and dehydrated for 2 min each in solutions of increasing ethanol concentration. The sections were then dried.

Sense and antisense probes were generated from a full-length *RS1* cDNA clone in Bluescript KS^+ (a generous gift of Dr B.H.F. Weber, Universität Würzburg, Germany). Plasmid DNA was linearized using either *Not*I or *Hin*dIII and digoxigenin-labelled riboprobes synthesized using T7 or T3 RNA polymerase (Boehringer Mannheim, Lewes, UK), respectively.

For hybridization, probes were diluted in hybridization buffer (2× SSC, 5% dextran, 0.2% Marvel, 50% deionized formamide) and denatured at 80°C for 2 min. Hybridization reactions were left overnight at 60°C and then washed in decreasing concentrations of 2× SSC at 60°C for 45 min, 1× SSC 50% formamide at 60°C for 45 min and two 10 min washes in 1× and 0.5× SSC, respectively, at room temperature. Signals were detected by firstly soaking in buffer 1 (100 mM Tris–HCl pH 7.5, 100 mM NaCl, 2 mM $MgCl_2$, 0.05% Triton X-100, 0.3% Tween), blocking in buffer 2 for 30 min [0.5–1% blocking reagent (Boehringer Mannheim)] then incubating with 400 μl of anti-digoxigenin alkaline phosphatase-conjugated antibody diluted to 1:500 in blocking buffer for 1 h. Sections were washed once in buffer 1 and soaked in buffer 3 for 5 min (100 mM Tris–HCl pH 9.5, 100 mM NaCl, 50 mM $MgCl_2$). Sections were incubated with colour change solution (4.5 μl of nitroblue tetrazolium salt, 3.5 μl of 3-bromo-3-indoyl-phosphate in 1 ml of buffer 3) in darkness until colour development and the slides mounted.

Antibody, SDS–PAGE and immunoblotting

Rabbit polyclonal antiserum was raised against peptide STEDEGEDPWYQKA (amino acid residues 24–37) conjugated to KLH (Genosys Biotechnologies, Pampisford, UK) and affinity-purified on the peptide (24), yielding antibody RS24–37. The Pierce (Rockford, IL) BCA kit was used to assay protein levels in tissue and cell samples to ensure even loading on gels. Protein samples were prepared by homogenization of tissues or cells in sample buffer (200 mM Tris–HCl, 5 mM EDTA, 1 M sucrose, 0.1% bromophenol blue) containing 4% SDS (with the addition of DTT to a final concentration of 10 mM for reduced samples), subjected to SDS–PAGE on 15% gels and electroblotted on to ECL nitrocellulose (Amersham, Little Chalfont, UK). Following blocking in 6% Marvel/1× PBS/0.1% Tween 20 (blocking buffer) for 1 h at room temperature blots were hybridized overnight with the affinity-purified primary antibody RS24–37 (1:1000 dilution) at 4°C. Subsequently, anti-rabbit polyclonal secondary antibody conjugated to peroxidase (Amersham) was used at 1:3000 for 2 h at room temperature. Bands were visualized using enhanced chemiluminescence (Amersham). When pre-adsorbed RS24–37 was used as a probe, 1 μg/ml of the peptide used to generate the antibody was incubated with RS24–37 at 1:750 dilution for 4 h on ice in blocking buffer. These blots were then reacted with anti-actin antibody (Sigma, Poole, UK) at a dilution of 1:2000.

Immunohistochemistry

After deep anaesthetic, mice were perfused with lactated Ringer's (20–50 ml) and fixative (4% paraformaldehyde in 0.066 M PBS at pH 7.4, 100 ml). After dissection, retinae were

further fixed in fixative, cryoprotected in 30% sucrose–PBS (pH 7.4, 4°C), frozen on dry ice and stored at –80°C. Paraffin embedded human retina sections were gifts of Prof. Philip Luthert (Institute of Ophthalmology, London, UK). Cryostat mouse retina sections (10 μm) were mounted on glass slides, permeabilized with cold methanol (–80°C, 3 min), blocked with 2% fish gelatin (1 h, room temperature), incubated with RS24–37 in 2% fish gelatin (1:1000, 4°C, overnight), and finally with biotin-conjugated goat anti-rabbit IgG in 2% fish gelatin (1:200, 25°C, 1 h). The immunoreaction was visualized with the biotin–avidin–peroxidase (Vector Laboratories, Burlingame, CA) and 3′,3′-diaminobenzidine (DAB, 1 mg/ml; H_2O_2, 0.03%) (Sigma). The human retina sections were deparaffined successively with xylene, 100% ethanol and 95% ethanol before proceeding with the immunohistochemistry. Control (omitting the primary antiserum) was included included in each experiment. To verify the specificity of the immunostaining, retina sections were also stained with preimmune serum and RS24–37 pre-absorbed with the peptide epitope (25 μg/μl).

RT–PCR

RNA was extracted from undifferentiated cells using the RNeasy kit from Qiagen (Crawley, UK), following the manufacturer's instructions. RT–PCR was performed using SuperScript Preamplification System (Gibco BRL, Paisley, UK) to obtain the first strand cDNA with either random hexamer primers or oligo(dT) primers as per the manufacturer's protocol. PCR was performed using exonic primers RSPEP10 (TTTTGAATTCCATATGTCTACCGAGGATGAAGGC) and RSPEP5 (TTTTGTCGACCTCGAGTCAGTTTGCAGTCCACGA) from exons 2 and 4, respectively (product size 262 bp), and primers RSPEP3 (TTTTGGATCCCATATGGCCCGGCTCAACAGTCAA) and RSPEP6 (TTTTGTCGACCTCGAGTCCGGCACAGTTGC) from exons 4 and 6, respectively. The following conditions were used: 94°C for 5 min, then 40 cycles at 94°C for 30 s, 55°C for 30 s, 72°C for 1 min and a final extension of 72°C for 10 min.

Retinoblastoma cell culture

Weri–Rb1 human retinoblastoma cells (31) were obtained from the American Type Tissue Culture Collection (Manassas, VA). Cells were maintained in suspension culture in RPMI 1640 (Gibco BRL) supplemented with 10% fetal bovine serum, 2 mM L-glutamine, 100 U penicillin/ml and 100 μg streptomycin/ml (Sigma), with medium changes every 2–3 days. For analysis by western blotting, cells were transferred to 30 mm six-well dishes for attachment and differentiation. The dishes were treated with 0.2 mg/ml poly-D-lysine (Sigma) for 30 min at room temperature and rinsed with distilled water before 5 μg/ml fibronectin (Sigma) was added for 1 h at room temperature. After this time the excess fibronectin was removed and the cells were seeded directly on to the adhesive surface at a density of 1×10^5 cells/well. Cells were grown as monolayer cultures for 7 days before the addition of DBcAMP (Sigma) at a final concentration of 2 mM. DBcAMP was readministered every 2–3 days with the medium changes. A sample of the medium in which the cells had grown was taken at these times. Differentiation was assessed by the change in morphology of the cells (25). After 9 days of treatment the cells were gently scraped off the bottom of the wells and prepared for western blot analysis or determination of protein concentration.

ACKNOWLEDGEMENTS

We are very grateful to Prof. P. Luthert (Institute of Ophthalmology, UK) for providing human retina samples and to Dr Bernard H.F. Weber (Universität Würzburg, Germany) for providing the *RS1* cDNA. We are grateful for financial support from the Wellcome Trust (D.T. and C.G.), the Foundation Fighting Blindness and National Institutes of Health grant EY08285 (D.B.F. and S.N.M.R.), the Muscular Dystrophy Campaign (J.A.E.) and the Medical Research Council, UK (A.R. and J.C.S.). D.T. was a Wellcome Clinician Scientist Fellow and D.B.F. is the recipient of a Research to Prevent Blindness Senior Investigator's Award.

REFERENCES

1. Forsius, H., Krause, U., Helve, J., Voupala, V., Mustonen, E., Vainio-Mattila, B. and Fellman, J. (1973) Visual acuity in 183 cases of X-chromosomal retinoschisis. *Can. J. Ophthalmol.*, **8**, 385–393.
2. Condon, G.P., Brownstein, S., Wang, N.S., Kearns, J.A. and Ewing, C.C. (1986) Congenital hereditary (juvenile X-linked) retinoschisis. Histopathologic and ultrastructural findings in three eyes. *Arch. Ophthalmol.*, **104**, 576–583.
3. George, N.D., Yates, J.R. and Moore, A.T. (1995) X-liked retinoschisis. *Br. J. Ophthalmol.*, **79**, 697–702.
4. George, N.D., Yates, J.R., Bradshaw, K. and Moore, A.T. (1995) Infantile presentation of X linked retinoschisis. *Br. J. Ophthalmol.*, **79**, 653–657.
5. George, N.D., Yates, J.R., Bradshaw, K. and Moore, A.T. (1996) Clinical features in affected males with X-linked retinoschisis. *Arch. Ophthalmol.*, **114**, 274–280.
6. Kraushar, M.F., Stepens, C.L., Kaplan, J.A. and Freeman, H.M. (1972) Congenital retinoschisis. In Bellows, J.G. (ed.), *Contemporary Ophthalmology Honoring Sir Stewart Duke-Elder*. Williams and Wilkins, Baltimore, MD, pp. 265–290.
7. Tanino, T., Katsumi, O. and Hirose, T. (1985) Electrophysiological similarities between two eyes with X-linked recessive retinoschisis. *Doc. Ophthalmol.*, **60**, 149–161.
8. Peachey, N.S., Fishman, G.A., Derlacki, D.J. and Brigell, M.G. (1987) Psychophysical and electroretinographic findings in X-linked juvenile retinoschisis. *Arch. Ophthalmol.*, **105**, 513–516.
9. de Jong, P.T., Zrenner, E., van Meel, G.J., Keunen, J.E. and van Norren, D. (1991) Mizuo phenomenon in X-linked retinoschisis. Pathogenesis of the Mizuo phenomenon. *Arch. Ophthalmol.*, **109**, 1104–1108.
10. Manschot, W.A. (1972) Pathology of hereditary juvenile retinoschisis. *Arch. Ophthalmol.*, **88**, 131–137.
11. Kirsch, L.S., Brownstein, S. and de Wolff-Rouendaal, D. (1996) A histopathological, ultrastructural and immunohistochemical study of congenital hereditary retinoschisis. *Can. J. Ophthalmol.*, **31**, 301–310.
12. Sauer, C.G., Gehrig, A., Warneke-Wittstock, R., Marquardt, A., Ewing, C.C., Gibson, A., Lorenz, B., Jurklies, B. and Weber, B.H. (1997) Positional cloning of the gene associated with X-linked juvenile retinoschisis. *Nature Genet.*, **17**, 164–170.
13. van de Vosse, E., Walpole, S.M., Nicolaou, A., van der Bent, P., Cahn, A., Vaudin, M., Ross, M.T., Durham, J., Pavitt, R., Wilkinson, J. *et al.* (1998) Characterisation of SCML1, a new gene in Xp22, with homology to developmental polycomb genes. *Genomics*, **49**, 96–102.
14. Walpole, S.M., Hiriyana, K.T., Nicolaou, A., Bingham, E.L., Durham, J., Vaudin, M., Ross, M.T., Yates, J.R.W., Seiving, P.A. and Trump, D. (1999) Identification and characterisation of the human homologue (*RAI2*) of a mouse retinoic acid-induced gene in Xp22. *Genomics*, **55**, 275–283.
15. Montini, E., Andolfi, G., Caruso, A., Buchner, G., Walpole, S.M., Mariani, M., Consalez, G., Trump, D., Ballabio, A. and Franco, B. (1998) Identification and characterisation of a novel serine-threonine kinase gene from the Xp22 region. *Genomics*, **51**, 427–433.

16. Reid, S.N., Akhmedov, N.B., Piriev, N.I., Kozak, C.A., Danciger, M. and Farber, D.B. (1999) The mouse X-linked juvenile retinoschisis cDNA: expression in photoreceptors. *Gene*, **227**, 257–266.
17. The Retinoschisis Consortium (1998) Functional implications of the spectrum of mutations found in 234 cases with X-linked juvenile retinoschisis (XLRS). *Hum. Mol. Genet.*, **7**, 1185–1192.
18. Baumgartner, S., Hofmann, K., Chiquet-Ehrismann, R. and Bucher, P. (1998) The discoidin family revisited: new members from prokaryotes and a homology based fold prediction. *Protein Sci.*, **7**, 1626–1631.
19. He, X. and Tessier-Lavigne, M. (1997) Neuropilin is a receptor for the axonal chemorepellent Semaphorin III. *Cell*, **90**, 739–751.
20. Bellen, H.J., Lu, R., Beckstead, R. and Bhat, M.A. (1998) Neurexin IV, caspr and paranodin—novel members of the neurexin family: encounters of axons and glia. *Trends Neurosci.*, **21**, 444–449.
21. Ensslin, M., Vogel, T., Calvete, J.J., Thole, H.H., Schmidtke, J., Matsuda, T. and Topfer-Peterson, E. (1998) Molecular cloning and characterisation of P47, a novel boar sperm-associated zona-pellucida-binding protein homologous to a family of mammalian secretory proteins. *Biol. Reprod.*, **52**, 1057–1064.
22. Hidai, C., Zupancic, T., Penta, K., Mikhail, A., Kawana, M., Quertermous, E.E., Aoka, Y., Fukagawa, M., Matsui, Y., Platika, D. *et al.* (1998) Cloning and characterisation of developmental endothelial locus-1: an embryonic endothelial cell protein that binds the anb3 integrin receptor. *Genes Dev.*, **12**, 21–33.
23. Vogel, W. (1999) Discoidin domain receptors: structural relations and functional implications. *FASEB J.*, **13**, S77–S82.
24. Luzio, J.P., Ellis, J.A., Thomas, S. and Banting, G. (1995) Antibody screening of bacterial expression systems. In Hames, B.D. and Higgins, S.J. (eds), *Gene Probes: A Practical Approach*. IRL Press, Oxford, UK, pp. 77–101.
25. Seigel, G.M. (1999) The golden age of retinal cell culture. *Mol. Vis.*, **5**, 4.
26. Springer, W.R., Cooper, D.N. and Barondes, S.H. (1984) Discoidin I is implicated in cell-substratum attachment and ordered cell migration of *Dictyostelium discoideum* and resembles fibronectin. *Cell*, **39**, 557–564.
27. Foehr, E.D., Tatavos, A., Tanabe, E., Raffioni, S., Goetz, S., Dimarco, E., De Luca, M. and Bradshaw, R.A. (2000) Discoidin domain receptor 1 (DDR1) signaling in PC12 cells: activation of juxtamembrane domains in PDGFR/DDR/TrkA chimeric receptors. *FASEB J.*, **14**, 973–981.
28. Vogel, W., Brakebusch, C., Fssler, R., Alves, F., Ruggiero, F. and Pawson, T. (2000) Discoidin domain receptor 1 is activated independently of β_1 integrin. *J. Biol. Chem.*, **275**, 5779–5784.
29. Kane, W.H. and Davie, E.W. (1988) Blood coagulation factors V and VIII: structural and functional similarities and their relationship to hemorrhagic and thrombotic disorders. *Blood*, **71**, 539–551.
30. Penta, K., Varner, J.A., Liaw, L., Hidai, C., Schatzman, R. and Quertermous, T. (1999) Del1 induces integrin signalling and angiogenesis by ligation of $\alpha V\beta 3$. *J. Biol. Chem.*, **274**, 11101–11109.
31. McFall, R.C., Sery, T.W. and Makadon, M. (1977) Characterisation of a new continuous cell line derived froma human retinoblastoma. *Cancer Res.*, **37**, 1003–1010.

Human Molecular Genetics, 2001, Vol. 10, No. 15 1571–1579

Temporal and spatial expression patterns of the *CRX* transcription factor and its downstream targets. Critical differences during human and mouse eye development.

Lindsay C. Bibb, James K.L. Holt[1], Emma E. Tarttelin, Matthew D. Hodges, Kevin Gregory-Evans[2], Adam Rutherford[1], Robert J. Lucas[3], Jane C. Sowden[1] and Cheryl Y. Gregory-Evans*

Section of Cell and Molecular Biology, Imperial College School of Medicine, Sir Alexander Fleming Building, Exhibition Road, London SW7 2AZ, UK, [1]Developmental Biology Unit, Institute of Child Health, University College London, 30 Guilford Street, London WC1N 1EH, UK, [2]Department of Ophthalmology, The Western Eye Hospital, Marylebone Road, London NW6 5YE, UK and [3]Department of Integrative and Molecular Neuroscience, Imperial College School of Medicine, St Dunstan's Road, London W6 8RF, UK

Received April 11, 2001; Revised and Accepted June 1, 2001

Cone–rod homeobox (*CRX*), a paired-like homeobox transcription factor, plays a major role in photoreceptor development and maintenance of the retina. Fifteen different mutations in the *CRX* gene have been identified as a cause of blinding retinal dystrophy. As a step towards characterizing the underlying pathophysiology of disease, temporal and spatial gene expression patterns during human and mouse eye development were investigated for *CRX* and for downstream retinally expressed genes, postulated to be transactivated by CRX. We found that human *CRX* was expressed at 10.5 weeks post-conception (p.c.). This was significantly later than observed in mouse development. Immunocytochemistry in human retina showed that CRX protein was not detected until >4 weeks later at 15 weeks p.c., implying that it would be unable to transactivate *PDEB*, *IRBP* and arrestin, which were all expressed before 15 weeks. These data therefore eliminate CRX as the major transcriptional activator of these three genes from a wide group of retinal genes that can be transactivated by CRX *in vitro*. Additionally, *PDEB* was expressed 2 weeks before *CRX* whereas murine *Pdeb* was expressed after *Crx*, highlighting a potential difference for the role of *PDEB* in human eye development. Previous data had shown *CRX* expression in the adult human retina to be photoreceptor-specific; however, we demonstrate that this gene is also expressed in the inner nuclear layer (INL) of the human and mouse retina by *in situ* hybridization and immunocytochemistry. INL localization of murine *Crx* was confirmed in *rd/rd,cl* mice, as in this mouse model the photoreceptors are absent. We have found important differences in the temporal expression of this gene in human and mouse retina, although spatial expression of the *CRX* gene appears to be conserved. In addition, downstream targets of *CRX in vitro* might not represent *in vivo* function during development. These data support concerns about the extent to which we can extrapolate from rodent models regarding embryonic development and disease pathophysiology.

INTRODUCTION

The process of retinal development involves a hierarchy of transcription factors regulating increasingly complex programmes of gene expression and cell fate determination (1,2). One such transcription factor is the cone–rod homeobox (*CRX*) gene (3–5). *CRX* is a member of the *OTX*-like homeobox gene family, a group of transcription factors that encode paired-like (*prd*) homeodomain proteins. The OTX proteins are involved in the regulation of anterior head structure and sensory organ development (6). Localized to human chromosome 19q13.3, mutations in the *CRX* gene have been found to cause autosomal dominant cone-rod dystrophy (4,7–9) and autosomal recessive Leber congenital amaurosis (8,10–12). Both these diseases are clinically and genetically heterogeneous. Cone-rod dystrophy is a severe form of retinal dystrophy, which often begins in the second decade of life and is untreatable and incurable (13). Leber congenital amaurosis is characterized by total blindness at birth or shortly thereafter (14), with no detectable electroretinogram (derived from photoreceptor cells).

The CRX protein binds to a conserved site or CRX-binding element (CBE 1), C/TTAATC/T, which is present in the upstream region of many photoreceptor-specific genes such as rhodopsin, arrestin and interphotoreceptor retinoid-binding protein (IRBP) (3,5). Recently, a second and weaker CBE-like motif has been identified, giving an 11-base motif in a head-to-tail

*To whom correspondence should be addressed. Tel: +44 20 7594 3007; Fax: +44 20 7594 3015; Email: c.gregory-evans@ic.ac.uk

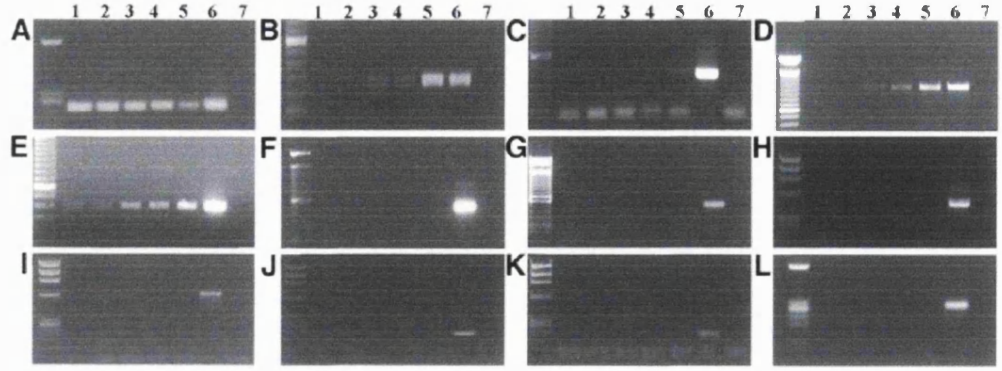

Figure 1. RT–PCR analysis during early human eye development. Lanes 1–5 are cDNA samples from 8.5, 9.5, 10.5, 11.0, and 13.5 weeks p.c., respectively. Lane 6 is adult cDNA and lane 7 is a negative control. The retinally expressed genes tested by RT–PCR were (**A**) *SIX3*, (**B**) *CRX*, (**C**) arrestin, (**D**) *IRBP*, (**E**) *PDEB*, (**F**) rhodopsin, (**G**) *RS1*, (**H**) *PDEA*, (**I**) *PDEG*, (**J**) red/green cone opsin, (**K**) blue cone opsin and (**L**) *NRL*. The DNA marker for (A) and (H–L) is ϕX174 (Gibco) and for (B–G) is 100 bp ladder (Gibco).

arrangement with CBE1 (C/TTAATC/TG/AGA/CTT/C). This motif has been identified in the upstream regions of retinally expressed genes, which are down-regulated in the absence of *Crx* in mouse retina (15,16). *In vitro*, CRX is capable of transactivating retinal gene reporter-constructs carrying the C/TTAATC/T binding site (3,5); however, transactivation by CRX *in vivo* remains to be confirmed.

The CRX transcription factor has been shown to be critical for the differentiation of photoreceptors during retinal development and also the maintenance of these structures in adult tissue (3). Over-expression of retroviral *Crx* in developing retinal cells results in a marked increase in rod photoreceptors and an almost complete absence of amacrine interneurons (3), highlighting the importance of this transcription factor in morphogenesis and the determination of cell function. Targeted disruption of murine *Crx* results in the failure of photoreceptor outer segment (OS) growth and thus the absence of phototransduction (16). Characterization of gene expression in the *Crx* null mouse has indicated that a number of photoreceptor genes are down-regulated in the absence of *Crx* (16), and the majority of these genes are crucial either to phototransduction or to the structural formation of the photoreceptor cells.

Studying the temporal and spatial expression of developmental genes can be used for dissecting biological development and disease pathophysiology (17). To date in adult tissues, *CRX* expression has been shown to be specific to the photoreceptor cell layer of the retina (3–5) and the pinealocytes of the brain (5). In the developing murine retina, *Crx* expression, as detected by *in situ* hybridization, is observed at embryonic day (E)12.5, coinciding with cone photoreceptor cell genesis (3). At postnatal day 6 (P6), peak expression is seen in correlation with the increase in photoreceptor cells expressing rhodopsin and other phototransduction genes. The expression pattern of *CRX* during human development has not been reported, and the data on expression of some of the retinal genes that CRX is believed to regulate is limited. In the present study, RT–PCR and *in situ* hybridization analysis were carried out to evaluate temporal and spatial gene expression during human retinal development, and immunocytochemistry was undertaken to confirm protein expression. Much of what is reported about this gene's function is based on mouse studies. Comparative gene expression patterns in the retina were therefore investigated to highlight any potential human/mouse differences in the expression of this and related genes during development.

RESULTS

RT–PCR analysis of *CRX* expression in the human and mouse developing eye

To identify the point during human eye development at which *CRX* is expressed, RT–PCR analysis was carried out on total RNA extracted from human fetal and adult eyes. Initially, the *sine oculis* homeobox gene 3 (*SIX3/Six3*) was amplified from both human and mouse cDNA as a positive control. *SIX3* is expressed in the developing human eye as early as 5–7 weeks gestation and expression is also maintained in mature ocular tissue (18). In the mouse, *Six3* expression is seen in the optic vesicles at E9.5 and by E11.5 expression is observed in the neural retina (19). *SIX3/Six3* was present in all ages tested of both human (Fig. 1A) and mouse cDNA (Fig. 2A), confirming RNA integrity of all samples. Exonic primers were designed to span intron 1 of the *CRX* gene, to avoid the possibility of amplifying from contaminating genomic DNA. Amplification of the *CRX* gene produced positive results from 10.5, 11.0 and 13.5 weeks post-conception (p.c.) and from the adult control (Fig. 1B). It was not possible to amplify *CRX* from either of the two younger fetal samples (8.5 and 9.5 weeks p.c.) and therefore the onset of *CRX* expression must occur between 9.5 and 10.5 weeks of development. Gene expression is presumably maintained from 10.5 weeks to adult, as shown with *CRX* expression studies in the mouse (3). An identical procedure was used to amplify *Crx* from embryonic mouse eyes. Expression was seen first at E10.5 and this expression was maintained in all cDNAs tested, both embryonic and postnatal (Fig. 2B).

Retinal-specific gene expression

A number of retinal-specific genes containing *CRX* binding sites in their promoter were also analysed by RT–PCR to

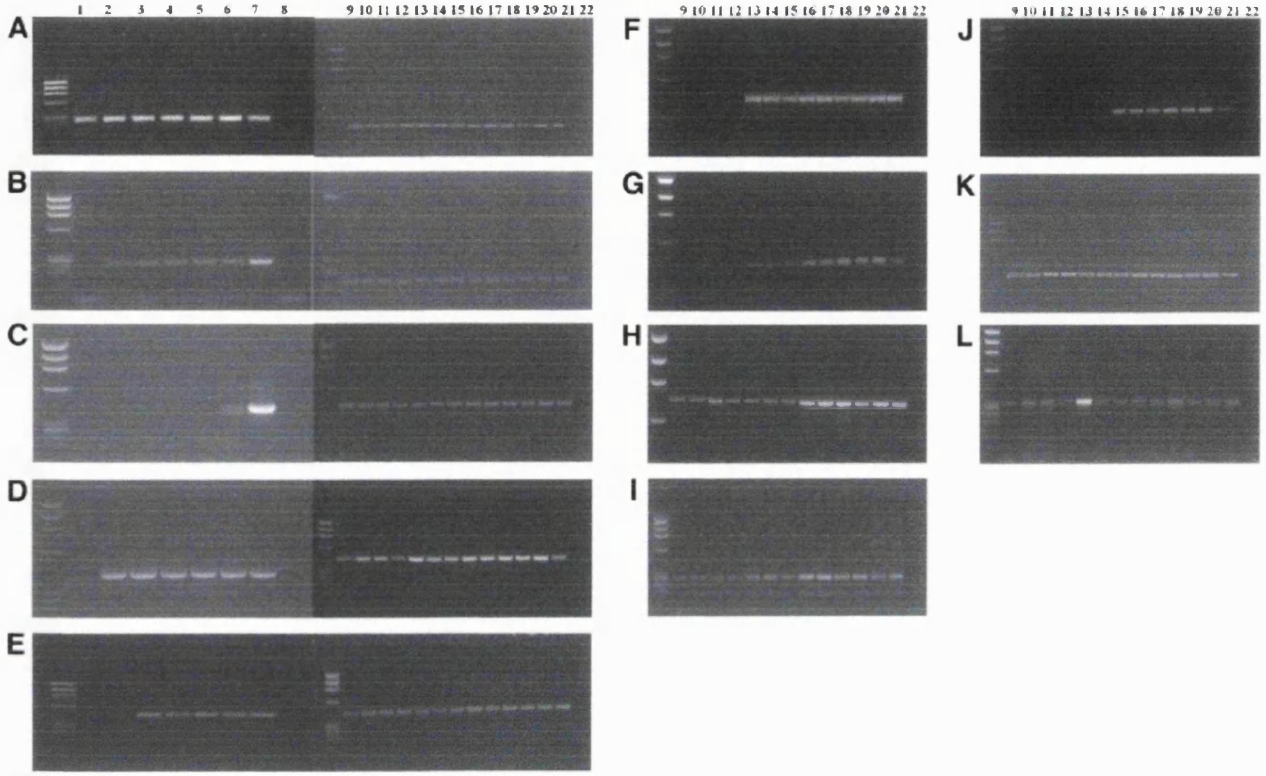

Figure 2. RT–PCR analysis during mouse eye development. Lanes 1–6 are cDNA samples from E9.5, E10.5, E11.5, E12.5, E13.5 and E14.5, respectively. Lane 7 is adult cDNA and lane 8 is a negative control. Lanes 9–20 are cDNA samples from P1–P12, respectively. Lane 21 is adult cDNA and lane 22 is a negative control. The genes tested by RT–PCR were (**A**) *Six3*, (**B**) *Crx*, (**C**) arrestin, (**D**) *Irbp*, (**E**) *Pdeb*, (**F**) rhodopsin, (**G**) *Rs1*, (**H**) *Pdea*, (**I**) *Pdeg*, (**J**) green opsin, (**K**) blue opsin and (**L**) *Nrl*. The DNA marker used was ϕX174 (Gibco).

determine their onset of expression relative to that of *CRX*. If *CRX* was expressed before these genes, it is possible that *CRX* could transactivate them *in vivo*. Arrestin was expressed at 13.5 weeks p.c. in the human eye (Fig. 1C) and at E14.5 in the mouse eye (Fig. 2C), although a low level of expression was observed. Human *IRBP* is expressed at the same time as *CRX* (10.5 weeks), therefore CRX could potentially transactivate *IRBP in vivo* (Fig. 1D). *Irbp* in mouse was detected at E10.5, the same time as *Crx* is first expressed (Fig. 2D), thus showing conserved temporal expression of *IRBP/Irbp* and *CRX/Crx* between man and mouse. A striking result was obtained for *PDEB* in the human retina, where it was expressed from an early stage (8.5 weeks p.c.) of development (Fig. 1E) preceding *CRX* expression by 2 weeks, whereas expression of *Pdeb* in the murine retina begins at E11.5 (Fig. 2E), after *Crx* gene expression was first detected. Hence, comparative temporal expression of *PDEB/Pdeb* and *CRX/Crx* is not conserved between species.

Rhodopsin expression was absent from all human fetal cDNAs, but was observed in the adult retinal control cDNA (Fig. 1F). In the mouse, rhodopsin expression was only observed postnatally, from P5 onwards, corresponding with rod photoreceptor OS development (Fig. 2F). In other species such as rat (20) and in human fetal retina (21) opsins have been detected before birth by immunocytochemical studies. Other studies in rats report later onset of expression (22). These differences may be due in part to detecting cell-specific expression, rather than a more global RT–PCR approach. We have tested our 13.5 and 15 week retinal sections for rhodopsin expression by *in situ* hybridization and found no expression (data not shown). Retinoschisin (*RS1*) was not expressed in any of the human fetal ages tested and neither were the α- and γ-subunits of phosphodiesterase (*PDEA/PDEG*), nor green or blue cone opsin (Fig. 1G–K). Comparable results were observed with mouse samples, with each gene having a specific time-of-onset during postnatal retinal maturation (Fig. 2G–K). Expression of *NRL* was not seen at any of the developmental stages tested in human fetal retina (Fig. 1L) and in mouse it was first observed at P1 (Fig. 2L).

In situ analysis of *CRX* expression in human fetal and adult retina

The expression of *CRX* was further investigated in the developing human retina by *in situ* hybridization analysis. Retinal sections of 10 and 12 weeks of development were tested, since the RT–PCR data had shown *CRX* expression at these times. However, we were unable to detect expression of *CRX*, indicating that it is likely that the *in situ* analysis was not sensitive enough to detect *CRX* expression at low levels. At 13 weeks p.c., *CRX* expression was observed in the neural retina adjacent to the retinal pigment epithelium (RPE), where newly born

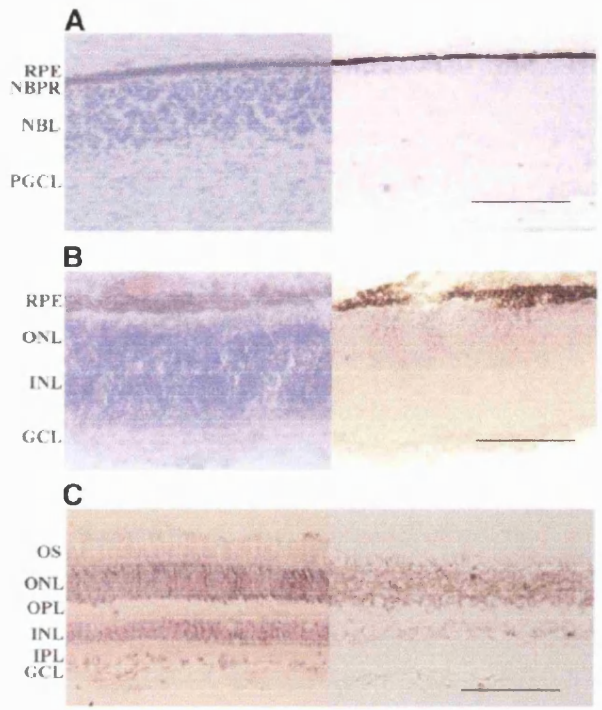

Figure 3. *In situ* hybridization analysis of *CRX* expression in human fetal and adult retina. Left panels are haematoxylin and eosin (H&E) stained sections adjacent to corresponding *in situ* in right panels. (**A**) In human fetal retina at 13 weeks p.c., staining is observed in newly born photoreceptors (NBPR), lying just vitreal to the RPE. NBL, neuroblastic layer; PGCL, presumptive ganglion cell layer. (**B**) In human fetal retina at 15 weeks p.c., expression is seen throughout the developing ONL, and is absent from the developing INL. (**C**) In adult human retina, *CRX* is localized to both ONL and INL. Scale bars, 100 µm.

photoreceptors are present (Fig. 3A). At 15 weeks p.c., *CRX* expression was much stronger and was localized specifically to the developing outer nuclear layer (ONL) of the retina (Fig. 3B), consistent with the *in situ* expression pattern in mouse embryonic retina (3). In adult tissue *CRX* is expressed in the ONL of the retina, which contains the nuclei of the rod and cone cells (Fig. 3C). However, expression was not limited to the ONL of the adult retina, as staining was also detected within the inner nuclear layer (INL) of the retina. Whereas the staining in the ONL was strong and diffuse, presumably in both the rod and cone nuclei, staining in the INL was weaker and punctate, suggesting that *CRX* expression in the INL may be localized to a particular subset of retinal cells.

CRX immunocytochemistry in human retina

We generated an N-terminal peptide antibody, which detected a specific 37 kDa band by western blotting of total mouse retinal extract (Fig. 4A). The specificity of detection was confirmed by western blotting with pre-immune serum (which did not detect this band) and pre-incubation of the antibody with the peptide used to generate it (this removed the ability of the antibody to detect the band; data not shown). Using this antibody we first saw immunochemical localization of CRX protein in the fetal retina at 15 weeks p.c., where strong staining was present in the photoreceptor cells adjacent to the RPE (Fig. 4B). Weak staining of the ganglion cell layer (GCL) was also noted at 15 weeks p.c. Similar GCL staining was present in controls without primary antibody, suggesting non-specific staining by the secondary antibody. No staining of the GCL was detected by *in situ* hybridization (Fig. 3B) in the same age embryos. Using the same conditions for immunohistochemistry, we did not detect protein at 13 weeks p.c. (Fig. 4C). Thus, CRX protein was only detected 2 weeks after we could detect *CRX* mRNA by *in situ* hybridization (at 13 weeks p.c.). This apparent interval between mRNA expression and protein localization may, however, reflect a difference in threshold of sensitivity of *in situ* hybridization compared with the immunocytochemistry technique.

Crx gene and protein expression in rodless coneless (*rd/rd,cl*) retina

To corroborate *CRX* expression in the INL of human retina, we took advantage of the *rd/rd,cl* mouse, where the ONL of the retina degenerates completely by P80 due to a lesion of rods (*rd/rd*) and a transgenic ablation (*cl*) of cone photoreceptors (23). *Crx* was amplified from *rd/rd,cl* retinal cDNA and also from wild-type mouse retinal cDNA isolated at P80. *Crx* RT–PCR products were observed in both samples, confirming that *Crx* expression is not confined to the ONL of the retina (Fig. 5A). It was not possible to amplify rhodopsin, green or blue cone opsin from the *rd/rd,cl* mice (Fig. 5B), inferring that the RT-PCR products were not due to any remaining rod and cone photoreceptor nuclei.

To confirm that *Crx* expression in *rd/rd,cl* mice was localized to the INL, *in situ* hybridization was performed on eyes taken from adult *rd/rd,cl* mice, which were then compared with wild-type eyes. The spatial expression of *Crx* in wild-type eyes reflected that of the human adult retina, as staining was observed in both the ONL and INL of the retina (Fig. 6A). It was evident that INL *Crx* staining was noticeably weaker than that of the ONL, consistent with the human data (compare Fig. 6A with Fig. 3C). Expression was also observed in the INL of the *rd/rd,cl* mice (Fig. 6B), confirming the RT–PCR data. By immunocytochemistry, Crx protein was localized to both the ONL and INL in wild-type adult mouse retina (Fig. 6C). In the *rd/rd,cl* mouse retina, Crx protein was localized to the INL (Fig. 6D). Interestingly, by both *in situ* hybridization and immunocytochemistry, the INL staining of the *rd/rd,cl* retina was stronger than previously observed in either the INL of the adult human sections or the wild-type mouse. This suggests that either the ONL acts as a competitor for the *Crx* probe during hybridization or, alternatively, that *Crx* expression is up-regulated in mice lacking rod and cone photoreceptors. To investigate this possibility, sections of *rd/rd,cl* eyes were taken before (P9) and after (P13) retinal degeneration had started. By immunocytochemistry we were unable to detect up-regulation of Crx protein, with similar levels of Crx detected at each time point examined (data not shown).

DISCUSSION

Between 8 and 20 weeks of fetal development, the human retina progresses from a basic two-layered structure comprising the inner and outer neuroblastic layers to a highly differentiated and multicellular structure (24,25). During this

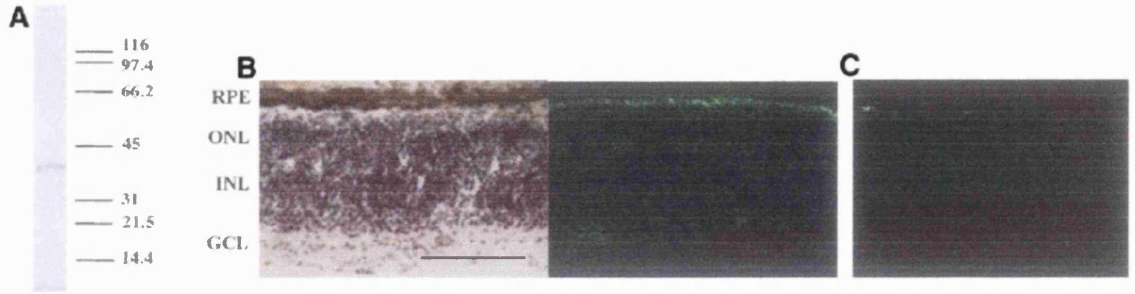

Figure 4. Immunocytochemical localization of CRX in fetal human retina. (**A**) Western blot of N-terminal peptide antibody showing a single band at 37 kDa. (**B**) Left panel, H&E staining; right panel, antibody localization at 15 weeks p.c. Green fluorescence present in newly formed photoreceptors. (**C**) No antibody detected at 13 weeks p.c. Scale bars, 100 μm.

time the cells destined to become photoreceptors begin to develop in the outer neural layer of the retina. Cone nuclei are born earlier than those of rod photoreceptors, first appearing at ~10 weeks of development during formation of the fovea (21). Rod nuclei, however, are born a little later than this and are subsequently not present until ~12 weeks of development (24,25). Our own observations show that *CRX* is not expressed until 10.5 weeks in the human retina. Therefore, it is likely that the first cells to express *CRX* in the developing human retina are the newly born cone photoreceptor nuclei. Continued *CRX* expression in the outer retina coincides with cone and rod specification and structural maturation of the photoreceptors. It is important to note that the onset of expression occurs later in human development than it does in the mouse. In the mouse retina we detected *Crx* expression at E10.5. This equates to ~30 days (~4 weeks) in human development based on Carnegie comparisons, highlighting a difference in temporal *CRX* expression between species. At birth the photoreceptors are fully differentiated in the human retina. In mouse retina, however, rod maturation is not complete until ~P16 (26). The role of *CRX* in the timing of differentiation is therefore different in mouse than human, suggesting that other factors/cues are involved.

The early expression of *PDEB* was unexpected and suggests that transactivation of *PDEB* occurs independently of *CRX*. Furthermore, presence of a *CRX* binding site in the promoter region of a gene, as is the case for *PDEB*, should not be regarded as evidence that CRX transactivates the gene *in vivo*, even though it is possible to drive expression of a *PDEB* reporter construct with CRX (5). Previous work on *PDEB* has indicated the presence of a conserved AP-1 element in both the human and the mouse proximal 5′ regions of the gene (27). Additionally, mutation of the *CRX* binding site in the *PDEB* promoter had no effect on transcription of a reporter gene, suggesting that *CRX* is not important in transactivation of *PDEB* (27). The reason for such an early expression of *PDEB* is unclear, although this observation suggests that the *PDEB* may have a role during the development of the human retina that is alternative to its role in phototransduction in mature retina. The early expression of *Pdeb* is not mirrored within mouse retinal development, where it occurs after Crx gene expression. This highlights a potential difference for the role of *PDEB/Pdeb* between these two species.

The expression pattern of *NRL* was included in this study, as previous work has suggested that *CRX* and *NRL* work synergistically in the activation of a number of retinal targets (5). Expression of *NRL* was not detected in any of the fetal tissues we tested. Therefore, if CRX is responsible for activation of retinal genes expressed at 13.5 weeks or earlier, such as *IRBP* and arrestin, then it must do so independently of NRL. Very recent data have shown that *Nrl* null mice completely lack rod photoreceptors and imply that Nrl plays an important role in directing gene expression in rod photoreceptors (28). *Nrl* expression has been detected slightly earlier than in our study at E18.5 in mice, in line with our view that Crx is acting independently of Nrl early in development. Another anomaly we found with *Nrl* expression was that in mouse, *Nrl* was expressed much later (P1) than *Pdeb* (E12). However, in rat retina it has been shown by northern blotting that *Nrl* expression precedes *Pdeb* by two postnatal days (22). Thus, even between species of the rodent lineage there seem to be differences in temporal gene expression.

Although, *IRBP* has a CRX binding site in its promoter, it seems unlikely that *IRBP* is itself regulated by *CRX in vivo* since it is not down-regulated in the absence of *Crx* in the null mouse (16). Furthermore, it has been shown recently that *OTX2* binds specifically to the *IRBP* promoter in yeast one-hybrid studies, whereas *CRX* was not identified (29). Thus, *IRBP* is another example of a gene containing a *CRX* binding site in its promoter, which can be transactivated by CRX *in vitro*; however, other studies show that *CRX* is unlikely to be the main transcription factor involved in *IRBP* gene expression.

Whether CRX can function as a transcriptional activator *in vivo* relies on the protein being present, rather than just evidence that the gene is being expressed. We detected *CRX* expression by RT–PCR at 10.5 weeks p.c. and by *in situ* hybridization at 13 weeks. In contrast, significant levels of CRX protein were only detected at 15 weeks p.c., whereas no protein was detectable at 13 weeks p.c. using the same immunohistochemical conditions. Although limitations to the sensitivity of the immunostaining mean that we cannot rule out the presence of low levels of protein before 15 weeks, our data does point to the possibility of post-transcriptional control of CRX expression.

Transcript localization and translational regulation are two post-transcriptional mechanisms for the spatial and temporal regulation of protein production (30). There are a number of

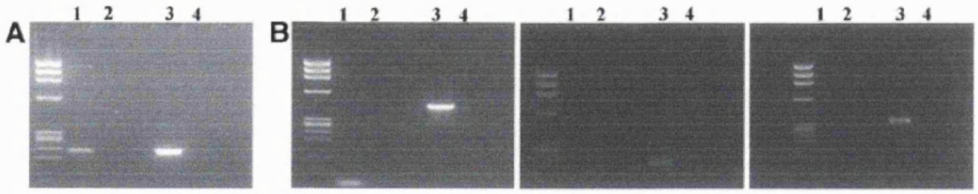

Figure 5. RT–PCR analysis from wild-type and *rd/rd,cl* mouse retinal cDNA. Lane 1, *rd/rd,cl* cDNA; lane 3, wild-type cDNA; lanes 2 and 4 are negative controls. The genes amplified were (**A**) *CRX*, (**B**) rhodopsin, green opsin and blue opsin, respectively. The DNA marker used was ϕX174 (Gibco).

examples showing that even though a gene is transcribed (e.g. *nanos* and *oskar* mRNAs), and is localized in the right cells, it is translationally repressed by proteins binding to *cis*-acting elements in 3′-untranslated region (3′-UTR) sequences (31,32). Translation is activated at the appropriate time by proteins binding to 5′-UTR sequences (33,34). Thus, we propose that retinally-expressed genes transcribed before 15 weeks p.c. in human fetal retina occur independently of CRX. Thus, in addition to *PDEB* and *IRBP*, we would exclude arrestin from transactivation by CRX *in vivo*.

The *in situ* hybridization and immunocytochemistry data convincingly demonstrate that the *CRX* gene and protein are expressed in the INL of both human and mouse retina. This is consistent with previous expression data observed in mouse (35) and zebrafish retina (36). INL expression of *CRX* has been previously documented in the retina of P6 mice (3) and this was thought to correspond to developing photoreceptors trapped on the vitreal side of the inner plexiform layer (37). However, we have clearly shown INL layer *CRX* expression in human adult retina. This was verified in the *rd/rd,cl* mouse retina which has no photoreceptor cells present. It is clear that expression of retinal *CRX* is not exclusive to the photoreceptors of the ONL and that its role in development may not be limited to differentiation and regulation of the photoreceptors as previously thought. The exact role of CRX in the inner retina remains to be determined. However, in *Crx* null mice circadian entrainment is attenuated (16). This is the only retinal modification, other than complete lesion, that has been shown to impair circadian photo-entrainment in mammals. This suggests that Crx may have a role, directly or indirectly, in circadian rhythmicity, and perhaps this is mediated via cells of the inner retina. We are following a number of lines of investigation to test this hypothesis.

The reliance on extrapolation from rodent embryonic expression studies to humans has been justified by strong similarities in the organization, morphology and evolutionary conservation of many key genes. However, recent studies have shown that there are both temporal and spatial differences between species (38). This could explain why attempts to make mouse models by gene targeting often produce either no phenotype or phenotypes that do not resemble the human condition (39). The extent to which our findings represent true functional differences for CRX remains to be determined. The *Crx* null mouse shows attenuated circadian photo-entrainment, whereby it takes approximately twice as long to entrain to a new light stimulus compared with wild-type mice (16). No circadian rhythm disturbance, such as abnormal sleep pattern or symptoms akin to prolonged 'jet-lag', has been reported. Such disturbances, however, have not been thoroughly investigated in humans with the CRX mutation. If humans do not have these disturbances it would suggest, in the mouse, that Crx has other functions, or in humans, that there is a compensatory mechanism. Species differences in longevity or modifier genes could be involved in this human/mouse difference; however, this deserves further investigation. The current work emphasizes the value of comparative studies in validating animal models of human disease and the limited degree of extrapolation that can be drawn from *in vitro* experiments.

MATERIALS AND METHODS

Tissues utilized for studies

Human fetal tissue collected from social terminations of pregnancy was obtained from the MRC Tissue Bank, Hammersmith Hospital, London, with ethical approval. Staging of fetal embryos was by last menstrual period and crown–rump length. Specimens were transferred, <4 h post-operatively, to liquid N_2 for RT–PCR, or to 4% (w/v) paraformaldehyde in phosphate-buffered saline (PBS) for fixation at 4°C for 18 h for *in situ* hybridization analysis. Mouse embryos were obtained from matings of C57BL/6 × CBA mice. The day on which the vaginal plug was detected was designated as E0.5. Tissue from *rd/rd,cl* mice was taken at P80 and tissue from age-matched wild-type eyes was taken when the ONL was absent by histological analysis.

Expression analysis using RT–PCR

Total RNA was extracted from human eyes using the RNAzol RNA extraction kit (Biogenesis), whilst TRIzol (Gibco BRL) was used to isolate total RNA from mouse eyes according to the manufacturer's instructions. The SuperScript pre-amplification system (Gibco BRL) was used to generate cDNA for PCR from 1 μg of total RNA. Identical aliquots of cDNA were used for amplification using gene-specific primers. The *CRX* exon 1 forward primer (5′-CCCTGACTTGGGCCTCAGT-3′) and exon 2 reverse primer (5′-CCACCTCCTCACGGGCATA-3′) were designed to span intron 1 and amplify a product of 250 bp. The PCR profile typically incorporated an initial denaturing step at 94°C for 5 min followed by 30 cycles of denaturation at 94°C for 45 s, annealing at 55°C for 45 s and extension at 72°C for 45 s, with a final extension at 72°C for 5 min. The time of expression for each gene was tested on three independent tissue samples at each time point. Primers used to amplify other retinal genes were as follows:
Rhodopsin (436 bp), 5′-ACCAGATCACCTGCTCTAAC/5′-TCTTGGACACGGTAGCAGAGG;

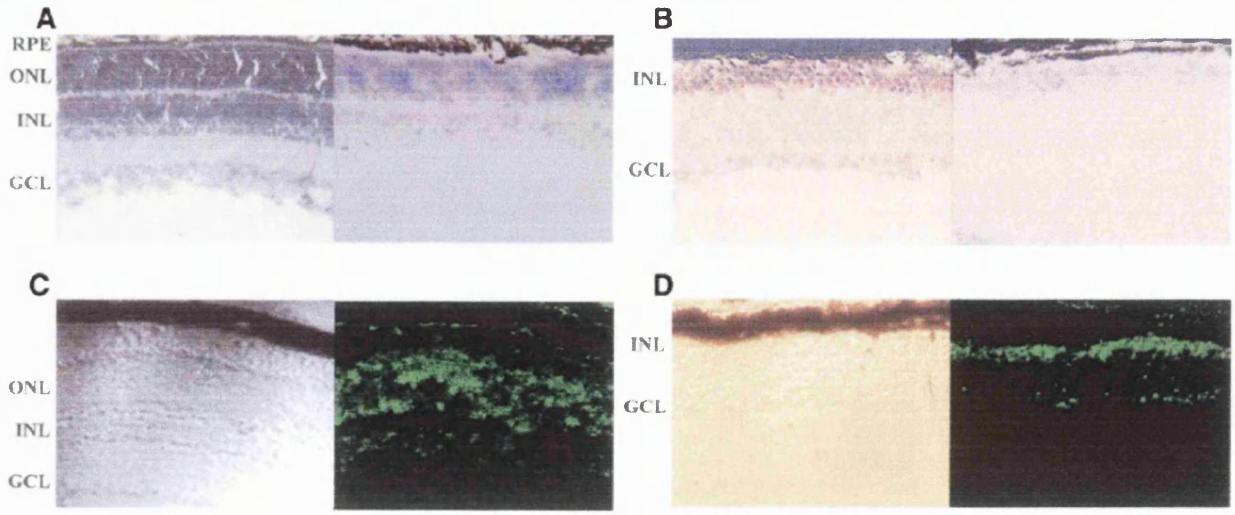

Figure 6. *In situ* hybridization and immunocytochemical (ICC) analyses in wild-type and *rd/rd,cl* retinal sections. (**A**) *Crx* mRNA expression in wild-type retina present in ONL and more weakly in INL. Left panel, H&E; right panel, *in situ*. (**B**) *Crx* mRNA expression in *rd/rd,cl* retina present in INL. Left panel, H&E; right panel, *in situ*. (**C**) CRX antibody localization in wild-type retina. Left panel, phase contrast; right panel, ICC. (**D**) CRX antibody localization in *rd/rd,cl* retina in the INL. Left panel, phase contrast; right panel, ICC. (A and B), 10× magnification; (C and D), 20× magnification.

PDEB (425 bp), 5′-AGGAGACCCTGAACATCTACC/5′-ATGAAGCCCACTTGCAGC;
PDEA (464 bp), 5′-CTCCATGGGTCCTCTATC/5′-CCGACTTGAAGCTTAGGG;
PDEG (594 bp), 5′-GCAGCAGGAGGGAGTC/5′-GACCAAGCCTCTCTGTGG;
arrestin (406 bp), 5′-AAAAAGTGCCACCAAACAGC/5′-GCGTCATTCTTGTCTCTCTTCC;
RS1 (434 bp), 5′-ACCAGATCACCTGCTCTAAC/5′-ACACTTGCTGACGCACTCC;
IRBP (1097 bp), 5′-CCTTTGCACACACCATGC/5′- CATGATATAGGTGAACTCC;
NRL (287 bp), 5′-GTGCCTCCTTCACCCACC/5′-CAGACATCGAGACCAGCG;
green opsin (231 bp), 5′-GCCCAGACGTGTTCAGCG/5′-GACCATCACCACCACCAT;
blue opsin (176 bp), 5′-GGTCACTGGCCTTCCTGG/5′-TGCAGGCCCTCAGGGATG;
SIX3 (242 bp), 5′-AGTCCACACACACTCCCAC/5′-CGTCATGCAGGTGGGGTCG.

Where primers designed against the human gene sequence were not compatible with mouse, specific primers to mouse homologous genes were used:
Pdeg (282 bp), 5′-GTCTCTGCCAGCCTCACC/5′-CTAAATGATGCCATACTGGG;
Pdea (717 bp), 5′-CTCCATGGGTCCTCCATC/5′-CTGGATGCAACAGGACTT;
Rs1 (434 bp), 5′-ATCAGATCACTTGCACCA/5′-ACACTTGCCGGCACACTC;
blue opsin (339 bp), 5′-CAGCCTTCATGGGATTTG/5′-GTGCATGCTTGGAGTTGA;
Irbp (427 bp), 5′-CCCTCCCCAGAAGTCTTT/5′-CAGCCTCTTCATGATGTA;
Nrl (287 bp), 5′-GTGCCTCCTTCACCCACC/5′-GCTGCCGGCAACTCGC;
arrestin (390 bp), 5′-AAAAAGTGCAGCCAAACAGC/5′-CATCTTTCTTCCCTTCTGTG.

In situ hybridization

Fresh human or murine eyes were fixed overnight in 4% paraformaldehyde in PBS and incubated overnight again in 20% sucrose in PBS at 4°C. The eyes were orientated and flash frozen in O.C.T. compound (BDH) using a chamber of dry ice and isopentane. *In situ* hybridization analysis was performed with digoxigenin-labelled riboprobes on 10 µm cryostat sagital sections through the central retina. The probes were generated from a pGEM-T plasmid (Promega) into which either a 445 bp fragment of the human 3′ *CRX* cDNA (forward primer, 5′-GGACTACAAGGATCAGAGTGCCTG-3′; reverse primer, 5′-GTTAAGTTATCAAGCCCCCCTACC-3′) or a 300 bp 3′ *Crx* mouse fragment (forward primer, 5′-CTCCTCCAGCTTAGATTC-3′; reverse primer, 5′-CCCGGAGTTCTAAGCCAA-3′) had been cloned. The plasmids were linearized with either *Not*I (for antisense probe) or *Nco*I (for sense probe). Digoxigenin-labelled riboprobes were generated using either SP6 RNA polymerase (antisense) or T7 RNA polymerase (sense) in the presence of digoxigenin RNA labelling mix (Roche) in accordance with the manufacturer's instructions. Immediately before use, the probes were diluted to a concentration of 1 ng/µl in hybridization buffer (10 mM Tris–HCl pH 7.5, 200 mM NaCl, 5 mM NaH_2PO_4, 5 mM Na_2HPO_4, 5 mM EDTA, 1 mg/ml tRNA, 50% formamide, 10% dextran sulphate, 1× Denhardt's). The probes were denatured for 5 min at 70°C and quenched on ice. Hybridization was performed overnight at 65°C in a humidified chamber of 50% formamide and 2× SSC. Immunodetection was carried out using a 1:1000 dilution of anti-digoxigenin alkaline phosphatase-conjugated Fab fragments (Roche). Hybrids were visualized with the BCIP/NBT substrate (Roche). Images were viewed using a Leitz Aristoplan microscope with digital image capture

(Olympus DP10 camera). *In situ* experiments were repeated on three different eyes at each time point.

Generation of an N-terminal antibody to human CRX

A peptide was synthesized commercially using Fmoc chemistry (Sigma-Genosys) corresponding to the first 24 amino acids of CRX protein. The peptide was conjugated to keyhole limpet hemocyanin and then used to generate a rabbit polyclonal antibody by standard protocols. Serum samples were desalted prior to IgG fraction by DEAE affi-gel chromatography (Bio-Rad). Protein concentrations were estimated using a Bradford assay (Pierce).

Western blotting

Mouse retinal tissue was dissected in ice-cold PBS, added to solubilization buffer (150 mM NaCl, 1% Tergitol, 0.5% sodium deoxycholate, 0.1% SDS, 50 mM Tris–HCl pH 8.0) containing protease inhibitor cocktail (Sigma) and kept on ice for 15 min. Tissue was sonicated, placed on ice for 10 min and then centrifuged at 10 000 *g* for 2 min. The supernatant was then mixed 1:1 with Laemmli sample buffer, denatured for 5 min at 100°C and the proteins were separated by 12% SDS–PAGE relative to low molecular weight standards (Biorad). Each sample loaded on a gel contained protein equivalent to one mouse retina in a 10 µl volume. Proteins were electrophoretically transferred onto nitrocellulose membrane (Schleicher and Schuell) using a Tris-glycine buffer system (48 mM Tris, 39 mM glycine, 0.037% SDS, 20% methanol). The membrane was pre-incubated in blocking buffer (5% non-fat milk, 0.1% Tween-20 in PBS) at 4°C for several hours followed by incubation with primary CRX antibody (diluted 1:250 in blocking buffer) for 1 h at room temperature. After three washes in PBS, 0.1% Tween-20, the membrane was incubated for 1 h at room temperature with a 1:3000 dilution of goat anti-rabbit conjugated-HRP in blocking buffer. After three final washes the peroxidase reaction was visualized by enhanced chemiluminescence (Amersham Pharmacia Biotech).

Immunocytochemistry

The sections for immunocytochemistry were taken from the same eyes that were used for *in situ* hybridization at each time point. To reduce non-specific labelling, 10 µm cryostat sections were incubated for 2 h at room temperature in blocking solution (PBS, 0.5% bovine serum albumin, 0.2% Triton X-100, 0.5% sodium azide) containing 2% normal donkey serum (Sigma). The sections were incubated with the primary CRX antibody in the same buffer (1:40) for 16 h at 4°C, rinsed in blocking solution and then incubated for 30 min at room temperature in secondary antibody (1:200) conjugated to fluorescein isothiocyanate (affinity-purified and species-absorbed donkey anti-rabbit IgG, Chemicon). Immunolabelled sections were mounted with Immunofluore (ICN) and were examined with a Leica laser scanning confocal microscope. Phase and fluorescence confocal images were exported to Photoshop 4.0 (Adobe) for annotation and dye-sublimation prints were generated.

ACKNOWLEDGEMENTS

The authors acknowledge the MRC Tissue Bank for provision of human fetal tissue. This work was supported by Fight for Sight prize studentships (L.C.B. and A.R.), British Retinitis Pigmentosa Society (GR518), Medical Research Council (J.C.S.) and the Child Health Research Appeal Trust (J.K.L.H.).

NOTE ADDED IN PROOF

A novel 12 bp deletion mutation in *CRX* has been identified by Tzekov, R.T. *et al.* (40).

REFERENCES

1. Zipursky, S.L. and Rubin, G.M. (1994) Determination of neuronal cell fate: lessons from the R7 neuron of *Drosophila*. *Annu. Rev. Neurosci.*, **17**, 373–397.
2. Cepko, C., Austin, C., Yang, X., Alexiades, M. and Ezzeddine, D. (1996) Cell fate determination in the vertebrate retina. *Proc. Natl Acad. Sci. USA*, **93**, 589–595.
3. Furukawa, T., Morrow, E.M. and Cepko, C.L. (1997) *Crx*, a novel *otx*-like homeobox gene, shows photoreceptor-specific expression and regulates photoreceptor differentiation. *Cell*, **91**, 531–541.
4. Freund, C.L., Gregory-Evans, C.Y., Furukawa, T., Papaioannou, M., Looser, J., Ploder, L., Bellingham, J., Ng, D., Herbrick, J.-A.S., Duncan, A. *et al.* (1997) Cone-rod dystrophy due to mutations in a novel photoreceptor-specific homeobox gene (*CRX*) essential for maintenance of the photoreceptor. *Cell*, **91**, 543–553.
5. Chen, S., Wang, Q.-L., Nie, Z., Sun, H., Lennon, G., Copeland, N.G., Gilbert, D.J., Jenkins, N.A. and Zack, D.J. (1997) Crx, a novel otx-like paired-homeodomain protein, binds to and transactivates photoreceptor cell-specific genes. *Neuron*, **19**, 1017–1030.
6. Finkelstein, R. and Boncinelli, E. (1994) From fly head to mammalian forebrain: the story of otd and OTX. *Trends Genet.*, **10**, 310–315.
7. Swain, P.K., Chen, S., Wang, Q.-L., Affatigato, L.M., Copats, C.L., Brady, K.D., Fishman, G.A., Jacobson, S.G., Swaroop, A., Stone, E. *et al.* (1997) Mutations in the cone-rod homeobox gene are associated with cone-rod dystrophy photoreceptor degeneration. *Neuron*, **19**, 1329–1336.
8. Sohocki, M.M., Sullivan, L.S., Mintz-Hittner, H.A., Birch, D., Heckenlively, J.R., Freund, C.L., McInnes, R.R. and Daiger, S.P. (1998) A range of clinical phenotypes associated with mutations in *CRX*, a photoreceptor transcription factor gene. *Am. J. Hum. Genet.*, **63**, 1307–1315.
9. Sankila, E.M., Joensuu, T.H., Hamalainen, R.H., Raitanen, N., Valle, O., Ignatius, J. and Cormand, B. (2000) A CRX mutation in a Finnish family with dominant cone-rod retinal dystrophy. *Hum. Mutat.*, **16**, 94.
10. Freund, C.L., Wang, Q.-L., Chen, S., Muskat, B.L., Wiles, C.D., Sheffield, V.C., Jacobson, S.G., McInnes, R.R., Zack, D.J. and Stone, E.M. (1998) *De novo* mutations in the *CRX* homeobox gene associated with Leber congenital amaurosis. *Nat. Genet.*, **18**, 311–312.
11. Swaroop, A., Wang, Q.-L., Wu, W., Cook, J., Coats, C., Xu, S., Zack, D.J. and Sieving, P.A. (1999) Leber congenital amaurosis caused by homozygous mutation (R90W) in the homeodomain of the retinal transcription factor CRX: direct evidence for the involvement of CRX in the development of photoreceptor function. *Hum. Mol. Genet.*, **8**, 299–305.
12. Silva, E., Yang, J.-M., Li, Y., Dharmaraj, S., Sundin, O.H. and Maumenee, I.H. (2000) A *CRX* null mutation is associated with both Leber congenital amaurosis and a normal ocular phenotype. *Invest. Ophthalmol. Vis. Sci.*, **41**, 2076–2079.
13. Evans, K., Duvall-Young, J., Fitzke, F.W., Arden, G.B., Bhattacharya, S.S. and Bird, A.C. (1995) Chromosome 19q cone-rod retinal dystrophy: ocular phenotype. *Arch. Ophthalmol.*, **113**, 195–201.
14. Schroeder, R., Mets, M.B. and Maumenee, I.H. (1987) Leber's congenital amaurosis. *Arch. Ophthalmol.*, **105**, 356–359.
15. Livesey, F.J., Furukawa, T., Steffen, M.A., Church, G.M. and Cepko, C.L. (2000) Microarray analysis of the transcriptional network controlled by the photoreceptor homeobox gene *Crx*. *Curr. Biol.*, **10**, 301–310.
16. Furukawa, T., Morrow, E.M., Li, T., Davis, F.C. and Cepko, C.L. (1999) Retinopathy and attenuated circadian entrainment in *Crx*-deficient mice. *Nat. Genet.*, **23**, 466–470.

17. Kumar, R. and Zack, D.J. (1995) Regulation of visual pigment gene expression. In Wiggs, J. (ed.), *Molecular Genetics of Ocular Disease*. Wiley-Liss Inc., New York, NY, pp. 139–160.
18. Granadino, B., Gallardo, M.E., Lopez-Rios, J., Sanz, R., Ramos, C., Ayuso, C., Bovolenta, P. and Rodriguez de Cordoba, S. (1999) Genomic cloning, structure, expression pattern and chromosomal location of the human *SIX3* gene. *Genomics*, **55**, 100–105.
19. Oliver, G., Mailhos, A., Wehr, R., Copeland, N.G., Jenkins, N.A. and Gruss, P. (1995) *Six3*, a murine homologue of the *sine oculis* gene, demarcates the most anterior border of the developing neural plate and is expressed during eye development. *Development*, **121**, 4045–4055.
20. Cepko, C.L. (1996) The patterning and onset of opsin expression in vertebrate retinae. *Curr. Opin. Neurobiol.*, **6**, 542–546.
21. Xiao, M. and Hendrickson, A. (2000) Spatial and temporal expression of short, long/medium, or both opsins in human foetal cones. *J. Comp. Neurol.*, **425**, 545–559.
22. He, L., Campbell, M.L., Srivastava, D., Blocker, Y.S., Harris, J.R., Swaroop, A. and Fox, D.A. (1998) Spatial and temporal expression of AP-1 responsive rod photoreceptor genes and bZIP transcription factors during development of the rat retina. *Mol. Vis.*, **4**, 32.
23. Freedman, M.S., Lucas, R.J., Soni, B., von Schantz, M., David-Gray, Z. and Foster, R. (1999) Regulation of mammalian circadian behaviour by non-rod, non-cone ocular photoreceptors. *Science*, **284**, 502–504.
24. Remington, L.A. and McGill, E.C. (1997) Ocular embryology. In McGill, E.C. (ed.), *Clinical Anatomy of the Visual System*. Butterworth-Heinemann, Oxford, UK, pp. 103–121.
25. Jakobiec, F.A. and Ozanics, V. (1982) Prenatal development of the eye and its adenexa. In Jakobiec, F.A. and Ozanics, V. (eds), *Ocular Anatomy, Embryology and Teratology*. Harper and Row, London, UK, pp. 11–96.
26. Rohrer, B., Korenbrot, J.I., LaVail, M.M., Reichardt, L.F. and Xu, B (1999) Role of neurotrophin receptor TrkB in the maturation of rod photoreceptors and establishment of synaptic transmission to the inner retina. *J. Neurosci.*, **19**, 8919–8930.
27. Di polo, A., Lerner, L.E. and Farber, D.B. (1996) Transcriptional activation of the human rod cGMP-phosphodiesterase β-subunit gene is mediated by an upstream AP-1 element. *Nucleic Acids Res.*, **25**, 3863–3867.
28. Mears, A.J., Kondo, M., Takada, Y., Swain, P.K., Nelson, B., Sieving, P.A. and Swaroop, A. (2001) NRL is a major determinant of rod photoreceptor cell fate: study of a knockout mouse. *Invest. Ophthalmol. Vis. Sci.*, **42**, S527.
29. Fong, S.L. and Fong, W.B. (1999) Elements regulating the transcription of human interstitial retinoid binding protein (IRBP) gene in cultured retinoblastoma cells. *Curr. Eye Res.*, **18**, 283–291.
30. Lipshitz, H.D. and Smibert, C.A. (2000) Mechanisms of RNA localisation and translational regulation. *Curr. Opin. Genet. Dev.*, **10**, 476–488.
31. Kim-Ha, J., Kerr, K. and Macdonald, P.M. (1995) Translational regulation of *oskar* mRNA by Bruno, an ovarian RNA-binding protein, is essential. *Cell*, **81**, 403–412.
32. Smibert, C.A., Wilson, J.E., Kerr, K. and Macdonald, P.M. (1996) Smaug protein represses translation of unlocalised nanos mRNA in the *Drosophila* embryo. *Genes Dev.*, **10**, 2610–2620.
33. Wilson, J.E., Connell, J.E. and Macdonald, P.M. (1996) *aubergine* enhances *oskar* translation in the *Drosophila* ovary. *Development*, **122**, 1631–1639.
34. Crucs, C., Chatterjee, S. and Gavis, E.R. (2000) Overlapping but distinct RNA elements control repression and activation of *nanos* translation. *Mol. Cell*, **5**, 457–467.
35. Chen, S., McMahan, B. and Xu, S. (2000) Localisation of the CRX protein in the mature and developing mouse retina. *Invest. Ophthalmol. Vis. Sci.*, **41**, S392.
36. Liu, Y., Shen, Y.-C., Rest, J.S., Redmond, P.A. and Zack, D.J. (2001) Isolation and characterization of a zebrafish homologue of the cone rod homeobox gene. *Invest. Ophthalmol. Vis. Sci.*, **42**, 481–487.
37. Young, R.W. (1985) Cell death during differentiation of the retina in the mouse. *J. Comp. Neurol.*, **229**, 362–373.
38. Fougerousse, F., Bullen, P., Herasse, M., Lindsay, S., Richard, I., Wilson, D., Suel, L., Durand, M., Robson, S., Abitbol, M. *et al.* (2000) Human-mouse differences in the embryonic expressions patterns of developmental control genes and disease genes. *Hum. Mol. Genet.*, **9**, 165–173.
39. Wynshaw-Boris, A. (1996) Model mice and human disease. *Nat. Genet.*, **13**, 259–260.
40. Tzekov, R.T., Liu, Y., Sohocki, M.M., Zack, D.J., Daiger, S.P., Heckenlively, J.R. and Birch, D.G. (2001) Autosomal dominant retinal degeneration and bone loss in patients with a 12-bp deletion in the *CRX* gene. *Invest. Ophthalmol. Vis. Sci.*, **42**, 1319–1327.

CORRECTIONS TO TEXT

Page 43: *Pax6*$^{-/-}$ mice develop incorrectly patterned forebrains and morphologically normal optic vesicles. However, optic cups are not formed because lens induction fails when the vesicle meets the mutant surface ectoderm, and homozygous mice are neonatally fatal owing to CNS defects (Grindley *et al.* 1997).

Page 51: Retinoic acid (RA), which is known to regulate many aspects of development (Ross *et al.* 2000), is produced is large quantities in the developing vertebrate retina, although its role is poorly understood (Drager *et al.* 2001) (see Appendix D).

Page 121: In the adult retina, *Chx10* expression is restricted to cells within the outer aspect of the inner nuclear layer (inl).

Page 124a: At this stage the retina is divided into two layers (a), and while *BRN3B* expression can be readily detected in both (b), it is certainly expressed at lower levels in the outer layer.

Page 124b: *PAX6* expression (c) is uniform throughout both layers, possibly reflecting both the presence of dividing cells and ganglion cells.

Page 134: Histological analysis of the adult *or*^{J} and wild-type retina.

Page 170: The *or*^{J} phenotype is on the sv129 background, and this demonstrates that the observed phenotype of delayed *Crx* expression in the *or*^{J} retina is not caused by an effect of its strain.

Page 180: (a) shows H and E stained postnatal (P) day 2 retinal section.

Page 219: As predicted by the RT-PCR experiments described above, where fragments of the novel Chx10-like cDNA were, at best, only very weakly amplified from developmental eye tissue from 9 to 15 weeks pc, no *in situ* hybridisation was observed in foetal eyes or retina (data not shown).

Page 243 (and in all text references): Furukawa, T., Kozak, C. A., & Cepko, C. L. *rax*, a novel paired-type homeobox gene, shows expression in the anterior neural fold and developing retina. *Proc.Natl.Acad.Sci.U.S.A* **94**, 3088-3093 (1997a).
Furukawa, T., Morrow, E. M., & Cepko, C. L. *Crx*, a novel otx-like homeobox gene, shows photoreceptor-specific expression and regulates photoreceptor differentiation. *Cell* **91**, 531-541 (1997b).

Page 258: Expression is first detected as early as E11, and thus may precede onset of *Crx* expression, which, first detected at E12.5, is presumed to be the earliest known genetic marker for photoreceptors (Freund *et al.* 1997).

Pages 259 and 166: The 5' promoter region of *Irbp* also contains a Crx preferred binding site (although the match is not perfect) (Livesey *et al.* 2000), suggesting that Crx might be involved with transcription of this photoreceptor specific gene.

Page 267: APPENDIX D – THE ROLE OF RETINOIDS IN DEVELOPMENT (ROSS *ET AL.* 2000).

The application of knockout mouse models to retinoid ligands has demonstrated that vitamin A and its derivatives are essential for normal embryonic development. Retinoic acid (RA), the oxidised form of retinol, regulates developmental processes by activation of gene transcription, predominantly by a signal transduction cascade prompted by the retinoic acid receptor families RAR and RXR. However, gene specific transcriptional activation is dependent not only on the presence of a RA receptor, but also on the concentration of RA in the cellular milieu [shown by the RARE mouse, see main text for details (Enwright and Grainger, 2000)]. Distribution of RA and its receptors is not homogeneous in developing tissue, exemplified, as shown by Drager *et al.* (2001), in the retina. Analysis of specific members of the RA catabolic pathway, such as the retinaldehyde dehydrogenases AHD2 and V1, show well characterised specific areas of expression: AHD1 in the dorsal and V1 in the ventral retina. These regions represent specific levels of RA synthesis, which are clearly demarcated by a stripe of expression of another RA catabolic enzyme CYP26. The tyrosine receptor kinase EphB2 and its ligand ephrin B2 are thought to regulate the targeted outgrowth of retinal axons in a dorso-ventrally-patterned manner. Ephrin B2 has an expression pattern restricted to the dorsal retina, whereas EphB2 is ventrally expressed. Although the specific pathways are yet to be elucidated, the similarities in expression patterns of regulators of cell-specific differentiation and RA catabolites suggest that RA is involved in this level of differentiation in a precise concentration-dependent fashion.

The intricate but highly organised nature of the retina suggests that patterning retinal tissue is very complex. The information that RA receptors form homo- and hetero-dimers with other receptors suggests a level of complexity for regulating differentiation of myriad cell types. RXR can form heterodimers with RAR, the thyroid receptor TR, the vitamin D_3 receptor VDR, and others. Transcription of specific genes is dependent not only on the heterodimeric RXR partner, but also on the presence of the partner's ligand. These levels of complex analysis are required to fully understand the potential role of RA in the differentiation of photoreceptors, as suggested in this thesis.

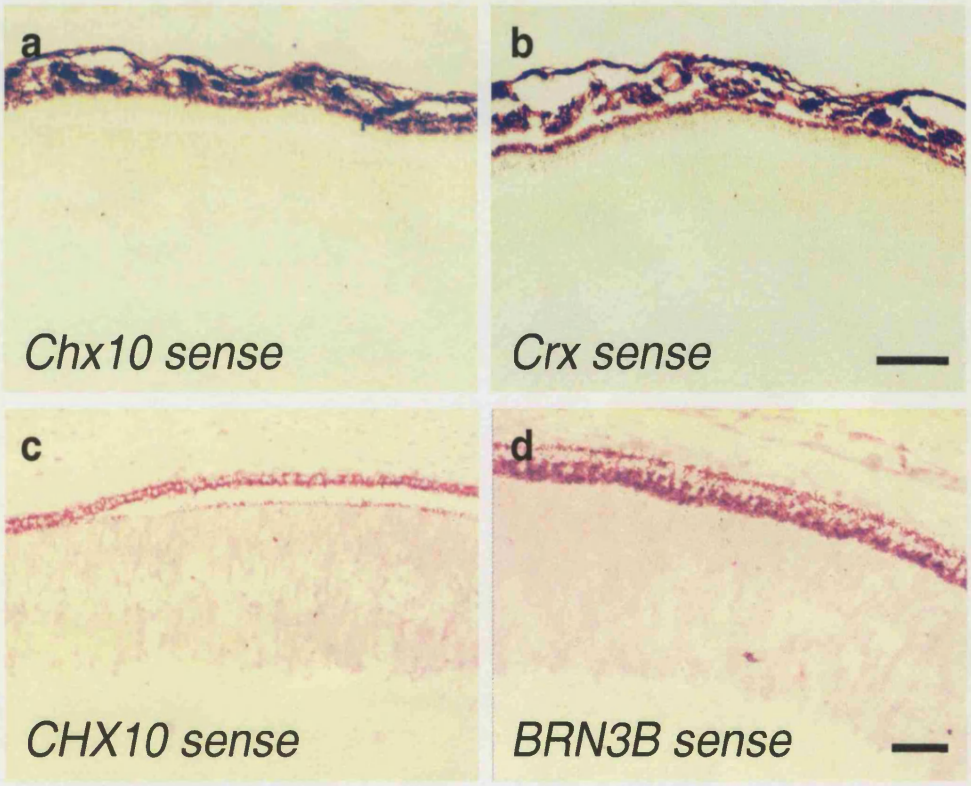

Figure addendum. *In situ* hybridisation sense riboprobe controls. When performing *in situ* hybridisation experiments with antisense riboprobes transcribed from specific genes, tissue from the same specimens was also incubated with sense probes from the same gene. This internal control was designed to determine whether the expression patterns observed with the antisense riboprobes were not an artefact caused by non-specific binding. Tissue was processed identically to the antisense experiments, and invariably, sense controls showed no digoxygenin labelling. (a) and (b) show *Chx10* and *Crx* sense riboprobes, respectively, on adult mouse retina. (c) and (d) show CHX10 and *BRN3B* sense riboprobes on 8wpc human retina. Scale bars = 100μm.